

The physicochemical characterisation, compatibility testing and solid-state form screening of terizidone - pyridoxine combinations

By

Ngabo Yves Musafili

A full thesis submitted in the partial fulfilment of the requirements for the degree of

Magister Pharmaceuticiae

Faculty of Natural Science, School of Pharmacy,

Discipline of Pharmaceutics

University of the Western Cape, Bellville, South Africa.



Supervisor: Prof. Marique Aucamp

Co-Supervisor: Prof Halima Samsodien

November 2021

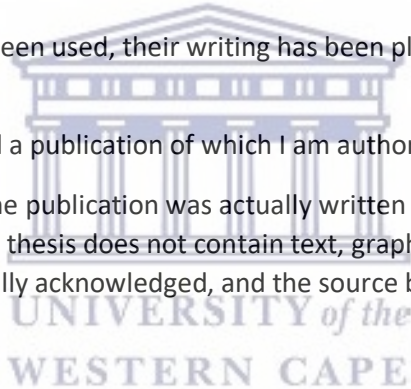
<http://etd.uwc.ac.za/>


Declaration (plagiarism declaration)

DECLARATION

INgabo Yves Musafili..... declare that

- (i) The research reported in this thesis, except where otherwise indicated, is my original work.
- (ii) This thesis has not been submitted for any degree or examination at any other University.
- (iii) This thesis does not contain other persons' data, pictures, graphs or other information, unless specifically acknowledged as being sourced from other persons.
- (iv) This thesis does not contain other persons' writing, unless specifically acknowledged as being sourced from other researchers. Where other written sources have been quoted, then:
 - a) their words have been re-written but the general information attributed to them has been referenced;
 - b) where their exact words have been used, their writing has been placed inside quotation marks, and referenced.
- (v) Where I have reproduced a publication of which I am author, co-author or editor, I have indicated in detail which part of the publication was actually written by myself alone and have fully referenced such publications. This thesis does not contain text, graphics or tables copied and pasted from the Internet, unless specifically acknowledged, and the source being detailed in the thesis and in the References sections.



Signed:  _____

Date: _11 November 2021_

Dedication

I would like to dedicate the thesis to myself, for having self-belief and working hard to provide good and quality research.

I dedicate this work to my parents and to my siblings and most importantly to my father, Lambert Musafili who is no longer with us and died shortly before my thesis submission. They supported me financially and allowed me to do this work.

I would like also to thank the almighty God for keeping me alive until today and giving me the courage and spiritual force to keep going even when time were difficult.



Abstract

Introduction: Terizidone (TZD) is considered an essential anti-tuberculosis drug and in South Africa it is prescribed as part of the multi-drug resistant tuberculosis (MDR-TB) treatment regimen. From a literature study it became apparent that very little is known in terms of the physicochemical characteristics of TZD and only one literature source mentions one polymorphic form of this drug. Furthermore, it exhibits neurotoxicity as an adverse effect, leading to the concomitant administration of pyridoxine (PDX) to counteract the TZD-induced side effects. MDR-TB patients experience major side effects from taking the drug for a long period (18 months) and it often results in resistance and poor adherence. This study therefore focused on the possibility to combine TZD and PDX either as co-crystals or as co-amorphous solid-state forms. In order to achieve this a complete physicochemical profile of TZD was determined, since very limited information could be found in literature. The compatibility between TZD and PDX were investigated and stood central in this study, finally, an attempt was made to prepare potential novel solid-state forms of TZD in combination with PDX. The purpose of this work was to obtain scientific evidence which could inform the potential formulation of a fixed-dose combination (FDC) containing TZD and PDX, thus aiming at reducing patient “pill burden” which could potentially improve patient adherence which in turn will improve patient quality of life.

Methods: The physicochemical properties of TZD, PDX and a 1:1 (w/w) TZD:PDX physical mixture were characterised utilising differential scanning calorimetry (DSC), thermogravimetric analysis (TGA), hot stage microscopy (HSM), spectroscopy (Fourier-transform infrared and Raman) and powder X-ray diffraction (PXRD). A complete equilibrium solubility profile of TZD in all relevant aqueous pH buffered media (pH 1.2, 4.5, 6.8, distilled water) and organic solvents, typically used in pharmaceutical recrystallisation studies and preformulation techniques, was determined. Compatibility of TZD and PDX were studied utilising spectroscopy and thermal analyses (DSC, TGA and HSM). High performance liquid chromatography (HPLC) was used to identify and quantify TZD, PDX and associated degradation products. Three methods typically utilised to prepare novel solid-state forms of drugs, namely, solvent evaporation, quench cooling of the melt and liquid assisted grinding (LAG) were investigated as potential methods to potentially prepare novel solid-state forms combining TZD and PDX.

Results: To aid in the simultaneous identification and quantification of TZD and PDX a sensitive and robust HPLC method was developed and validated. Physicochemical characterisation of TZD showed it to be a partially crystalline compound that is poorly soluble in most organic solvents and aqueous buffered media. An in-depth compatibility testing of TZD in combination with PDX showed the two compounds to be compatible. The poor solubility associated with TZD made typical recrystallisation processes challenging, resulting in phase separation of TZD and PDX during recrystallisation through solvent evaporation. Due to the thermal behaviour of both compounds but specifically linked to that of PDX, which showed rapid degradation almost immediately after melting, made the use of the quench cooling of the melt method as preparation technique for a co-amorphous solid-state form impossible. LAG showed the most promise, however no novel solid-state forms could be prepared. It was found that the solvent, DMSO, facilitates rapid degradation of both compounds during the LAG process.

Conclusion: To conduct thorough physicochemical characterization of pharmaceutical compounds, sensitive and accurate analytical methods are a necessity. The solid-state form screening of TZD proved that only a single solid-state form of the drug exists and that no other solid-state forms which allows molecular level combination of TZD with PDX could be prepared using various techniques. Despite this very important and impactful information was gained throughout this study, adding value to the current gap in the knowledge base pertaining to TZD.

Keywords: Tuberculosis (TB), Multi-drug resistant tuberculosis (MDR-TB), terizidone, pyridoxine HCl, solid-state, fixed dose combination (FDC), physicochemical characterization, drug-drug compatibility.

Acknowledgment

I would like to thank my supervisors, Prof Marique Aucamp and Prof. Halima Samsodien who guided me throughout the period of the research, for their efforts and attention. I am greatly humbled by their contributions and their guidance in the course of this work.

I would like also to acknowledge my colleagues: Nnamdi, Candidah, Sandrine, Geoffrey, Omobolanle, Bjorn and Marise; we shared laboratory, assisted, and motivated each other whenever needed.

I am grateful to the University of Western Cape, to the Faculty of Natural Sciences and more importantly to the Department of Pharmaceutics for providing access to the laboratory, equipment, and materials to conduct the research.



List of abbreviations

ACN: acetonitrile

AIDS: Acquired Immunodeficiency Syndrome

API: Active Pharmaceutical Ingredient.

ATS : American Thoracic Society

DSC: Differential Scanning Calorimetry

DMSO : Dimethyl sulfoxide

EMA : European Medicine Agency

FDA: Food and Drug administration

FDC: Fixed-dose combination

FTIR : Fourier-Transform infrared spectroscopy

GFA : Glass-Forming Ability

HIV: Human Immunodeficiency Virus

HPLC : High Performance Liquid Chromatography

HSM : Hot stage Microscopy

ICH: International Council for Harmonisation .

IGRA: Interferon-gamma Release Assay

LAG: Liquid Assisted Grinding

MDR-TB : multi-drug resistant TB

MeOH: Methanol

NDOH: National Department of Health

PDX: Pyridoxine HCl

PXRD: Powder X-Ray Diffraction

TB : Tuberculosis

TZD: Terizidone

TGA : Thermogravimetric analysis

USA: United state of America

WHO: World Health Organisation

w/w: Weight per weight

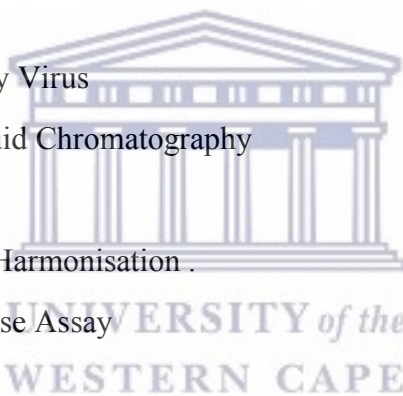


Table of contents

Declaration	ii
Dedication	iii
Abstract	iv
Acknowledgement	vi
List of abbreviations	vii
Table of contents	viii

Chapter 1

Introduction

1.1	A brief introduction to tuberculosis	1
1.2	A pharmaceutical perspective towards the eradication of TB	3
1.3	A brief overview of TZD and PDX linked to the study rationale	4
1.4	Study design and objectives	5
1.5	Outline of thesis chapters	5
1.6	Conclusion	6
1.7	References	7

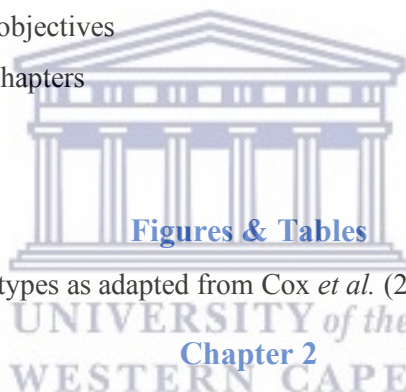


Table 1.1:	TB drug resistant types as adapted from Cox <i>et al.</i> (2017)	2
------------	--	---

An overview of tuberculosis (TB) and associated drug treatment

2.1	Introduction	9
2.2	Risk factors	10
2.3	Transmission	10
2.4	Pathogenesis of <i>Mycobacterium tuberculosis</i>	11
2.5	Detection and diagnosis	12
2.6	Clinical symptoms associated with TB	14
2.7	Multi-drug resistant tuberculosis (MDR-TB)	14
2.8	Treatment	15
2.8.1	Latent tuberculosis	15
2.9	Active TB and MDR-TB	15
2.10	Adverse drug reactions of anti-TB medications	17
2.11	Eradication of TB – the WHO vision	17
2.12	PDX and TZD as part of the TB treatment regimen	18

2.12.1	Pharmacological action of PDX	18
2.12.2	Pharmacological action of TZD	19
2.13	The route of synthesis and physicochemical properties	20
2.13.1	PDX	20
2.13.2	TZD	22
2.14	Conclusion	23
2.15	References	24

Figures and Tables

Figure 2.1:	TB incidence estimation in 2019, for countries with at least 100 000 incident cases, adapted from WHO (WHO, 2020).	10
Figure 2.2 :	The pathogenesis cycle of Mtb, as adapted from Cambier, Falkow and Ramakrishnan (2014).	12
Figure 2.3:	Molecular structure of PDX (Scifinder, 2021)	20
Figure 2.4:	Molecular structure of TZD (Scifinder, 2019)	22
Table 2.1:	MDR-TB regimen standard in South Africa for adults (NDOH, 2020)	16
Table 2.2:	Physicochemical properties of PDX (Aboul-Enein and Loutfy, 1984; Ph. Eur 2005)	21
Table 2.3:	Physicochemical properties of TZD (Scifinder, 2019)	23

Chapter 3

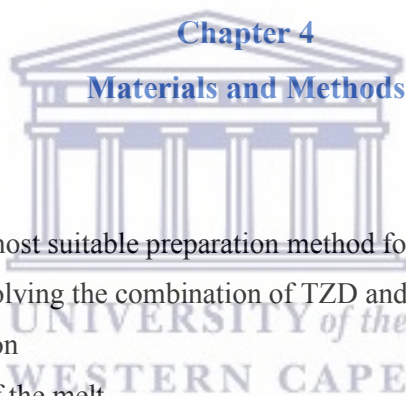
An overview on the solid-state chemistry and physicochemical properties of drugs in relation to pharmaceutical preformulation.

3.1	Introduction	29
3.2	Solid-state forms of active pharmaceutical ingredients (APIs)	29
3.2.1	Polymorphism	30
3.2.2	Hydrates and solvates	32
3.2.3	Co-crystals	33
3.2.4	Salts	35
3.2.5	Amorphous and co-amorphous solid-state forms	36
3.2.6	Solid dispersions	39
3.2.6.1	Eutectic mixtures	40
3.2.6.2	Solid solution	41
3.2.6.3	Glass solutions and glass suspensions	42
3.3	Solubility	43
3.4	Compatibility	44
3.5	Fixed dose combinations (FDC)	45
3.6	Conclusion	47

3.7	References	48
-----	------------	----

Figures and Tables

Figure 3.1:	Solid-state forms of APIs as adapted from Healy <i>et al.</i> , (2017).	30
Figure 3.2:	Crystalline solid-state form preparation methods depicting longer duration methods that yield stable polymorphs and shorter duration methods that yield less stable polymorphs as adapted from Cains, (2009).	32
Figure 3.3:	Schematic representation of PDX (a) and of TZD (b) with hydrogen bond donor (+) and (-) acceptor potential region.	34
Figure 3.4	Solid dispersions classification as adapted from Dengale <i>et al.</i> , 2016.	40
Figure 3.5:	BCS classification of pharmaceutical compounds based on permeability and solubility. Adapted from Williams <i>et al.</i> , 2013.	43
Figure 3.6:	FDC types of system: monolithic (1), multiple-layer system (2) and multiparticulate systems (3) as adapted from (Fernández-García, et al., 2020).	46



4.1	Introduction	55
4.2	Materials	55
4.3	Screening of the most suitable preparation method for potential solid-state modifications involving the combination of TZD and PDX	55
4.3.1	Solvent evaporation	56
4.3.2	Quench cooling of the melt	57
4.3.3	Liquid assisted grinding (LAG)	57
4.4	Analytical methods used to characterise TZD:PDX preparations	58
4.4.1	Hot stage microscopy (HSM)	58
4.4.2	Thermogravimetric analysis (TGA)	59
4.4.3	Differential scanning calorimetry (DSC)	59
4.4.4	Powder X-Ray Diffraction (PXRD)	60
4.4.5	Fourier-Transform infrared spectroscopy (FTIR)	60
4.4.6	Raman spectroscopy	61
4.4.7	High performance liquid chromatography (HPLC)	61
4.5	Equilibrium solubility studies	62
4.6	Investigation of compatibility between TZD and PDX	62
4.7	Conclusion	63

Figures & Tables

Figure 4.1: Schematic diagram depicting the raw materials, LAG combination method and the characterisation techniques used in the study. 58

Table 4.1: Safety classes and boiling point of the solvents used in the experiment (Joshi and Adhikari, 2019; Prat *et al.*, 2015). 56

Chapter 5

Development and validation of a reversed-phase high performance liquid chromatography (RP-HPLC) method for the simultaneous detection of TZD and PDX.

5.1	Introduction	67
5.2	HPLC method development considerations	68
5.2.1	Analyte properties	68
5.2.2	Suitable solvent selection	70
5.2.3	Determination of optimal wavelength	71
5.2.4	Column choice	71
5.3	HPLC method optimisation	73
5.4	Method validation	84
5.4.1	Linearity	84
5.4.2	Accuracy	85
5.4.3	Precision	86
5.4.4	Limit of detection (LOD) and limit of quantification (LOQ)	87
5.4.5	Specificity	88
5.4.6	Robustness	90
5.4.7	Sample solution stability	90
5.5	Conclusion	94
5.6	References	96



Figures & Tables

Figure 5.1: Pictogram displaying a(A) typical, ideal Gaussian peak and (B) the characteristic peaks obtained with varying levels of column selectivity and efficiency (Adapted from Kazakevich and LoBrutto, 2007a). 72

Figure 5.2: The HPLC chromatogram of simultaneous analysis of TZD and PDX obtained using MeOH: H₂O (50:50 %v/v) as mobile phase and solvents with an ACE[®] Excel[™] C18 (250 x 4.6 mm, 3 μ m) column. 74

Figure 5.3 :	The HPLC chromatogram of TZD and PDX obtained using a mobile phase of ACN: H ₂ O (80:20 %v/v) and the Phenomenex [®] Kinetex [®] C ₁₈ 250 x 4.6 mm, 5µm column stationary phase.	75
Figure 5.4:	The HPLC chromatogram of TZD and PDX obtained using the mobile phase consisting of ACN: H ₂ O (90:10 %v/v) and the Phenomenex [®] Kinetex [®] C ₁₈ 150 x 4.6 mm, 5µm column stationary phase.	76
Figure 5.5 :	The HPLC chromatogram of TZD and PDX obtained using the mobile phase consisting of ACN: H ₂ O (30:70 %v/v) and the Phenomenex [®] Kinetex [®] C ₁₈ 150 x 4.6 mm, 5µm column stationary phase.	77
Figure 5.6:	The HPLC chromatogram of TZD and PDX obtained using the 30:70 %v/v ACN:H ₂ O, with 1 ml glacial acetic acid using a Supelco [™] , Discovery [®] C ₁₈ , 150 x 4.6 mm, 5µm column as stationary phase.	78
Figure 5.7:	Regression plots of PDX and TZD obtained from concentration (µg/ml) versus peak area (mAu).	85
Figure 5.8:	Chromatograms of the different media used in the specificity study	89
Figure 5.9:	Chromatogram obtained after TZD:PDX solution was stored for 24 hours at 60.0°C ± 2.0°C.	93
Figure 5.10:	Chromatogram obtained after sample was stored in direct sunlight for a period of 12 hours.	94
Table 5.1:	The molecular structures and related physicochemical properties of PDX and TZD.	69
Table 5.2:	Roadmap of the HPLC method development and optimisation for the simultaneous detection of TZD and PDX	79
Table 5.3:	Obtained analytical responses during the linearity testing for PDX and TZD	84
Table 5.4:	Summary of validation parameters and results obtained during the method development process.	88
Table 5.5:	Outline of the detected AUC values for PDX and TZD after deliberate adjustments in the detection wavelength obtained during the injection of a solution containing 100 µg/ml PDX and TZD, respectively	90
Table 5.6:	Stability data of PDX and TZD under different temperature conditions, exposure to light, pH changes and oxidation, over the course of three days.	92

Chapter 6

Physicochemical characterisation, solid-state form screening and compatibility testing of TZD in combination with PDX

6.1	Introduction	99
6.2	Physicochemical characterisation of TZD and PDX	100
6.2.1	Spectroscopic analyses of TZD and PDX	100
6.2.1.1	Fourier-transform infrared spectroscopy (FTIR)	101
6.2.1.2	Raman spectroscopy	104
6.2.2	X-ray powder diffraction (PXRD)	106
6.2.3	Thermal analyses of pure TZD and PDX	107
6.2.3.1	Hot-stage microscopy (HSM)	108
6.2.3.2	Thermogravimetric analysis (TGA)	109
6.2.3.3	Differential Scanning Calorimetry (DSC)	111
6.2.4	Equilibrium solubility of TZD and PDX in various solvents	113
6.3	Physicochemical characterisation of TZD and PDX in combination	114
6.4	Investigation of different solid-state form modification techniques to prepare TZD:PDX co-crystals or co-amorphous solid-state forms	122
6.4.1	Solvent evaporation	123
6.4.2	Quench cooling of the melt	123
6.4.3	Liquid assisted grinding (LAG)	124
6.5	Physicochemical characterisation of TZD:PDX combinations prepared by LAG	124
6.5.1	FTIR analysis of obtained TZD:PDX LAG samples	124
6.5.2	Raman spectroscopy of samples obtained during LAG	126
6.5.3	PXRD of samples manipulated <i>via</i> LAG	127
6.5.4	Thermal behaviour characterisation of TZD:PDX manipulated <i>via</i> LAG	136
6.5.4.1	Hot stage microscopy (HSM)	136
6.5.4.2	Thermogravimetric analysis (TGA)	139
6.5.4.3	Differential scanning calorimetry (DSC)	139
6.6	The investigation of the effect of LAG on TZD and PDX as single compounds using HSM and DSC analyses	142
6.7	Compatibility study of TZD and PDX in combination with another	146
6.8	Conclusion	152
6.9	References	154

Figures and Tables

Figure 6.1:	Fourier transform infrared (FTIR) spectra of TZD raw material versus a certified reference standard with the molecular structure of TZD provided as an inset. Molecular structure adapted from Scifinder (2019).	102
Figure 6.2:	Fourier transform infrared (FTIR) spectrum of PDX.	104
Figure 6.3:	An overlay of the Raman spectra for TZD raw material and TZD reference standard obtained at ambient temperature and collected across a range of 200-2000 with laser excitation of 1064 nm.	105
Figure 6.4:	Raman spectrum of PDX collected across a range of 100-2000 cm ⁻¹ at room temperature with a laser excitation of 1064 nm.	106
Figure 6.5:	X-ray powder diffraction patterns obtained for TZD and PDX across a 2θ range of 4-40°, collected at ambient conditions.	107
Figure 6.6:	Photomicrographs depicting the thermal behaviour of TZD observed during heating of the sample at a rate of 10 °C/min with silicon oil. The temperatures at which the micrographs were captured is indicated on each relevant micrograph.	108
Figure 6.7:	Micrographs depicting the thermal behaviour of PDX observed when heated at 10 °C/min with silicon oil. The temperatures at which the micrographs were captured is indicated on each relevant micrograph.	109
Figure 6.8:	Thermogravimetric analysis (TGA) results of TZD and its first derivative heated at 10 °C/min.	110
Figure 6.9:	TGA results of PDX obtained during a heating program of 10 °C/min. The thermogram also depicts the first derivative showing the major thermal event as a peak .	111
Figure 6.10:	Thermogram obtained using DSC analysis of TZD heated at a heating rate of 10 °C/min.	112
Figure 6.11:	DSC thermogram obtained with PDX during heating at 10 °C/min across a temperature range of 30 – 230 °C.	113
Figure 6.12:	Figure 6.12: Overlay of FTIR spectra obtained for TZD, PDX and the TZD:PDX physical mixture 1:1 (w/w).	115
Figure 6.13:	Raman spectra overlay of TZD, PDX and TZD:PDX physical mixture.	117
Figure 6.14:	PXRD diffractograms of TZD, PDX and TZD:PDX physical mixture 1:1 (w/w).	119
Figure 6.15:	Overlay of the DSC thermograms obtained for TZD, PDX and TZD:PDX physical mixture 1:1/ (w/w).	120
Figure 6.16:	Photomicrographs depicting the thermal behavior of PDX, TZD and TZD:PDX physical mixture 1:1/ (w/w).	121

Figure 6.17:	Overlay of the TGA thermograms obtained for TGA, PDX and TZD:PDX physical mixture 1:1/ (w/w).	122
Figure 6.18:	FTIR spectrum of binary mixtures 1:1 (w/w) of TZD and PDX prepared by LAG in different solvents.	125
Figure 6.19:	Overlay of Raman spectra obtained with (a) PDX, (b) TZD, (c) LAG with acetone, (d) LAG with ACN, (e) LAG with butanol, (f) LAG with ethanol, (g) LAG with methanol, (h) LAG with propanol, (i) TZD:PDX 1:1 w/w mixture and (j) LAG with DMSO.	127
Figure 6.20:	Overlay of the PXRD diffractogram obtained for the sample subjected to LAG using acetone as grinding fluid in comparison with the physical mixture.	129
Figure 6.21:	Overlay of the PXRD diffractogram obtained for the sample subjected to LAG using ACN as grinding fluid in comparison with the physical mixture.	130
Figure 6.22:	Overlay of the PXRD diffractogram obtained for the sample subjected to LAG using butanol as grinding fluid in comparison with the physical mixture.	131
Figure 6.23:	Overlay of the PXRD diffractogram obtained for the sample subjected to LAG using ethanol as grinding fluid in comparison with the physical mixture.	132
Figure 6.24:	Overlay of the PXRD diffractogram obtained for the sample subjected to LAG using methanol as grinding fluid in comparison with the physical mixture.	133
Figure 6.25:	Overlay of the PXRD diffractogram obtained for the sample subjected to LAG using propanol as grinding fluid in comparison with the physical mixture.	134
Figure 6.26:	Overlay of the PXRD diffractogram obtained for the sample subjected to LAG using DMSO as grinding fluid in comparison with the physical mixture.	135
Figure 6.27:	HSM data of binary mixtures of TZD and PDX prepared by LAG (1:1(w/w) indicating the initial, the onset, the peak and the end of the main thermal events (left-to-right) in the following solvents: A: acetone, B: acetonitrile, C: Butanol, D: DMSO E: Ethanol, F: Methanol, and G: Propanol.	138
Figure 6.28:	DSC thermograms obtained with all samples prepared via LAG in comparison with pure TZD, pure PDX and the TZD:PDX (1:1 w/w) mixture.	141
Figure 6.29:	DSC thermograms obtained with TZD subjected to LAG using acetone, ACN, ethanol, DMSO and no solvent (dry grinding).	142
Figure 6.30:	HSM micrographs depicting the thermal behaviour (°C) of TZD samples prepared by LAG with (A) grinded TZD - without solvent, (B) acetone, (c) ethanol, (D) ACN, (E) DMSO heated at 10 °C/min under silicone oil.	143
Figure 6.31:	Overlay of DSC thermograms of PDX prepared by LAG using acetone, ACN, ethanol and DMSO as grinding fluids and dry grinding as a control sample.	144

Figure 6.32:	HSM micrographs depicting thermal events displayed in (°C) for PDX samples prepared by LAG with (E) grinded PDX alone, (F) acetone (G) ACN, (H) ethanol and (I) DMSO heated at 10 °C per min under silicon oil.	145
Figure 6.33:	Overlay of the obtained FTIR spectra obtained for PDX during isothermal storage at 60 ± 0.5 °C and analysed on a weekly basis for a period of 28 days.	149
Figure 6.34:	Overlay of the obtained FTIR spectra obtained for TZD during isothermal storage at 60 ± 0.5 °C and analysed on a weekly basis for a period of 28 days.	150
Figure 6.35:	Overlay of the obtained FTIR spectra obtained for the TZD:PDX (1:1 w/w) mixture during isothermal storage at 60 ± 0.5 °C and analysed on a weekly basis for a period of 28 days.	151
Table 6.1:	Theoretical and experimental wavenumbers associated with TZD with their corresponding functional bonds (Smith, 2018).	103
Table 6.2:	Theoretical and experimental wavenumber found in PDX chemical structure with their corresponding functional bonds (Smith, 2018; Larkin, 2017).	104
Table 6.3:	Equilibrium solubility obtained for TZD and PDX in various solvent systems at 25 °C	114
Table 6.4 :	Investigation of appearance and disappearance of wavenumbers of spectra of TZD, PDX and TZD:PDX (1:1 w/w)	116
Table 6.5:	X-ray diffraction peaks obtained for TZD, PDX and TZD:PDX physical mixture 1:1 (w/w).	118
Table 6.6:	Theoretical and experimental FTIR wavenumbers of TZD and PDX LAG mixtures with their respective functional bonds (Smith, 2018; Larkin, 2017) .	126
Table 6.7:	Visually observed onset of degradation of samples prepared using LAG in comparison with the TZD:PDX (1:1 w/w) physical mixture.	137
Table 6.8:	TGA onset of degradation and percentage weight loss (%) of samples prepared using LAG in comparison with the TZD:PDX (1:1 w/w) physical mixture.	139
Table 6.9:	Onset of degradation and percentage weight loss (%) of samples prepared using LAG in comparison with the TZD:PDX (1:1 w/w) physical mixture	146
Table 6.10:	TGA compatibility data of pure PDX, pure TZD and TZD:PDX (1:1 w/w) combination stored at 60 °C and analysed on a weekly basis for a period of 28 days	148
Table 6.11:	Determined drug purity for TZD, PDX and both compounds in the TZD:PDX (1:1 w/w) mixture during isothermal exposure of the samples to 60 ± 0.5 °C.	152

Chapter 7

Concluding remarks , limitations, and recommendations

	Concluding remarks	156
7.1	References	159
	Appendix	
	Article submitted for peer review to Analytica journal	161



Chapter 1

Introduction

1.1 A brief introduction to tuberculosis

The history of tuberculosis (TB) dates back to as early as 5000 BC when it was found in mummies. In 1882, a German scientist, Robert Koch, discovered the causative organism namely, *Mycobacterium tuberculosis* (*Mtb*) (Viñuelas-Bayón, Vitoria and Samper, 2017). TB is a communicable infectious disease that produces silent, latent infection and active disease (Anon, 2015). Although TB is an old disease, it is still currently ranked globally among the top ten causes of death, and it is still the leading cause of death globally from a single infection (WHO, 2018). It is estimated that 1.3 billion people present with latent TB infection of which 10% are at risk of developing the active disease in their lifetime. The World Health Organisation (WHO) estimates that on a global level there is an annual incidence of 10.4 million new infections with a third of these new cases being unknown to the healthcare system. This being followed by an annual mortality rate of 1.4 million patients (WHO, 2018). The ultimate goal remains to eradicate TB since it is a treatable disease. Hence, there is a constant need for the discovery of new active pharmaceutical ingredients (APIs) but further to this the strategy to enhance older and already marketed APIs with the specific goal of improving patient adherence (Campaniço, Moreira and Lopes, 2018) also plays a substantial role in the fight against TB.

A significant amount of research is being dedicated to the effective treatment and possible eradication of TB. From literature sources, which will be discussed in greater detail in the following chapters, it will be highlighted that TB is a highly infective disease coupled with the ability of the organism to develop resistance to treatment. This, in combination with many other factors lead to a significant number of challenges in providing effective treatment options to patients. In terms of pharmaceutical sciences, dosage form pre-formulation and formulation, it remains the common goal to improve the bioavailability of some of the currently marketed anti-tuberculosis drugs. This, coupled with the effort to improve the physical and chemical stability of the drugs currently used to treat TB, as well as the goal to reduce the pill-burden

experienced by TB-infected patients allows for a vast number of research opportunities still unexplored. This global effort is highlighted when considering the funding target of approximately US\$13 billion per year from 2022 onwards which is focused on the prevention, treatment, and effective diagnosis, especially in middle-income countries that account for 97% of reported TB cases (WHO, 2020).

TB requires a combination of anti-tuberculosis drugs to be treated successfully. The WHO has set out a general guideline for treating TB, but each country provides its own guidelines depending on factors such as the economic standing of the country, TB causative strains and the healthcare system that facilitates the implementation of drug treatment regimens. Generally, after a positive diagnosis has been made, rifampicin, isoniazid, pyrazinamide, and ethambutol are the four drugs used in an intensive treatment phase of two months followed by a continuation phase of four months with only rifampicin and isoniazid (NDOH, 2019). This treatment strategy forms the current first-line treatment regimen followed by numerous countries stricken by TB infections.

Several *mycobacterium* strains have developed resistance to the current first-line treatment and different types of drug resistant TB exist. These different categories of resistance are outlined in Table 1.1 and are mainly classified based on the type of anti-TB drugs that the infecting organism shows resistance to.

Table 1.1: TB drug resistant types as adapted from Cox. et al, (2017)

TB drug resistant types	Drug resistant to
<i>Multi-Drug resistant TB (MDR-TB)</i>	Isoniazid and rifampicin
<i>Rifampicin-resistant TB (RR-TB)</i>	Rifampicin (regardless of resistance to other drugs)
<i>Extensively drug-resistant TB (XDR-TB)</i>	Isoniazid, rifampicin, moxifloxacin or levofloxacin and amikacin or kanamycin

In South Africa, the TB incidence is reported to have decreased within the period of 2010 - 2017 and it is largely attributed to the sustainable treatment of co-infections. The most prominent co-infection presenting in TB-infected patients is the human immunodeficiency

virus (HIV) and subsequent to that the acquired immunodeficiency syndrome (AIDS). This co-infection has a devastatingly negative impact on TB patients. Despite various interventions, on a global level, South Africa is still among the countries with the highest number of MDR-TB cases (WHO, 2018). From a thorough literature study that will be disseminated in subsequent chapters it became apparent that drug resistance is the greatest stumbling block in the current anti-TB drug regimen and all evidence points towards the need to enhance treatment. Realistically, considering the current rate at which new and highly potent drugs are being discovered, it might take 20 - 30 years to formulate another highly effective treatment regimen. The recent FDA approval of the new anti-TB drugs, bedaquiline and delamanid, is a very recent success story in the anti-TB drug discovery pipeline, but this is only after many drug synthesis attempts and hours of costly research and development. Bedaquiline and delamanid are currently used under certain conditions for MDR-TB in combination with other repurposed drugs, and they are expected to improve the MDR-TB cure rate with the additional advantage of better safety (Tiberi *et al.*, 2018; NDOH, 2020).

1.2 A pharmaceutical perspective towards the eradication of TB

Generally, it takes 15 - 20 years to discover a new pharmaceutically active compound, with every step in the drug discovery process being important in providing the foundation for the next step. This is a costly process associated with many failures along the way. Considering this it makes sense that pharmaceutical scientists investigate possibilities allowing the improvement of the physicochemical properties of existing drugs which currently detrimentally affects the performance thereof after administration to the patient.

Most drug molecules exist in the solid-state. Solid-state chemistry of drugs is a subject area which studies the physicochemical properties associated with any given drug as well as strategies involving the molecular modification of a drug under investigation, whilst coupling it to pre-formulation studies. Such strategies ultimately aim to improve drug bioavailability, stability, manufacturability and potentially patient adherence (Wen *et al.*, 2015). These molecular modification strategies will be discussed in greater detail in subsequent chapters. Further to the already mentioned molecular modification strategies multiple advanced dosage formulations may also be explored in an effort to resolve the issues related to poor drug solubility, low membrane permeability and treatment adherence issues which is directly linked

to the high pill-burden patients need to endure. It is with these strategies and the issue of poor patient adherence due to a high pill-burden that focus was placed on the anti-TB drug, terizidone (TZD) and the well-known compound pyridoxine (PDX), also known to the general public as vitamin B₆. These two molecules are currently co-administered as two separate dosage forms in the treatment of TB and the question arose whether it would be possible to combine these two compounds in a molecular modification such as a co-crystal or a solid dispersion.

1.3 A brief overview of TZD and PDX linked to the study rationale

TZD is a World Health Organisation (WHO) categorised group IV anti-tuberculosis drug. It is effective against both *Mycobacterium tuberculosis* and *Mycobacterium avium*. Currently, it is used as a second-line treatment option in multi-drug resistant TB (MDR-TB) and extensively drug-resistant TB (XDR-TB) for non-psychotic patients. However, it is known to cause polyneuropathic side effects. These side effects include slurred speech, convulsions, tremors, insomnia, confusion, depression and the most dangerous being suicidal tendency (Vora, 2010). TZD inhibits PDX activity and therefore increases the potential for nervous system toxicities. Furthermore, increasing the risk of isoniazid associated symptomatic symmetrical peripheral neuropathy (Conradie *et al.*, 2013). It is also reported that cycloserine, an analogue of TZD, competes with γ -aminobutyric acid in the brain which causes central nervous system (CNS) side effects (Dooley *et al.*, 2012). It is recommended that patients considered to be at risk for developing polyneuropathy, such as those with alcohol dependency, malnutrition, diabetes, and HIV infection, receive PDX supplementation daily (van der Watt *et al.*, 2011). This results in increasing the dosage burden even more on patients already taking a significant number of tablets or capsules per day, which in turn leads to poor compliance of the patients due to the effects caused by adverse drug reactions. Furthermore, it causes a bigger problem in the effective treatment of TB by further increasing resistance which could result in mortality or the development of extensively drug-resistant TB. This creates a vicious cycle which is a threat to humanity and a burden to governments where more and more resources must be spent treating TB.

From a pharmaceutical pre-formulation and formulation perspective, TZD was found to be a poorly studied compound with very little information available for this molecule in the public

domain. On the other hand, PDX is a well-known molecule with significant information available in terms of physicochemical properties and even some molecular modifications such as co-crystals and solid dispersions (Thakuria and Sarma, 2018). Considering the mentioned challenges and drawbacks associated with the treatment of MDR-TB and XDR-TB patients the following research question that was investigated throughout this study was asked: *“Is it possible to combine the two compounds, TZD and PDX, on a molecular level which could potentially result in a single solid-state form that will allow easy formulation of a fixed-dose combination (FDC) consisting of the two drugs?”*

1.4 Study design and objectives

Due to the identified gap in the knowledge base in terms of the physicochemical properties of TZD this study focussed first and foremost on the investigation and reporting of the complete physicochemical profile of TZD. In order to complete a thorough physicochemical study of any drug a suitable analytical method allowing the quantification of drug concentration is imperative. Based on this as well as the intended objective to combine TZD and PDX on a molecular level the need arose for a sensitive high-performance liquid chromatography (HPLC) method. Such a method could not be sourced from literature and therefore a suitable method was developed and validated during this study. This was followed by an investigation into the possibility to prepare either co-crystal(s) or solid dispersion(s) containing TZD and PDX, which could provide a single molecular entity that would allow the co-administration of TZD and PDX in a single dosage form. Further to this it is imperative to assess and report on the compatibility for any drug-drug or drug-excipient combination, aspects which were also investigated during this study.

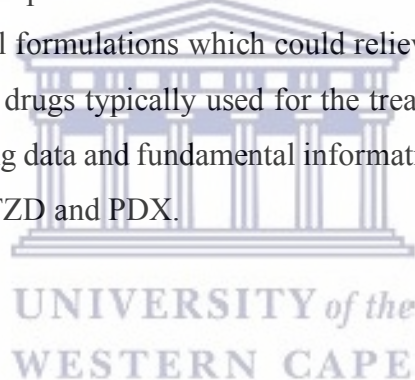
1.5 Outline of thesis chapters

This thesis consists of several chapters with the subsequent Chapter 2 providing a more in-depth overview of TB, highlighting the associated treatment challenges and how these challenges impact the development of bacterial resistance. Chapter 3 provides an in-depth discussion on solid-state chemistry and how this science links with the science of pharmaceutical pre-formulation and dosage form formulation. Following on this, Chapter 4 provides a thorough description of all relevant analytical methods used throughout this study.

Chapters 5 and 6 are disseminating the experimental results, hypotheses and conclusions drawn from this study and finally Chapter 7 provides insight into the knowledge gained during this study linked to future prospects and studies to be pursued.

1.6 Conclusion

This chapter provided the focus and outline of this study through a very brief overview of the debilitating disease, TB and how the aspect of the development of microbial resistance leads to severe challenges in terms of successful patient treatment. The avoidance of resistance development depends greatly on proper patient treatment and the adherence to treatment regimens; thus one could say that clinicians play a key role in the fight against this disease. However, proper patient care has its limits and clinicians, patients and caregivers must rely on pharmaceutical scientists to improve current marketed formulations or to develop and formulate novel pharmaceutical formulations which could relieve the pill-burden experienced by patients. Focussing on two drugs typically used for the treatment of MDR-TB and XDR-TB this study aimed at collecting data and fundamental information which would inform future FDC formulations containing TZD and PDX.



1.7 References

Anon. 2015. Tuberculosis. In: Wells, B.G., Dипiro, J.T., Schwinghammer, T.L., Dипiro, C.V. Ed(s). *Pharmacotherapy handbook*. 9th ed. New York: McGraw-Hill, 476-489.

Campaniço, A., Moreira, R. and Lopes, F. 2018. Drug discovery in tuberculosis. New drug targets and antimycobacterial agents. *European Journal of Medicinal Chemistry*, 150: 525-545. <https://doi.org/10.1016/j.ejmech.2018.03.020>.

Conradie, F., Mabiletsa, T., Sefoka, M., Mabaso, S., Louw, R., Evans, D., van Rie, A. 2014. Prevalence and incidence of symmetrical symptomatic peripheral neuropathy in patients with multidrug-resistant TB. *South African Medical Journal*, 104(1):24-26. Doi: <https://hdl.handle.net/10520/EJC146778>.

Cox, H., Dickson-Hall, L., Jassati, W., Moshabela, M., Kielmann, K., Grant, A., Nicoli, M., Black, J., Mlisana, K., Vanleeuwix, L., Loveday, M. 2017. Drug-resistant tuberculosis in South Africa: history, progress and opportunities for achieving universal access to diagnosis and effective treatment. In: Padarath, A., Barron, P. Ed(s). *South African Health Review 2017*. 20th ed. Durban: Health Systems Trust, 157–168.

Dooley, K., Mitnick, C., Ann DeGroot, M., Obuku, E., Belitsky, V., Hamilton, C., Makhene, M., Shah, S., Brust, J., Durakovic, N. and Nuermberger, E. 2012. Old Drugs, New Purpose: Retooling Existing Drugs for Optimized Treatment of Resistant Tuberculosis. *Clinical Infectious Diseases*, 55(4):572-581. Doi: <https://doi.org/10.1093/cid/cis487>.

NDOH see National Department of Health.

National Department of Health (NDOH). 2019. *Standard Treatment Guidelines and Essential Medicines List: Hospital level (Adults)*. [online] Available at: <https://www.knowledgehub.org.za/elibrary/hospital-level-adults-standard-treatment-guidelines-and-essential-medicines-list-2nd> [Accessed 8 November 2021].

Takhuria, R. and Sarma, B. 2018. Drug-Drug and Drug-Nutraceutical Cocrystal/Salt as alternative medicine for combination therapy: A crystal engineering approach. *Crystals*, 8(2), 101:1-39. <https://doi.org/10.3390/cryst8020101>.

Tiberi, S., Muñoz-Torrico, M., Duarte, R., Dalcolmo, M., D'Ambrosio, L. and Migliori, G.B. 2018. New drugs and perspectives for new anti-tuberculosis regimens. *Pulmonology*, 24(2):86-98. Doi: <https://doi.org/10.1016/j.rppnen.2017.10.009>.

Van der Watt, J., Harrison, T., Benatar, M. and Heckmann, J. 2011. Polyneuropathy, anti-tuberculosis treatment and the role of pyridoxine HCl in the HIV/AIDS era: a systematic review [Review article]. *The International Journal of Tuberculosis and Lung Disease*, 15(6): 722-728. Doi: <https://doi.org/10.5588/ijtld.10.0284>.

Viñuelas-Bayón, J., Vitoria, M. and Samper, S. 2017. Rapid diagnosis of tuberculosis. Detection of drug resistance mechanisms. *Enfermedades infecciosas y microbiología clinica (English ed.)*, 35(8): 518-526. Doi: <https://doi.org/10.1016/j.eimce.2017.08.009>.

Vora, A. 2010. Terizidone. *Journal of Association Physician of India*. Volume 58.

Wen, H., Jung, H. and Li, X. 2015. Drug Delivery Approaches in Addressing Clinical Pharmacology-Related Issues: Opportunities and Challenges. *The AAPS Journal*, 17(6):1327-1340. Doi: 10.1208/s12248-015-9814-9.

WHO see World Health Organisation.

World Health Organization. 2018. *Global tuberculosis report 2018*. Geneva. [online]. Available at: <<https://apps.who.int/iris/handle/10665/274453>> [Accessed 15 August 2019].

World Health Organization. 2020. *Global tuberculosis report 2020*. Geneva. [online]. Available at: <<https://www.who.int/publications/i/item/9789240013131>> [Accessed 10 November 2020].



Chapter 2

An overview of tuberculosis (TB) and associated drug treatment

2.1 Introduction

Mycobacterium tuberculosis (*Mtb*) is an infectious disease that has been affecting humankind for a very long time and the human body is a perfect environment for its replication. The bacteria can hide as they become hydrophobic and escape the body's innate immune system (Cambier, Falkow and Ramakrishnan, 2014). It affects a very large number of populations, and it is disastrous to vulnerable individuals with comorbidities. *Mtb* is a treatable disease but, it requires timely diagnosis, correct intervention, and good adherence to achieve successful treatment. According to the WHO 2020 global TB report, *Mtb* is still synonymous to high infection and mortality rates, as it shows a total of 10 million people who got infected with *Mtb*, particularly affecting southeast Asia (44%), Africa (25%) and the western Pacific countries (18%), as mapped out in Figure 2.1 (WHO, 2020). This WHO report furthermore highlights the emergence of newly diagnosed MDR-TB incidences, which complicates the matter and calls for serious actions. The intervention is still needed, as the global TB report of 2021 recorded 132,222 cases of MDR/RR-TB and 25,681 cases of XDR-TB of people diagnosed with bacteriologically confirmed pulmonary TB in 2020.



Figure 2.1: TB incidence estimation in 2019, for countries with at least 100 000 incident cases, adapted from WHO (WHO, 2020).

2.2 Risk factors

Mtb. easily infects immunocompromised individuals who includes HIV positive patients and corticosteroids or immunosuppressive drug users (ATS, 2000). HIV positive patients are 100 times more likely of being infected with *Mtb.* compared to HIV-seronegative patients. Other significant risk factors include patients suffering from diabetes and individuals consuming high volumes of alcohol. There are also social factors that ties to health assurance such as malnutrition and living in a crowded environment and in close contact with TB patients (WHO, 2019). *Mtb.* is also associated with other human diseases such as lung cancer, systemic lupus erythematosus (SLE) and obesity (Chai, Zhang and Liu, 2018).

2.3 Transmission

TB is caused by the infection of an individual by any of the mycobacteria grouped in the *Mycobacterium tuberculosis* Complex (MTBC). These mycobacteria are intracellular pathogens of humans and animals. In the past, *M. bovis* infected people through milk before the process of milk pasteurisation was discovered and implemented. *M. bovis* is the most common strain of zoonotic TB and in 2019, 140,000 humans were infected with it (WHO, 2020). *M. caprae* is known to cause TB infection through livestock, *M. pinnipedii* can infect people through sea lions and *M. microti* through pet animals. There are also typical human

associated species of MTBC such as, *M. africanum*, and *M. canettii*, with *Mtb* being the most prevalent strain of the MTBC in humans and it still affects a large population today (Jagielski *et al.*, 2016). TB is transmitted from one person to another through airborne droplets. It spreads by inhaling the *Mtb* containing droplet nuclei (1 to 5 μm in size). The droplets are produced through the action of coughing, talking, sneezing, or singing by a person with pulmonary or laryngeal tuberculosis (Patterson and Wood, 2019). They can also be inhaled from sputum induction, aerosol treatments and through processing or manipulating secretions in the laboratory (ATS, 2000). The transmission depends on bacilli load and virulence, the level of ventilation of a room, UV light exposure of bacilli and the immune status of the individual inhaling the droplets. Therefore, effective TB screening, proper room designing, and wearing safety gear and treatment of active diseases can halt its transmission (Nardell, 2016). In low incidence countries, transmission can be halted by tracing individuals who have been in close contact with TB patients. Meanwhile, high incidence countries, also being mostly low and middle-income countries, find themselves being overloaded by active cases having insufficient resources to do a thorough investigation and tracing close-contact individuals (Morrison, Pai and Hopewell, 2008).

2.4 Pathogenesis of *Mycobacterium tuberculosis*

As described, *Mtb* is an airborne infection. As depicted in Figure 2.2, the inhaled droplets containing *Mtb* settle in the respiratory alveoli or bronchioles *via* the bronchial tree. The bacterial virulence and the microbicidal ability of the host macrophages are a determining factor for the likelihood of the inhaled tubercle bacilli to cause infection. *Mtb* does not trigger an immediate host response since it does not contain endo- or exotoxins. It is the failure of the alveolar macrophage defence that allows the slow growth of tubercle bacilli which divide every 25 - 32 hours within the macrophage (ATS, 2000). The infected macrophages release cytokines and chemokines which attracts other phagocytic cells forming a nodular granulomatous called a tubercle. If the tubercle is not controlled, it invades the draining lymph nodes and develops into lymphadenopathy, which cause lesions in the lungs called the Ghon complex (Wani, 2013). After 2 - 12 weeks, the higher number of tubercle bacilli (10^3 to 10^4) can initiate an immune response, which can be detected by the tuberculin skin test. Tubercle bacilli can reach other parts of the body through the blood stream *via* the lymphatic system to the hilar lymph nodes. This is then termed extra-pulmonary TB.

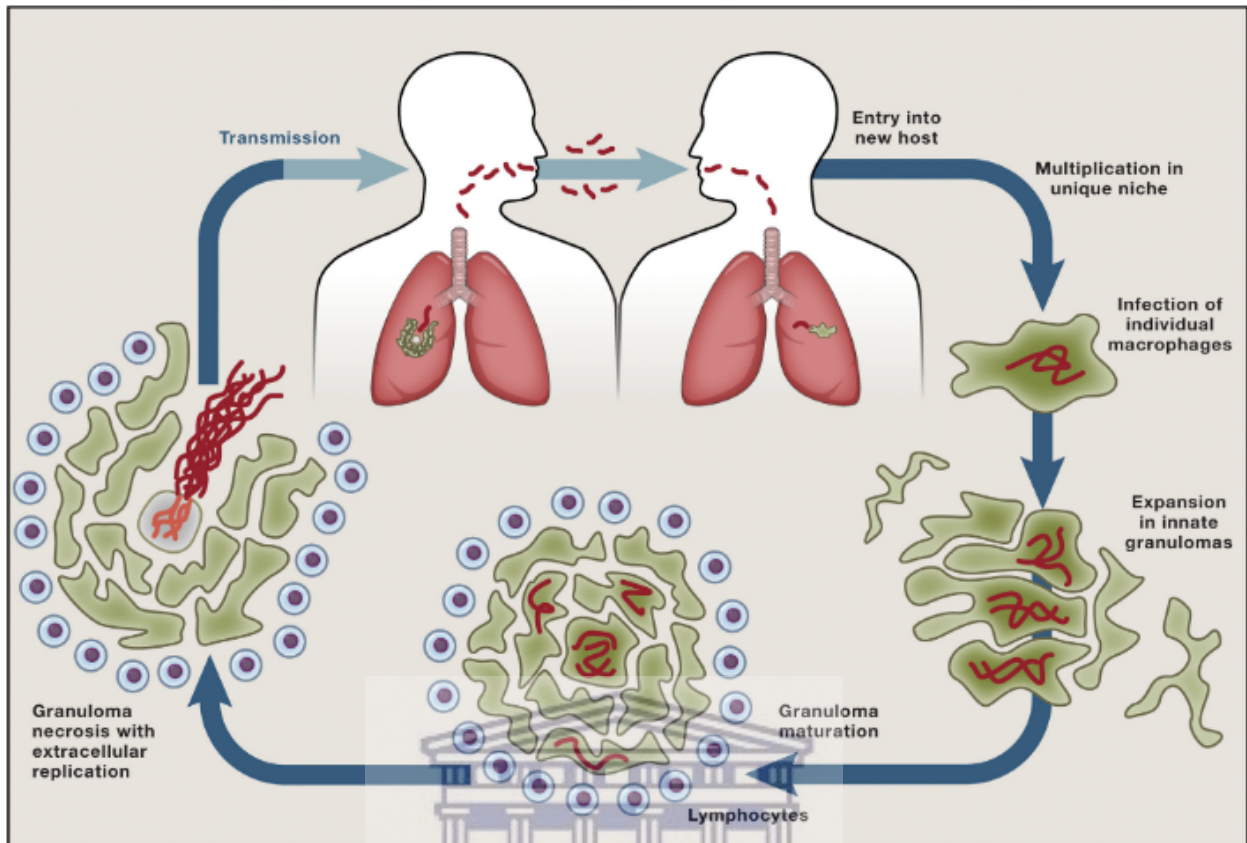


Figure 2.2: The pathogenesis cycle of *Mtb*, as adapted from Cambier, Falkow and Ramakrishnan (2014).

Individuals with strong cell-mediated immunity form granulomas through T-cells and macrophages, which limits the growth and spread of the organism, further causing the development of latent tuberculosis infection. Approximately, 10% of patients with latent tuberculosis may develop active disease. The risk for latent tuberculosis to progress towards active TB is very high in the first two years after infection and more so in individuals with higher risk factors such as diabetes mellitus and diseases associated with the suppression of the immune system such as human immunodeficiency virus (HIV) infection. Often the development of active TB from latent TB is triggered by re-exposure of the patient to the causative organism (ATS, 2000).

2.5 Detection and diagnosis

The early detection of the disease and obtaining rapid susceptibility results is important in controlling the disease. People at higher risk of being infected by TB can be discovered and be subjected to screening and if necessary, go through confirmatory tests (van't Hoog, Onozaki

and Lonnroth, 2014). Once patients have been diagnosed, adequate prescribing of anti-TB medication, progress monitoring, adherence, and response to the treatment by the patients for a successful TB treatment should be implemented (Viñuelas-Bayón, Vitoria and Samper, 2017).

According to the Center for Disease Control and Prevention (CDC), two tests are typically used to detect *Mtb* in the human body and include the TB skin test and TB blood tests. A positive outcome of any of these two tests informs that a patient has been infected with TB, but other tests are necessary to inform whether a person has active TB disease (CDC, 2021). To accurately diagnose active TB the use of a culture method has proven to be the most sensitive method, though it takes 3 - 5 weeks to produce results and it requires the use of a high-level biosafety laboratory and highly skilled technicians (Gómez, Gonzalez-Martin, and Garcia-Basteiro, 2017). The presence of acid-fast bacilli colonies indicates the presence of *Mtb.*, while the absence of colonies indicates no active disease. This method delays the onset of the treatment, the interruption of the transmission chain and makes disease control harder due to the time needed to produce accurate test results (Malacarne *et al.*, 2019). Bacilloscopy is the most accessible method utilising the Ziehl-Neelsen stain to diagnose smear positive cases, which is cheap, fast and provides 25 - 90% susceptibility compared to the culture method. Moreover, it depends on the studied sample and the bacterial load (Viñuelas-Bayón, Vitoria and Samper, 2017).

The WHO recommends the use of the GeneXpert[®] system, an automated system which simultaneously detects *Mtb* and rifampicin resistant *Mtb*. This is particularly useful in countries presenting with a significant incidence of MDR-TB. It provides results within two hours of testing, but it does not distinguish between different MTBC strains (WHO, 2011; Gómez, Gonzalez-Martin and Garcia-Basteiro, 2017). The use thereof has been implemented since 2010 and has contributed significantly to the early diagnosing of drug-resistant tuberculosis. The goal is to provide results at the point-of-care, resulting in rapid therapy initiation. Another test of Interferon-gamma Release Assay (IGRA) is used as a replacement for the tuberculin skin test to detect or exclude latent TB infection, and it is used to complement the diagnosis of active TB (Meier and Enders, 2020). IGRA is an *ex vivo* blood test that detects interferon- γ (INF- γ) released when the antigens found in MTBC stimulate the T-cells. IGRA is specific and largely reduces the number of false-positive results in children vaccinated by BCG (Starke, 2014).

2.6 Clinical symptoms associated with TB

TB symptoms are presented by an individual exposed to any *Mycobacterium tuberculosis* Complex (MTBC) specie. Symptoms vary depending on the part of the body affected and the health profile of the infected individual. Cough is the most common symptom for pulmonary TB patients and is also the primary mode of transmission for the causative organism. A prolonged cough exceeding two weeks, fever, night sweats, unexplained weight loss and haemoptysis are the most common TB symptoms (Morrison, Pai and Hopewell, 2008; NDOH, 2019). These symptoms in addition to laboratory tests and chest radiography are used as confirmatory test for TB infection (Anon, 2015).

2.7 Multi-drug resistant tuberculosis (MDR-TB)

Mtb presents with two types of drug resistance, namely, genetic and phenotypic. The genetic resistance occurs in a growing bacterium due to mutations in the chromosomal genes, while phenotypic resistance, also termed drug tolerance occurs in non-growing bacteria caused by epigenetic changes in gene expression and protein modification (Zhang and Yew, 2015; Allué-Guardia, Garcia and Torrelles, 2021). These *Mtb* drug resistances are manifested through different mechanisms such as epistasis, compensatory evolution, clonal interference, efflux pumps, cell envelope impermeability and drug degradation and modification. These mechanisms slow the TB treatments, increase the potential risk of post-treatment relapse, and pose a challenge for global public health and therapeutics. It is a well-known fact that drug resistance can also originate from poor prescribing practices or lack of adherence, and it thus justifies the interventions of multiple drugs in MDR-TB treatment (Singh *et al.*, 2020).

MDR-TB medications are taken for a longer period to achieve a better outcome without relapse, but also presenting their challenges such as increased side effects to patients or the development of lack of adherence to the intensive treatment regimens by patients (Sloan and Lewis, 2016). The HIV comorbidity with *Mtb*. increases the chances of contracting MDR-TB due to the reduction of anti-TB medication efficacy. Antiretroviral (ARV) medication in combination with second line anti-TB medication has overlapping toxicity, which makes it hard to manage MDR-TB in HIV patients (Bhunja *et al.*, 2015). The remedy is to shorten the regimen period with fewer drugs. New anti-TB medications are emerging and slowly being integrated into national and international treatment guidelines. Among these are, bedaquiline, linezolid and

delamanid showing potential to treat MDR-TB and XDR-TB in a short period, with fewer side effects and improved patient adherence (Sloan and Lewis, 2016). TB, in addition to other drug resistant infections has resulted in antimicrobial stewardship programs, which is aimed at the rational use of already available medication for best treatment outcomes (Miller-Petrie, Pant and Laxminaraya, 2017).

2.8 Treatment

2.8.1 Latent tuberculosis

Treatment of latent TB infection (LTBI) is vital to the eradication of TB even though it is currently reserved only for higher risk populations. These are people living with HIV and children aged under five living with a household bacteriologically confirmed to have TB (WHO, 2018a). Bacille Calmette-Guérin (BCG) is a recommended vaccine for infants in countries with a high incidence of tuberculosis and/or leprosy. It is only effective up to ten years after administration, but it can provide residual vaccine effectiveness up to 20 - 25 years post administration (Cernuschi *et al.*, 2018), hence there is a need for a vaccine for adults and more research are underway for a latent TB vaccine. The recommended therapy for latent TB is a daily dose of isoniazid for 36 months for people with HIV and six months or three to four months with a combination with rifampicin or rifapentine for children and adults less than 15 years old in countries with high *Mtb.* incidence (WHO, 2018a).

2.9 Active TB and MDR-TB

In 1943, the first TB drug, streptomycin was discovered, followed by isoniazid and rifampicin in 1952 and 1959, respectively (Viñuelas-Bayón, Vitoria and Samper, 2017). *Mtb* treatment requires a combination of drugs and adequate time to be treated successfully. As already emphasised, TB is one of the most significant disease burdens in South Africa. The South African TB treatment guideline recommends a regimen of four drugs, which are rifampicin, isoniazid, ethambutol, and pyrazinamide for an intensive phase of two months and rifampicin and isoniazid for a continuation phase of four months (NDOH, 2019).

MDR-TB treatment requires the administration of second-line drugs which are more costly and associated with more side effects than first-line drugs (Table 2.1). MDR-TB treatment is

associated with an intensive treatment phase consisting of bedaquiline, linezolid, levofloxacin, clofazimine and TZD taken for six months, followed by a continuation treatment phase of 12 months using the same regimen but without bedaquiline and linezolid. This regimen may be subject to change depending on the patient's history in terms of treatment with first-line TB-drugs and the susceptibility test towards this treatment regimen (NDOH, 2020). In 2018, there were half a million global incidences of rifampicin-resistant TB (RR-TB) of which 78% cases had MDR-TB and were dominated by Asian countries namely, Russia, China and India (WHO, 2019). Extensive drug resistant TB (XDR-TB) refers to MDR-TB strains showing resistance to one of the fluoroquinolones and one of the first-line injectable drugs. A high mortality rate is associated with XDR-TB it and it is difficult to treat. In 2017, the WHO reported TB treatment success rates of 85% for active TB disease, 56% for MDR/RR-TB, 75% for HIV co-infected patients and only 39% for XDR-TB patients (WHO, 2019). There are still challenges such as obtaining missing data with regards to treatment outcomes in some countries, the prevention of dropouts and the attainment of uninterrupted regimen compliance. TB patients have been known to be non-adherent and direct observed therapy has been implemented in some instances and provided positive results (Balasubramanian, Oommen and Samuel, 2000). Treatment duration and the side effects plays a major role in the outcomes. TZD and isoniazid are known to cause neurotoxicity.

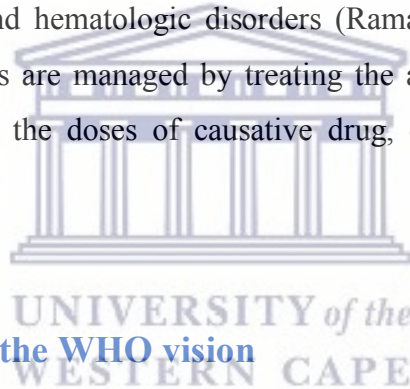
Table 2.1: MDR-TB regimen standard in South Africa for adults (NDOH, 2020)

Medications	Dosage (daily)	Duration (Months)
Bedaquiline	400 mg *	6
Linezolid	600mg	6
Levofloxacin	1000mg	18
Clofazimine	100mg	18
Terizidone	750 mg	18

*400 mg daily for first two weeks, followed by 200mg three times a week.

2.10 Adverse drug reactions of anti-TB medications

The determination of side effects due to a single anti-TB drug is not easy since there are aspects such as co-morbidity and multiple drugs administered at once that plays a role. Many side effects are determined during a short course period and during direct observed therapy of single drugs and not necessarily administration of FDCs (Singh *et al.*, 2015). Patients taking anti-TB medication are very likely to develop adverse drug reactions. It is recommended to perform baseline testing before administering the drugs and monitoring during treatment is imperative. Ototoxicity, nephrotoxicity, and electrolyte imbalances are the main side effects caused by the aminoglycosides. Fluoroquinolone are known to cause tendon rupture, neurotoxicity, photosensitivity, and QT prolongation. Isoniazid, cycloserine, TZD and linezolid are known to cause adverse drug reaction associated with central nervous system disturbances. Among other side effects known to be caused by anti-TB regimen are hypersensitivity, visual disturbances, hepatotoxicity and hematologic disorders (Ramanathan, Howell and Sanders, 2019). Adverse drug reactions are managed by treating the adverse drug reaction with an additive medication, adjusting the doses of causative drug, or being replaced by a more tolerable drug.



2.11 Eradication of TB – the WHO vision

The WHO vision, as set out in their “end TB strategy” which was initiated in 2014 is aimed at reducing TB deaths by 95% and TB incidence rates by 90% by the year 2035. This will be accomplished by evaluating achieved progress in 2020 and 2025. The target is a decline of 5% per year between 2015 and 2020 and 10% per year between 2020 and 2025. This will be achieved through an integrated and patient-centred care approach, strong policies and supportive systems, intensified research and innovation. Universal health coverage and social protection is also important to prevent financial loss experienced by *Mtb.* patients and their households. Unfortunately, the 2020 milestone was not achieved globally, except in some European countries. The cumulative decline observed during 2015 – 2020 was 6.3 % instead of 10 - 15 %. Ultimately, the goal is to shorten the duration of TB treatment and reduce the current pill-burden experienced by patients in an effort to effectively eradicate TB on a global level (WHO, 2019).

2.12 PDX and TZD as part of the TB treatment regimen

As discussed above, it was shown that several dosage forms are employed in treating tuberculosis for a prolonged period and from this point forward, the study will be primarily focusing on TZD and PDX that are administered together in treating MDR-TB and XDR-TB. PDX is a vitamin recommended for patients who are taking isoniazid or TZD for the prevention of peripheral neuropathy, and TZD is an antimycobacterial and antituberculosis drug but mainly used in treating MDR-TB.

2.12.1 Pharmacological action of PDX

PDX, also well-known as Vitamin B₆ is a water-soluble molecule. It is a vitamin found in food ingredients and is regularly used as a dietary supplement. It is prevalent in brewer's yeast, eggs, chicken, carrots, fish, liver, kidneys, peas, wheat germ and walnuts. Its deficiency may cause anaemia, nerve damage, seizures, skin problems, and sores in the mouth. It is essential in haemoglobin production which is responsible for the transport of oxygen to tissues (Srivastava *et al.*, 2014). Bacteria, fungi, and plants make their own PDX, whereas parasitic organisms and higher animals obtain PDX through food intake (Ristilä *et al.*, 2006). It is recommended that patients considered to be at risk for developing polyneuropathy, such as those with alcohol dependency, malnutrition, diabetes, and HIV, receive daily PDX supplementation (van der Watt *et al.*, 2011). PDX is usually interconverted into pyridoxal (aldehyde) and pyridoxamine (amine) derivatives. PDX, pyridoxamine, and their phosphorylated forms are major forms of vitamin B₆ in plant-based food, while pyridoxal and pyridoxal-5'-phosphate (PLP) are the main forms observed in foods obtained from animals. PLP acts as co-factor for many enzymes which catalyse the phosphorolytic cleavage of glycogen, variety of metabolic reactions of amino acids such as racemization, transamination, a-decarboxylation, aldolic cleavages, b- and c-eliminations and replacements. Pyridoxine hydrochloride (HCl) is the hydrochloride salt form of vitamin B₆ and which get converted into its active co-enzymatic form pyridoxal-5'-phosphate (PLP) through the vitamin B₆ salvage pathway involving three enzymes: pyridoxal kinase, pyridox(am)ine phosphate oxidase and pyridoxal phosphatase (Branton and Jana 2017). . PDX 5'-phosphate esters, pyridoxal 5'-phosphate (PLP), pyridoxine 5'-phosphate (PNP) and pyridoxamine 5'-phosphate (PMP) are dephosphorylated by alkaline phosphatase (ALP) before crossing the cell membranes and subsequently producing its pharmacological effect. These mentioned co-factors are are

phosphorylated by pyridoxal kinase inside the cell back into the 5'-phosphate ester form. Subsequently, the 5'-phosphate ester form is catabolised into 4-pyridoxic acid before being excreted in the urine (Ramos *et al.*, 2019). An overdose of PDX supplementation can cause sensory neuronal pain. It has also been shown that the inactive form of PDX competitively inhibits the active pyridoxa-5'-phosphate which produce symptoms of overdose, that are similar to the symptoms associated with deficiency (Vrolijk *et al.*, 2017). PDX is excreted in urine as 4-pyridoxic acid and it is inversely associated with protein intake (Ueland *et al.*, 2015). It also stays longer in the body with a half-life of 18-38 days (Johansson *et al.*, 1966).

2.12.2 Pharmacological action of TZD

TZD, is an anti-TB drug consisting of two molecules of D-cycloserine joined together with a terephthalaldehyde molecule. This drug molecule exhibits a bacteriostatic mechanism of action in the treatment of MDR-TB. It blocks the action of D-alanine racemase and D-alanine ligase to inhibit the synthesis of the cell wall peptidoglycan. D-cycloserine shows a wide minimum inhibitory concentration (MIC), ranging from 1.5 to 30 µg/ml depending on the culture medium used to ascertain MIC (Zhang and Yew, 2015). Zitkova and Tousek conducted a study in 1974 comparing TZD and cycloserine pharmacokinetics following administration of single doses of 250, 500 and 750 mg of each drug. The quantified TZD blood concentration was higher at all time intervals compared to cycloserine, but this was found not to be statistically significant given that TZD is a double cycloserine molecule. The maximum peak concentration was achieved after 2 and 3 hours for cycloserine and TZD, respectively. The concentration range for both drugs was roughly between 5 and 19 µg/ml across a 30-hour period. The excretion was slower in elderly people compared to young people, with approximately 40% excreted unchanged in the urine, providing possibility of using the drugs in cases of genitourinary TB infection (Zitkova and Toušek, 1974). The metabolism of TZD is not yet known, it is thought to be hydrolysed into cycloserine and para-phthalate. Mugabo and Mulubwa studied the pharmacological comparison between TZD and cycloserine. They found that only 29% of TZD was converted into cycloserine and both drugs cannot be used interchangeably (Mulubwa and Mugabo, 2019). TZD is given as a daily dose of 15 - 20 mg/kg within a range of 500 - 1000 mg divided into 3 - 4 doses as shown in Table 2.1. The few reported side effects of TZD are dizziness, slurred speech, headache, and convulsions. Others include tremors, insomnia, confusion and depression and the most dangerous side effect is suicidal tendency (Vora, 2010).

In the metanalysis study comparing the safety of cycloserine versus that of TZD in Asian populations, no significant differences were observed in the prevalence of adverse drug reactions, though TZD is recommended for patients who discontinue cycloserine due to toxicity or with psychiatric comorbidity (Hwang *et al.*, 2013; Vora, 2010). The mechanism through which TZD causes side effects is not well understood. Cycloserine, an analogue of TZD has been reported to compete with γ -aminobutyric acid in the brain which causes central nervous system (CNS) side effects (Dooley *et al.*, 2012). Additionally, TZD is suspected to inhibit PDX activity and thereby increasing the nervous system toxicities and the risk of isoniazid associated symptomatic symmetrical peripheral neuropathy (Conradie *et al.*, 2013).

2.13 The route of synthesis and physicochemical properties

2.13.1 PDX

PDX (Figure 2.3) is synthesised through alkyl substitution of oxazoles reacted with maleic acid to yield a substituted pyridine ring which is ready to be converted to PDX. The complete route of synthesis constitutes that the starting material ethyl D, 1-alaninate hydrochloride is combined with formic-acetic anhydride which forms ethyl N-formyl D, 1-alaninate. Subsequently, it is refluxed with phosphorous pentoxide in chloroform. This reaction produces 4-methyl-5-ethoxyoxazole which is then quenched with aqueous potassium hydroxide and the subsequent distillation of the formed organic layer, resulting in an oxazole.

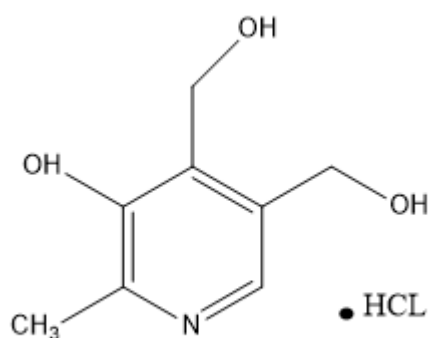


Figure 2.3: Molecular structure of PDX (Scifinder, 2021)

The obtained oxazole can be condensed with dienophiles to generate 2-methyl-3-hydroxy-4,5-disubstituted-pyridine. This resultant product is mixed and heated with two moles of diethyl maleate and the adduct is cleaved with ethanolic hydrogen chloride to form the diethyl ester of

2-methyl-3-hydroxy-pyridine-4,5-dicarboxylic acid hydrochloride. The latter is reduced to pyridoxine with lithium aluminum hydride collected as its hydrochloride. (Aboul-Enein and Loutfy, 1984; Itov and Gunar, 1988).

Table 2.2: Physicochemical properties of PDX (Aboul-Enein and Loutfy, 1984; Ph. Eur 2005)

Properties	PDX
Physical characteristics	PDX appears white or almost white of crystalline powder. It is odorless and it has a bitter saline taste.
pH	2.0 to 3.0
Molecular weight	205.64 g/mol
Loss on drying	0.5% when 1g is dried in oven at 105°C
Solubility	Soluble in water, propylene glycol, not in chloroform and ether
Melting point	202 - 212°C (Free base: 160°C) with decomposition
Dissociation constant	pKa of 5.0 and 9.0

Table 2.2 outlines the physicochemical properties of PDX found to be relevant to this study. PDX is highly soluble in water, alcohol, and propylene glycol and insoluble in chloroform and ether. PDX is more stable compared to pyridoxamine and pyridoxal and is reported to be more stable in acidic solutions than in neutral or alkaline solution (Aboul-Enein and Loutfy, 1984). Thermal analysis of PDX conducted by Branton and Jana (2017), showed a single sharp endothermic peak at 214.14°C which marked its melting point, with no solid-state transformations occurring during heating. It is also stable even if it is heated at 120°C for 30 minutes without decomposition in acidic solutions. PDX falls under class I of the Biopharmaceutical Classification System (BCS) since it is highly soluble and highly permeable (Lindenberg *et al.*, 2004). It shows instability unstable with various food products with the possibility of forming complex addition products between the typical colourants used in food.

Further to this it should be noted that PDX gets degraded by UV radiation in neutral and alkaline solutions (Aboul-Enein and Loutfy, 1984).

2.13.2 TZD

TZD is synthesised through condensation of two cycloserine molecules joined by terephthalaldehyde. Cycloserine was discovered in 1954 in *Streptomyces orchidaceus* and *streptomyces garyphalus* species. Its formula name is D-4-amino-3-isoxazolidone. Many cycloserine synthetic pathways have been developed. This synthesis uses D-serine which is readily available and can be easily transformed into D-cycloserine (Li *et al.*, 2010; Kim and Park, 2012). Table 2.3 highlights the physicochemical properties of TZD that could be collected through a thorough literature search. This compound presents as a slightly hygroscopic, white to yellowish coloured powder (WHO, 2018b). Its molecular weight is 302.29 g/mol and shows a melting point of 204 - 205°C (Scifinder, 2019). According to literature, TZD shows polymorphism, and one polymorph is consistently produced. This polymorphic form exhibits low solubility (WHO, 2018b). TZD lacks literature on solid-state forms in terms of aqueous solubility, physical and chemical stability. There is no known BCS classification of this drug. Considering this, it will be of great importance to know all relevant physicochemical properties and how these properties may affect its therapeutic efficacy.

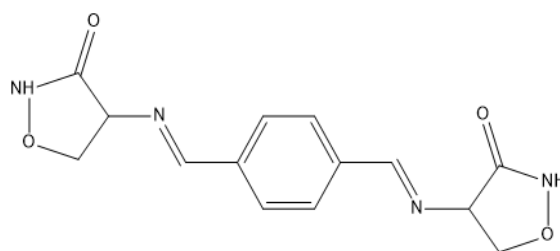


Figure 2.4: Molecular structure of TZD (Scifinder, 2019)

Table 2.3: Physicochemical properties of TZD (Scifinder, 2019)

Properties	TZD
Molecular weight	302.29 g/mol
Melting point (Experimental)	204 - 205°C
Density (Predicted)	1.52±0.1 g/cm ³
pKa (Predicted)	14.08±0.40

2.14 Conclusion

TB remains a debilitating disease with millions of people being affected by it on an annual basis. To make matters even more challenging is the emergence and alarming high incidence rate of MDR-TB. The treatment of TB and especially that of MDR-TB requires the administration of multiple drugs over an extended period of time (6 - 24 months) to infected patients. The treatment success rate remains problematic due to the challenges that patients must overcome in taking the anti-TB medications. Many evidence exist that their exist a direct correlation between the pill-burden experienced by patients and the treatment outcome. This being said, it is clear to see why there is a need for new medicines which are efficient and convenient to be administered to patients, to bring forth a better therapeutic outcome. The design and formulation of FDC products is one of the strategies that proves to be successful in these complex treatment regimens, typically associated with the treatment of TB and this can be ascribed to the reduction in the number of dosage forms patients must ingest on a daily basis.

As outlined in Chapter 1, this project investigated the possibility to combine TZD and PDX through possible molecular modifications which could potentially lead to the incorporation of both these active compounds into an FDC formulation containing reduced doses of both molecules. Thus, addressing the aspect of pill-burden for at least two of the drugs that MDR-TB patients must take daily. The engineering and design of new solid-state forms of drugs in an effort to enhance the physicochemical properties of the individual molecules also plays an imperative role in the research and development associated with FDCs. As will be disseminated and described in detail in Chapter 3, solid-state form modifications of drugs may result in improved solubility, faster dissolution rates and ultimately increased bioavailability

which could potentially lead to dosage reduction potentially linking to better treatment outcomes.

2.15 References

Aboul-Enein, H.Y. and Loutfy, M.A. 1984. Pyridoxine hydrochloride. In: Florey K. Ed. *Analytical Profiles of Drug Substances*. Vol. 13. New York: Academic Press, 447-486.

Allué-Guardia, A., Garcia, J.I. and Torrelles, J.B. 2021. Evolution of drug-resistant Mycobacterium tuberculosis strains and their adaptation to the human lung environment. *Frontiers in Microbiology*, 12, p.137. Doi: <https://doi.org/10.3389/fmicb.2021.612675>.

ATS see American Thoracic Society.

American Thoracic Society. 2000. Diagnostic Standards and Classification of Tuberculosis in Adults and Children. *American Journal of Respiratory and Critical Care Medicine* 161(4): 1376-1395. Doi: <https://doi.org/10.1164/ajrccm.161.4.16141>.

Anon. 2015. Tuberculosis. In: Wells, B.G., Dipro, J.T., Schwinghammer, T.L., Dipiro, C.V. Ed(s). *Pharmacotherapy handbook*. 9th ed. New York, McGraw-Hill, 476-489.

Balasubramanian, V.N. Oommen, K. and Samuel, R.D.O.T. 2000. DOT or not? Direct observation of anti-tuberculosis treatment and patient outcomes, Kerala State, India. *The International Journal of Tuberculosis and Lung Disease*, 4(5): 409-413.

Bhunja, S., Sarkar, M., Banerjee, A. and Giri, B. 2015. An update on pathogenesis and management of tuberculosis with special reference to drug resistance. *Asian Pacific Journal of Tropical Disease*, 5(9): 673-686. Doi: 10.1016/S2222-1808(15)60912-4.

Branton, A., Jana, S. 2017. Evaluation of the Effect of the Energy of Consciousness Healing Treatment on Physico-chemical and Thermal Properties of Pyridoxine Hydrochloride. *American Journal of Physical Chemistry*, 6(4): p.49-58. doi: 10.11648/j.ajpc.20170604.11.

Cambier, C.J., Falkow, S. and Ramakrishnan, L. 2014. Host evasion and exploitation schemes of Mycobacterium tuberculosis. *Cell*, 159(7):1497-1509. Doi: <https://doi.org/10.1016/j.cell.2014.11.024>.

Centers for Disease Control and Prevention (CDC). 2021. *Testing for TB Infection*. [online] Available at: <<https://www.cdc.gov/tb/topic/testing/tbtesttypes.htm>> [Accessed 31 October 2021].

Chai, Q., Zhang, Y., and Liu, C.H. 2018. Mycobacterium tuberculosis: an adaptable pathogen associated with multiple human diseases. *Frontiers in Cellular and Infection Microbiology*, 8:158. Doi: 10.3389/fcimb.2018.00158.

- Censi, R. and Di Martino, P.** 2015. Polymorph impact on the bioavailability and stability of poorly soluble drugs. *Molecules*, 20(10):18759-18776. Doi: <https://doi.org/10.3390/molecules201018759>.
- Cernuschi, T., Malvolti, S., Nickels, E. and Friede, M.** 2018. Bacillus Calmette-Guérin (BCG) vaccine: a global assessment of demand and supply balance. *Vaccine*, 36(4): 498-506. <https://doi.org/10.1016/j.vaccine.2017.12.010>.
- Conradie, F., Mabiletsa, T., Sefoka, M., Mabaso, S., Louw, R., Evans, D. and Van Rie, A.** 2013. Prevalence and incidence of symmetrical symptomatic peripheral neuropathy in patients with multidrug-resistant TB. *South African Medical Journal*, 104(1):24. Doi: <https://hdl.handle.net/10520/EJC146778>.
- Dooley, K.E., Mitnick, C.D., Ann DeGroot, M., Obuku, E., Belitsky, V., Hamilton, C.D., Makhene, M., Shah, S., Brust, J.C., Durakovic, N. and Nuermberger, E.** 2012. Old drugs, new purpose: retooling existing drugs for optimized treatment of resistant tuberculosis. *Clinical infectious diseases*, 55(4):572-581. Doi: <https://doi.org/10.1093/cid/cis487>.
- European Pharmacopoeia (Ph. Eur).** 2005. Pyridoxine Hydrochloride in: *Monographs medicinal and related substances*. 5th ed. Strasbourg: Council of Europe, 2342.
- Gómez, A.V., Gonzalez-Martin, J. and Garcia-Basteiro, A.L.** 2017. Xpert® MTB/RIF: Usefulness for the diagnosis of tuberculosis and resistance to rifampicin. *Medicina Clínica (English Edition)*, 149(9):399-405. Doi: [10.1016/j.medcli.2017.06.007](https://doi.org/10.1016/j.medcli.2017.06.007).
- Hwang, T.J., Wares, D.F., Jafarov, A., Jakubowiak, W., Nunn, P. and Keshavjee, S.** 2013. Safety of cycloserine and terizidone for the treatment of drug-resistant tuberculosis: a meta-analysis. *The International Journal of Tuberculosis and Lung Disease*, 17(10):1257-1266. Doi: <https://doi.org/10.5588/ijtld.12.0863>.
- Itov, Z.I. and Gunar, V.I.** 1988. Methods of synthesis and technology of production of drugs synthesis of pyridoxine. *Pharmaceutical Chemistry Journal*, 22(2):151-157.
- Jagielski, T., Minias, A., Van Ingen, J., Rastogi, N., Brzostek, A., Żaczek, A. and Dziadek, J.** 2016. Methodological and clinical aspects of the molecular epidemiology of Mycobacterium tuberculosis and other mycobacteria. *Clinical Microbiology Reviews*, 29(2):239-290. Doi: [10.1128/CMR.00055-15](https://doi.org/10.1128/CMR.00055-15).
- Johansson, S., Lindstedt, S., Register, U. and Wadstrom, L.** 1966. Studies on the metabolism of labeled pyridoxine in man. *The American journal of clinical nutrition*, 18(3):185-196. Doi: <https://doi.org/10.1093/ajcn/18.3.185>.
- Kim, H.K. and Park, K.J.J.** 2012. Novel practical synthesis of d-cycloserine. *Tetrahedron Letters*, 53(32):4090-4092. Doi: <https://doi.org/10.1016/j.tetlet.2012.05.120>.
- Li, X., Meng, X., Duan, H., Wang, L., Wang, S., Zhang, Y. and Qin, D.** 2010. Original and efficient synthesis of d-cycloserine. *Archiv Der Pharmazie*, 343(8):473-475. Doi: <https://doi.org/10.1002/ardp.200900316>.

Malacarne, J., Heirich, A.S., Cunha, E.A.T., Kolte, I.V., Souza-Santos, R. and Basta, P.C. 2019. Performance of diagnostic tests for pulmonary tuberculosis in indigenous populations in Brazil: the contribution of Rapid Molecular Testing. *Journal Brasileiro de Pneumologia*, 45(2), e20180185. Doi: <http://dx.doi.org/10.1590/1806-3713/e20180185>.

Meier, T. and Enders, M. 2020. High reproducibility of the interferon-gamma release assay T-SPOT. TB in serial testing. *European Journal of Clinical Microbiology & Infectious Diseases*, 40(1):85-93. Doi: <https://doi.org/10.1007/s10096-020-03997-3>.

Miller-Petrie, M. Pant, S. and Laxminaraya, R. 2017. Drug-Resistant Infections. In: Holmes K., Bertozzi, S., Bloom, B. and Jha, P. Ed(s). *Major infectious disease*. 3rd ed. Washington: World Bank, 433-448. Doi: 10.1596/978-1-4648-0524-0.

Morrison, J., Pai, M. and Hopewell, P. 2008. Tuberculosis and latent tuberculosis infection in close contacts of people with pulmonary tuberculosis in low-income and middle-income countries: a systematic review and meta-analysis. *The Lancet Infectious Diseases*, 8(6):359-368. Doi:10.1016/S1473-3099(08)70071-9.

Mulubwa, M. and Mugabo, P. 2019. Amount of cycloserine emanating from terizidone metabolism and relationship with hepatic function in patients with drug-resistant tuberculosis. *Drugs in R&D*, 19(3):289-296. Doi: 10.1007/s40268-019-00281-4.

NDOH see National Department of Health.

National Department of Health. 2019. *Standard Treatment Guidelines and Essential Medicines List: Hospital level (Adults)*. [online] Available at: <<https://www.knowledgehub.org.za/elibrary/hospital-level-adults-standard-treatment-guidelines-and-essential-medicines-list-2nd>> [Accessed 8 November 2021].

National Department of Health. 2020. Management of rifampicin resistant tuberculosis: a clinical reference guide. [online]. Available at: <<https://www.health.gov.za/wp-content/uploads/2020/11/management-of-rifampicin-resistant-tb-booklet-0220-v11.pdf>> [Accessed 6 November 2021].

Nardell, E.A. 2016. Transmission and institutional infection control of tuberculosis. *Cold Spring Harbor Perspectives in Medicine*, 6(2):018192. Doi: <https://doi.org/10.1101/cshperspect.a018192>.

Patterson, B. and Wood, R. 2019. Is cough necessary for TB transmission?. *Tuberculosis*, 117:31-35. <https://doi.org/10.1016/j.tube.2019.05.003>.

Ramanathan, M.R., Howell, C.K. and Sanders, J.M. 2019. Drugs in tuberculosis and leprosy. In: Ray S. D. *Side Effects of Drugs Annual*. Vol 41. Amsterdam: Elsevier, 321-338. Doi: <https://doi.org/10.1016/bs.seda.2018.06.014>.

Ramos, R.J., Albersen, M., Vringer, E., Bosma, M., Zwakenberg, S., Zwartkruis, F., Jans, J.J. and Verhoeven-Duif, N.M. 2019. Discovery of pyridoxal reductase activity as part of human vitamin B6 metabolism. *Biochimica et Biophysica Acta (BBA)-General Subjects*, 1863(6):1088-1097. Doi: <https://doi.org/10.1016/j.bbagen.2019.03.019>.

Ristilä, M., Matxain, J., Strid, Å. and Eriksson, L. 2006. pH-Dependent Electronic and Spectroscopic Properties of Pyridoxine (Vitamin B6). *The Journal of Physical Chemistry B*, 110(33):16774-16780. Doi: <https://doi.org/10.1021/jp062800n>.

Scifinder. 2019. *SciFinderⁿ Login*. [online] Available at: <<https://scifinder-n.cas.org/searchDetail/substance/616186e93e8b173419f5787f/substanceDetails>> [Accessed 9 October 2021].

Scifinder. 2021. *SciFinderⁿ Login*. [online] Available at: <<https://scifinder-n.cas.org/search/substance/6187bcae8bc1a11b91cf8c5a/1>> [Accessed 7 November 2021].

Singh, A., Prasad, R., Balasubramanian, V., Gupta, N. and Gupta, P. 2015. Prevalence of adverse drug reaction with first-line drugs among patients treated for pulmonary tuberculosis. *Clinical Epidemiology and Global Health*, 3:80-90. Doi: <https://doi.org/10.1016/j.cegh.2015.10.005>.

Singh, R., Dwivedi, S.P., Gaharwar, U.S., Meena, R., Rajamani, P. and Prasad, T. 2020. Recent updates on drug resistance in Mycobacterium tuberculosis. *Journal of Applied Microbiology*, 128(6):1547-1567. Doi: <https://doi.org/10.1111/jam.14478>.

Sloan, D. and Lewis, J. 2016. Management of multidrug-resistant TB: novel treatments and their expansion to low resource settings. *Transactions of The Royal Society of Tropical Medicine and Hygiene*, 110(3):163-172. Doi: <https://doi.org/10.1093/trstmh/trv107>.

Srivastava, M., Rani, P., Singh, N. and Yadav, R. 2014. Experimental and theoretical studies of vibrational spectrum and molecular structure and related properties of pyridoxine (vitamin B6). *Spectrochimica Acta Part A: Molecular and Biomolecular Spectroscopy*, 120:274-286. Doi: <https://doi.org/10.1016/j.saa.2013.09.133>.

Starke J.R. 2014. Interferon- γ release assays for diagnosis of tuberculosis infection and disease in children. *Pediatrics*, 134. Doi: <https://doi.org/10.1542/peds.2014-2983>.

Ueland, P.M., Ulvik, A., Rios-Avila, L., Midttun, Ø. and Gregory, J.F. 2015. Direct and functional biomarkers of vitamin B6 status. *Annual Review of Nutrition*, 35:33-70. Doi: <https://doi.org/10.1146/annurev-nutr-071714-034330>.

van der Watt, J., Harrison, T., Benatar, M. and Heckmann, J. 2011. Polyneuropathy, anti-tuberculosis treatment and the role of pyridoxine in the HIV/AIDS era: a systematic review [Review article]. *The International Journal of Tuberculosis and Lung Disease*, 15(6):722-728. Doi: <https://doi.org/10.5588/ijtld.10.0284>.

van't Hoog, A.H., Onozaki, I. and Lonnroth, K. 2014. Choosing algorithms for TB screening: a modelling study to compare yield, predictive value and diagnostic burden. *BMC Infectious Diseases*, 14(1): 532. <https://doi.org/10.1186/1471-2334-14-532>.

Viñuelas-Bayón, J., Vitoria, M.A. and Samper, S. 2017. Rapid diagnosis of tuberculosis. Detection of drug resistance mechanisms. *Enfermedades infecciosas y microbiología clinica (English ed.)*, 35(8):518-526. Doi: [10.1016/k.eimce.2017.08.009](https://doi.org/10.1016/k.eimce.2017.08.009).

Vora, A. 2010. Terizidone. *Journal of Association Physician of India*. Volume 58.

Vrolijk, M.F., Opperhuizen, A., Jansen, E.H., Hageman, G.J., Bast, A. and Haenen, G.R. 2017. The vitamin B6 paradox: supplementation with high concentrations of pyridoxine leads to decreased vitamin B6 function. *Toxicology In Vitro*, 44:206-212. Doi: <https://doi.org/10.1016/j.tiv.2017.07.009>.

Wani, R.L.S. 2013. Tuberculosis 2: Pathophysiology and microbiology of pulmonary tuberculosis. *South Sudan Medical Journal*, 6(1):10-12.

WHO see World Health Organization.

World Health Organization. 2011. *Rapid Implementation of the Xpert MTB/RIF diagnostic test*. Geneva. [online] Available at: https://apps.who.int/iris/bitstream/handle/10665/44593/9789241501569_eng.pdf;jsessionid=577C223408B115DDCFAB99EDE3FA24CA?sequence=1 > [Accessed 25 June 2020].

World Health Organization. 2018a. *Latent tuberculosis infection: updated and consolidated guidelines for programmatic management*. Geneva. [online] Available at: <https://apps.who.int/iris/bitstream/handle/10665/260233/9789241550239-eng.pdf> [Accessed 10 November 2019].

World Health organization. 2018b. Terizidone 250mg capsules WHOPAR part 6. Available at <https://extranet.who.int/pqweb/sites/default/files/TB303part6v1.pdf>. [Accessed 10 November 2019]

World Health Organization. 2019. *Global tuberculosis report 2019*. Geneva: World Health Organization Press; 2019. [online] Available at: <https://www.who.int/teams/global-tuberculosis-programme/tb-reports/global-report-2019> > [Accessed 04 May 2019].

World Health Organization. 2020. *Global Tuberculosis Report 2020*. [online] Available at: <https://www.who.int/publications/i/item/9789240013131> > [Accessed 1 December 2020].

World Health Organization. 2021. Global tuberculosis report 2021. [online] Available at: <https://www.who.int/teams/global-tuberculosis-programme/tb-reports/global-tuberculosis-report-2021> > [Accessed 5 November 2021].

Zhang, Y. and Yew, W.W. 2015. Mechanisms of drug resistance in Mycobacterium tuberculosis: update 2015. *The International Journal of Tuberculosis and Lung Disease*, 19(11):1276-1289. Doi: 10.5588/ijtld.15.0389.

Zitkova, L. and Toušek, J. 1974. Pharmacokinetics of cycloserine and terizidone. *Chemotherapy*, 20(1):18-28. Doi: <https://doi.org/10.1159/000221787>.

Chapter 3

An overview on the solid-state chemistry and physicochemical properties of drugs in relation to pharmaceutical preformulation

3.1 Introduction

In this chapter, an in-depth discussion pertaining to the solid-state chemistry of API(s) relating to chemical and physical stability and how this fundamental information informs preformulation and pharmaceutical product formulation processes is presented. The latest literature was reviewed to provide an overview of the different solid-state forms, highlighting critical differences, and linking it to key aspects in pharmaceutical formulation.

3.2 Solid-state forms of active pharmaceutical ingredients (APIs)

Solid-state chemistry information linked to a specific API(s) is important since it not only informs preclinical studies and formulation processes but could also highlight potential bioavailability challenges. The majority of pharmaceutical compounds are produced to exist in the solid-state and many end up in dosage forms such as tablets, capsules or powders. The physicochemical characteristics of drug molecules determine the solubility behaviour, dissolution rate, powder flowability, compressibility and stability of the finished pharmaceutical products in which they are incorporated and ultimately their bioavailability (El-Yafi and El-Zein, 2015).

Pharmaceutical solids may be comprised of different solid-state habits or more correctly termed solid-state forms. These may broadly be classified into: (a) thermodynamically stable crystalline or (b) metastable amorphous forms. It is these differences in the solid-state that often lead to differences in thermodynamic parameters and physicochemical properties such as: solubility, dissolution rate, stability, and mechanical properties of a particular active pharmaceutical ingredient (API). Crystallisation influences the dissolution rate and offers habit modifications of crystalline materials. The increase of wettability and dissolution rate of crystalline materials is dependent on a combination of the nature of the crystal packing, size, and associated polymorphic form(s) (Blagden *et al.*, 2007). Crystallisation is also a process often utilised to manufacture and/or purify solid compounds (Byrn, Zografí and Chen, 2010). Within the pharmaceutical arena, different solid-state forms are not only an occurrence with

APIs but also with excipients. Different solid-state forms occur due to differences in the packing of the compound molecules within the unit cell. Molecules may be packed in a highly organised manner, exhibiting three-dimensional long-range order or in a randomly oriented manner, thus having a short-range order of molecules (Healy *et al.*, 2017). Crystalline and amorphous forms of the same drug may exist in various solid-state forms, it can be broadly classified into single-component or multi-component solid-state forms, as depicted in Figure 3.1. Subsequent paragraphs will provide a more in-depth review of the different crystalline and amorphous solid-state forms in which any given drug may exist.

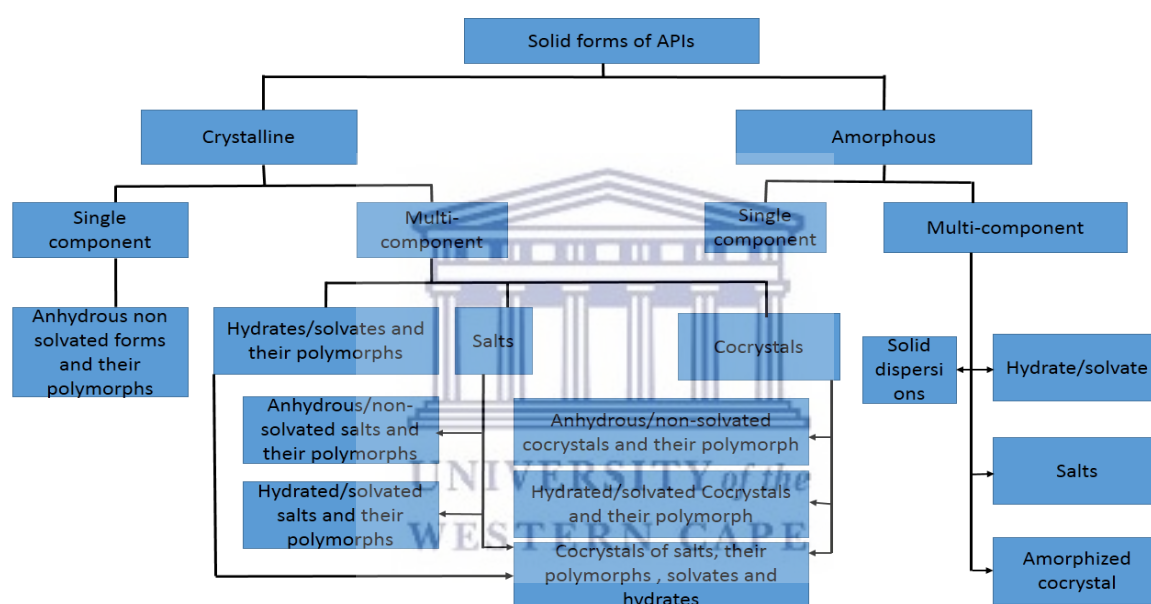


Figure 3.1: Solid-state forms of APIs as adapted from Healy *et al.*, (2017).

3.2.1 Polymorphism

Polymorphism is defined as the ability of a chemical compound to exist in more than one crystal packing or molecular arrangement. This is caused by a variety of intermolecular interactions; typically weak bonds such as van der Waals forces or hydrogen bonds, that constitutes different forms of crystal structure. Polymorphs may be subdivided into two types, namely, (a) packing polymorphism, where molecules keep the same molecular conformation to one another but are differently arranged in three-dimensional space and (b) conformational polymorphism which is due to flexible moieties rearranging thereby resulting in the existence of different solid-state forms due to molecular conformation differences (Omar, Makary, and Wlodarski, 2015; Lee, 2014). These crystalline forms may either be stable or metastable forms. The prior is known

to be chemically stable due to higher packing density and optimised orientation and it is favoured in pharmaceutical manufacturing because it does not convert to other forms as compared to metastable forms, even though it is less soluble compared to its counterpart (Acharya *et al.*, 2018). Metastable forms can only be favoured if the most soluble metastable form can remain physically and chemically stable during the shelf-life of the finished pharmaceutical product or if the therapeutic dose is limited by the solubility of the drug with no need to increase the dissolution of the drug to shorten T_{max} and/or increase the maximum concentration for rapid relief of acute symptoms (Buckton, 2018; Singhal, 2003).

Polymorphs affect the mechanical properties, physical and chemical stability, solubility and dissolution rate of the compound. It is essential that a pharmaceutical manufacturing company is aware of the produced polymorph, and evidence must be provided to substantiate the stability thereof during manufacturing, usage and storage to ensure reproducible bioavailability after administration (Censi and Martino, 2015). During preformulation studies, it is recommended to apply high throughput polymorph screening to avoid unexpected solid-state changes within the finished pharmaceutical product which could affect API solubility and bioavailability detrimentally. The goal is to find the most stable form for further development and avoid poor reproducibility and low physical stability (Kawakami, 2009).

Several polymorphic form preparation processes exist and includes: recrystallisation through solvent evaporation, spray drying, slurring, grinding, antisolvent addition, vapor diffusion, vapor deposition, crash cooling and crystallisation from the melt or from an amorphous intermediary. Figure 3.2 depicts more preparation methods and the relation between stability and the time taken to prepare the solid-state form (Byrn, Zografi and Chen, 2010; Cains, 2009). From a polymorphic form preparation perspective, it is advantageous to employ the same method used to produce a specific polymorph throughout to ensure repeatability and to have a sound understanding of the preparation method and how it determines the preparation of the specific polymorphic form. Slow and well controlled conditions will lead to the production of stable crystalline forms compared to extreme conditions with greater driving force that produces metastable crystalline forms and/or amorphous forms. There are marketed pharmaceutical products containing APIs which exhibit one or more polymorphic forms such as ritonavir which is known to exist in five polymorphic forms and Form II being the most

stable. Acetaminophen (paracetamol) have three forms, but Form I is the only one that is used in commercialised pharmaceutical products since Form II is not stable and it transforms to Form I during storage and compression. Axitinib have 60 solvates, polymorphs of the solvates, and five anhydrous forms. The marketed Form (Inylta[®]) is an anhydrous form obtained by reslurrying of the solvates at an elevated temperature (Lee, 2014).

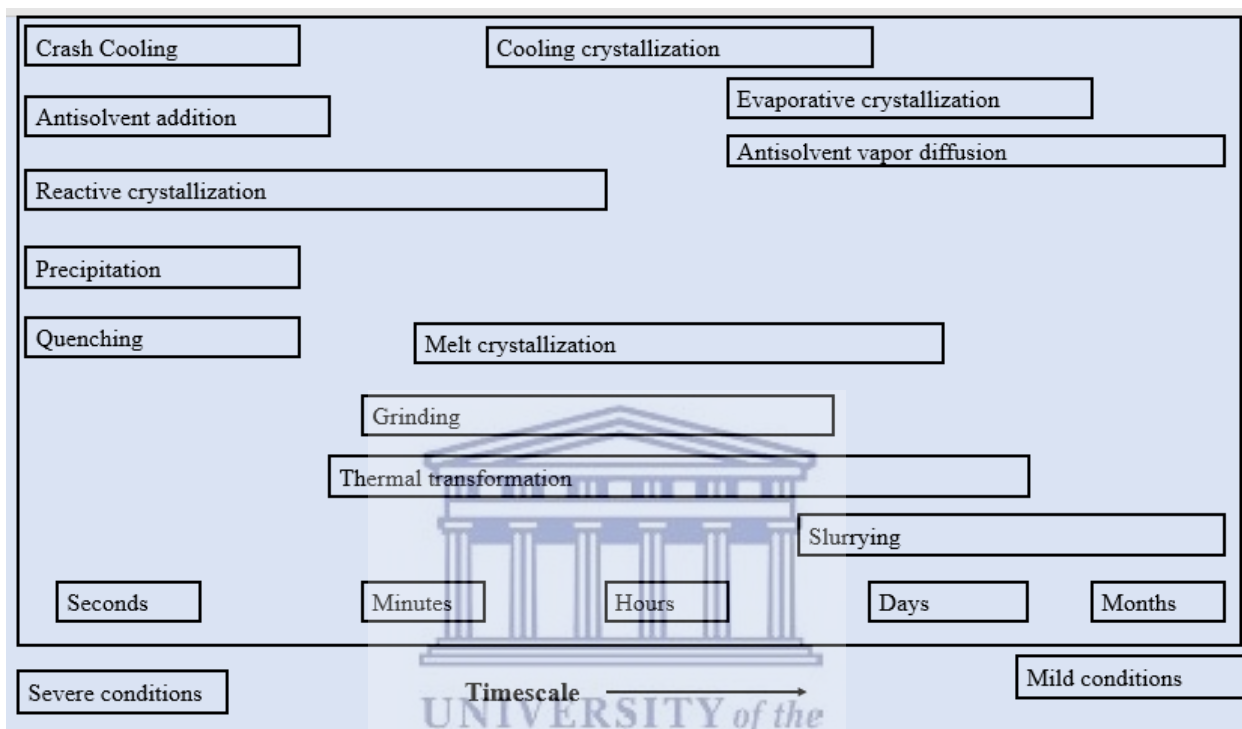


Figure 3.1: Crystalline solid-state form preparation methods depicting longer duration methods that yield stable polymorphs and shorter duration methods that yield less stable polymorphs as adapted from Cains, (2009).

3.2.2 Hydrates and solvates

Hydrates and solvates are multicomponent solid forms that contain a host molecule (API or excipient) and a guest molecule (water (hydrate) or other solvents (solvate)) incorporated into the molecular structure. Just as with polymorphic forms, hydrates and solvates exhibit differences in their physicochemical properties in comparison with their anhydrous form (Healy *et al.*, 2017). Hydrates and solvates are typically produced, but not restricted, using solvents of FDA Class 3 that are safe in manufacturing (Stahly, 2007). Water is safe as a crystal adduct and depending on how it is incorporated in the crystal lattice, hydrates are classified into hydrates where water molecules exist as isolated sites, channel hydrates and ion-coordinated site hydrates.

Hydrates may form easily, primarily due to the small size of the water molecule and its ability to act both as a hydrogen bond donor and acceptor and its ability to fill structural voids (Byrn, Zografí and Chen, 2017b). Water inclusion in the structure affects the dimension, shape, symmetry and capacity of the unit cell. It disrupts the internal energy and therefore the thermodynamic activity of the solid which can modify the bioavailability and the product performance (Khankari and Grant, 1995). Hydrates and solvates are discovered through the process of polymorph screening. The processing or storage of a pharmaceutical solid in a solvent during crystallisation, refluxing, wet granulation and water evaporation facilitates the formation of solvates or hydrates. The exposure to high humidity during moisture sorption experiments may also be used to identify the possibility of hydrate formation (Byrn, Zografí and Chen, 2017b). Water is essential for the preservation of the hydrate structure and any significant change in composition of the structure due to dehydration or desolvation could lead to phase changes and therefore the formation of a different crystal structure (Braun and Griesser 2016). Examples of marketed hydrates include cefadroxil (monohydrate) and paroxetine hydrochloride (hemihydrate), creatine phosphate sodium tetrahydrate, ampicillin hydrate and cephalexin monohydrate, to name just a few (Healy *et al* 2017). Many others are found in commonly used pharmaceutical excipients such as magnesium stearate, calcium diphosphate, glucose, and lactose (Khankari and Grant, 1995).

3.2.3 Co-crystals

A co-crystal is defined as a single crystalline structure of two or more components with no proton transfer occurring between the components and existing as a physical solid at room temperature (Zhou *et al.*, 2016). Co-crystals are developed to enhance the improvements in dissolution rate, solubility, bioavailability, and physical stability of a given API. Furthermore, these solid-state forms may lead to improved powder flowability and compressibility, chemical and physical stability as well as lower hygroscopicity (Qiao *et al.*, 2011). Co-crystals are formed between APIs and suitable co-formers *via* strong intermolecular interactions such as hydrogen bonding which may result in a thermodynamically stable combination of two compounds (Zhou *et al.*, 2016). Co-former selection is a crucial step, and these molecules are usually compounds that are typically used as food additives and should be pharmaceutically acceptable and generally regarded as safe (GRAS). Apart from improving the physicochemical

properties, the co-former may provide additional benefits of nutrition and health (Qiao *et al.*, 2011). A good co-former is characterised as a compound more likely to form a strong intermolecular bond with the API. The crystal engineering principles predicts that compounds with a carboxylic acid moiety with one or more hydroxyl moieties have the potential to form supramolecular co-crystal arrangements. These are compounds with acidic, amide and alcohol functional groups such as amino acids, citric acid and tartaric acid (Ouiyangkul *et al.*, 2020). In this study, TZD and PDX were combined and screened to inform the possibility of possible co-crystal formation. Looking at the molecular structures of both compounds Figure 3.3 (a) and (b), the presence of a hydrogen bond donor species on the PDX molecular structure and hydrogen bond acceptor species on the TZD molecule is considered advantageous for the formation for a supramolecular synthon and the spatial arrangements of intermolecular non-covalent interactions (Sahoo *et al.*, 2011). To date few co-crystals have reached the market: valsartan-sacubitril (Enteresto[®], Novartis), ipragliflozin-proline (Suglat[®], by Astellas Pharma and Kotobuki Pharmaceutical in Japan, Korea and Thailand market) and many more are still in clinical trials. Co-crystals are not a recent development but there is still significant research to be done in terms of proper classification and a common registration guideline. The United States Food and Drug Administration (FDA) classify co-crystals as a special form of solvates or hydrates whilst the European Medicines Agency (EMA) classify them as a new chemical entity (Chavan *et al.*, 2018).

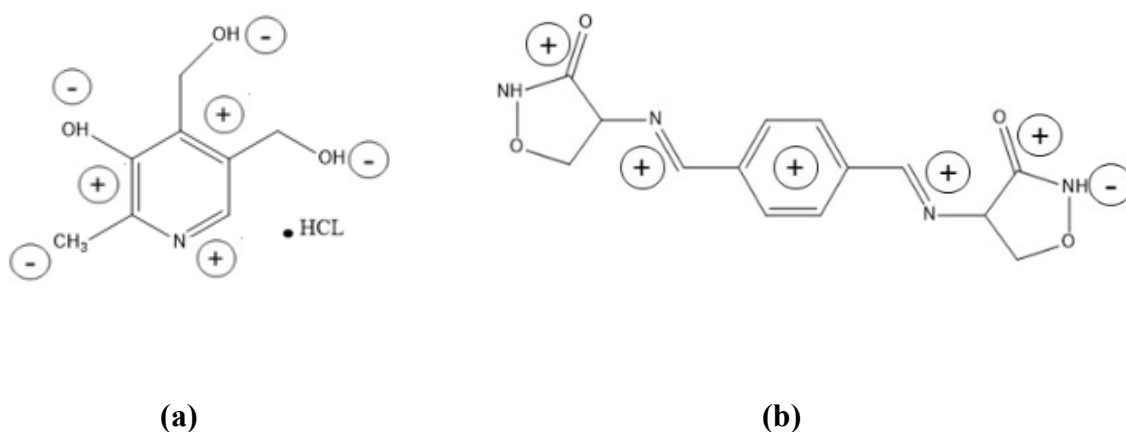


Figure 3.2: Schematic representation of PDX (a) and of TZD (b) with hydrogen bond donor (+) and (-) acceptor potential region.

In order to prepare co-crystals, one has to rely on co-crystallisation techniques and these techniques are divided into solvent-based and solvent-free methods. Solvent-based methods are commonly used on laboratory scale because they are simple to set up and the properties of

the final product can be controlled either by changing the solvent and/or temperature. Solvent-free methods are supported by academia and industry because they are scalable, associated with green chemistry and in general have less toxic by-products. An example of solvent-based methods includes solvent evaporation, spray drying, freeze drying and vapor diffusion while solvent free methods account for neat grinding, liquid assisted grinding (LAG), hot melt extrusion (HME) and spray congealing. Spray drying, spray congealing and HME are so far the methods employed in industry and further studies are needed to fully understand the mechanism behind them (Rodrigues *et al.*, 2018). One of the obstacles that the pharmaceutical industry is facing in the development of pharmaceutical co-crystals, that could be furthered to the market, is that of process upscaling, moving from the method of LAG on small scale to large scale production remains challenging. Further to this is the issue of having two compounds with different solubilities. However, a study conducted on the formation of a carbamazepine-nicotinamide co-crystal illustrated how proper initial measurements of intermolecular interactions and crystal lattice energies informs the understanding of the strength and structure of the binding synthons. This being followed by measuring the solubilities of each individual pure component, solid form stability domains, speciation in solution and nucleation kinetics may be further used to optimise solution crystallisation (Brittain, 2011). In terms of co-crystallisation techniques there exist multiple techniques and the choice of a suitable technique(s) should be based on preliminary solid-state characteristic investigations of the pure compounds.

3.2.4 Salts

Salts are formed when an ionisable API interacts with a counterion within a definite stoichiometry creating a charge balance. Amino acids are largely used as counterions since they exhibit high water solubility therefore showing to be suited for enhancing solubility of salifiable API(s). Counterions exert the common-ion effect in solution which influences the solubility of the resulting salt form. Overall salt solubility is governed by the pKa, solubility product constant (K_{sp}) of the compounds and the pH of the medium (Serajuddin, 2007). Salts are formed during an acid-base reaction between an API and a basic or an acidic counterion. It is formed through the transfer of a proton from an acid to a base (Pindelska, Sokal, and Kolodziejcki, 2017). Salt formation is one of the most utilised strategies to improve the physicochemical properties of APIs and it is considered a favourable process due to its simplicity, ease to synthesise, crystallisation yield and reliability of the resulting product

(Vioglio, Chierotti and Gobetto 2017). Salts can increase an API's purity, water solubility, crystallinity, possibility of isolation, and stability. It is a requirement that the difference in pKa of both components must be greater than 3 to enable the formation of a potential salt (Karagianni, Malamataris and Kachrimanis, 2018). The pKa rule is based on the solubility enhancement that is obtained once both species are charged in solution. Furthermore, a pH-unit difference of 3 between the pKa values of the given molecules is sufficient to enable salt formation and prevent the risk of disproportionation in pure water (Berry and Steed, 2017). Salt selection is important during preclinical development. Salt characteristics such as basicity/acidity, molecular size, shape, flexibility, relevant physicochemical properties, degree of crystallinity, aqueous solubility, crystal habit, physical and chemical stability are evaluated to check the suitability for product development (Bastin, Bowker and Slater, 2004). A mentionable drawback of salt forms is that in order to produce a clinical effect, a high dose is needed since typically about 20 - 50% of the molecule consists of the inactive counterion component. Thus, increasing the molecular weight of the compound significantly and in order to allow the correct dose of the API to be included into the dosage form weight compensation should be employed. This results in usage of high volume of powder and in the instances of capsule formulation may become difficult to fit a high volume of powder into a capsule shell or may result in the formation of significantly larger tablet sizes. (Bastin, Bowker and Slater, 2000).

3.2.5 Amorphous and co-amorphous solid-state forms

Amorphous state molecules are molecules that possess short-range order, while having the macroscopic mechanical properties of a solid, local properties of a liquid, with elevated molecular energy and greater molecular mobility, compared to the molecules in the crystalline state (Byrn, Zografi, and Chen 2017a). These solid-state forms have unique properties of higher apparent solubilities and dissolution rate, and in some instances better compressibility compared to the crystalline solid-state forms of the same drug. Compounds such as proteins, some sugars, and many pharmaceutical excipients naturally exist in an amorphous state (Yu, 2001). In comparison with the crystalline form(s) of the same drug the amorphous form(s) possess excess thermodynamics in terms of enthalpy, entropy and Gibbs free energy. The higher thermodynamic energy is advantageous to the solubility of the compound but detrimentally affects the physical stability. Amorphous solid-state forms tend to recrystallise

during storage when thermodynamic properties and kinetic mobility favours the reorganisation of the molecular packing to the less energised, more organised state (Graeser *et al.*, 2010; Toby *et al.*, 2009). Since stability is considered a major drawback for these solid-state forms, numerous strategies have been developed to stabilise amorphous forms. These strategies include:

- (a) the preparation of polymeric amorphous solid dispersion (ASDs) which improve stability compared to pure amorphous forms as the API is kinetically entrapped between the polymer chains (Rumondor *et al.*, 2009), thus reducing molecular mobility.
- (b) Co-amorphous formulation, which is a multi-component single phase amorphous solid system which lacks periodicity in the molecular lattice and is associated by weak and discrete intermolecular interactions between the two components (Ainurofiq *et al.*, 2018). These co-amorphous forms can be drug-drug or drug-excipient combinations. The goal with these solid-state forms is not only to stabilise the amorphous API but also to increase the bioavailability of the API, thus providing improved therapeutic outcomes. This is possible since the co-former acts as a dissolution-enhancing and amorphous stabilising agent (Dengale *et al.*, 2016). Co-former screening selection is a very complex process since it often requires the application of computational methods or theoretical approaches such as identification of miscibility in the amorphous state as a primary requirement.

Just as with co-crystal formation the greatest challenge associated with amorphous and co-amorphous solid-state forms is the production on large scale and manufacturing for commercialisation. The few marketed pharmaceutical products containing pure amorphous drugs are: zafirlukast (Accolate[®]), cefuroxime axetil (Ceftin[®]) and quinapril hydrochloride (Accupril[®]) (Chavan *et al.*, 2019). The co-amorphous forms of carvedilol prepared using different amino acids, as reported by Mishra *et al.* (2018) showed an improvement of dissolution rate by changing crystalline carvedilol to amorphous and co-amorphous forms using ball milling, liquid assisted grinding (LAG) and spray drying. The novobiocin amorphous cream was found to be 10 times more soluble in 0.1N hydrochloric acid compared to its crystalline form, but unstable due to conversion into its crystalline form (Mansour *et al.*, 2018). Current research is focused on stabilising the amorphous forms long enough to prevent

recrystallisation prior to patient administration and epithelial permeation. Other methods of amorphous form stabilisation have been reported in literature and includes, storing the amorphous form at temperatures lower than the glass transition temperature and entrapment of the amorphous form in the nanopores of mesoporous inorganic silicates (Mansour *et al.*, 2018).

Several preparation methods may be employed to render crystalline APIs into the amorphous state. Amorphous solid-state forms are formed by keeping a highly disordered molecular arrangement from reorganising back to into a highly organised molecular packing. Depending on the starting materials it can be achieved by lattice disruption through roller compaction, milling, desolvation of solvates or hydrates, condensation and quench cooling of the melt (Byrn, Zografi and Chen, 2017a). Furthermore, these forms can be prepared by freeze drying, rapid precipitation by antisolvent addition, spray drying and hot melt extrusion (HME). Compounds showing good glass forming ability forms amorphous solid-state forms easier than compounds that is characterised as poor glass formers (Yu, 2001). The glass-forming ability (GFA) of a material is defined as the potential of a material to vitrify on cooling from the melted state or forming a glass due to spray-drying or mechanical activation. Compounds with a molecular weight above 300 g/mol have demonstrated a good GFA. Furthermore, parameters of molecular flexibility, branched carbon skeletons, electronegative atom presence and a low number of aromatic rings are predictors of a good GFA compound (Alhalaweh *et al.*, 2014).

Co-amorphous compounds are typically prepared using methods such as melting, solvent and mechanical activation. During melting the process of HME is typically applied. Solvent techniques include techniques such as solvent evaporation, freeze drying and spray drying. The use of solvents can be employed on a large scale, but it is important to note that solvent residues remaining in the preparation may destabilise the co-amorphous form *via* recrystallisation or solvate formation. Milling methods include cryomilling and vibrational ball milling. The latter is the main method currently used in the preparation of co-amorphous forms. Advantages of this method is that it is conducted at low temperatures, resulting in low chemical degradation and high recovery compared to some of the other mentioned methods. During the milling process, successful co-amorphous formation relies on milling time, vibrational frequency, and temperature. Quench cooling is another method used to produce co-amorphous forms. During this method, samples are heated in a closed system until the mixture of the components has

reached a completely molten state. Subsequently, the temperature of the system is brought down abruptly by quenching it with ice or liquid nitrogen. (Chavan *et. al* 2016).

3.2.6 Solid dispersions

In 1971, Chiou and Riegelman defined a solid dispersion as a dispersion of one or more API in an inert carrier within the solid state prepared by the melting (fusion), solvent, or melting-solvent methods. From this provided definition it is evident that pharmaceutical solid dispersions are a very broad class which includes eutectic mixtures, solid solutions, glass solutions which are often called amorphous solid dispersion (ASD) and glass suspensions. Further to this, ASDs are further divided into subcategories based on the excipients that stabilise the amorphous API whether it is polymeric or non-polymeric and the former are further divided in mesoporous silica-based glass solution and co-amorphous formulation as shown in Figure 3.4. It is important to note that by definition, solid dispersions and solid solutions can be differentiated from one another based on the molecular state of the API within the carrier matrix. If the API is transformed to an amorphous form and the preparation process forms a one phase system with the polymer the solid dispersion can be classified as a solid solution (further discussed in paragraph 3.2.8). Whilst, if the API exists as a microcrystalline dispersion, in other words two distinct phases can be distinguished (crystalline and amorphous) the system is generally characterised as a solid dispersion (Goldberg, Gibaldi, and Kanig, 1965; Chokshi *et al.*, 2007).

Polymeric ASDs are very common these days with many marketed pharmaceutical products containing ASDs (Dengale *et al.*, 2016). Examples of marketed pharmaceutical products containing solid dispersions include: Kaletra[®] (lopinavir, ritonavir), Intelence[®] (etravirin), Certican[®] (everolimus), Prograf[®] (tacrolimus), and Sporanox[®] (itraconazole). Successful ASD preparation entails using amorphous carriers exhibiting elevated glass transition temperatures (Janssens and van den Mooter, 2009). It is a prerequisite condition for the drug and the polymer to be miscible to form a physically stable ASD (He and Ho, 2015). The downside of solid dispersions is the crystallisation of amorphous drug during storage. This is orchestrated by the presence of water which might increase drug mobility and promote drug crystallisation. Furthermore, some hygroscopic polymers used in solid dispersions can promote phase separation, crystal growth or conversion from a metastable crystalline (Jermain, Brough, and

Williams, 2018). The two major processes used in preparing solid dispersions are melting and solvent evaporation methods. Melting is done by melting the drug within the carrier followed by cooling and pulverisation of the obtained product while solvent evaporation is done by solubilisation of the drug and carrier in a volatile solvent which is later evaporated. Solvent methods require the solubility of carriers in organic solvents for solid dispersion formation (Aggarwal, Gupta and Chaudhary, 2010).

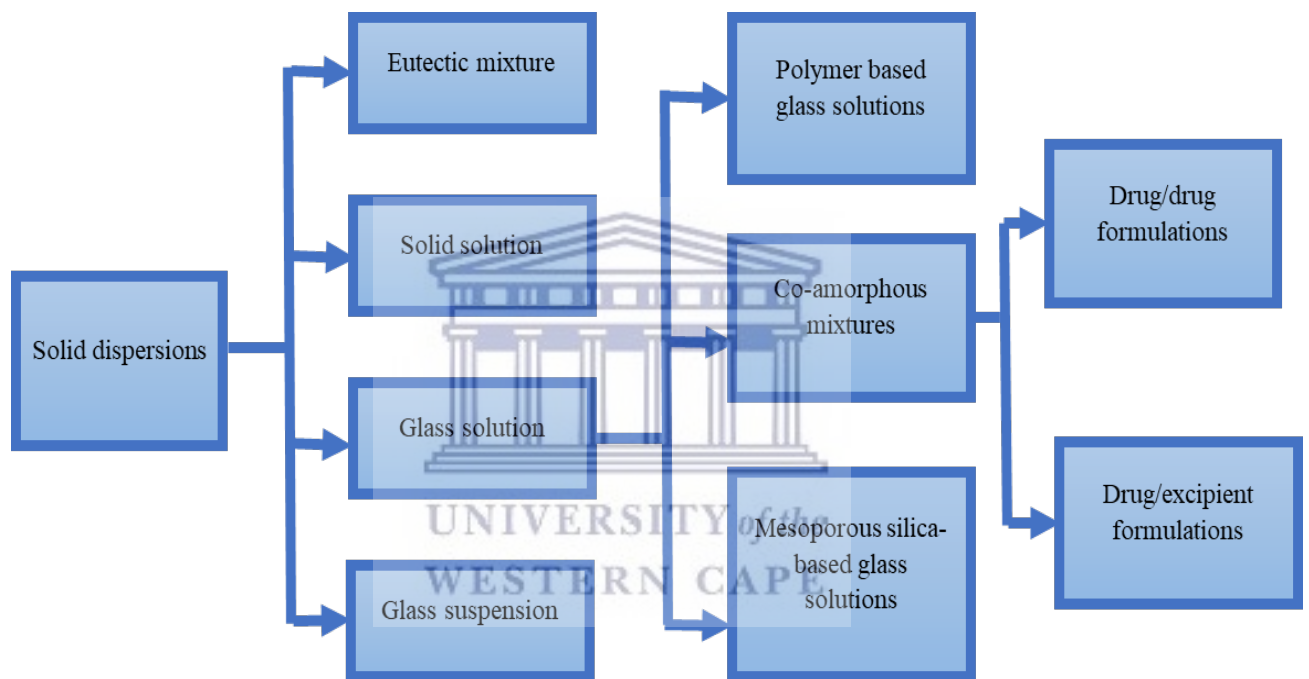


Figure 3.3: Solid dispersions classification as adapted from Dengale et al., 2016.

3.2.6.1 Eutectic mixtures

Eutectic mixtures have several definitions. These mixtures or solid-state forms may be defined by an isothermal, reversible reaction that produces a single liquid phase between two or more solid phases during the heating of a system (Thipparaboina *et al.*, 2017). They are also defined as a fixed proportion mixture of substance, that melts and freezes at a single temperature that is lower than the melting points of any the raw material that constitute the mixture. The resulting crystal structure is characterised as a heterogeneous solid solution or in another term, discontinuous solid solutions. Like solid dispersions, eutectic mixtures gain their solubility

and dissolution advantage, from their higher thermodynamic properties such as free energy, enthalpy, and entropy. The marketed pharmaceutical product, EMLA[®], contains an eutectic mixture of lidocaine and prilocaine. This eutectic mixture exhibits rapid skin permeation, lower melting point and an improved pharmacological effect compared to the individual drugs (Cherukuvada and Nangia, 2014). There are not many eutectic systems produced in the pharmaceutical industry, and it is probably due to the lack of understanding of their microstructures and characterisation difficulties. Eutectic mixtures can be prepared by gentle mechanical mixing, compaction, fusion and solvent based methods. Rifampicin and isoniazid eutectic mixture were successfully produced by neat grinding for 15 minutes and produced a stable eutectic mixture (Cherukuvada and Nangia 2012).

3.2.6.2 Solid solution

A solid solution is a subdivision of ASDs, and it is defined as the formation of a homogenous mixture of a drug and a crystalline carrier which are fully soluble with one another (Kim *et al.*, 2011). An important characteristic of solid solutions that is worthy of noting is that it consists of one phase irrespective of the number of components and the associated particle size of the drug is at an absolute minimum with regards to its molecular dimensions. Solid solutions are grouped either based on the miscibility of the different compounds with one another (continuous or discontinuous) or according to the manner in which the solute molecules are distributed in the solvent molecules (substitutional, interstitial, and amorphous). It is worthy to mention that to understand these concepts better the solid state should not be confused here with the liquid state, in other words true to the term “solid solution”, the molecules remain in the solid state (Chiou, and Riegelman, 1971).

- (a) *Continuous solid solutions*: In such a system the components are miscible regardless of the proportions of the components, it means that the intermolecular bonding would be greater than intramolecular bonding, except that this type of solid solutions has not been reported yet in the literature;
- (b) *Discontinuous solid solutions*: In these systems the solubility of the one compound in the other is limited, existing at a specific composition of the mixture. Moreover, it is temperature dependent, maximum at the eutectic temperature and decreasing with temperature reduction. In this case, the term solid solution only applies if the mutual

solubility of the two components is above 5% (Goldberg, Gibaldi, and Kanig, 1965, (Laitinen *et al.*, 2014).).

The other types of solid solutions differ either by solute substituting solvent molecules in the crystal lattice or the solutes occupying the interstitial spaces between the solvent molecules and lastly if solutes are dispersed within the solvent in a molecular ratio but in an irregularly. The most common preparation methods for solid solutions are hot melt and solvent evaporation (Leuner and Dressman, 2000). The solid solution prepared by Chokshi *et al.* (2007) using PVPK30 (polyvinylpyrrolidone K30), poloxamer 188 and a hydrophobic model drug marked an elevated dissolution rate due to conversion of the crystalline form of the drug to an amorphous form. The study compared the physical mixture, the solid dispersion, and the solid solution with one another. The solid dispersion was approved as the best choice due to the conversion of the amorphous drug in the solid solution converting back to the crystalline form of the drug during stability stress testing conditions.

3.2.6.3 Glass solutions and glass suspensions

Glass suspensions are derived from glass solutions when there is a limited miscibility of an amorphous drug in an amorphous carrier. Glass solutions are homogenous mixtures of an amorphous carrier and amorphous drug, existing as one phase. The viscosity associated with glass solutions requires mixing to ensure the homogeneous mixture of the amorphous drug and carrier. When drug content increases and causes phase separation in a glass solution, it creates a drug-rich amorphous phase, which leads to glass suspension conversion (Laitinen *et al.*, 2014). A glass solution exhibits one T_g while a glass suspension shows two T_g phases, and it is therefore considered to be heterogeneous. Glass suspensions form part of the second generation of solid dispersions and drugs with high melting points are good candidates for glass suspension formation. There is also a mixture of both, glass solution and suspension, when there is heterogeneous structure with mixed properties (Vasconcelos, Sarmiento and Costa, 2007, Van Drooge *et al.*, 2006). During this literature review process, it was noted that there is limited literature available describing glass suspensions and many experiments are reported as solid dispersions without necessarily indicating which type of solid dispersion they are.

3.3 Solubility

Solubility is an ability of a solute to form a homogenous solution when dissolved in a solvent and it is dependent on temperature and pressure. Though many drugs are in a solid form, they must be dissolved in solution for absorption to take place to reach the intended site of action (Censi and Di Martino, 2015). Pharmaceutical compounds are classified in categories based on their solubility and permeability levels. Figure 3.5 illustrates the BCS of pharmaceutical compounds. The drug is classified as highly soluble if the highest dose is soluble in 250 ml of water. It is highly permeable if the absorption is $> 90\%$ or the assessed *in vitro* or *in vivo* permeability is equal or greater to the reference than that of a reference compound that is 90% absorbed. Low drug solubility is a major concern in pharmaceutical development since it affects the other systems that depend on it such as, drug permeation, dosage, and the present environment within the GIT. It is the reason why a great number of strategies have been developed to increase the solubility of drugs. To name a few, there is particle size reduction, polymorphs, salts, surfactants, cosolvents, cocrystals, amorphous solid dispersions, lipid-based systems formation (Williams *et al.*, 2013). These strategies are greatly explored due to numerous compounds that are being discovered with poor solubility. In this study, TZD and PDX solubility will be quantified and compared before and after combination.

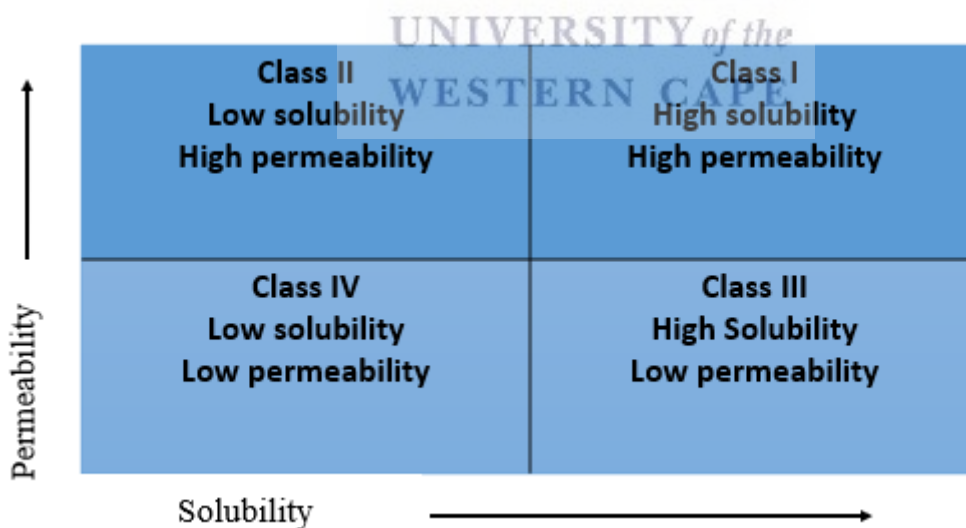


Figure 3.5: BCS classification of pharmaceutical compounds based on permeability and solubility. Adapted from Williams *et al.*, 2013.

Bioavailability (BA) is defined as the rate and extent to which the API or active moiety is absorbed from a drug product, and it is available at the site of action. Three factors affect BA:

(1) physicochemical characteristics of a drug, (2) dosage factors and (3) physiological factors associated with the gastro-intestinal tract (Zhu, Zhou and Seitz, 2016). A significant difference in solubility of different solid-state forms of a drug may result in difference in the oral absorption and thus affecting the oral BA. It was observed that metastable polymorphs of a compound have higher BA compared to the stable polymorph (Singhal and Curatolo, 2004). Therefore, BA can be enhanced by solid-state modification such as formation of amorphous solid dispersion and consequently improving the therapeutic efficiency of the poorly soluble drugs (Pandi *et al.*, 2020).

3.4 Compatibility

Pharmaceutical formulation requires the combination of an API with multiple APIs or just with excipients. Excipients are mostly considered to be pharmacologically inert, but there are cases where chemical or physical interaction/incompatibilities were reported. This compromises the purity of the API(s) or the specific solid-state form in which the API(s) exists which in turn could potentially lead to changes in API solubility, dissolution rate, bioavailability, and clinical efficacy. Compatibility studies are mandated at early stages of drug development and technology research to prevent wastage of costly materials and to achieve a suitable pharmaceutical formulation quickly (Chadha and Bhandari, 2014).

Compatibility studies can become very complex and intricate and thermal techniques such as differential scanning calorimetry (DSC) is a powerful technique used to detect the occurrence of incompatibilities between the API(s)-API(s) or API(s)-excipients. Hot-stage microscopy (HSM) and thermogravimetric analysis (TGA) are typically used in conjunction with DSC to determine the type of incompatibilities present in a mixture under investigation (Sims *et al.*, 2003; Clas, Dalton and Hancock, 1999).

Spectroscopic techniques such as Fourier-Transform infrared spectroscopy (FTIR), are also used for compatibility studies to detect vibrational changes of potential intermolecular interactions between the components of the mixture. The interactions may cause polymorphic changes or transformations, dehydration, hydrate formation and desalting, which could lead to an undesirable effect (Chadha and Bhandari, 2014). Traditional compatibility studies are time

consuming and often rely on the researcher's experience. Novel experimental methods such as PharmDE, an online system that establish drug-excipient incompatibility risk evaluation are being developed to predict the compatibilities of components easily and efficiently using an automated response system (Wang *et al.*, 2021).

3.5 Fixed dose combinations (FDC)

Fixed dose combination (FDC) is a pharmaceutical formulation containing two or more APIs with different pharmacological action formulated in a fixed ratio into a single dosage form (Desai *et al.*, 2013). Co-crystals or solid dispersions enables FDC formulation where the final pharmaceutical product will exhibit superior performance in terms of drug solubility and bioavailability due to the use of enhanced solid-state forms. When considering the formulation of and FDC, the combination must be rational, such that it offers an advantage to the patient. Risks and benefits must be evaluated before the combination is pursued and properties of combined drugs must be investigated (Gautam and Saha, 2008).

Chronic conditions of cardiovascular diseases, HIV, TB, and malaria rely on FDCs due to the high pill-burden experienced by patients suffering from these mentioned diseases. The utilisation of FDCs as part of treatment regimens results in improvement of patient care and adherence with less expenditure. The profit margin for FDC production is higher compared to the separate products, as the manufacturing and distribution is easier and the shelf-life of the product gets extended (Moon and Oh, 2016). FDCs are typically divided into three types or drug release systems, namely: monolithic, multiple-layer and multi-particulate systems. Monolithic systems are easy to manufacture, and it is typically used when a similar dissolution rate is required. Limitations associated with monolithic FDCs are (a) the compatibility of the APIs, and (b) a wide differential in the API doses can induce formulation separation. Multi-layer FDC systems are used when the APIs to be incorporated into the FDC are incompatible with one another and different dissolution profiles are required. Hot melt extrusion, dry and wet granulation are typical methods used to prepare these multi-layered systems. Atripla[®] is an example of a multi-layer system consisting of 600 mg efavirenz, 245 mg tenofovir disoproxil fumarate and 200 mg emtricitabine.

Lastly, multi-particulate FDC systems includes differing drug releasing units such as coated pellets or granules. The simplest manufacturing method is to encapsulate the granules or pellets in capsule shells as demonstrated in Figure 3.6. The process involves coating of each API or

forming layers within a capsule. This process uses advanced formulation techniques such as roller compaction with milling, wet granulation, hot-melt extrusion, co-crystallisation, and spray drying. FDCs can provide APIs in such a manner to the human body that it may function and provide a pharmacological effect in a synergistic manner. FDCs containing antibiotics are typically used to combat microbial resistance, target multiple infections at once and due to potential synergistic pharmacological effects might require lower minimum inhibitory concentration (Fernández-García, *et al.*, 2020). In comparison with FDC formulations, co-crystal or solid dispersion formation share the same if not more benefits because of the formation of physicochemically improved crystalline or amorphous structures. The formulation of an API with a co-drug have potential to increase the solubility, dissolution rate, bioavailability, chemical and physical stabilisation through intermolecular interactions (Rossi *et al.*, 2018). The hypothesis for this study is that the combination of PDX with TZD, either as a co-crystal or a solid dispersion, will not only reduce TZD side effects, but it might also improve its physicochemical properties.

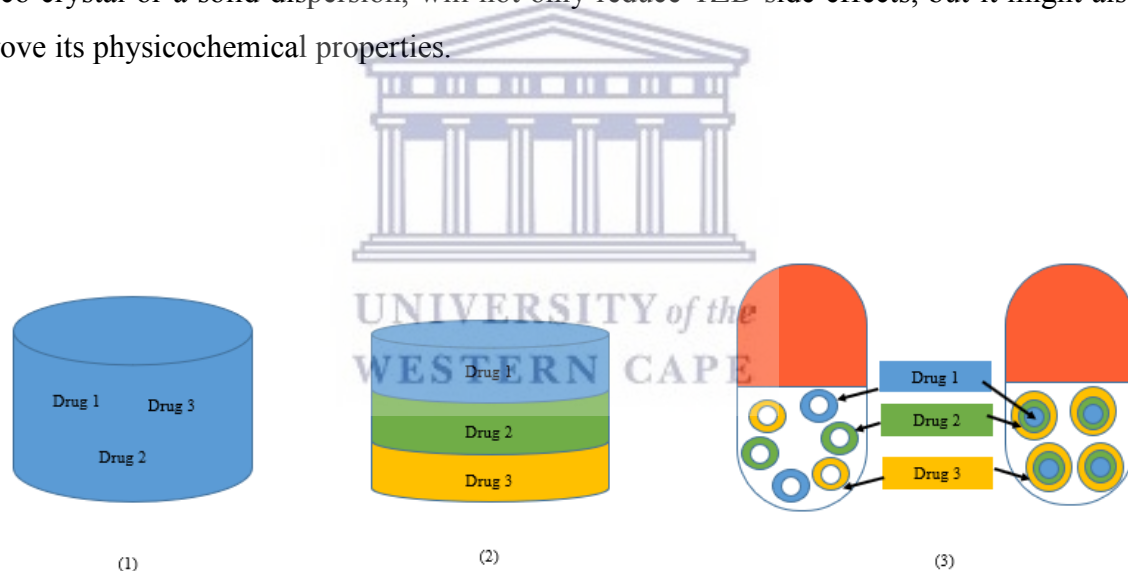


Figure 3.6: FDC types of system: monolithic (1), multiple-layer system (2) and multiparticulate systems (3) as adapted from (Fernández-García, *et al.*, 2020).

3.6 Conclusion

This is an investigational study into the possible combination of TZD and PDX. It was therefore paramount to study and come to terms with the subject of solid-state chemistry of drugs as a whole. This chapter highlighted the importance of knowing the solid-state form(s) in which a particular drug may exist, and which methods and strategies may be explored in order to improve the physicochemical properties of an API that proves to be detrimental to the overall performance thereof. Further to this the associated advantages and disadvantages for each solid-state form has been described. In each instance, marketed dosage forms and experimental research examples were provided for each type of solid-state form. Overall, the subject area of solid-state chemistry of drugs and its linkage to pharmaceutical dosage form formulation is broad and complex.



3.7 References

- Acharya, P.C., Shetty, S., Fernandes, C., Soares, D., Maheshwari, R. and Tekade, R.K.** 2018. Preformulation in Drug Research and Pharmaceutical Product Development. In: Tekade R.K. (Ed). *Dosage Form Design Considerations*. Amsterdam: Elsevier, 1-55. Doi: <https://doi.org/10.1016/B978-0-12-814423-7.00001-0>.
- Aggarwal, S., Gupta, G.D. and Chaudhary, S.** 2010. Solid dispersion as an eminent strategic approach in solubility enhancement of poorly soluble drugs. *International Journal of Pharmaceutical Sciences and Research*, 1(8):1-13. Doi: [http://dx.doi.org/10.13040/IJPSR.0975-8232.1\(8-S\).1-135](http://dx.doi.org/10.13040/IJPSR.0975-8232.1(8-S).1-135).
- Ainurofiq, A., Mauludin, R., Mudhakir, D. and Soewandhi, S.** 2018. A Novel Desloratadine-Benzoic Acid Co-Amorphous Solid: Preparation, Characterization, and Stability Evaluation. *Pharmaceutics*, 10(3):85. Doi:10.3390/pharmaceutics10030085.
- Alhalaweh, A., Alzghoul, A., Kaialy, W., Mahlin, D. and Bergström, C.A.** 2014. Computational predictions of glass-forming ability and crystallization tendency of drug molecules. *Molecular Pharmaceutics*, 11(9):3123-3132. Doi: <dx.doi.org/10.1021/mp500303>.
- Bastin, R.J., Bowker, M.J. and Slater, B.J.** 2000. Salt selection and optimisation procedures for pharmaceutical new chemical entities, *Organic Process Research and Development*, 4(5):427–435. Doi: <https://doi.org/10.1021/op000018u>.
- Berry, D.J. and Steed, J.W.** 2017. Pharmaceutical cocrystals, salts and multicomponent systems; intermolecular interactions and property-based design. *Advanced Drug Delivery Reviews*, 117:3-24. Doi: 10.1016/j.addr.2017.03.003.
- Blagden, N., de Matas, M., Gavan, P. and York, P.** 2007. Crystal engineering of active pharmaceutical ingredients to improve solubility and dissolution rates. *Advanced Drug Delivery Reviews*, 59(7):617-630. Doi: <https://doi.org/10.1016/j.addr.2007.05.011>.
- Braun, D.E. and Griesser, U.J.** 2016. Why do hydrates (solvates) form in small neutral organic molecules? Exploring the crystal form landscapes of the alkaloids brucine and strychnine. *Crystal Growth & Design*, 16(11):6405-6418. Doi: <https://doi.org/10.1021/acs.cgd.6b01078>.
- Buckton, G.** Solid-state properties 2018. In: Aulton, M.E. and Taylor, K.M.G. ed(s). *Aulton's Pharmaceutics E-Book: The Design and Manufacture of Medicines*. 5th ed. Edinburgh: Elsevier, p. 131. Available at < <https://web-b-ebsohost-com.ezproxy.uwc.ac.za/ehost/ebookviewer/ebook/bmxlYmtfXzE2OTcxNTVfX0FO0?sid=51838e41-0d39-4658-b9ed-4fc951f9a5a3@sessionmgr103&vid=0&format=EB&rid=1>> (Accessed: 9 October 2021).
- Brittain, H.G.** 2011. Cocrystal systems of pharmaceutical interest: 2009. In: Brittain, H.G. (Ed.). *Profiles of Drug Substances, Excipients and Related Methodology*. San Diego, Elsevier, Vol. 36:361-381. Doi:10.1016/B978-0-12-387667-6.00010-5.

- Byrn, S.R., Zografi, G. and Chen, X.S.** 2010. Accelerating proof of concept for small molecule drugs using solid-state chemistry. *Journal of Pharmaceutical Sciences*, 99(9):3665-3675. Doi: <https://doi.org/10.1002/jps.22215>.
- Byrn, S.R., Zografi, G. and Chen, S.** 2017a. Amorphous solids. In: Byrn, S.R., Zografi, G. and Chen, S. Ed(s). *Solid state properties of pharmaceutical materials*. Hoboken, NJ: Wiley, 69-87.
- Byrn, S.R., Zografi, G. and Chen, S.** 2017b. Solvates and hydrates . In: Byrn, S.R., Zografi, G. and Chen, S. Ed(s). *Solid state properties of pharmaceutical materials*. Hoboken, NJ: Wiley, 38-46.
- Cains, P.W.** 2009. Classical methods of preparation of polymorphs and alternative solid forms. In: Brittain, H.G. (Ed). *Polymorphism in Pharmaceutical Solids*. Vol.192. New York: CRC Press, 76-138.
- Censi, R. and Di Martino, P.** 2015. Polymorph impact on the bioavailability and stability of poorly soluble drugs. *Molecules*, 20(10):18759-18776. Doi: <https://doi.org/10.3390/molecules201018759>.
- Chadha, R. and Bhandari, S.** 2014. Drug–excipient compatibility screening—role of thermoanalytical and spectroscopic techniques. *Journal of pharmaceutical and Biomedical Analysis*, 87:82-97. Doi: <https://doi.org/10.1016/j.jpba.2013.06.016>.
- Chavan, R.B., Rathi, S., Jyothi, V.G.S. and Shastri, N.R.** 2019. Cellulose based polymers in development of amorphous solid dispersions. *Asian Journal of Pharmaceutical Sciences*, 14(3):248-264. <https://doi.org/10/1016/j.ajps.2018.09.003>.
- Chavan, R., Thipparaboina, R., Yadav, B. and Shastri, N.** 2018. Continuous manufacturing of co-crystals: challenges and prospects. *Drug Delivery and Translational Research*, 8(6):1726-1739. Doi: <https://doi.org/10.1007/s13346-018-0479-7>.
- Cherukuvada, S. and Nangia, A.** 2012. Fast dissolving eutectic compositions of two anti-tubercular drugs. *CrystEngComm*, 14(7):2579-2588. Doi: <https://doi.org/10.1039/C2CE06391C>.
- Cherukuvada, S. and Nangia, A.** 2014. Eutectics as improved pharmaceutical materials: design, properties and characterization. *Chemical Communications*, 50(8):906-923. Doi: <https://doi.org/10.1039/C3CC47521B>.
- Chiou, W.L. and Riegelman, S.** 1971. Pharmaceutical applications of solid dispersion systems. *Journal of Pharmaceutical Sciences*, 60(9):1281-1302. Doi: <https://doi.org/10.1002/jps.2600600902>.
- Chokshi, R.J., Zia, H., Sandhu, H.K., Shah, N.H. and Malick, W.A.** 2007. Improving the dissolution rate of poorly water soluble drug by solid dispersion and solid solution—pros and cons. *Drug Delivery*, 14(1):33-45. Doi: <https://doi.org/10.1080/10717540600640278>.

- Clas, S.D., Dalton, C.R. and Hancock, B.C.** 1999. Differential scanning calorimetry: applications in drug development. *Pharmaceutical Science & Technology Today*, 2(8):311-320. Doi: [https://doi.org/10.1016/S1461-5347\(99\)00181-9](https://doi.org/10.1016/S1461-5347(99)00181-9).
- Dengale, S., Grohganz, H., Rades, T. and Löbmann, K.** 2016. Recent advances in co-amorphous drug formulations. *Advanced Drug Delivery Reviews*, 100:116-125. <https://doi.org/10.1016/j.addr.2015.12.009>.
- Desai, D., Wang, J., Wen, H., Li, X. and Timmins, P.** 2013. Formulation design, challenges, and development considerations for fixed dose combination (FDC) of oral solid dosage forms. *Pharmaceutical Development and Technology*, 18(6):1265-1276. Doi: <https://doi.org/10.3109/10837450.2012.660699>.
- El-Yafi, A.K.E.Z. and El-Zein, H.** 2015. Technical crystallization for application in pharmaceutical material engineering. *Asian Journal of Pharmaceutical Sciences*, 10(4):283-291. Doi: <https://doi.org/10.1016/j.ajps.2015.03.003>.
- Fernández-García, R., Prada, M., Bolás-Fernández, F., Ballesteros, M.P. and Serrano, D.R.** 2020. Oral fixed-dose combination pharmaceutical products: Industrial manufacturing versus personalized 3D printing. *Pharmaceutical Research*, 37(7):1-22. <https://doi.org/10.1007/s11095-020-02847-3>.
- Gautam, C. S. and Saha, L.** 2008 'Fixed dose drug combinations (FDCs): rational or irrational: a view point', *British Journal of Clinical Pharmacology*, 65(5):795–796.
- Goldberg, A.H., Gibaldi, M. and Kanig, J.L.** 1965. Increasing dissolution rates and gastrointestinal absorption of drugs via solid solutions and eutectic mixtures I: Theoretical considerations and discussion of the literature. *Journal of Pharmaceutical Sciences*, 54(8):1145-1148.
- Graeser, K.A., Patterson, J.E., Zeitler, J.A. and Rades, T.** 2010. The role of configurational entropy in amorphous systems. *Pharmaceutics*, 2(2):224-244. Doi: <https://doi.org/10.3390/pharmaceutics2020224>.
- He, Y. and Ho, C.** 2015. Amorphous solid dispersions: utilization and challenges in drug discovery and development. *Journal of Pharmaceutical Sciences*, 104(10):3237-3258. Doi: <https://doi.org/10.1002/jps.24541>.
- Healy, A., Worku, Z., Kumar, D. and Madi, A.** 2017. Pharmaceutical solvates, hydrates and amorphous forms: A special emphasis on cocrystals. *Advanced Drug Delivery Reviews*, 117:25-46. Doi: <https://doi.org/10.1016/j.addr.2017.03.002>.
- Janssens, S. and van den Mooter, G.** 2009. Physical chemistry of solid dispersions. *Journal of Pharmacy and Pharmacology*, 61(12):1571-1586. Doi: 10.1211/jpp/61.12.0001.
- Jermain, S.V., Brough, C. and Williams, R.O.** 2018. Amorphous solid dispersions and nanocrystal technologies for poorly water-soluble drug delivery – An update, *International Journal of Pharmaceutics*, 535(1–2):379–392. Doi: <https://doi.org/10.1016/j.ijpharm.2017.10.051>.

Khankari, R.K. and Grant, D.J. 1995. Pharmaceutical hydrates. *Thermochimica Acta*, 248:61-79. Doi: [https://doi.org/10.1016/0040-6031\(94\)01952-D](https://doi.org/10.1016/0040-6031(94)01952-D).

Karagianni, A., Malamataris, M. and Kachrimanis, K. 2018. Pharmaceutical cocrystals: New solid phase modification approaches for the formulation of APIs. *Pharmaceutics*, 10(1):1–30. Doi: <https://doi.org/10.3390/pharmaceutics10010018>.

Kawakami, K. 2009. Current status of amorphous formulation and other special dosage forms as formulations for early clinical phases. *Journal of Pharmaceutical Sciences*, 98(9):2875-2885. Doi: <https://doi.org/10.1002/jps.21816>.

Kim, K.T., Lee, J.Y., Lee, M.Y., Song, C.K., Choi, J.H. and Kim, D.D. 2011. Solid dispersions as a drug delivery system. *Journal of Pharmaceutical Investigation*, 41(3):125-142. Doi : <https://doi.org/10.4333/KPS.2011.41.3.125>.

Laitinen, R., Priemel, P.A., Surwase, S., Graeser, K., Strachan, C.J., Grohganz, H. and Rades, T. 2014. Theoretical considerations in developing amorphous solid dispersions. In: Shah, N. Sandhu, H. and Choi, D. S. *Amorphous Solid Dispersions*. New York : Springer, 35-90.

Lee, E.H. 2014. A practical guide to pharmaceutical polymorph screening & selection. *Asian Journal of Pharmaceutical Sciences*, 9(4):163-175. <https://doi.org/10.1016/j.ajps.2014.05.002>.

Leuner, C. and Dressman, J. 2000. Improving drug solubility for oral delivery using solid dispersions. *European Journal of Pharmaceutics and Biopharmaceutics*, 50(1):47-60. Doi: 10.1016/S0939-6411(00)00076-X.

Mansour, R.S., Deb, P.K. and Tekade, R.K. 2018. Role of Amorphous State in Drug Delivery. In: Tekade, R. *Dosage Form Design Parameters*. London: Academic Press, 105-154. Doi: <https://doi.org/10.1016/B978-0-12-814421-3.00004-X>.

Mishra, J., Löbmann, K., Grohganz, H. and Rades, T. 2018. Influence of preparation technique on co-amorphization of carvedilol with acidic amino acids. *International Journal of Pharmaceutics*, 552(1-2):407-413. Doi : <https://doi.org/10.1016/j.ijpharm.2018.09.070>.

Morissette, S.L., Almarsson, Ö., Peterson, M.L., Remenar, J.F., Read, M.J., Lemmo, A.V., Ellis, S., Cima, M.J. and Gardner, C.R. 2004. High-throughput crystallization: polymorphs, salts, co-crystals and solvates of pharmaceutical solids. *Advanced Drug Delivery Reviews*, 56(3):275-300. Doi: <https://doi.org/10.1016/j.addr.2003.10.020>.

Moon, C. and Oh, E. 2016. Rationale and strategies for formulation development of oral fixed dose combination drug products. *Journal of Pharmaceutical Investigation*, 46(7):615-631.

Omar, M., Makary, P. and Wlodarski, M. 2015. A review of polymorphism and the amorphous state in the formulation strategy of medicines and marketed drugs. *UK Journal of Pharmaceutical and Biosciences*, 3(6):60-66. Doi: 10.1007/s40005-016-0286-4.

Ouiyangkul, P., Tantishaiyakul, V. and Hirun, N. 2020. Exploring potential cofomers for oxyresveratrol using principal component analysis. *International Journal of Pharmaceutics*, 587, p.119630. Doi: <https://doi.org/10.1016/j.ijpharm.2020.119630>.

Pandi, P., Bulusu, R., Kommineni, N., Khan, W. and Singh, M. 2020. Amorphous solid dispersions: An update for preparation, characterization, mechanism on bioavailability, stability, regulatory considerations and marketed products. *International Journal of Pharmaceutics*, 586, p.119560. Doi: <https://doi.org/10.1016/j.ijpharm.2020.119560>.

Pindelska, E., Sokal, A. and Kolodziejcki, W. 2017. Pharmaceutical cocrystals, salts and polymorphs: Advanced characterization techniques. *Advanced Drug Delivery Reviews*, 117:111-146. Doi: <https://doi.org/10.1016/j.addr.2017.09.014>.

Qiao, N., Li, M., Schlindwein, W., Malek, N., Davies, A. and Trappitt, G. 2011. Pharmaceutical cocrystals: an overview. *International Journal of Pharmaceutics*, 419(1-2):1-11. Doi: <https://doi.org/10.1016/j.ijpharm.2011.07.037>.

Rodrigues, M., Baptista, B., Lopes, J. and Sarraguça, M. 2018. Pharmaceutical cocrystallization techniques. Advances and challenges. *International Journal of Pharmaceutics*, 547(1-2):404-420. Doi: <https://doi.org/10.1016/j.ijpharm.2018.06.024>.

Rossi, F., Cerreia Vioglio, P., Bordignon, S., Giorgio, V., Nervi, C., Priola, E., Gobetto, R., Yazawa, K. and Chierotti, M. 2018. Unraveling the Hydrogen Bond Network in a Theophylline–Pyridoxine Salt Cocrystal by a Combined X-ray Diffraction, Solid-State NMR, and Computational Approach. *Crystal Growth & Design*, 18(4):2225-2233. Doi: <https://doi.org/10.1021/acs.cgd.7b01662>.

Rumondor, A.C., Ivanisevic, I., Bates, S., Alonzo, D.E. and Taylor, L.S. 2009. Evaluation of drug-polymer miscibility in amorphous solid dispersion systems. *Pharmaceutical Research*, 26(11):2523-2534. Doi: [10.1007/s11095-009-9970-7](https://doi.org/10.1007/s11095-009-9970-7).

Sims, J.L., Carreira, J.A., Carrier, D.J., Crabtree, S.R., Easton, L., Hancock, S.A. and Simcox, C.E. 2003. A new approach to accelerated drug-excipient compatibility testing. *Pharmaceutical Development and Technology*, 8(2):119-126. Doi: <https://doi.org/10.1081/PDT-120018476>.

Singhal, D. 2003. Drug polymorphism and dosage form design: a practical perspective. *Advanced Drug Delivery Reviews*, 56(3):335–347. Doi: [10.1016/j.addr.2003.10.008](https://doi.org/10.1016/j.addr.2003.10.008).

Sahoo, P., Kumar, D., Raghavan, S. and Dastidar, P. 2010. Supramolecular Synthons in Designing Low Molecular Mass Gelling Agents: L-Amino Acid Methyl Ester Cinnamate Salts and their Anti-Solvent-Induced Instant Gelation. *Chemistry - An Asian Journal*, 6(4):1038-1047. Doi: [10.1002/asia.201000560](https://doi.org/10.1002/asia.201000560).

Serajuddin, A.T. 2007. Salt formation to improve drug solubility. *Advanced Drug Delivery Reviews*, 59(7):603-616. Doi: [10.1016/j.addr.2007.05.010](https://doi.org/10.1016/j.addr.2007.05.010).

- Singh, A. and Van den Mooter, G.** 2016. Spray drying formulation of amorphous solid dispersions. *Advanced Drug Delivery Reviews*, 100: 27-50. <https://doi.org/10.1016/j.addr.2015.12.010>.
- Singhal, D. and Curatolo, W.** 2004. Drug polymorphism and dosage form design: a practical perspective. *Advanced Drug Delivery Reviews*, 56(3):335-347. Doi: <https://doi.org/10.1016/j.addr.2003.10.008>.
- Stahly, G.P.** 2007. Diversity in single-and multiple-component crystals. The search for and prevalence of polymorphs and cocrystals. *Crystal Growth & Design*, 7(6):1007-1026. Doi: <https://doi.org/10.1021/cg060838j>.
- Tobyn, M., Brown, J., Dennis, A.B., Fakes, M., Gamble, J., Khimyak, Y.Z., McGeorge, G., Patel, C., Sinclair, W., Timmins, P. and Yin, S.** 2009. Amorphous drug-PVP dispersions: application of theoretical, thermal and spectroscopic analytical techniques to the study of a molecule with intermolecular bonds in both the crystalline and pure amorphous state. *Journal Of Pharmaceutical Sciences*, 98(9):3456-3468. Doi: <https://doi.org/10.1002/jps.21738>.
- Thipparaboina, R., Thumuri, D., Chavan, R., Naidu, V.G.M. and Shastri, N.R.** 2017. Fast dissolving drug-drug eutectics with improved compressibility and synergistic effects. *European Journal of Pharmaceutical Sciences*, 104:82-89. Doi: <https://doi.org/10.1016/j.ejps.2017.03.042>.
- Vasconcelos, T., Sarmiento, B. and Costa, P.** 2007. Solid dispersions as strategy to improve oral bioavailability of poor water-soluble drugs. *Drug Discovery Today*, 12(23-24):1068-1075. Doi: <https://doi.org/10.1016/j.drudis.2007.09.005>.
- Van Drooge, D.J., Hinrichs, W.L.J., Visser, M.R. and Frijlink, H.W.** 2006. Characterization of the molecular distribution of drugs in glassy solid dispersions at the nano-meter scale, using differential scanning calorimetry and gravimetric water vapour sorption techniques. *International Journal of Pharmaceutics*, 310(1-2):220-229. Doi: <https://doi.org/10.1016/j.ijpharm.2005.12.007>.
- Vioglio, P.C., Chierotti, M.R. and Gobetto, R.** 2017. Pharmaceutical aspects of salt and cocrystal forms of APIs and characterization challenges. *Advanced Drug Delivery Reviews*, 117:86-110. Doi:10.1016/j.addr.2017.07.001.
- Wang, N., Sun, H., Dong, J. and Ouyang, D.** 2021. PharmDE: A new expert system for drug-excipient compatibility evaluation. *International Journal of Pharmaceutics*, 607:120962. Doi: <https://doi.org/10.1016/j.ijpharm.2021.120962>.
- Williams, H.D., Trevaskis, N.L., Charman, S.A., Shanker, R.M., Charman, W.N., Pouton, C.W. and Porter, C.J.** 2013. Strategies to address low drug solubility in discovery and development. *Pharmacological Reviews*, 65(1):315-499. Doi: <https://doi.org/10.1124/pr.112.005660>.
- Yu, L.** 2001. Amorphous pharmaceutical solids: preparation, characterization, and stabilization. *Advanced Drug Delivery Reviews*, 48(1):27-42. [https://doi.org/10.1016/S0169-49X\(01\)00098-9](https://doi.org/10.1016/S0169-49X(01)00098-9).

Zhu, H., Zhou, H. and Seitz, K. 2016. Bioavailability and bioequivalence. *In: Qiu, Y., Chen, Y., Zhang, G.G., Yu, L. and Mantri, R.V. Eds. Developing Solid Oral Dosage Forms.* New York, Academic Press, 341-364.

Zhou, L., Dodd, S., Capacci-Daniel, C., Garad, S., Panicucci, R. and Sethuraman, V. 2016. Co-crystal formation based on structural matching. *European Journal of Pharmaceutical Sciences*, 88:191-201. Doi: <https://doi.org/10.1016/j.ejps.2016.02.017>.



Chapter 4

Materials and methods

4.1 Introduction

The aim of physicochemical characterisation of pharmaceutical compounds is to investigate the physical, chemical, and bulk properties thereof. As described in Chapters 1 and 2, limited physicochemical characterisation data is currently available for TZD. Therefore, the first part of this study consisted of studying and documenting these characteristics associated with this anti-TB drug. Secondly, the possibility of supramolecular modifications through the combination of TZD and PDX was explored through typical co-crystallisation or co-morphisation techniques. This study relied on a series of characterisation techniques, used in conjunction, to complement one another and to obtain physicochemical characteristics of TZD and PDX separately as well as in combination with one another. This chapter will disseminate all materials and analytical methods used throughout this study.

4.2 Materials

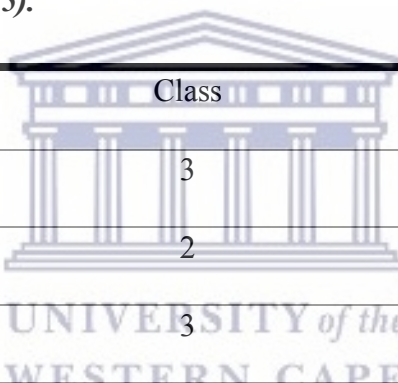
Terizidone (TZD) was an in-kind donation from Chemical Process Technologies (Pretoria, South Africa). The purity of this bulk material was validated against a reference standard with a certified purity of 99.3%, purchased from Toronto Research Chemicals, Canada (Lot No: 2-MJK-168-2). PDX, dimethyl sulfoxide (DMSO), sodium hydroxide (NaOH), hydrochloric acid (HCl), glacial acetic acid, anhydrous sodium acetate, disodium hydrogen orthophosphate and potassium dihydrogen orthophosphate were purchased from Sigma-Aldrich (Johannesburg, South Africa). Ultrapure water with a resistivity of $18.2 \text{ M}\Omega \cdot \text{cm}^{-1}$ was obtained from a Purite, Lasec (Johannesburg, South Africa) water purification system. Chromatography grade acetonitrile and methanol were purchased from Merck (Johannesburg, South Africa).

4.3 Screening of the most suitable preparation method for potential solid-state modifications involving the combination of TZD and PDX

As highlighted in Chapter 3, different techniques are available to facilitate the combination of compounds on a molecular level. The techniques were screened based on equipment availability in the laboratory, or whether it is feasible upon consideration of the determined

physicochemical properties of TZD and PDX. These methods are used to enhance the intermolecular bonding between two or more molecules and formation of new solid-state habits and included (a) solvent evaporation, (b) quench cooling of the melt and (c) liquid assisted grinding (LAG). Table 4.1 outlines some of the typical organic solvents which may be used during recrystallisation, or LAG preparations of drugs and it is this information that informed the safety associated with each organic solvent. Solvents are classified in four classes, the first one being undesirable to work in the laboratory, the second is to be used with precaution within pharmaceutical formulation, the third and fourth pose a lower risk to humans when used in formulation (Prat *et al.*, 2015; ICH, 2016). Table 4.1 indicates the class levels of used solvents, and they are predominantly in class 3, which is safe to use in the laboratory.

Table 4.1: Safety classes and boiling point of the solvents used in the experiment (Joshi and Adhikari, 2019; Prat *et al.*, 2015).



Solvents	Class	Boiling point (°C)
Acetone	3	56.3
Acetonitrile	2	81.65
Butanol	3	117.7
DMSO	3	189.0
Ethanol	3	78.3
Methanol	2	64.7
Propanol	3	97.2

4.3.1 Solvent evaporation

Solvent evaporation is a simple and effective method useful in the screening process of co-crystals on laboratory scale. However, it is known to be environmentally hazardous, and it might facilitate the formation of solvates (Rodrigues *et al.*, 2018). The method was screened by dissolving the TZD and PDX in different solvents (Table 4.1). Equivalent amount of the TZD:PDX mixture was dissolved in different solvents. Enough solvent was placed in a beaker,

placed on a magnetic heating stirrer and the heating temperature was subsequently set at 10 °C below the boiling point of each solvent. The solution was stirred using a magnetic stirrer bar until all TZD was dissolved. The resulting solution was covered with pierced Parafilm® (Bemis, Menasha, USA) and left for solvent evaporation to occur.

4.3.2 Quench cooling of the melt

Melt quenching is the rapid cooling of a molten drug and it is used to prepare amorphous materials (Shi, Moinuddin, and Cai, 2019). Furthermore, it is suitable for compounds which are stable around the melting temperature (Byrn, Zografí and Chen, 2017). This method was pursued in an attempt to form a co-amorphous solid-state form between TZD and PDX. TZD:PDX, 1:1 w/w were placed on aluminium foil and heated using a heating plate (Dragon Lab, China), until melting was observed. The sample was subsequently removed from the heating plate and cooled rapidly on a cold surface.

4.3.3 Liquid assisted grinding (LAG)

LAG is a technique that is also known as solvent drop grinding or wet granulation. It typically enhances the degrees of orientation and conformational freedom of the molecules as well as the possibility of molecular collisions (Shan, Toda, and Jones, 2002). Furthermore, LAG produces higher yield, facilitate crystallinity and the ability to control polymorph formation (Rodrigues *et al.*, 2018). It uses less amount of solvent compared to slow evaporation, which makes it affordable, safe for the environment and it is suitable for discovering new cocrystals and preparing existing ones (Qiao *et al.*, 2011). This is manual mechano-chemical methods and dissolution of the molecules is not required (Malamatari *et al.*, (2017) which is considered advantageous for many drugs. TZD, PDX and the TZD:PDX (1:1 %w/w) mixture were grinded in a mortar by slowly adding different solvents dropwise at regular time intervals. An average of 5 minutes were used for grinding and the samples were characterised after preparation with relevant techniques as depicted in Figure 4.1.

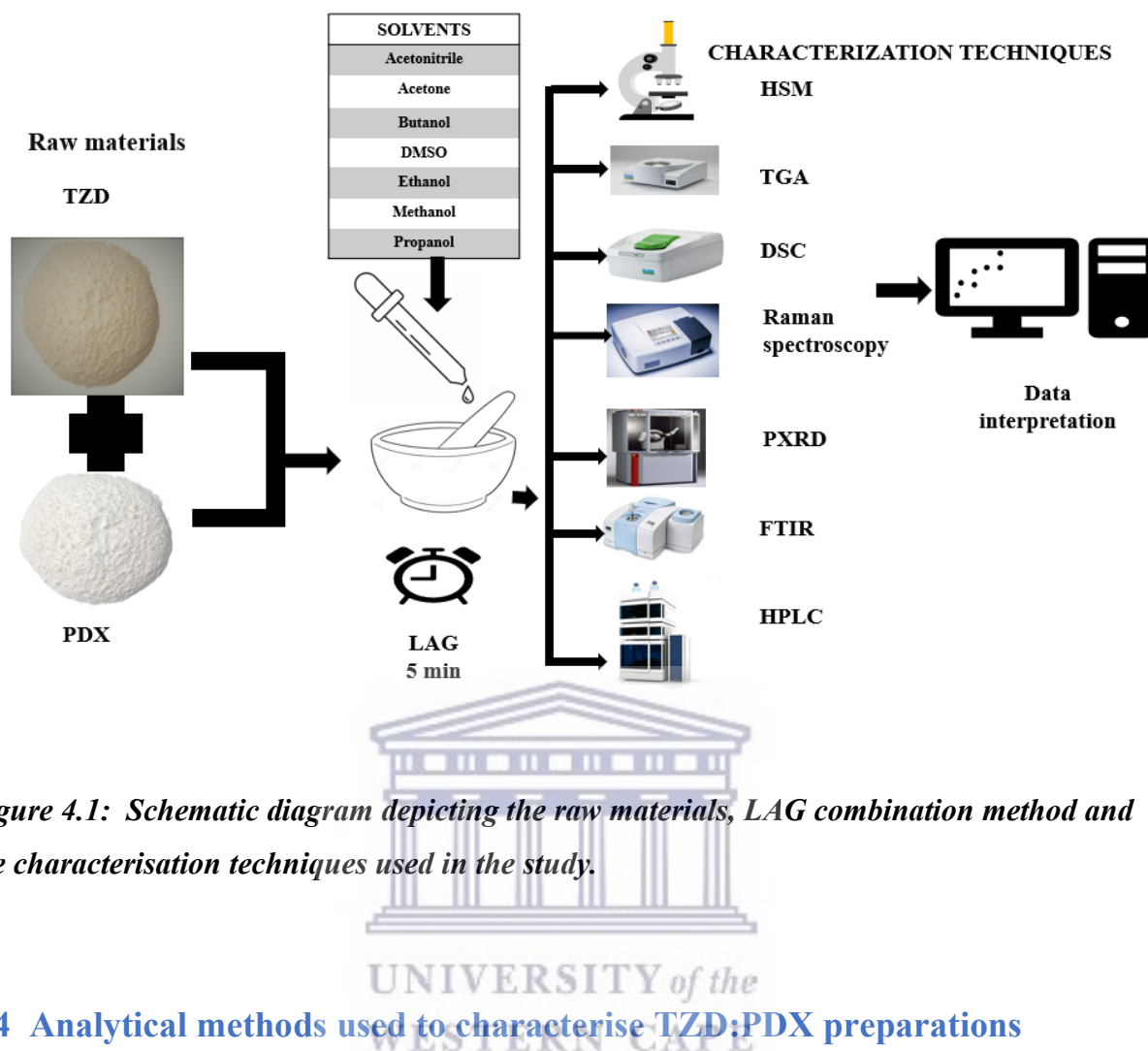


Figure 4.1: Schematic diagram depicting the raw materials, LAG combination method and the characterisation techniques used in the study.

4.4 Analytical methods used to characterise TZD:PDX preparations

4.4.1 Hot stage microscopy (HSM)

Hot stage microscopy (HSM) is an analytical technique that use a microscope to observe the physical properties of compounds as a function of temperature. It is substantially used in the pharmaceutical industry in conjunction with other thermo-analytical techniques to determine the solid-state characteristics of drugs, evaluation of solid-state forms in terms of stability and associated phase transformations which may include, among others, dehydration, desolvation, vapour deposition as well as observations such as melting processes, crystal habits and amorphisation or recrystallisation. (Vitez *et al.*, 1998; Stieger *et al.*, 2012). An Olympus SZX7 (Tokyo, Japan) microscope equipped with a Linkam THMS600 heating stage (Surrey, UK) was used. A temperature range of 25 - 300 °C set at a heating rate of 10 °C/min was used for all HSM analyses conducted during this study. A small amount of either TZD, PDX or TZD:PDX combinations was placed on a microscope slide, then a small drop of silicon oil was placed on the sample followed by the fixing of a cover slip. This preparation was subsequently

placed on the heating stage and the microscope was focused so that the samples were clearly visible. Micrographs were taken at the start of each heating program, and on regular intervals thereafter to allow accurate observation of thermal events. The obtained data served as information for other thermo-analytical techniques, such as thermogravimetric analysis (TGA) and differential scanning calorimetry (DSC), and all these thermal techniques were analysed in conjunction to complement each other.

4.4.2 Thermogravimetric analysis (TGA)

TGA is a thermal technique, in which a substance is subjected to a controlled temperature program, in a controlled atmosphere and its behaviour is observed based either as a function of time or temperature (Perkin Elmer, 2010). It is also used in the study of decomposition of materials and their related kinetics (Fan *et al.*, 2016). In combination with DSC, it provides information of desolvation, dehydration and compound decomposition (Law and Zhou, 2017). TGA was conducted using a TGA 4000 (PerkinElmer, Waltham, USA). The samples, weighing 1-3 mg each were placed in a porcelain crucible. Subsequently, a heating program of 10 °C/min from ambient temperature to 600 °C was used, under a nitrogen purge of 40 ml/min. The weight lost during heating of the sample were subsequently documented using the Pyris® (Perkin Elmer, Waltham, USA) software.

4.4.3 Differential scanning calorimetry (DSC)

DSC is a thermal analytical tool which measures the difference in heat flow between a sample and a reference, observed as a function of time and temperature (Kodre *et al.*, 2014). It enables the measurement of the energy associated with thermal events such as melting, dehydration, desolvation, glass transition, recrystallisation, to name just a few. The principle of DSC relies on measuring the heat flow difference between the sample and the reference when heated at the same time and temperature after a short equilibration time. The process may involve heating, cooling or isothermal conditions and the energy absorbed (endothermic) or released (exothermic) by the sample is translated as a measurement signal, followed by the quantification of the area under the curve (Fortunato, 2013). DSC is also a useful technique during the investigation for possible interactions among formulation components based on the appearance or disappearance of phase transition peaks and/or differences in the corresponding enthalpy or heat capacity values in generated thermal curves of drug-drug or drug-excipient

combinations (Skotnicki *et al.*,2015). A PerkinElmer DSC 8000 (Waltham, USA), equipped with an intracooler was used. Approximately 1 – 3 mg of sample was accurately weighed into an aluminium sample pan and sealed. Nitrogen was used as purge gas at a flow rate of 20 ml/min and a heating rate of 10 °C / min over a range of 25 °C - 250 °C. The resultant DSC trace obtained was analysed and it was used to identify the thermal properties of TZD, PDX and the compatibility between the two drugs by determining phase transformations, melting points, and other relevant properties.

4.4.4 Powder X-Ray Diffraction (PXRD)

PXRD facilitate the study of crystalline phases as materials diffract X-rays in a typical manner. The peak shape and intensity generate information of atomic position and crystallite size. It is generally used for identification and determination of the amounts of the phases present in the materials (Epp, 2016). The three-dimensional crystalline lattice of the material diffracts X-rays as they are passing through and every phase produce a unique pattern. Crystalline and quasicrystalline phases produce sharp peaks while amorphous phases produce nonlinear, halo-like patterns (Freeman, Brockbank, and Sabathier, 2017). PXRD was used for the determination of the solid-state habit of TZD, PDX and associated combinations of the two compounds. During the PXRD analysis the samples were lightly grinded using an agate mortar and pestle. The samples were thereafter distributed evenly on a suitable sample holder. PXRD patterns were obtained using a Bruker D8 Advance (Massachusetts, USA) diffractometer operated at ambient conditions across a scanning range of $4 - 40^{\circ} 2\theta$.

4.4.5 Fourier-Transform infrared spectroscopy (FTIR)

IR light exists in the spectroscopic region ranging from $4000-400\text{ cm}^{-1}$ which corresponds to the wavelengths between 2500 and 25000 nm. It is principled on vibrational spectroscopy since its energy is too low to cause electron transition in molecules (Van Eerdenbrugh and Taylor, 2011). Molecules absorb electromagnetic radiation depending on functional groups present in a molecular structure which leads to bond vibration. The absorbed energy is measured at each specific wavelength and subsequently its corresponding functional bond is deduced (Law and Zhou, 2017). The spectrum is plotted from the intensity of absorbance or transmittance versus the wavenumber, and it correlates to the energy difference between the ground and the excited vibrational states (Larkin, 2017). In this study, a Perkin Elmer Spectrum 400 FTIR (Waltham,

USA) was used to obtain information on the functional groups present in TZD, PDX and potential solid-state modifications consisting of both compounds. The surface on which the sample was placed, it was wiped clean with ethanol prior to the analysis. Subsequently, a small amount of sample was placed upon the scanning surface of the FTIR and a scanning range of 650 to 4000 cm^{-1} was used to obtain a spectroscopic spectrum.

4.4.6 Raman spectroscopy

Raman spectroscopy involves the principle of molecules scattering monochromatic light provided by a laser beam. The Raman spectrum is constructed from the differences between the scattered and the incident light due to the different frequency (Bumrah and Sharma, 2016). In this study, Raman spectroscopy was performed using an Anton Paar Cora 5700 Raman spectrophotometer (Anton Paar, Graz, Austria). The wavelength was set to 1064 nm and scans were collected across the range of 200 to 2000 cm^{-1} .

4.4.7 High performance liquid chromatography (HPLC)

The following method was developed and validated according to ICH guidelines (ICH, 2005). A Knauer (Berlin, Germany) Azura HPLC system equipped with a DAD 2.1L detector, 6.1L autosampler, quaternary pump and column thermostat was used during this method development and validation study. A mobile phase consisting of 30:70 v/v acetonitrile: HPLC grade water with 1 mL of glacial acetic acid added was utilised. The stationary phase was a Supelco™ (Bellefonte, United States) Discovery® C₁₈ (150 × 4.6 mm, 5 μ m) reversed-phase column. Compound detection was done at 260 nm and the sample injection volume was 10 μ L. The HPLC analysis was performed at a flow rate and temperature of 1 ml/min and 25 °C respectively. For HPLC method validation purposes, stock solutions containing 200 $\mu\text{g/ml}$ of TZD and PDX, respectively were prepared using a 50:50 v/v acetonitrile : ultrapure water solution as solvent. Due to the poor solubility of TZD in almost all organic solvents, it was necessary to dissolve TZD first in DMSO. For every 10 mg TZD used, 150 μl of DMSO was used. Subsequently, serial dilutions of the stock solutions were made to achieve solutions in the concentration range of 50.0 – 800.0 $\mu\text{g/ml}$. This method was validated according to the following method development parameters: linearity and range, accuracy, precision, limit of detection (LOD), limit of quantification (LOQ), specificity, robustness, and solution stability. The obtained results obtained was processed using the Analysis Toolpak in Excel.

4.5 Equilibrium solubility studies

The equilibrium solubility was measured using the shake-flask method. It is a method of manually transferring the compound in excess into a vial/flask containing a solvent, then the resultant suspension is shaken for a known period of time and temperature with or without pH adjustment. Samples are collected at a known time interval, filtered, and quantified by HPLC (Alsenz and Kansy, 2007). Excess powder of TZD, PDX and the TZD:PDX mixture were added to a polytop vial containing different media; acidic buffer (pH 1.2), acetate buffer (pH 4,6), distilled water, and phosphate buffer (pH 6.8). The following organic solvents were also used as solvents: acetone, acetonitrile, ethanol and methanol. The contents were left stirring at 380 rotations per min for a period of 24 hours, with the temperature maintained at 37 ± 0.5 °C. The resulting solutions were filtered through 0.22 µm PVDF filters and the solubilised concentrations were subsequently determined using HPLC analysis.

4.6 Investigation of compatibility between TZD and PDX

It is useful to demonstrate and link the influence of excipient choice, concentration, and characteristics to the overall drug performance. Furthermore, fixed dose combination requires demonstration of compatibility between the API-API and API-excipient, and they are useful when the APIs are compatible with each other and/or with possible excipients under stress conditions (WHO, 2005). The compatibility studies were run by storing the powder in the AccuBlock™ digital dry bath (Labnet International, USA) with the temperature set at a 60 ± 0.5 °C. TZD, PDX and the TZD:PDX binary mixture of 1:1 w/w were analysed on a weekly basis for a period of 28 days, by using TGA, FTIR and HPLC, to detect any changes influenced by the heat to the sample before and after the storage.

4.7 Conclusion

This chapter presented the materials and methods used to conduct the study. Materials were used as received, and identification tests were carried out where necessary. The study used the suitable characterisation techniques to provide accurate and reliable data. The used materials and instruments were of acceptable standard, and calibration of equipment were done to allow accurate and precise measurement. Experiments and data analysis were repeated, twice or three times to substantiate the observed results. The novel HPLC method was developed and validated, and it is fully discussed in Chapter 5. The screening of a suitable method for combination of TZD and PDX was conducted in conjunction with an in-depth compatibility study and the results are disseminated in Chapter 6.



4.8 References

- Alsenz, J. and Kansy, M.** 2007. High throughput solubility measurement in drug discovery and development. *Advanced Drug Delivery Reviews*, 59(7):546-567. Doi: 10.1016/j.addr.2007.05.007.
- Brady, J., Dürig, T., Lee, P.I. and Li, J.X.** 2017. Polymer properties and characterization. In: Qiu, Y., Chen, Y., Zhang, G.G., Yu, L. and Mantri, R.V. Ed(s). *Developing solid oral dosage forms*. New York: Academic Press, 181-223. Doi: <https://doi.org/10.1016/B978-0-12-802447-8.00007-8>.
- Bumbrah, G.S. and Sharma, R.M.** 2016. Raman spectroscopy–Basic principle, instrumentation and selected applications for the characterization of drugs of abuse. *Egyptian Journal of Forensic Sciences*, 6(3):209-215. Doi: <https://doi.org/10.1016/j.ejfs.2015.06.001>.
- Byrn, S.R., Zografis, G. and Chen, S.** 2017. Product development. In: Byrn, S.R., Zografis, G. and Chen, S. Ed(s). *Solid state properties of pharmaceutical materials*. Hoboken, NJ: Wiley, 69-87.
- European medicines Agency (EMA).** 2009. ICH Topic Q 8 (R2) Pharmaceutical Development. [online] Available at: https://www.ema.europa.eu/en/documents/scientific-guideline/note-guidance-pharmaceutical-development_en.pdf [Accessed 26 October 2021].
- Epp, J.** 2016. X-ray diffraction (XRD) techniques for materials characterization. In : Hübschen, G., Altpeter, I., Tschuncky, R., and Herrmann, H.G. Ed(s). *Materials characterization using nondestructive evaluation (NDE) methods*. Sawston: Woodhead publishing, 81-125.
- Fan, H., Chen, Y., Huang, D. and Wang, G.** 2016. Kinetic analysis of the thermal decomposition of latex foam according to thermogravimetric analysis. *International Journal of Polymer Science*. 1-7. Doi: <https://doi.org/10.1155/2016/8620879>.
- Fortunato, A.** 2013. DSC: history, instruments, and devices. In: Pignatello, R. Ed. *Drug-Biomembrane Interaction Studies: The application of calorimetric techniques*. Sawston: Woodhead Publishing, 169-212. Doi: <https://doi.org/10.1533/9781908818348.169>.
- Freeman, T., Brockbank, K. and Sabathier, J.** 2017. Characterising powder flow properties—the need for a multivariate approach. In *EPJ Web of Conferences* (Vol. 140, p. 03008). EDP Sciences. Doi: <https://doi.org/10.1051/epjconf/201714003008>.
- Iglesias, N., Galbis, E., Romero-Azogil, L., Benito, E., Lucas, R., García-Martín, M.G. and de-Paz, M.** 2020. In-depth study into polymeric materials in low-density gastroretentive formulations. *Pharmaceutics*, 12(7):636. <https://doi.org/10.3390/pharmaceutics12070636>.
- International Council for Harmonisation (ICH).** 2016. Impurities: guideline for residual solvents q3c(r6). [online] Available at: https://database.ich.org/sites/default/files/Q3C-R6_Guideline_ErrorCorrection_2019_0410_0.pdf [Accessed 2 November 2020].

International Council on Harmonization (ICH). 2005. *ICH Official web site: ICH.* [online] Available at: <<https://database.ich.org/sites/default/files/Q2%28R1%29%20Guideline.pdf>> [Accessed 4 October 2021].

Kodre, K., Attarde, S., Yendhe, P., Patil, R. and Barge, V. 2014. Differential Scanning Calorimetry: A Review. *Research and Reviews: Journal of Pharmaceutical Analysis*, (3):11 - 22.

Larkin, P. 2017. Basic principles. In: Larkin, P. (ed). *Infrared and Raman spectroscopy: principles and spectral interpretation.* Amsterdam: Elsevier, 7-27.

Law, D. and Zhou, D. 2017. Solid-state characterization and techniques. In : Qiu, Y., Chen, Y., Zhang, G.G., Yu, L. and Mantri, R.V. Ed(s). *Developing solid oral dosage forms: pharmaceutical theory and practice.* New York: Academic press, 59-84. Doi: <https://doi.org/10.1016/B978-0-12-802447-8.00003-0>.

Malamatari, M., Ross, S.A., Douroumis, D. and Velaga, S.P. 2017. Experimental cocrystal screening and solution based scale-up cocrystallization methods. *Advanced Drug Delivery Reviews*, 117:162-177. Doi: <http://dx.doi.org/10.1016/j.addr.2017.08.006>.

Newman, A. 2017. Rational design for amorphous solid dispersions. In: Qiu, Y., Chen, Y., Zhang, G.G., Yu, L. and Mantri, R.V. Ed(s). *Developing Solid Oral Dosage Forms.* New York: Academic press, 497-518.

Pereira, G.G., Figueiredo, S., Fernandes, A.I. and Pinto, J.F. 2020. Polymer selection for hot-melt extrusion coupled to fused deposition modelling in pharmaceuticals. *Pharmaceutics*, 12(9):795. Doi: <https://doi.org/10.3390/pharmaceutics12090795>.

Perkin Elmer. 2010. Thermogravimetric analysis (TGA) a beginner's guide. *United States of America: Perkin Elmer.* Available online at: <https://resources.perkinelmer.com/lab-solutions/resources/docs/FAQ_Beginners-Guide-to-Thermogravimetric-Analysis_009380C_01.pdf> [Accessed 30 May 2020].

Prat, D., Wells, A., Hayler, J., Sneddon, H., McElroy, C.R., Abou-Shehada, S. and Dunn, P.J. 2015. CHEM21 selection guide of classical-and less classical-solvents. *Green Chemistry*, 18(1):288-296. Doi: 10.1039/C5GC01008J.

Qiao, N., Li, M., Schlindwein, W., Malek, N., Davies, A. and Trappitt, G. 2011. Pharmaceutical cocrystals: An overview. *International Journal of Pharmaceutics*, 419(1-2):1-11. Doi: <https://doi.org/10.1016/j.ijpharm.2011.07.037>.

Rodrigues, M., Baptista, B., Lopes, J. and Sarraguça, M. 2018. Pharmaceutical cocrystallization techniques. Advances and challenges. *International Journal of Pharmaceutics*, 547(1-2):404-420. Doi: <https://doi.org/10.1016/j.ijpharm.2018.06.024>.

Shan, N., Toda, F. and Jones, W. 2002. Mechanochemistry and co-crystal formation: effect of solvent on reaction kinetics. *Chemical Communications*, (20):2372-2373. Doi: <https://doi.org/10.1039/B207369M>.

Shi, Q., Moinuddin, S.M. and Cai, T. 2019. Advances in coamorphous drug delivery systems. *Acta Pharmaceutica Sinica B*, 9(1) : 19-35. Doi: <https://doi.org/10.1016/j.apsb.2018.08.002>.

Skotnicki, M., Aguilar, J.A., Pyda, M. and Hodgkinson, P. 2015. Bisoprolol and bisoprolol-valsartan compatibility studied by differential scanning calorimetry, nuclear magnetic resonance and X-Ray powder diffractometry. *Pharmaceutical Research*, 32(2):414-429. Doi: <https://doi.org/10.1007/s11095-014-1471-7>.

Stieger, N., Aucamp, M., Zhang, S.W. and De Villiers, M.M. 2012. Hot-stage optical microscopy as an analytical tool to understand solid-state changes in pharmaceutical materials. *American Pharmaceutical Review*, 15(2).

Van Eerdenbrugh, B. and Taylor, L.S. 2011. Application of mid-IR spectroscopy for the characterization of pharmaceutical systems. *International Journal of Pharmaceutics*, 417(1-2):3-16. Doi: <https://doi.org/10.1016/j.ijpharm.2010.12.011>.

Varges, P.R. Costa, C.M. Fonseca, S. B., F. Naccache, M. and De Souza Mendes, P. 2019. Rheological Characterization of Carbopol® Dispersions in Water and in Water/Glycerol Solutions. *Fluids*, 4(1): 3. Doi: <https://doi.org/10.3390/fluids4010003>.

Vitez, I., Newman, A., Davidovich, M. and Kiesnowski, C. 1998. The evolution of hot-stage microscopy to aid solid-state characterizations of pharmaceutical solids. *Thermochimica Acta*, 324(1-2):187-196. Doi: [https://doi.org/10.1016/S0040-6031\(98\)00535-8](https://doi.org/10.1016/S0040-6031(98)00535-8).

World Health Organization (WHO). 2005. Annex 5: Guidelines for registration of fixed-dose combination medicinal product. [online] Available at: https://www.who.int/medicines/areas/quality_safety/quality_assurance/GuidelinesRegistrationFixedDoseCombinationTRS929Annex5.pdf [Accessed 27 October 2021].

Chapter 5

Development and validation of a reversed-phase high performance liquid chromatography (RP-HPLC) method for the simultaneous detection of TZD and PDX.

5.1 Introduction

As thoroughly described in the preceding chapters, pyridoxine (PDX) is often prescribed in TB patients taking isoniazid and TZD to reduce the occurrence of polyneuropathy side effects. TZD is a poorly studied drug and very little is known of its solubility and physicochemical properties. In order to investigate the physicochemical properties of a drug, it is necessary to quantify and qualify it. To that extent, HPLC is a powerful analytical tool for quantitative and qualitative compound analysis. During physicochemical and compatibility studies of TZD in combination with PDX, it became necessary to have a sensitive analytical method that will allow the simultaneous detection of the two compounds. Currently, there are only three literature sources discussing the HPLC analysis of TZD. One of the sources investigated the quantification of TZD from human plasma (Mulubwa and Mugabo, 2018), while the other sources reported stability indicating HPLC methods which allow the accurate detection of TZD degradation products when exposed to stress conditions (Gandhi, Shevale and Choudhari, 2018; Vanavi and Rajput, 2021).

However, in terms of the detection and quantification of TZD in combination with PDX, it was not possible to replicate any of these analytical methods, and they all resulted in poor peak retention and sub-optimal chromatographic characteristics. Furthermore, none of these methods allowed the simultaneous detection and quantification of PDX, thus the need arose to develop and validate an analytical method that was deemed suitable for this particular study. This HPLC method was developed in a stepwise manner. The objective was to develop an HPLC method which can be used either for the simultaneous detection of TZD and PDX, or only for the identification and quantification of TZD in bulk material, but also in potential solid-state modifications. Validation of an analytical method is required to demonstrate that it is reliable and

adequate for its intended purpose (LoBrutto and Patel 2007). This chapter describes the steps followed during the method development process and the documented evidence of accuracy, precision, linearity, selectivity, robustness, limit of detection and limit of quantification as proof of the method validity will be discussed.

5.2 HPLC method development considerations

Liquid chromatography is relatively easy to use, fast and has different ranges of selectivity to choose from, hence it is used in the pharmaceutical industry for purification and quantification of many compounds and preservatives (Driver and Raynie, 2007). HPLC is a separation technique relying on the distribution (separation) of an analyte between a mobile phase (the solvent) and a stationary phase (column packing). This separation of a given analyte is governed by the chemical structure thereof, since intermolecular interactions between the molecule under investigation and the packing material of the column will influence the retention of the compound (Böttcher, Margraf and Monks, 2021; Belanger *et al.* 1997). Based on this principle, it is evident that many factors need to be considered when developing a suitable HPLC method. Initial steps include the collection or determination of physicochemical properties such as pKa, logP and solubility. This will further reveal aspects such as solvent selection, not only for sample preparation but also for the mobile phase (Belanger *et al.* 1997; LoBrutto, 2007). HPLC is commonly used in pharmaceutical development in determining; drug assays, dissolution testing, stability, and drug impurity determination (Zacharis 2009).

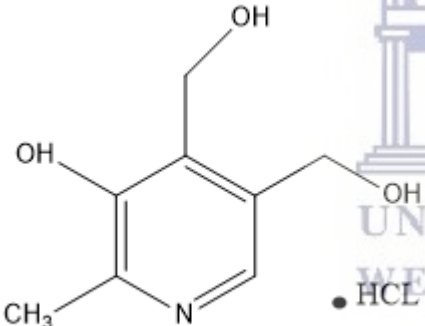
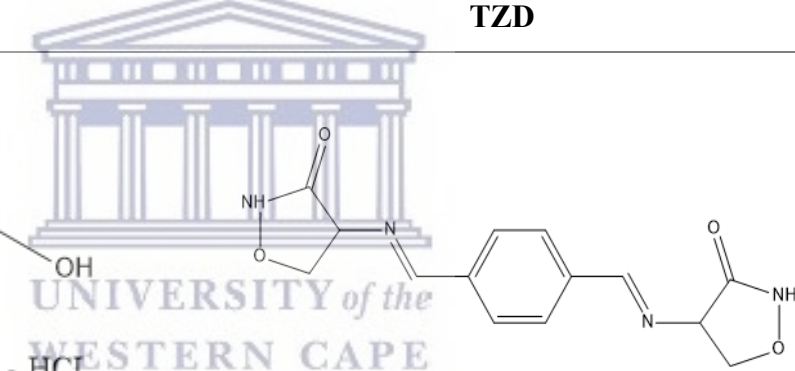
5.2.1 Analyte properties

As mentioned, the physicochemical properties of PDX and TZD had to be investigated to generate a successful method. Table 5.1 provides a summary of known physicochemical properties of the two drugs. Based on this information and the scrutiny of the molecular structures, it was deduced that PDX is a salt with alcohol functional bonds, and it will be ionised in solution by donating hydrogen ions from its hydrogen bonds. TZD can accept hydrogen bonds which will be attached to its amide bond once dissolved in water. It is recommended to establish the initial mobile phase pH for development of separation methods for analytes with known pKa values. The methods with

close pKa and pH values are not advisable, since they can generate distorted peaks which are adjusted by salt increase or buffer concentration changes. The minimum of one unit value difference between a pH mobile phase and a pKa analyte is sufficient to allow a single predominant ionisation state of an analyte (Kazakevich and LoBrutto, 2007b).

pKa values of compounds are indirectly proportional to the acidic strength (Kotz *et al.*, 2014). PDX has a strong acidic pKa value of 9.4 and a strong basic value of 5.0 while TZD has a pKa value of 14.08, therefore PDX is more acidic than TZD. The ionisation probability was taken into consideration during HPLC development and the pH of the mobile phase was adjusted by the addition of glacial acetic acid.

Table 5.1: The molecular structures and related physicochemical properties of PDX and TZD.

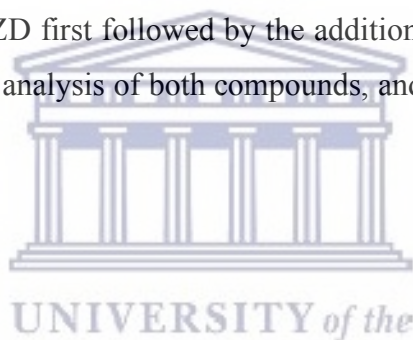
PDX	TZD
	
<p>pKa: 5.0 and 9.0 (Aboul-Enein and Loutfy, 1984)</p>	<p>pKa (Predicted): 14.08 ± 0.40 (Scifinder 2019)</p>
<p>logP: No information</p>	<p>logP: No information</p>
<p>Solubility: Soluble in water, propylene glycol, slightly soluble in alcohol (1g/100ml) and insoluble in ether and chloroform (Aboul-Enein and Loutfy, 1984)</p>	<p>Solubility: No information</p>

5.2.2 Suitable solvent selection

As part of the analytical method development phase, it was imperative to know the solvents in which both compounds solubilise. Table 5.1 summarises the available solubility behaviour of both compounds. In terms of TZD, almost no information could be found in literature sources due to the sparse physicochemical characterisation data available in the public domain for this drug. From literature, it was concluded that PDX is soluble in water, propylene glycol, slightly soluble in alcohol (1g/100ml) and insoluble in ether and chloroform (Aboul-Enein and Loutfy, 1984). The lack of information resulted in screening different organic solvents in terms of PDX and TZD solubilisation by relying on visualisation since an analytical method was not available (at this point in time) to quantify drug solubility. This screening process revealed that TZD shows limited solubility in almost all pharmaceutically relevant organic solvents. Organic solvents screened for the solubilisation of TZD in combination with PDX included ultrapure water, acetonitrile, methanol, ethanol, iso-propanol and dimethyl sulfoxide (DMSO). In previous studies, Gandhi *et al.* (2018), Mulubwa and Mugabo, (2018) and Vanaci and Rajput, (2021) investigated the HPLC method development for detection and quantification of TZD alone, where DMSO was used in combination with other solvents. DMSO is a universal solvent, greatly used as a solubilising agent for many compounds. It exhibits a higher loading dose due to its high dielectric constant and its stereochemistry structure facilitates the solvation of many solute molecules (Balakin *et al.*, 2004). Furthermore, it has a higher boiling point which is advantageous for dynamic studies, it is used for storage of stock solutions with the advice to store in inert conditions since it is hygroscopic and known to cause hydrolysis (Kassel, 2007). It therefore became evident that DMSO should be used to completely solubilise TZD, and this resulted in the screening of various solvent systems in which DMSO was added to obtain the best possible solvent. Solvents ranging from 100% v/v DMSO and different ratios of DMSO in combination with chromatography grade methanol, ethanol, acetonitrile, and water were visually observed. These solvent systems were then also investigated during preliminary HPLC analysis, whilst the optimal mobile phase was also investigated as detailed in Table 5.2.

5.2.3 Determination of optimal wavelength

A detector is used to recognise the elution of a substance from the column. This is achieved by monitoring the change in mobile phase, translating it into an electric signal that differs from the baseline. UV detectors are commonly used due to their sensitivity, wide linear range, temperature tolerance and appropriateness for gradient elution. They detect elements that absorb UV and visible light. The molecular structure affects the UV absorption capacity of a compound, and compounds with aromatic ring and ketone structure, generally have higher UV absorption (Meyer, 2004b). A setting of 254 nm wavelength has been reported to generate strong absorption bands for proteins, enzymes, and nucleic acid (Belanger *et al.*, 1997). The research by Nawaz (2013) and Anayakora *et al.*, (2008) have used 254 nm to detect PDX in solution. Meanwhile, Gandhi *et al* (2018) used 264 nm for the detection of TZD and Mugabo and Mulubwa (2018) used 260 nm as an optimal wavelength. UV screening of solutions consisting of TZD and PDX in which 200 μ l DMSO was used to solubilise TZD first followed by the addition of ACN showed 260 nm as an optimum UV wavelength for the analysis of both compounds, and it was further used for method validation for the current study.



5.2.4 Column choice

Column choice is an integral part for HPLC method development and influences the ability to obtain accurate results. The column selectivity, robustness, loadability, efficiency and compatibility between mobile phase and the solvent should be considered (Ahuja and Rasmussen, 2007). The peak shapes indicate separation efficiency of a chromatographic system. Column overload may provide a “shark-fin” peak shape and this happens when the injected sample exceeds the stationary phase capacity (Jerkovich and Vivilecchi, 2007). A peak shape with a peak asymmetry value equivalent to 1, is called a symmetrical peak, also known as a Gaussian peak. A non-gaussian peak with the back spreading out to a certain extent is termed peak tailing and its peak asymmetry is greater than 1. If the front part of the peak is flatter than the back, it is termed as fronting with peak asymmetry of less than 1 (Meyer, 2004a). Narrower peak widths (Figure 5.1A) are an indication of good compound separation, and sharper peaks enable separation of more sample components in a certain time (Belanger *et al.*, 1997).

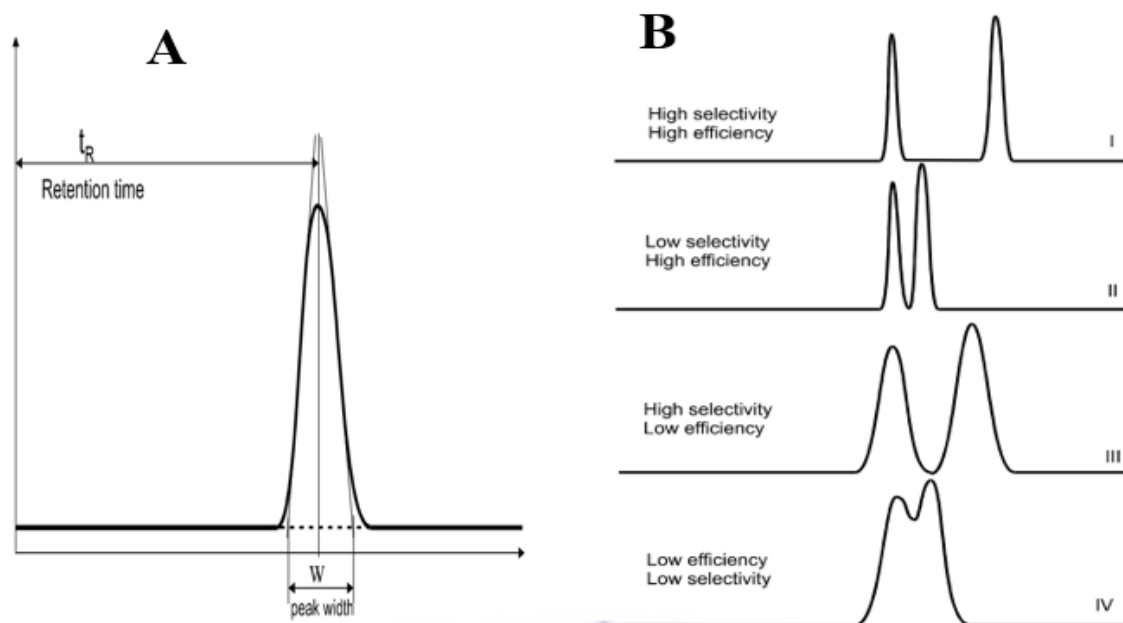


Figure 5.1: Pictogram displaying a(A) typical, ideal Gaussian peak and (B) the characteristic peaks obtained with varying levels of column selectivity and efficiency (Adapted from Kazakevich and LoBrutto, 2007a).

Retention time (t_R) is the peak maxima distance from the injection point. It is used to identify the analyte on a particular chromatographic system. The column efficiency is defined as the band-broadening degree when the analyte is injected in the column and it depends on kinetic factors of the chromatographic system such as mass-flow dynamics, flow rate, molecular diffusion and the properties of the column packing bed. The efficiency is higher when particles are smaller and have a uniform packing in the column. Furthermore, an optimum flow rate is needed to achieve an optimum efficiency for any given column. Column selectivity is the ability to distinguish different analytes being analysed using the same chromatographic setup and method and it is dependent on the interactions of the nature of the analytes and the stationary phase surface. Figure 5.1B shows different degree of selectivity and efficiency of a column (Kazakevich and LoBrutto, 2007a). Silica based packing columns are very popular due to the physical characteristics of the silica support, offering a wide range of pore sizes, particle size distribution and appropriate packing for both small and large molecules.

5.3 HPLC method optimisation

The poor solubility that TZD exhibits in most organic solvents as well as water, further complicated the optimisation of a suitable solvent and mobile phase system for TZD and PDX combinations. The potential suitable solvent systems and mobile phase for both compounds were simultaneously investigated, taking into consideration the solubility behaviour of both TZD and PDX. Acetonitrile (ACN) and ultrapure water combined in different (%v/v) ratios from 90:10 to 10:90 were tested. These ratios were supplemented by adding 1% v/v glacial acetic acid. Chromatography grade methanol and water combinations in the same %v/v ratios as used with the ACN : H₂O combinations were also tested, both as mobile phases and diluents. The following HPLC columns were further used to investigate suitable stationary phases: Luna C₁₈ (250 × 4.6 mm, 5µm), ACE C₁₈ (250 x 4.6 mm, 3µm), Kinetex C₁₈ (250× 4.6 mm, 5µm), Discovery C₁₈ column (150 × 4.6 mm, 5 µm) and Kinetex XB C₁₈ (250 × 4.6mm, 5 µm). Table 5.2 provides a summary of the different chromatographic conditions investigated.

Figure 5.2 depicts the chromatogram obtained using MeOH : H₂O (50:50 %v/v) as mobile phase and sample diluent and an ACE[®] Excel[™] C₁₈ (250 x 4.6 mm, 3µm) column as stationary phase. The chromatography was found to be unacceptable with split peaks observed for PDX. These observed split peak could be ascribed to overlapping of the PDX peak with the solvent used due to low selectivity and efficiency. TZD was detected at around 15 minutes with acceptable peak symmetry, but the analytical response was found to be poor, resulting in a small peak. Based on visual solubility observations as discussed in paragraph 5.2.2 it was concluded that TZD didn't solubilise completely in this solvent system therefore, despite affecting the peak size it will also not provide accurate analytical results since the poor solubility of TZD adds uncertainty in terms of the actual TZD concentration. On this basis, it was therefore decided not to pursue MeOH : H₂O (50:50 %v/v) as mobile phase or diluent any further in this method development process.

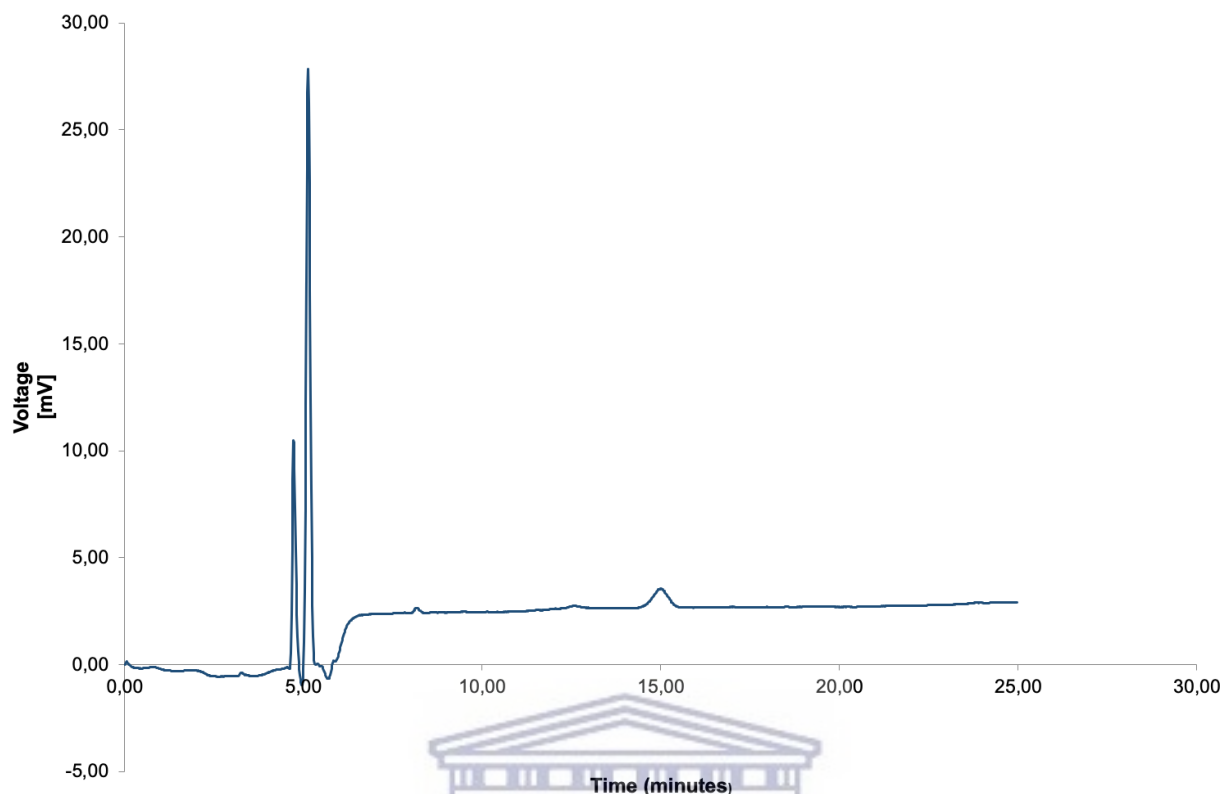


Figure 5.2: The HPLC chromatogram of simultaneous analysis of TZD and PDX obtained using MeOH: H₂O (50:50 %v/v) as mobile phase and solvents with an ACE[®] Excel[™] C18 (250 x 4.6 mm, 3 μm) column.

The next step was to investigate the chromatographic response when ACN:H₂O is used in various ratios as mobile phase with a solvent consisting of ACN:H₂O (50:50 %v/v) and 1 ml DMSO added to ensure complete solubilisation of TZD. Both Phenomenex[®] Kinetex[®] C₁₈ 250 x 4.6 mm, 5 μm and Phenomenex[®] Kinetex[®] C₁₈ 150 x 4.6 mm, 5 μm columns were tested as stationary phases. Figure 5.3 depicts a chromatogram obtained with a mobile phase of ACN:H₂O (80:20 %v/v), using a flow rate of 0.8 ml/min and the Phenomenex[®] Kinetex[®] C₁₈ 250 x 4.6 mm, 5 μm column. PDX presented with a small split peak, whilst TZD showed poor peak shape with significant fronting.

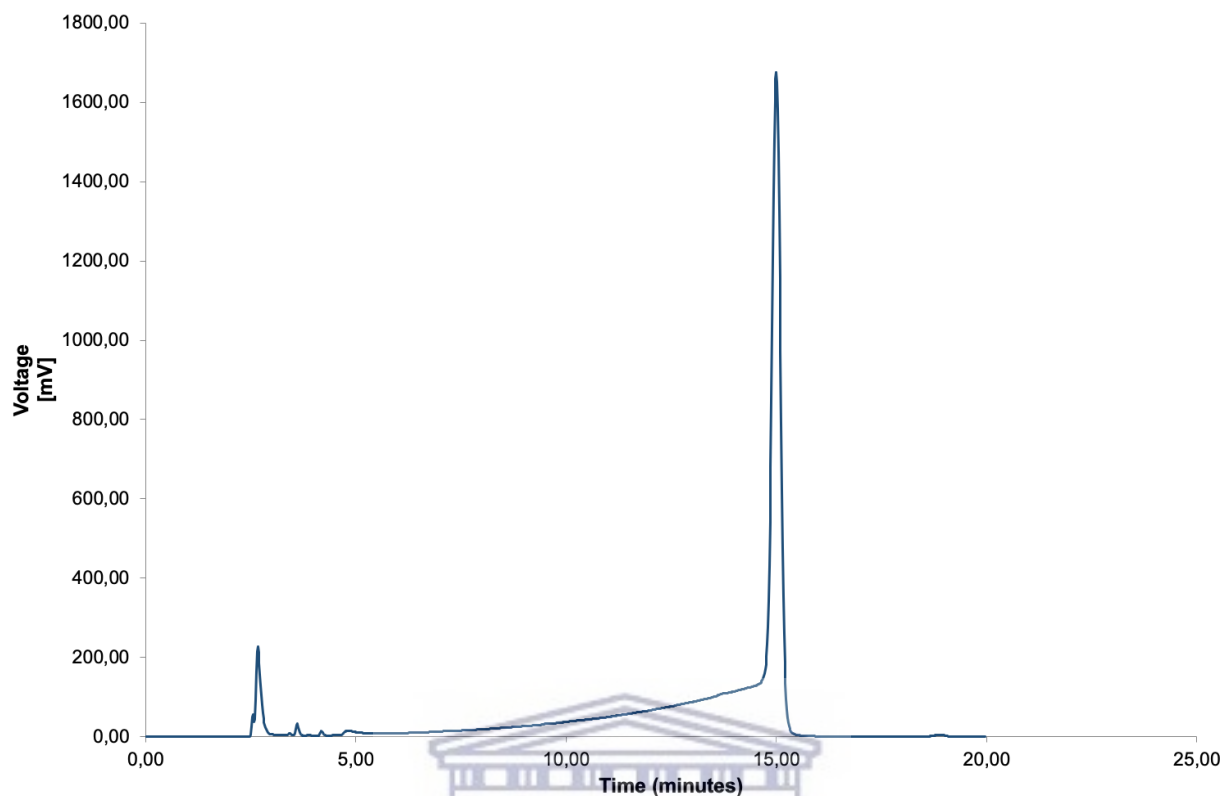


Figure 5.1: The HPLC chromatogram of TZD and PDX obtained using a mobile phase of ACN:H₂O (80:20 %v/v) and the Phenomenex® Kinetex® C₁₈ 250 x 4.6 mm, 5µm column stationary phase

The shorter Phenomenex® Kinetex® C₁₈ revealed similar results but overall shorter elution times. The worst chromatography with this column as stationary phase was obtained with the mobile phase consisting of ACN:H₂O (90:10 %v/v), as depicted in Figure 5.4, with other ACN:H₂O ratios improving the resolution between PDX and TZD but the split peak in front and overlapping with PDX remained (Figure 5.5). Furthermore, the increase in water concentration in the mobile phase was associated with an increase of TZD fronting, which could be due to increased polarity of the mobile phase.

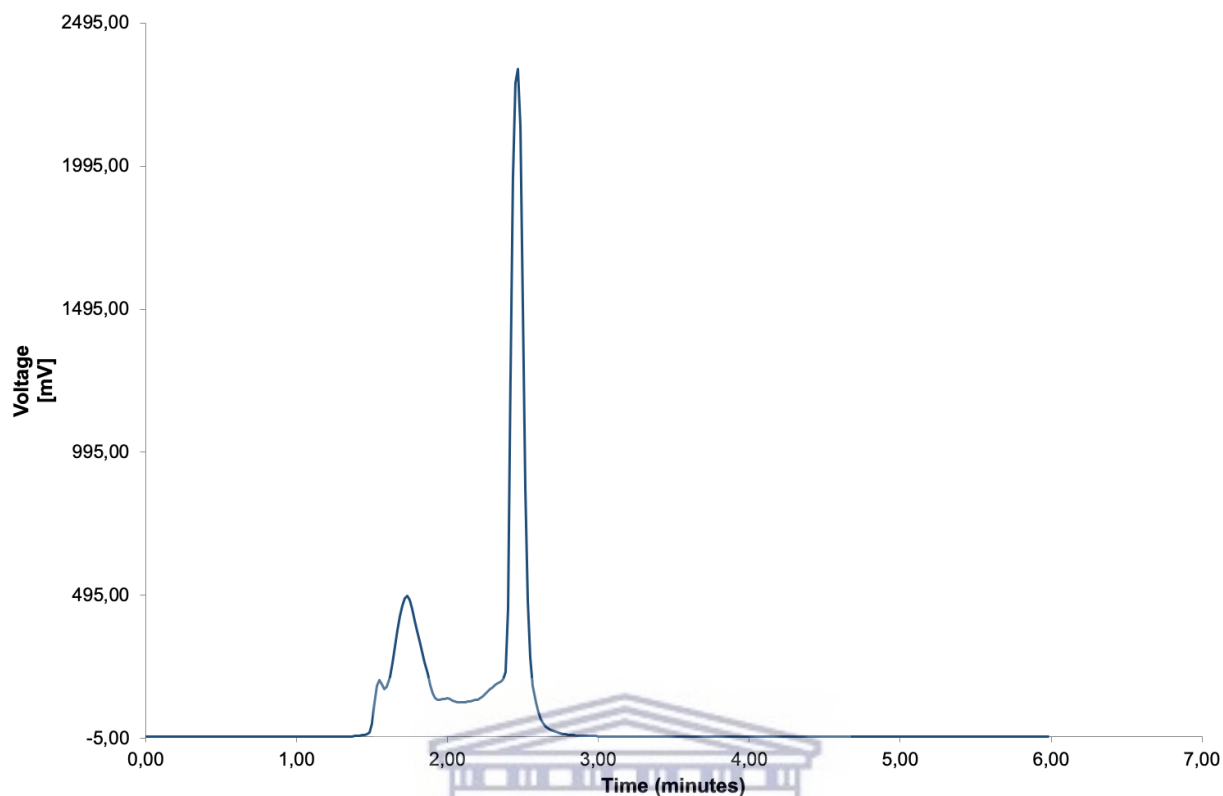


Figure 5.2: The HPLC chromatogram of TZD and PDX obtained using the mobile phase consisting of ACN:H₂O (90:10 %v/v) and the Phenomenex® Kinetex® C₁₈ 150 x 4.6 mm, 5µm column stationary phase.

UNIVERSITY of the
WESTERN CAPE

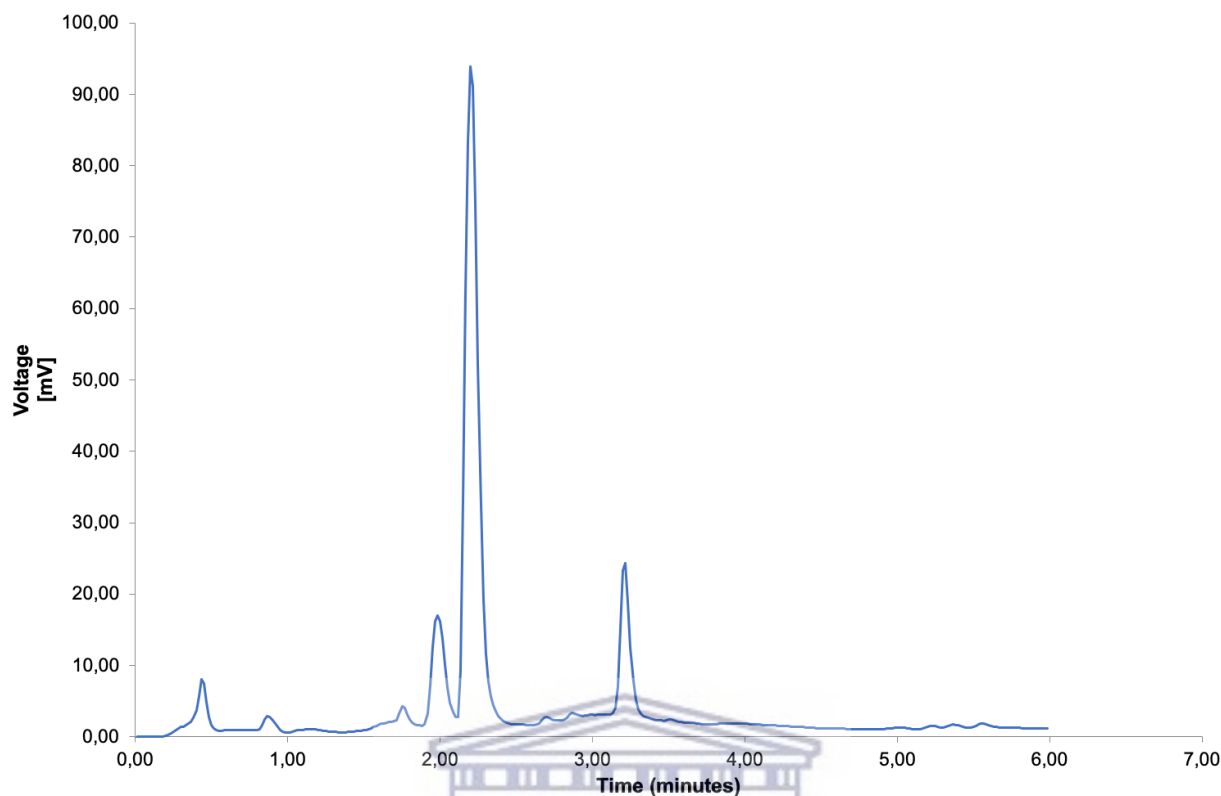


Figure 5.3: The HPLC chromatogram of TZD and PDX obtained using the mobile phase consisting of ACN: H₂O (30:70 %v/v) and the Phenomenex® Kinetex® C₁₈ 150 x 4.6 mm, 5µm column stationary phase.

Based on the above investigations the best chromatographic responses in terms of peak symmetry, resolution and retention time, were obtained with a mobile phase consisting of 30:70 %v/v ACN:H₂O with 1 ml glacial acetic acid added, following a flow rate program of 0.5 ml/min from 0 to 4 min, followed by an increase of the flow rate to 1.5 ml/min from 4.1 min to 8 min. The chosen stationary phase was a Supelco™, Discovery® C₁₈, 150 x 4.6 mm, 5µm column. The resulting chromatography for a standard solution containing 200µg/ml TZD and PDX, respectively is depicted in Figure 5.6.

It was observed that the more DMSO used as part of the diluent, the greater the peak fronting associated with the TZD peak and as the DMSO concentration was decreased, the fronting became markedly less. The phenomenon was interpreted as a “solvent mismatch” or what is known as a “diluent effect”. It is an effect known to decrease separation performance and it occurs when the elution strength of the sample solvent exceeds the starting mobile-phase strength, resulting in a

distorted peak either by fronting or splitting (Jerkovich and Vivilecchi, 2007). The DMSO solvent was minimized and the resultant TZD peak was still fronting. This result was however accepted since its symmetry value of 0.83 falls within the accepted symmetry range of 0.8 - 1.5 (EDQM, 2021).

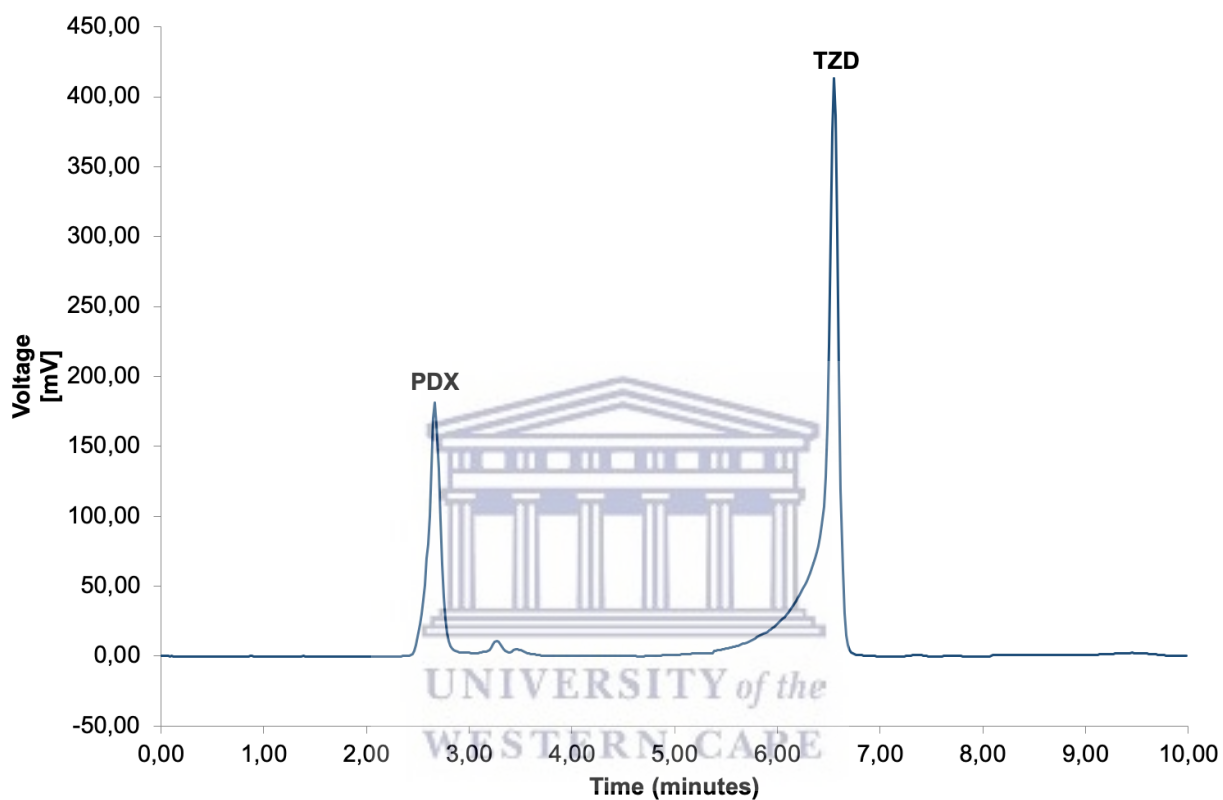


Figure 5.4 : The HPLC chromatogram of TZD and PDX obtained using the 30:70 %v/v ACN:H₂O, with 1 ml glacial acetic acid using a Supelco™, Discovery® C₁₈, 150 x 4.6 mm, 5µm column as stationary phase.

Table 5.1: Roadmap of the HPLC method development and optimisation for the simultaneous detection of TZD and PDX

Trial	Column	Mobile phase	Solvents	Flow rate(s) ml/min	Observation	Conclusion
1	ACE[®] Excel[™] C₁₈ (250 x 4.6 mm, 3μm)	MeOH: H ₂ O (50:50 %v/v)	MeOH: H ₂ O (50:50 %v/v)	0.5 0.8 1.0	Very poor chromatography with PDX split peaks. TZD peak exhibited good symmetry, but detection proved to be low with small resulting peak area.	Found not to be acceptable.
2	Phenomenex[®] Kinetex[®] C₁₈ 250 x 4.6 mm, 5μm	MeOH : H ₂ O (50:50 %v/v)	MeOH : H ₂ O (50:50 %v/v)	1	Multiple peaks without distinction of TZD.	TZD rejected and PDXH was not tested further.

Trial	Column	Mobile phase	Solvents	Flow rate(s) ml/min	Observation	Conclusion
3	Phenomenex® Kinetex® C ₁₈ 250 x 4.6 mm, 5µm	ACN : H ₂ O (10:90 % v/v) ACN : H ₂ O (20:80 % v/v) ACN : H ₂ O (40:60 % v/v) ACN : H ₂ O (50:50 % v/v) ACN : H ₂ O (60:40 %v/v) ACN : H ₂ O (70:30 %v/v) ACN : H ₂ O	ACN : H ₂ O (50:50 %v/v) with 1 ml DMSO added	0.8	PDX alone produced a sharp peak but with a split peak identified in peak front. TZD showed poor peak shape with significant fronting.	Found not to be acceptable.

		(80:20 %v/v)				
--	--	-----------------	--	--	--	--



Trial	Column	Mobile phase	Solvents	Flow rate(s) ml/min	Observation	Conclusion
4	Phenomenex® Kinetex® C ₁₈ 150 x 4.6 mm, 5µm	ACN : H ₂ O (10:90, (v/v) ACN : H ₂ O (20:80, (v/v) ACN : H ₂ O (40:60, (v/v) ACN : H ₂ O (50:50, (v/v) ACN : H ₂ O (60:40, (v/v) ACN : H ₂ O (70:30, (v/v)	ACN : H ₂ O (50:50 %v/v) with 1 ml DMSO added	0.8	Very poor separation between solvent peak and PDX. TZD distinguishable but poor separation from the solvent and PDX peaks.	Found not to be acceptable

Trial	Column	Mobile phase	Solvents	Flow rate(s) ml/min	Observation	Conclusion
5	Phenomenex® Kinetex® XB 250 x 4.6 mm, 3µm	ACN : H ₂ O (20:80, v/v) ACN : H ₂ O (40:60, v/v) ACN : H ₂ O (60:40, v/v) ACN : H ₂ O (50:50)ACN : H ₂ O (80:20, v/v)	ACN : H ₂ O (80:20 %v/v) with 1ml DMSO ACN : H ₂ O (20:80 %v/v) with 1ml DMSO ACN : H ₂ O (50:50, v/v) with 1ml DMSO	1.0	Good separation between the two products but lower sensitivity towards PDX.	The method is suitable for TZD only but not simultaneous analysis of the two.
6	Supelco™, Discovery® C ₁₈ , 150 x 4.6 mm, 5µm	30:70 %v/v ACN:H ₂ O with 1 ml glacial acetic acid.	ACN : H ₂ O (50:50, v/v) with TZD dissolved in 150 µl prior to	0.5 from 0 to 4 &1.5 from 4 to 8 min	The obtained chromatogram had acceptable peak symmetry, selectivity, and efficiency.	Despite TZD peak fronting, reproducibility of chromatography was possible and was therefore

			mix with PDX			accepted as best scenario.
--	--	--	-----------------	--	--	-------------------------------

5.4 Method validation

The next step was to conduct a complete method validation using the analytical setup as identified during the method optimisation process and described in the preceding paragraph.

5.4.1 Linearity

Linearity is the ability of an analytical procedure to produce test results which are directly proportional to the amount of an analyte in the sample (ICH, 2005). It is recommended to use at least five concentrations for linearity determination (EMA, 1995). This linearity is determined by plotting a calibration curve from which the regression coefficient is established. A goodness fit test is used as an acceptance criterion and a high correlation coefficient (r^2) of greater than 0.99 of the working range that fits the purpose is acceptable. (UNODC, 2021). Linearity for this analytical method was investigated across a concentration range of 50.00 – 800.00 $\mu\text{g/ml}$ for both compounds. The prepared solutions were analysed using the mobile phase and column which produced the best results as outlined in Table 5.2. Table 5.3 provides the analytical data obtained during linearity testing.

Table 5.2: Obtained analytical responses during the linearity testing for PDX and TZD

Concentration ($\mu\text{g/ml}$)	PDX peak area (% RSD)	TZD peak area (%RSD)
50.00	282.14 (0.20)	811.31 (0.09)
100.00	472.88 (0.55)	2124.04 (0.03)
200.00	904.97 (0.18)	4350.29 (0.03)
400.00	1863.14 (0.33)	8669.14 (0.03)
800.00	3590.90 (0.16)	17653.11 (0.13)
Regression coefficient (r^2)	0.9996	0.9998

Regression plots for TZD and PDX were obtained by plotting the concentration *versus* peak area obtained (Figure 5.7). For TZD, the obtained correlation equation was: $y = 22.30x - 190.7$ with a correlation factor (r^2) of 0.9998. For PDX, the correlation equation obtained was $y = 4.45x + 43.62$ with a r^2 of 0.9996. This indicates that the relationship between the concentration of the analytes and the area under the curve for each analyte is linear.

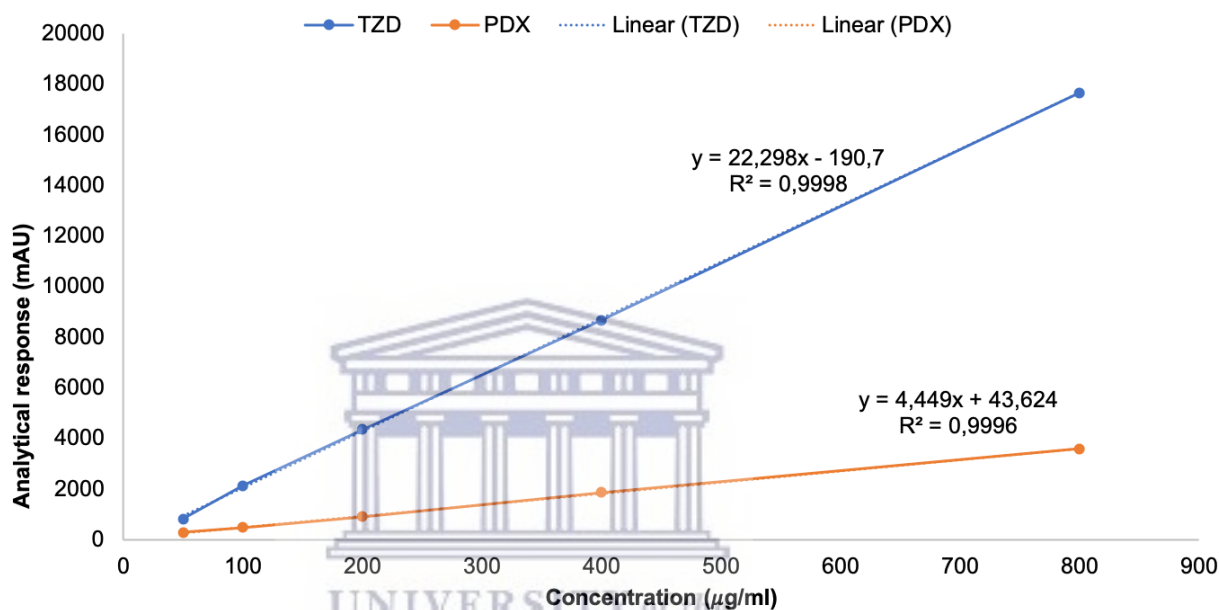


Figure 5.5: Regression plots of PDX and TZD obtained from concentration ($\mu\text{g/ml}$) versus peak area (mAu).

5.4.2 Accuracy

Accuracy represents the ability of an analytical procedure to give the measured results which are closer to the accepted reference value or conventional true value of an analyte added to the sample matrix (EMA, 1995; ICH, 2005). It is obtained by at least nine determinations using a minimum of three concentrations, and it is usually expressed as a percentage value with an acceptable range of 98.0-102.0% (LoBrutto and Patel, 2007). Accuracy of this analytical method was investigated through recovery studies, which was performed by the spiking of a standard solution resulting in five solutions at five

concentration levels: 50, 100, 200, 300 and 400 µg/ml for both APIs. Subsequently, these solutions were analysed against a reference solution of known concentration at 100% concentration level. The percentage recovery for TZD and PDX at each concentration level was quantified and is presented in Table 5.4.

For both API's, the accuracy across varying concentration levels were found to fall within a range of 92.00 – 102.00%, except the concentration of 50.50 µg/ml of TZD and 404 µg/ml of PDX which gave 46.48 µg/ml and 392.81 µg/ml respectively, thus falling out of range.

5.4.3 Precision

Precision is assessed by determining repeatability, intermediate precision, and reproducibility of an analytical procedure. It expresses the closeness of a series of measurements obtained from multiple sampling of the same homogenous sample under defined conditions. It is indicated as a variance, standard deviation, or coefficients of a variation of a series of measurements (EMA, 1995). Precision was determined on two levels: repeatability also termed intra-assay precision and reproducibility also termed intermediate precision. Method precision is determined over a series of measurements of a single sample and was thus conducted by analysing six replicates of solutions containing 200 µg/ml TDZ and PDX in combination. Intermediate precision can represent a variation of different days, analysts, or equipment. Reproducibility expresses the ability to replicate an analytical procedure in a different laboratory or when analysed by a different analyst on different days (BP, 2013). The intra-assay (repeatability) determination for a combination of TZD and PDX were calculated to be 1.04% and 0.87% respectively with the obtained data outlined in Table 5.3. The intermediate precision was calculated to be 0.23% and 0.15% for TZD and PDX respectively. Based on these results, the method is precise, the obtained results are within the accepted range since the %RSD acceptance criteria of analysis of repeatability and intermediate precision must be $\leq 2\%$ for drug products within the 80-120% assay range (Jimidar, Heylen and De Smet, 2007).

5.4.4 Limit of detection (LOD) and limit of quantification (LOQ)

LOD is the lowest concentration of an analyte that can be detected but not necessarily quantified while LOQ is the lowest amount of an analyte that can be quantified with suitable precision and accuracy (EMA, 1995). During LOD and LOQ determinations, TZD and PDX were analysed in a concentration range 50.00 – 800.00 µg/ml. Subsequently, the LOD and LOQ for TZD and PDX were calculated based on the standard deviation of the response and the slope as recommended by the ICH guidelines on analytical method development and validation, using ANOVA statistical analysis (FDA, 2015; ICH, 2005). This was done by applying the regression functionality provided by the Analysis Toolpak which forms part of the Microsoft Excel software package. The following equations were subsequently used to quantify both LOD and LOQ:

$$LOD = \frac{3.3\sigma}{b} \quad \text{Equation 5.1}$$

$$LOQ = \frac{10\sigma}{b} \quad \text{Equation 5.2}$$

With σ being the standard deviation of the response values across the concentration range used to determine linearity and range of the analytical method and b being the slope of the calibration curve. For TZD the LOD and LOQ were quantified as 13.49 µg/ml and 44.95 µg/ml, respectively and for PDX the LOD and LOQ were quantified as 21.49 µg/ml and 71.64 µg/ml respectively (Table 5.3). It means that the amount lower than 13.49 µg/ml for TZD and 21.49 µg/ml for PDX will not be detected by the developed method.

Table 5.3: Summary of validation parameters and results obtained during the method development process

Validation parameters	TZD		PDX	
Linearity (r^2)	0.999		0.999	
Slope	22.30		4.45	
y-intercept	190.70		43.62	
Accuracy				
Expected concentration ($\mu\text{g/ml}$)	% Recovery	Concentration ($\mu\text{g/ml}$)	% Recovery	Concentration ($\mu\text{g/ml}$)
50.50	92.04	46.48 \pm 0.05	102.04	51.53 \pm 0.05
104.00	101.74	105.81 \pm 0.77	98.04	101.96 \pm 0.54
202.10	100.25	202.61 \pm 0.87	100.37	202.85 \pm 2.56
312.00	99.55	310.60 \pm 0.25	98.62	307.69 \pm 0.60
404.00	99.77	403.07 \pm 0.54	97.23	392.81 \pm 0.16
Precision				
Repeatability (%)	1.04		0.87	
Intermediate precision (%)	0.23		0.15	
Limit of detection (LOD) ($\mu\text{g/ml}$)	13.49		21.49	
Limit of quantification (LOQ) ($\mu\text{g/ml}$)	44.95		71.64	

5.4.5 Specificity

Specificity is the ability to assess the analyte in the presence of other components, to serve as a test of identification, purity and assay determination (ICH, 2005). Firstly, the respective peak of each compound was identified by analysing samples, containing only one API, at a time. Subsequently, TZD and PDX were then combined, and these solutions were then analysed to ascertain whether a shift in retention time could be identified or any

other peak interference due to the combination. Further to this, the specificity of both compounds was studied when combined with typical pharmaceutical dissolution media. This was done since the focus of this study was to collect complete physicochemical characterisation data for TZD as well as to investigate potential solid-state modifications involving both APIs. To achieve this aim, solubility studies in various buffered aqueous media shall be necessary, making it important to investigate potential specificity issues during the method development process. Different solvents, namely hydrochloric acid (pH 1.2), acetate buffer (pH 4.5), phosphate buffer (pH 6.8) and distilled water were injected separately to ascertain whether any peak interference will occur once TZD and PDX are dissolved in these solvents. The resulting chromatograms are depicted in Figure 5.8 and shows no interference in the interval of the retention time of the PDX and TZD eluting zone. Therefore, the method is considered specific.

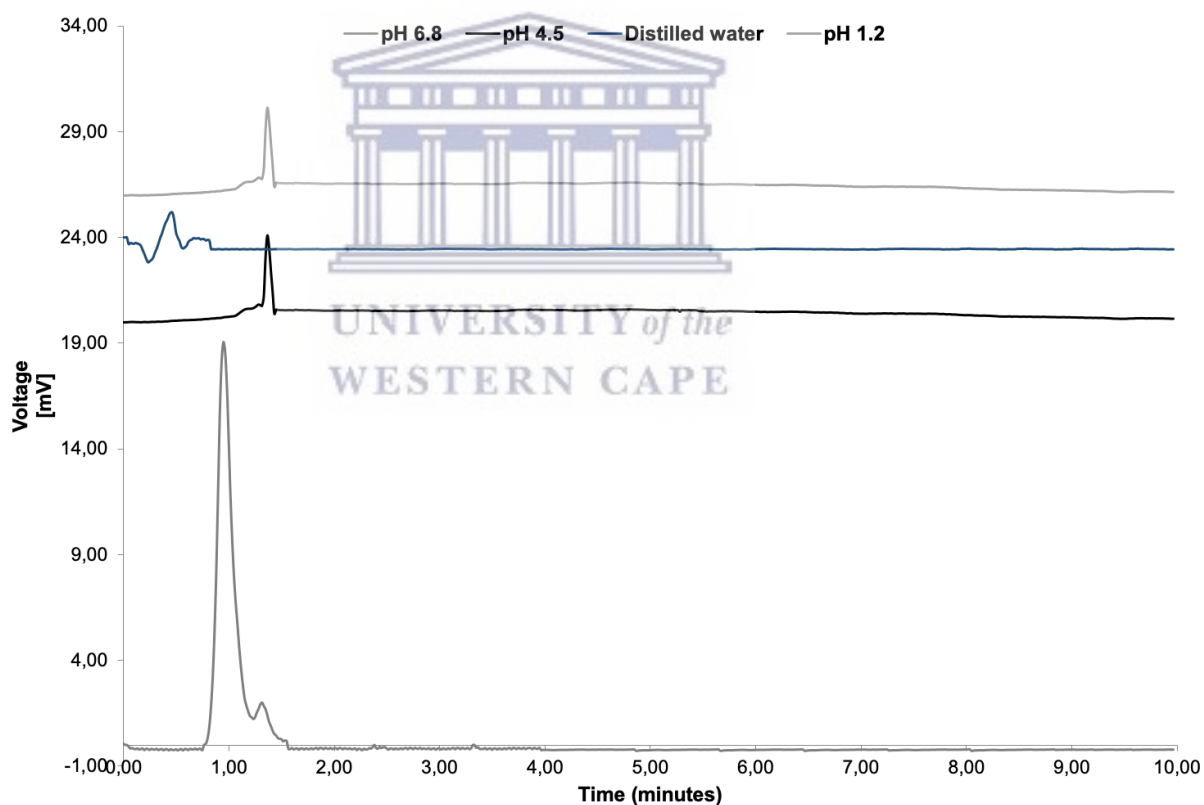


Figure 5.6: Chromatograms of the different media used in the specificity study

5.4.6 Robustness

Robustness of an analytical method indicates the extent at which the analytical method is affected by deliberate alterations of the method parameters. During the validation process robustness of the method was analysed by deliberate adjustment of the following parameters: column temperature ranging from ambient ($25\text{ }^{\circ}\text{C} \pm 0.3\text{ }^{\circ}\text{C}$) to $40\text{ }^{\circ}\text{C} \pm 0.3\text{ }^{\circ}\text{C}$, wavelength variation. Table 5.5 provides an outline of the obtained area under the curve (AUC) values for both PDX and TZD. From these deliberate changes it was observed that PDX exhibits a higher AUC at wavelength 250 nm whilst TZD shows the highest AUC response at 280 nm. Based on these results it was concluded that using a detection wavelength of 260 nm provides the best detection for both compounds in this specific combination. Deliberate changes to the column temperature was also tested during robustness testing. The column temperatures were varied from ambient temperature to 40°C . It was noted that changes in the column temperature didn't affect the retention time of each of the compounds significantly and was therefore not identified as a critical chromatographic parameter for this method.

Table 5.5: Outline of the detected AUC values for PDX and TZD after deliberate adjustments in the detection wavelength obtained during the injection of a solution containing $100\text{ }\mu\text{g/ml}$ PDX and TZD, respectively

Wavelength (nm)	PDX	TZD
230	383.57	4808.23
250	1606.21	2157.37
260 (chosen wavelength)	738.15	4627.39
280	237.31	4834.05

5.4.7 Sample solution stability

Stability is the ability of a pharmaceutical product to remain efficacious and safe for the shelf-life period by withstanding physical, chemical, and microbiological changes or decomposition due to different environmental conditions (Marshall, 2018). During HPLC method development it is important to ascertain how stable the compounds will remain throughout the analytical process. The stability studies were conducted over a course of

three days, under four conditions: photosensitivity (where the sample was exposed to sunlight), fridge ($5\text{ }^{\circ}\text{C} \pm 0.5\text{ }^{\circ}\text{C}$), ambient temperature ($25\text{ }^{\circ}\text{C} \pm 2.0\text{ }^{\circ}\text{C}$), and heat ($60\text{ }^{\circ}\text{C} \pm 2.0\text{ }^{\circ}\text{C}$). Further to this, the stability of the TZD and PDX in the sample solution were investigated through exposing the solution to stress conditions, which included the addition of 200 μl of either acid (pH 1.2), alkaline (1N NaOH) or oxidative species (3% H_2O_2) to three sample vials. Six HPLC vials containing a solution with a concentration of 200 $\mu\text{g/ml}$ of TZD and PDX, respectively were prepared and analysed over a period of three days. PDX showed stability when stored at $5\text{ }^{\circ}\text{C} \pm 0.5\text{ }^{\circ}\text{C}$ and degrades when exposed to heat and to sunlight. PDX is reported to be stable in heat, strong alkali, or acid but sensitive to light when it is in neutral or alkaline solutions (Harris 1988; Aboul-Enein and Loutfy 1984.). This confirmed what was observed in this study since PDX was extensively degraded by photolysis when combined with TZD in the solvent of the current study. Following this, different findings were observed in terms of the stability of PDX in strong alkali. From the obtained results (Table 5.6), PDX was not stable in the alkaline solution as it marked a % purity loss of 35.1%. It was also noticed that PDX is sensitive towards oxidative species based on a purity loss of 19.5% across a period of 3 days. The fact that PDX stability was different when in combination with TZD was noteworthy and it suggests that the stability of PDX when combined with TZD might be affected detrimentally.

TZD was stable in the studied conditions except during exposure to light where it was completely degraded and a loss of 27.24% during heat exposure ($60\text{ }^{\circ}\text{C}$) was observed (Figure 5.9). The stability data of TZD differs from the reported results by Gandhi, Shevale and Choudhari, (2018) where TZD was unstable in alkaline and oxidative conditions, and stable in heat and UV light illumination. This being said, it should be highlighted that the mobile phase, column, solvent, and the exposure times used in the mentioned study were different from what were applied in this study. Figure 5.10 shows that additional peaks formed at 3.42, 4.05, 4.33, 4.92, 6.25 minutes upon exposure of the TZD:PDX solution to sunlight followed by total sample degradation 12 hours later, and samples could not be quantified. It showed that the mixture is photosensitive, and it would not be recommended to expose it to UV-light. The TZD:PDX solution was overall unstable upon exposure to

UV, heat, alkaline conditions, and oxidative species, and PDX showed significant more instability compared to TZD, as Table 5.6, Figures 5.9 and 5.10 are showing.

This solution stability study proved that the developed method will allow the detection of degradation products. However, further investigation through coupling with other techniques such as mass spectroscopy should be considered to allow the accurate identification of the specific degradation compounds.

Table 5.6: Stability data of PDX and TZD under different temperature conditions, exposure to light, pH changes and oxidation, over the course of three days.

Conditions	5 °C	25 °C	60 °C	Photolysis	Acid hydrolysis	Alkaline hydrolysis	Oxidation
PDX	Day 1	100.00%	100.00%	100.00%	100.00%	100.00%	100.00%
	Day 2	98.08%	94.87%	34.94%	1.81%	100.02%	70.84%
	Day 3	95.13%	90.41%	0%	0%	93.75%	64.91%
TZD	Day 1	100.0%	100.0%	100.00%	100.00%	100.00%	100.00%
	Day 2	97.50%	97.43%	127.67%	0%	99.86%	101.97%
	Day 3	97.59%	97.58%	72.76%	0%	99.56%	100.63%

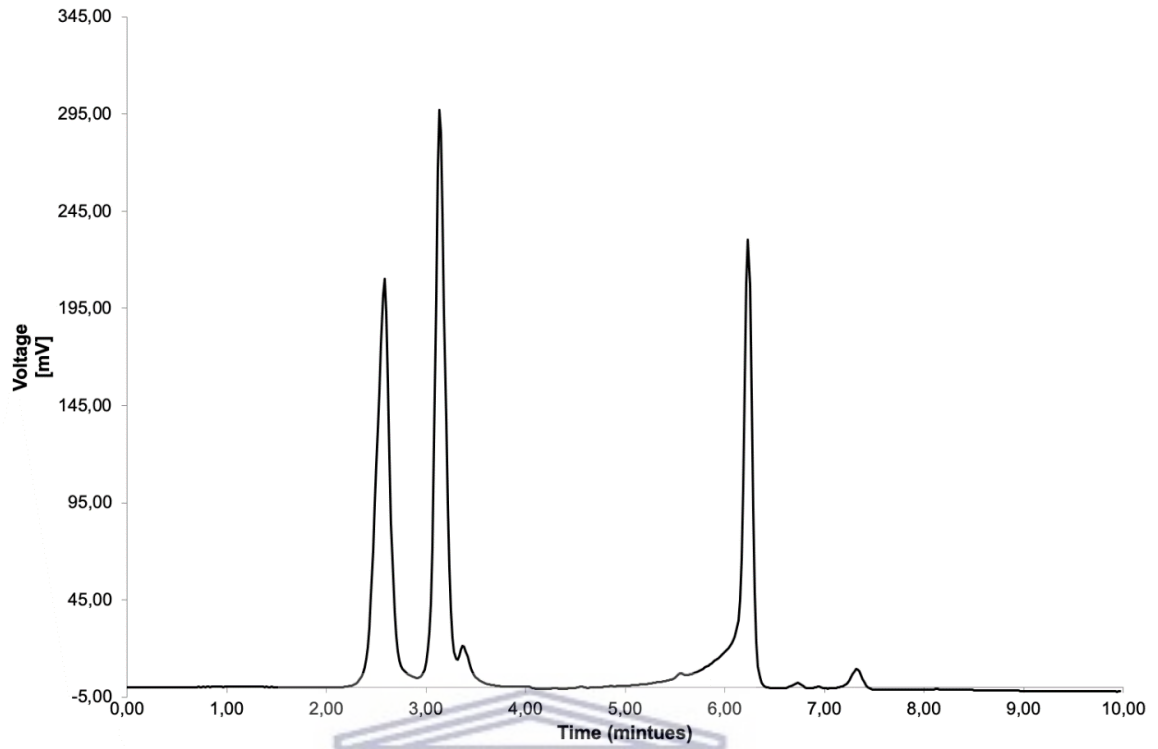
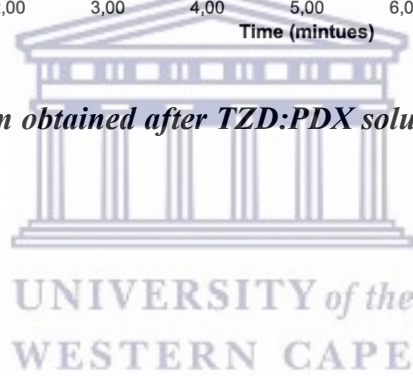


Figure 5.7: Chromatogram obtained after TZD:PDX solution was stored for 24 hours at $60.0^{\circ}\text{C} \pm 2.0^{\circ}\text{C}$.



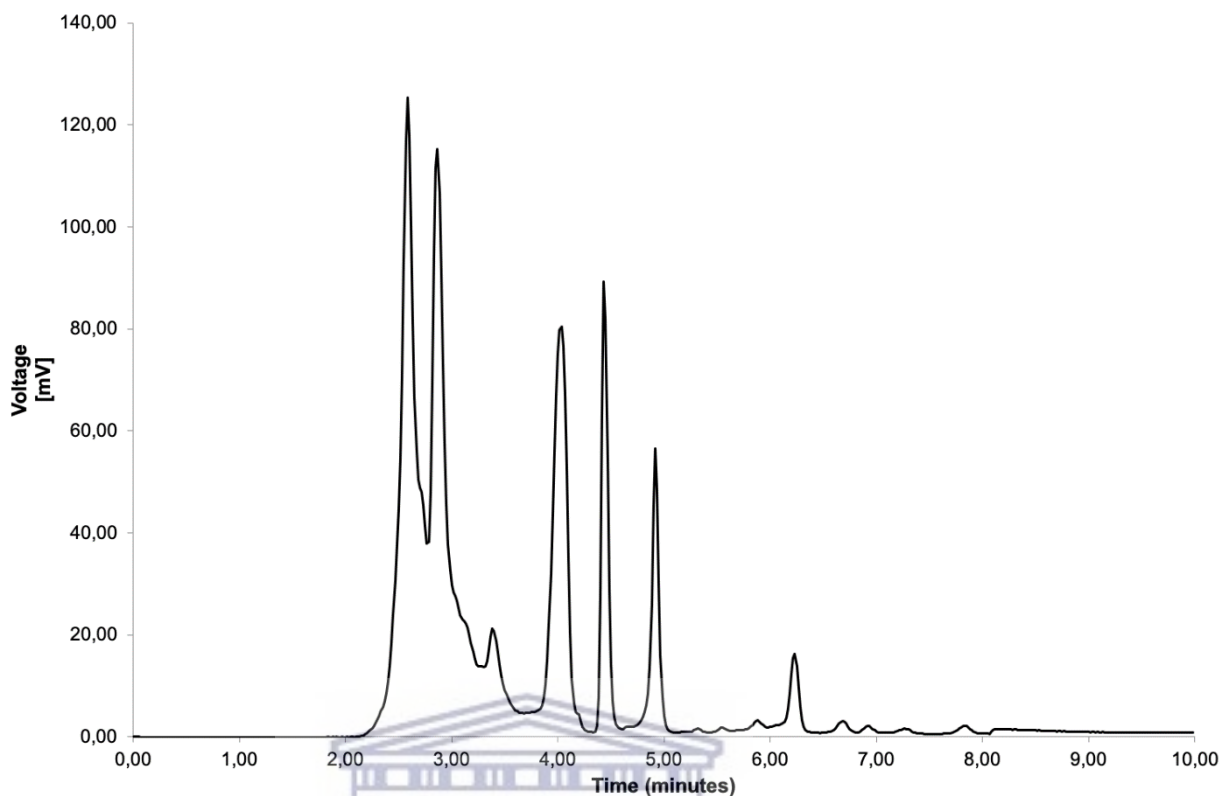


Figure 5.8: Chromatogram obtained after sample was stored in direct sunlight for a period of 24 hours.

UNIVERSITY of the
WESTERN CAPE

5.5 Conclusion

Herein, a novel method for the simultaneous analysis of TZD and PDX has been developed. It proved suitable and sufficiently sensitive to analyse both compounds simultaneously. The method development met with the challenges of lack of physicochemical properties of TZD in literature to guide in the development process, coupled with its poor solubility. Besides, it was problematic to adjust the methodology to suit both compounds concurrently. The solubility screening showed poor solubility of TZD in most of the organic solvents and only DMSO could dissolve TZD. The used concentration of DMSO for TZD solubilisation was found critical to obtain peaks with acceptable symmetry. The DMSO amount was greatly minimised and despite all efforts, the fronting associated with the TZD peak could not be eliminated entirely, though the TZD peak symmetry was found to be within acceptable range, although not an ideal Gaussian peak.

The obtained data were validated against ICH standard guidelines for method development and validation (ICH, 2005). Linearity, accuracy, precision, LOD, LOQ, robustness and solution stability were successfully determined. The stability studies highlighted considerable PDX and TZD compatibility issues when the solution of the binary mixture was exposed to heat, sunlight, and stress conditions of alkaline hydrolysis and oxidation. Necessary precautions should therefore be taken into account when combining these two drugs.

The method development obtained from pre-existing methods of TZD and PDX respectively were ameliorated to enable the detection and quantification of both TZD and PDX. It is important to note that there were trial methods that could be used for TZD detection and quantification only, such as using a Kinetex[®] XB 250 x 4.6 mm, 3 μ m as a column and ACN : H₂O (50:50, v/v) as both mobile phase and solvent, but this resulted in poor chromatography for PDX. The developed method can be used in formulation and preformulation of either single bulk material of TZD, PDX or in combination of both.



5.6 References

Aboul-Enein, H.Y. and Loutfy, M.A. 1984. Pyridoxine hydrochloride. In: Florey, K. ed. *Analytical Profiles of Drug Substances*. Vol. 13. Academic Press, pp. 447-486.

Ahuja, S. 2007. Overview of HPLC method development for pharmaceuticals. In: Ahuja, S and Rasmussen, H. Ed(s). *HPLC method development for pharmaceuticals*. Elsevier, pp.1-11.

Anyakora, C., Afolami, I., Ehianeta, T. and Onwumere, F. 2008. HPLC analysis of nicotinamide, pyridoxine, riboflavin and thiamin in some selected food products in Nigeria. *African Journal of Pharmacy and Pharmacology*, 2(2):029-036.

Balakin, K.V., Ivanenkov, Y.A., Skorenko, A.V., Nikolsky, Y.V., Savchuk, N.P. and Ivashchenko, A.A. 2004. In silico estimation of DMSO solubility of organic compounds for bioscreening. *Journal of biomolecular screening*, 9(1):22-31.

Belanger, J.M., Paré, J.J. and Sigouin, M. 1997. High performance liquid chromatography (HPLC): principles and applications. In: Paré, J.J. and Belanger, J. Ed(s). *Instrumental methods in food analysis*. Vol. 1. Elsevier, pp37-59.

Böttcher, J., Margraf, M., Monks, K. HPLC Basics – principles and parameters. Available at <https://www.knauer.net/Application/application_notes/VSP0019_HPLC%20Basics%20-%20principles%20and%20parameters_final%20-web-.pdf> Date accessed: 06 October 2021.

British Pharmacopoeia (BP). 2013. Department of health, Great Britain. Stationery office.

Driver, J.L. and Raynie, D.E. 2007. Method development for biomolecules. In: Ahuja, S. and Rasmussen, H. Ed(s). *HPLC Method Development for Pharmaceuticals*. Academic Press, pp. 425-439.

European Medicines Agency (EMA). 1995. *ICH Q2 (R1) Validation of analytical procedures: text and methodology* [online] Available at: <<https://www.ema.europa.eu/en/ich-q2-r1-validation-analytical-procedures-text-methodology>> [Accessed 9 October 2021].

European Pharmacopoeia (Ph. Eur). 2005. Pyridoxine Hydrochloride in: *Monographs medicinal and related substances*. 5th edn. Strasbourg: Council of Europe, pp. 2342.

European Directorate for the Quality of Medicines (EDQM). 2021. General methods, Control of impurities, FP monographs, Pharmacopoeial harmonisation. [online] Available at: <https://www.edqm.eu/sites/default/files/1710_1445_ur_genmethods-impurities-harmonisation-chinese_pharmacop._workshop.pdf> [Accessed 18 October 2021].

Gandhi, S.V. Shevale V. P. Choudhari G. B. 2018. Development and validation of a stability indicating RP-HPLC method for the determination of Terizidone. *Indo American Journal of Pharmaceutical Sciences*. pp353-1361.

Harris, R.S. 1988. General discussion on the stability of nutrients. In: Karmas, E. and Harris, R. Ed(s). *Nutritional evaluation of food processing*. Springer, Dordrecht, pp. 3-5.

International Council on Harmonization (ICH). 2005. *ICH Official web site: ICH*. [online] Available at: < <https://www.ich.org/page/quality-guidelines> > [Accessed 4 October 2021].

Jimidar, M.I., Heylen, P. and De Smet, M. 2007. Method validation. In: Ahuja, S. Rasmussen, H. Ed(s). *Separation Science and Technology*. (Vol. 8). Academic Press, pp. 441-458

Kassel, D.B. 2007. The expanding role of HPLC in drug discovery. In: Kazakevich, Y and LoBrutto, R. Ed(s). *HPLC for pharmaceutical scientists*. New Jersey: John Wiley & Sons, pp.533-575.

LoBrutto, R. 2007. Method development. In: Kazakevich, Y and LoBrutto, R. Ed(s). *HPLC for pharmaceutical scientists*. New Jersey: John Wiley & Sons, pp. 347 – 454.

LoBrutto, R. and Patel, T. 2007. Method validation. In: Kazakevich, Y and LoBrutto, R. Ed(s). *HPLC for pharmaceutical scientists*. New Jersey: John Wiley & Sons, pp. 455-502.

Kazakevich, Y. and LoBrutto, R. 2007a. Introduction. In: Kazakevich, Y. and LoBrutto, R. Ed(s). *HPLC for pharmaceutical scientists*. New Jersey: John Wiley & Sons, pp.3-24.

Kazakevich, Y. and LoBrutto, R. 2007b. Reversed-phase HPLC. In: Kazakevich, Y. and LoBrutto, R. Ed(s) *HPLC for Pharmaceutical Scientists*. New Jersey: John Wiley and Sons, pp. 139-195.

Jerkovich, A.D. and Vivilecchia, R.V. 2007. Development of fast HPLC methods. In: Kazakevich, Y. and LoBrutto, R. Ed(s). *HPLC for pharmaceutical scientists*. New Jersey: John Wiley & Son, pp.763-810.

Kotz, J.C., Treichel, P.M., Townsend, J. and Treichel, D. 2014. Principles of chemical reactivity: The chemistry of acids and bases. In: *Chemistry & chemical reactivity*. 8th edn. Cengage Learning, pp. 756-805.

Marshal, P. 2018. Product stability and stability testing. In: Aulton, M.E. and Taylor, K.M.G. Ed(s). *Aulton's Pharmaceutics E-Book: The Design and Manufacture of Medicines*. 5th ed. Edinburgh: Elsevier, p. 862. Available at: <https://search-ebshost-com.ezproxy.uwc.ac.za/login.aspx?direct=true&db=nlebk&AN=1697155&site=ehost-live&scope=site> (Accessed: 9 October 2021).

Meyer, V.R. 2004a. Theoretical principals. In: *Practical high-performance liquid chromatography*. 4th edn. John Wiley & Sons, pp 14-47.

Meyer, V.R. 2004b. Detectors. In: *Practical high-performance liquid chromatography*. 4th edn. John Wiley & Sons, pp 82-99.

Mulubwa, M. and Mugabo, P. 2018. Analysis of terizidone in plasma using HPLC-UV method and its application in a pharmacokinetic study of patients with drug-resistant tuberculosis. *Biomedical Chromatography*, 32(11).

Nawaz, M. 2013. A new validated stability indicating RP-HPLC method for simultaneous estimation of pyridoxine hydrochloride and meclizine hydrochloride in pharmaceutical solid dosage forms. *Chromatography Research International*.

Scifinder. 2019. *SciFinderⁿ Login*. [online] Available at: <<https://scifinder-n.cas.org/searchDetail/substance/616186e93e8b173419f5787f/substanceDetails>> [Accessed 9 October 2021].

Snyder, L.R., Kirkland, J.J. and Glajch, J.L. 2012. Column. In: Snyder, L.R., Kirkland, J.J. and Glajch, J.L. *Practical HPLC method development*. 2nd ed. John Wiley & Sons, pp537-615.

Srivastava, M., Rani, P., Singh, N. and Yadav, R. 2014. Experimental and theoretical studies of vibrational spectrum and molecular structure and related properties of pyridoxine (vitamin B6). *Spectrochimica Acta Part A: Molecular and Biomolecular Spectroscopy*, 120:274-286.

United Nation Office on Drug and Crimes (UNODC). 2021. Guidance for the Validation of Analytical Methodology and Calibration of Equipment used for Testing of Illicit Drugs in Seized Materials and Biological Specimens. [online] Available at: <https://www.unodc.org/documents/scientific/validation_E.pdf> [Accessed 9 October 2021].

U.S. Food and Drug Administration (FDA). 2015. *Analytical Procedures and Methods Validation for Drugs and Biologics*. [online] Available at: <<https://www.fda.gov/regulatory-information/search-fda-guidance-documents/analytical-procedures-and-methods-validation-drugs-and-biologics>> [Accessed 5 October 2021].

Vanavi P.J and Rajput S.J. 2021. Impurity profiling of first line anti-tb drug-terizidone using chromatographic and related techniques. *International Journal of Pharmacy and Pharmaceutical Sciences*, pp. 83-95.

Vora, A. 2010. TZD. *Journal of Association Physician of India*. Volume 58.

WHO Public Assessment Reports (WHOPAR). 2021. Terizidone 250mg capsules. [online] Available at: <<https://extranet.who.int/pqweb/sites/default/files/TB303part6v1.pdf>> [Accessed 10 October 2021].

Zacharis, C.K. 2009. Accelerating the quality control of pharmaceuticals using monolithic stationary phases: a review of recent HPLC applications. *Journal of chromatographic science*, 47(6):443-451.

Chapter 6

Physicochemical characterisation, solid-state form screening and compatibility testing of TZD in combination with PDX

6.1 Introduction

As detailed in Chapter 3, different solid-state forms of APIs and excipients may exist. It is a well-known fact that different solid-state forms of a compound have different crystal packing, lattice energy and associated entropy, which in turn leads to significant differences in the exhibited physicochemical properties. Inevitably, these physicochemical differences affect aspects and processes which form part of pharmaceutical product development and thus different APIs and excipients need to be processed differently during dosage form manufacturing. Furthermore, the differences in solubility and dissolution rate affects the absorption and the mass transport of the molecules, respectively (Vippagunta *et al.*, 2001). This calls for a deep understanding of the solid-state characteristics of APIs in order to ensure the safety and efficacy of finished pharmaceutical products reaching patients. Besides, as discussed in Chapter 3, compounds may be modified to improve specific physicochemical properties that are undesirable either for dosage form development or clinical outcomes. On a molecular level, possible fixed dose combinations may be obtained either through the preparation of co-crystals, eutectic systems, or co-amorphous solid dispersions. In a certain sense, the findings from the physicochemical characterisation of the pure molecules envisioned to be combined on a molecular level could potentially inform the possible route for solid-state formation.

The technology of combining ingredients is important in the age of co-infections and subsequent co-morbidities as the life expectancy of the human population is growing and the quality of life needs to be preserved. Diseases such as TB, which needs multi-drug combination therapies, calls for having the convenience of FDC-products for patients who must take many drugs at once (Blomberg *et al.*, 2001). As highlighted in Chapter 2, it is recommended to take TZD together

with PDX due to TZD associated neurotoxicity which leads to multiple adverse effects (Vora, 2010). It would be desirable if the two drugs are compatible and an FDC of the two molecules can be formed and/or if feasible, more of the drugs used in a typical TZD-based TB treatment regime can be added. Upon a thorough literature search conducted on the physicochemical properties of TZD, it was noted that very limited published literature is available in terms of the physicochemical properties and stability thereof, thus emphasising the need to establish the fundamental information on which the rest of this research study is based.

The first objective of this part of the study was therefore to investigate the physicochemical properties of TZD and PDX as single compounds and subsequently relating the obtained results with that available in literature. The obtained physicochemical properties were then utilised to inform possible molecular modifications involving the combination of both drugs. As documented in Chapter 3, compatibility studies using diverse analytical instruments may be used to determine the feasibility to combine two or more ingredients. Incompatibility between pharmaceutical compounds leads to undesired effects that cause changes in the clinical efficacy and safety of a finished pharmaceutical product. Considering this, compatibility studies are mandated early in the research and development process of finished pharmaceutical products in an effort to save valuable funds and time (Chadha and Bhandari, 2014).

The initial physicochemical investigations involved spectroscopy analysis, PXRD, thermal analysis and equilibrium solubility, which will be described in detail in subsequent paragraphs. TZD and PDX were characterised as single molecules using thermal analysis and spectroscopic techniques to lay a foundation for the rest of the study.

6.2 Physicochemical characterisation of TZD and PDX

6.2.1 Spectroscopic analyses of TZD and PDX

Spectroscopy investigates and measures the absorbance or transmittance produced by materials when in contact with electromagnetic radiation, and the information is used to identify and/or quantify materials based on the obtained pattern of molecular vibration or absorption (van der

Meer, 2018). As mentioned in Chapter 4, TZD was an in-kind donation from a local raw material manufacturing company, and it was therefore necessary to confirm the identity of the raw material against a certified reference standard. PDX was a purchased certified material and it was therefore not compared with a reference standard. Spectroscopic data was collected for both compounds, firstly to confirm the purity of TZD bulk material to that of the purchased reference standard and secondly to obtain baseline spectroscopic data for both compounds to allow comparison with preparations containing both APIs.

6.2.1.1 Fourier-transform infrared spectroscopy (FTIR)

Infrared spectra were collected across the wavenumber range of 650 - 4000 cm^{-1} . The TZD diagnostic region (4000-1500 cm^{-1}) contains strong asymmetric peaks at 1705 and 1636 cm^{-1} , respectively which can be attributed to carbonyl stretching vibration (R-C=O) of aliphatic ketones associated with a secondary amide functional group in the TZD structure, whilst the stretching at about 1636 cm^{-1} can be attributed to the -CH₂=CH₂- stretch present in the benzene ring (Smith, 2018). The stretch observed at 2873 cm^{-1} can be attributed to the saturated carbon stretch (R-CH-R). FTIR data and the associated spectrum of TZD has not been reported in literature, yet and therefore the TZD raw material was validated using a purchased reference standard, which produced an identical FTIR spectrum as depicted in Figure 6.1.

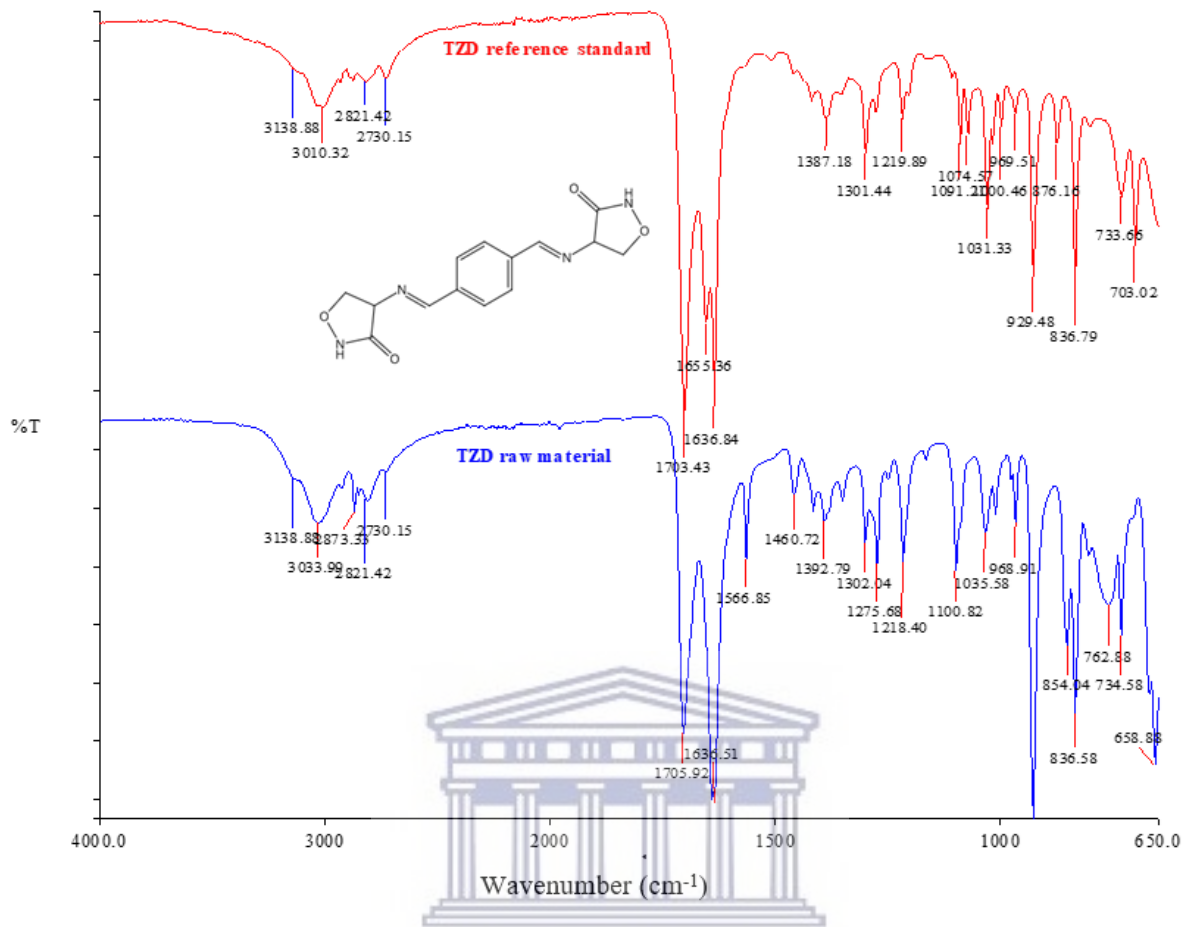


Figure 6.1: Fourier transform infrared (FTIR) spectra of TZD raw material versus a certified reference standard with the molecular structure of TZD provided as an inset. Molecular structure adapted from Scifinder (2019).

Table 6.1: Theoretical and experimental wavenumbers associated with TZD with their corresponding functional bonds (Smith, 2018).

Experimental wavenumber (cm ⁻¹)	Theoretical wavenumber (cm ⁻¹)	Description	Corresponding functional bonds
3033	3050-3000	Weak and broad	Alkene(R-CH ₂ =CH ₂ -R)
2873	3000-2840	Medium	Alkane (-CH-)
1706	1750 - 1680	Strong	Ketone (-CO)
1636	1680 - 1630	Strong	Alkene (R-CH ₂ =CH ₂ -)
1460	1600-1400	Weak	Benzene ring modes
1100	1300-1000	weak	Ether (-C-O-)
929, 836	1000-700	Strong	Out-of-plane -CH bends

The FTIR spectrum obtained for PDX displayed weak narrow stretches in the region ranging from 4000 - 1500 cm⁻¹, except for a strong broad band at 2811.96 cm⁻¹, which can be attributed to the alcohol functional group given its intensity and size, as the reference range being between 3200 - 2600 cm⁻¹ (Smith, 2018). The PDX spectra also produced a peak at 3087 cm⁻¹ belonging to the unsaturated carbon group. The pyridine ring produced the stretch at 1541 cm⁻¹ which is attributed to the quadrant stretch of the pyridine ring and the two sharp peaks at 1088.60 cm⁻¹ and 1016.96 cm⁻¹ are attributed to the C-O bond, as previously obtained by Radoman *et al.*, (2016). The same PDX FTIR spectrum (Figure 6.2) was obtained by Köse, *et al.*, (2014) and it is identical to the PDX FTIR found in the BP, (2013), therefore confirming its identity. Table 6.2 outlines all relevant absorbance bands observed for PDX.

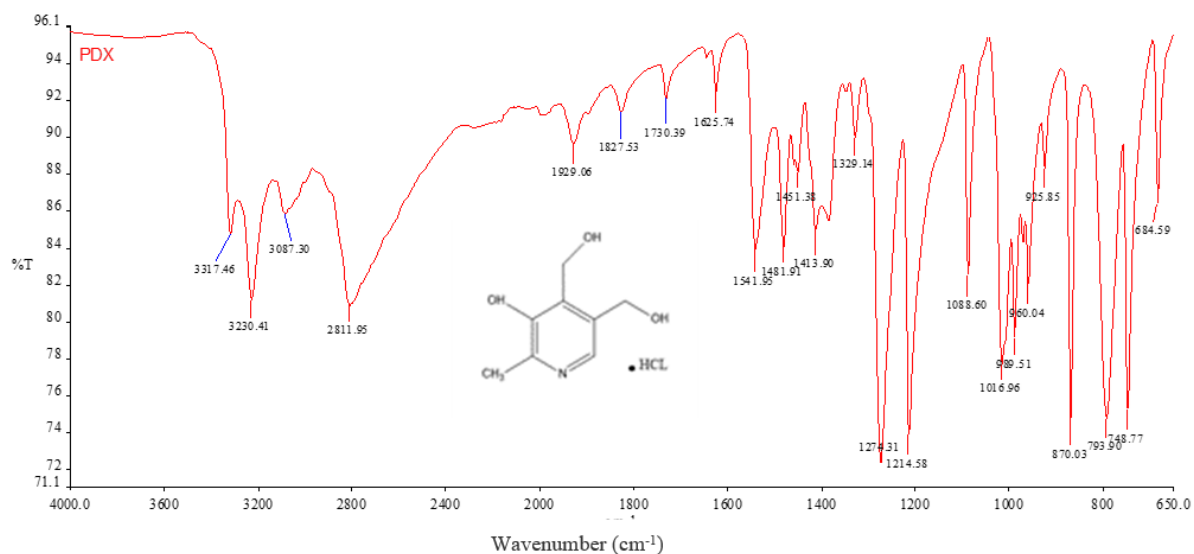


Figure 6.2: Fourier transform infrared (FTIR) spectrum of PDX.

Table 6.2: Theoretical and experimental wavenumber found in PDX chemical structure with their corresponding functional bonds (Smith, 2018; Larkin, 2017)

Experimental Wavenumber (cm ⁻¹)	Theoretical wavenumber (cm ⁻¹)	Description	Corresponding functional bonds or structure
3230,3325	3550-3200	Medium	Alcohol (-OH)
3087	3100-3000	Weak	Alkyl (CH)
2811	3200-2600	Weak and broad	Alcohol (-OH)
1274,1214	1300-1000	Strong	Ether (-C-O-)
1541	1560-1540	Medium	Pyridine
1016	1050-980	Medium	Pyridine

6.2.1.2 Raman spectroscopy

The Raman scattering observed when TZD was irradiated at a fixed wavelength of 1064 nm laser light (Figure 6.3) showed a dominant peak in the wavenumber range of 1600-1700 cm⁻¹, which is

an indication of an alkene functional bond of the benzene ring, and weak stretches between 1300-1000 cm^{-1} that can be attributed to the -C-O stretch of the TZD molecule. The Raman spectra obtained for both the TZD raw material, and the certified reference standard compared well, showing that the scattering of the monochromatic light occurs in a similar manner for both materials, therefore confirming the identity of the supplied TZD bulk material. Figure 6.4 displays the typical Raman spectrum of PDX, similar to that reported in literature by Cimpoiu *et al.*, (2005), where the dominant peak at 692 cm^{-1} is distinctive and belonging to the C=C-C functional group is associated with the PDX molecular structure and the stretch at 1230 cm^{-1} of the -C-O stretch.

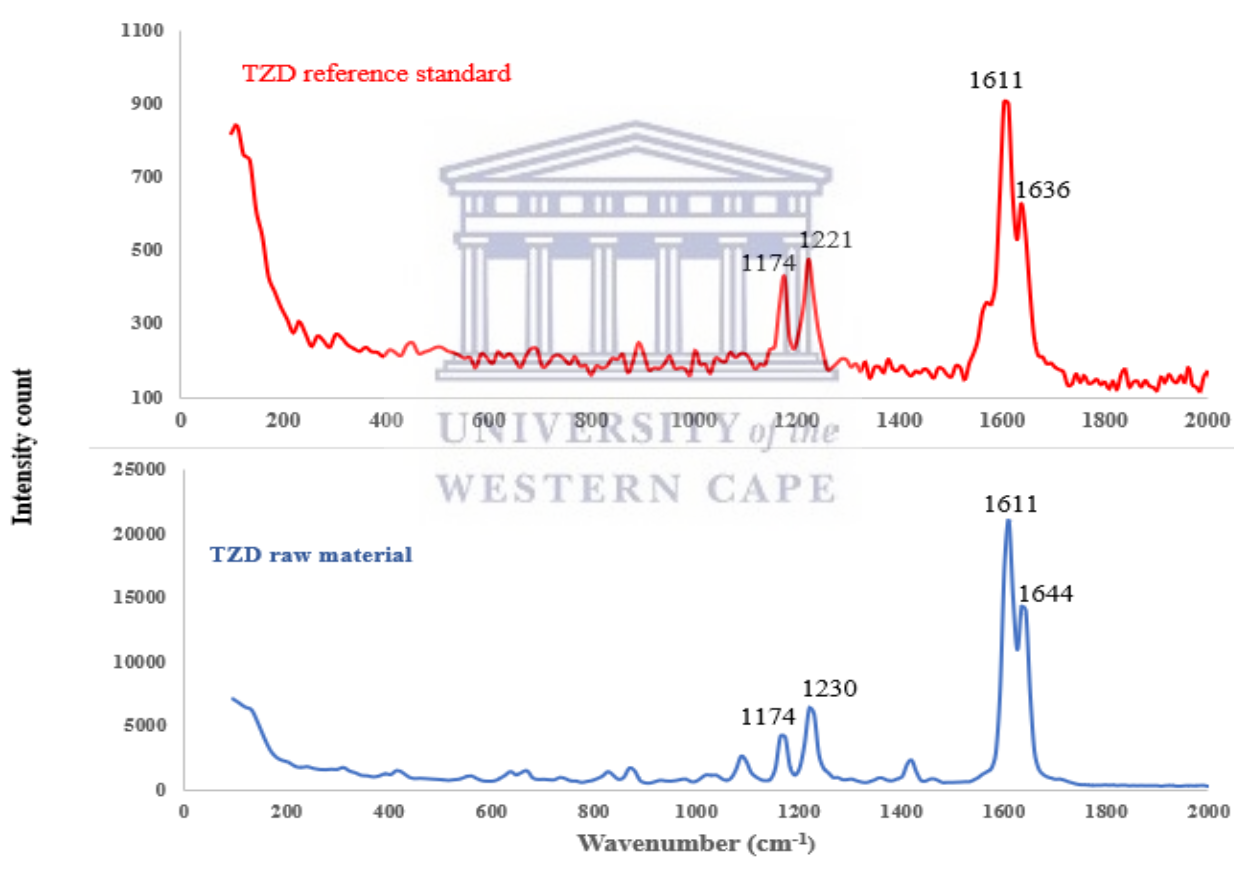


Figure 6.3: An overlay of the Raman spectra for TZD raw material and TZD reference standard obtained at ambient temperature and collected across a range of 200-2000 with laser excitation of 1064 nm.

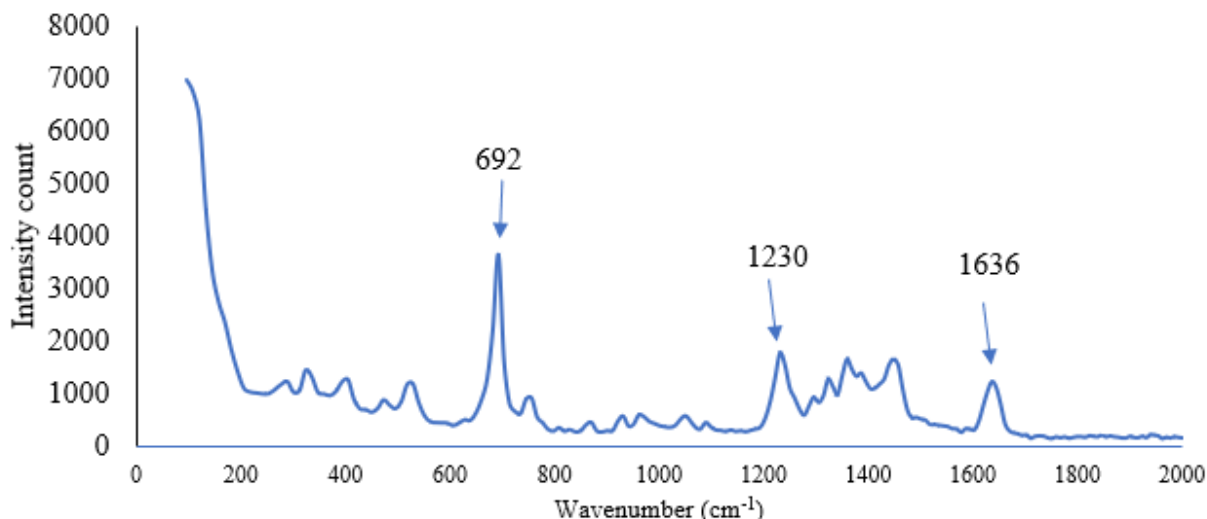


Figure 6.4: Raman spectrum of PDX collected across a range of 100-2000 cm^{-1} at room temperature with a laser excitation of 1064 nm.

6.2.2 X-ray powder diffraction (PXRD)

As part of the characterisation process, it was also important to investigate the solid-state habits in which TZD and PDX exist. TZD displayed a diffraction pattern which is associated with that of a partially crystalline compound with distinct diffraction observed at the following $^{\circ}2\theta$ angles: 16.33, 18.52, 18.88, 19.25, 23.17, 23.21, 23.86 and 25.07. Figure 6.5 depicts the PXRD pattern of TZD, and it should be mentioned that the diffraction peak at 16.33 $^{\circ}2\theta$ is a sharp, well-defined diffraction peak whilst the subsequent diffraction peaks are less defined thus leading to the conclusion that TZD exist as a partial crystalline solid-state form. PDX displayed characteristic and well-defined diffraction peaks at: 10.31, 15.56, 16.92, 20.65, 20.76, 21.11, 21.95, 23.43, 24.19, 25.0, 25.93, 27.83, 29.01 and 37.21 $^{\circ}2\theta$. This diffraction pattern was indicative of a highly crystalline character and the pattern observed in this study was found to be similar to the one reported by Han *et al.*, (2016).

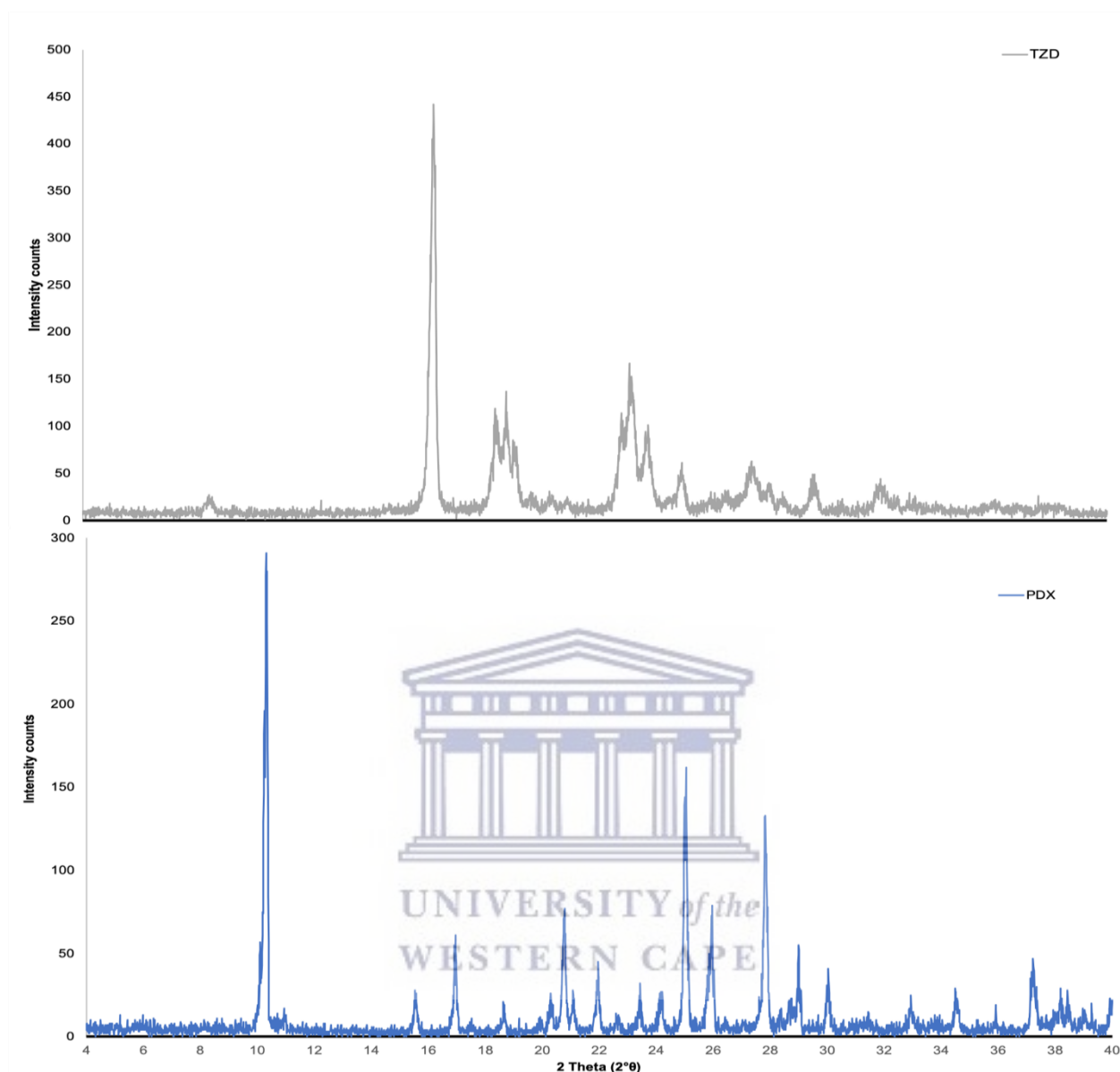


Figure 6.5: X-ray powder diffraction patterns obtained for TZD and PDX across a 2θ range of 4-40 $^{\circ}$, collected at ambient conditions.

6.2.3 Thermal analyses of pure TZD and PDX

The next phase of the initial physicochemical characterisation of the two individual compounds was performed utilising thermal analyses, and the results are presented in the subsequent paragraphs.

6.2.3.1 Hot-stage microscopy (HSM)

Micrographs obtained from HSM are presented in Figure 6.6, displaying the beginning to the end of the heating observation. Thermal analysis of TZD applying HSM was marked by a discoloration from a whitish to yellow colour and finally to a dark black color. This colour change was definitively observed from 210 °C, which marked the onset of decomposition and continued in a gradual manner up until complete charring of the compound, visually observed at 280 °C. The theoretical melting point of 204 - 205 °C (Scifinder, 2021), was neither observed for TZD raw material nor for the TZD reference standard. This emphasised the lack of literature documenting the physicochemical properties of TZD even more.

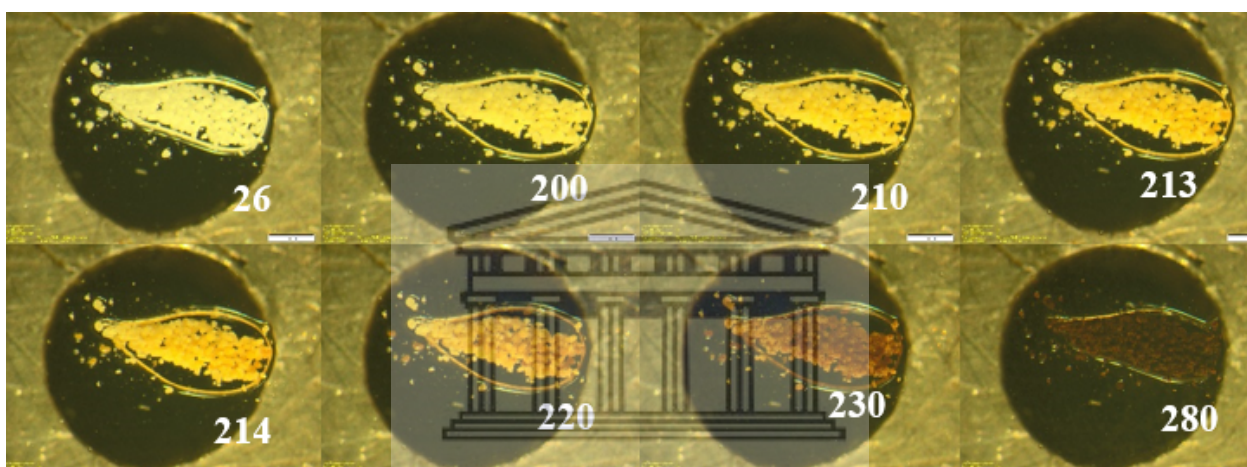


Figure 6.6: Photomicrographs depicting the thermal behaviour of TZD observed during heating of the sample at a rate of 10 °C/min with silicon oil. The temperatures at which the micrographs were captured is indicated on each relevant micrograph.

HSM of PDX showed an onset of melting at 210 °C followed by an immediate onset of degradation with complete melting and degradation observed at 226 °C. The obtained results closely correlate with the theoretical melting point (205 - 212 °C) reported in literature (Aboul-Enein et al. 1984).

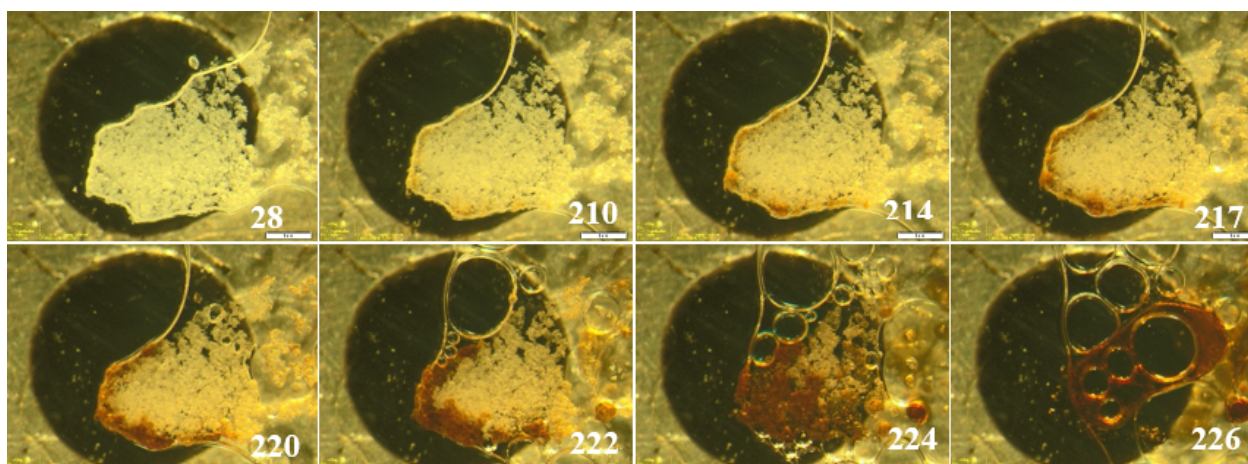


Figure 6.7: Micrographs depicting the thermal behaviour of PDX observed when heated at 10 °C/min with silicon oil. The temperatures at which the micrographs were captured is indicated on each relevant micrograph.

6.2.3.2 Thermogravimetric analysis (TGA)

The thermogram obtained during the TGA of TZD, as depicted in Figure 6.8, marked a rapid weight loss of 32.34% with an onset temperature of 209.19 °C. This rapid weight loss was ascribed to degradation based on the observed degradation during HSM (Figure 6.6). Subsequent to this rapid weight loss step, sample weight loss continued gradually with a total weight loss of 62.75% quantified over the temperature range of 30 – 600 °C, confirming as depicted by the thermogram that complete degradation only occurs at a heating temperature higher than 600 °C.

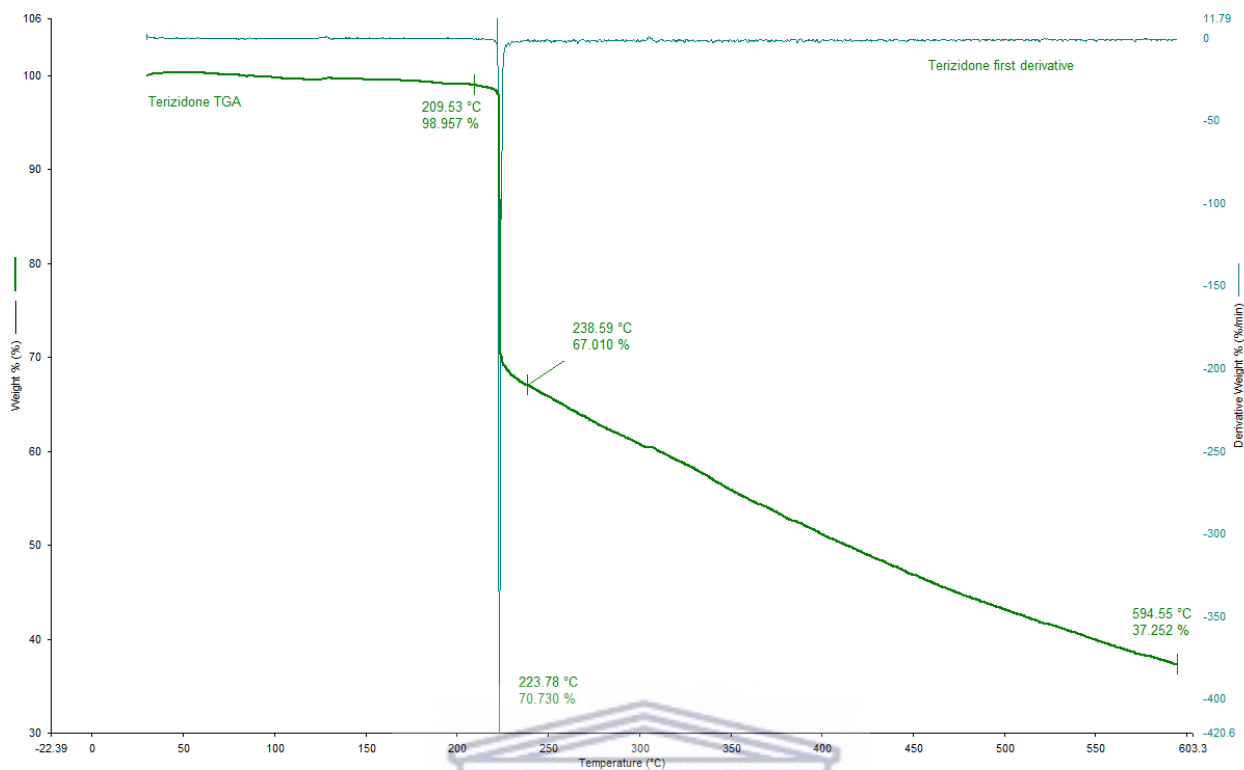


Figure 6.8: Thermogravimetric analysis (TGA) results of TZD and its first derivative heated at 10 °C/min.

The TGA of PDX (Figure 6.9) marked a major weight loss event between 209.53 – 238.59 °C which was calculated to be 31.95 % followed by a gradual weight loss. At the end of the heating run at 600 °C, a total degradation of 58.38% was quantified and just as with TZD, it was apparent that complete degradation of PDX will only occur beyond 600 °C. There was no indication of the inclusion of water molecules into the molecular structures of both TZD and PDX since none of the TGA traces showed weight loss prior to the onset of degradation. Thus, as observed with HSM, the weight loss quantified for both TZD and PDX is only due to degradation and not dehydration or desolvation.

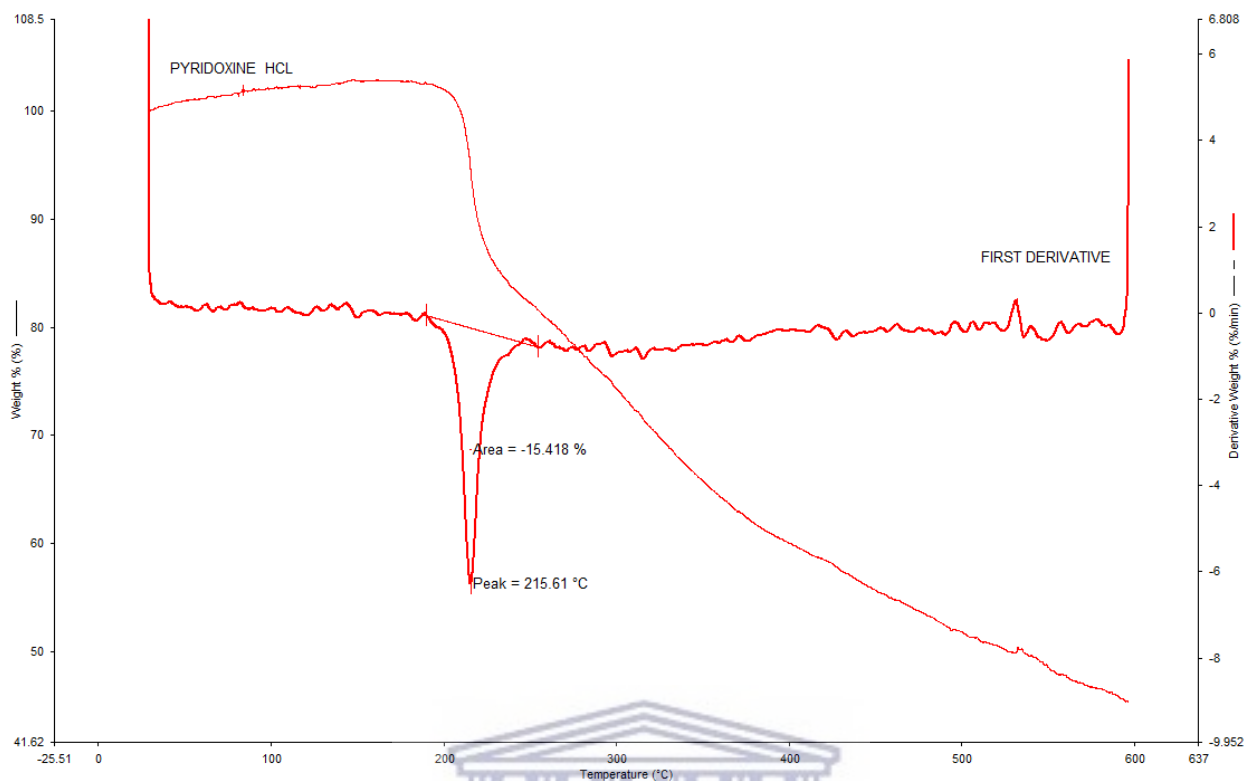


Figure 6.9: TGA results of PDX obtained during a heating program of 10 °C/min. The thermogram also depicts the first derivative showing the major thermal event as a peak .

6.2.3.3 Differential Scanning Calorimetry (DSC)

The thermogram obtained during the DSC analysis of TZD exhibited an exothermic peak with an onset at 202.65 °C, reaching the peak exothermic temperature at 215.84 °C and based on the preceding HSM and TGA data this exothermic peak was interpreted as a degradation process. TZD is derived from an alpha-amino acid, and it is an organooxygen and an organonitrogen, it is possible that the observed exothermic behavior is linked to nitrogen and oxygen since they are involved in the heating process during DSC analysis (Pubchem, 2021). The exothermic peak was associated with an enthalpy (ΔH) of -472.2845 J/g. This is an enthalpy that marks the kinetic intermolecular energy in the TZD molecule. The only literature source that reports a melting point of 204 - 205 °C (Scifinder, 2021) for TZD was thus not confirmed as part of the physicochemical characterisation performed during this study.

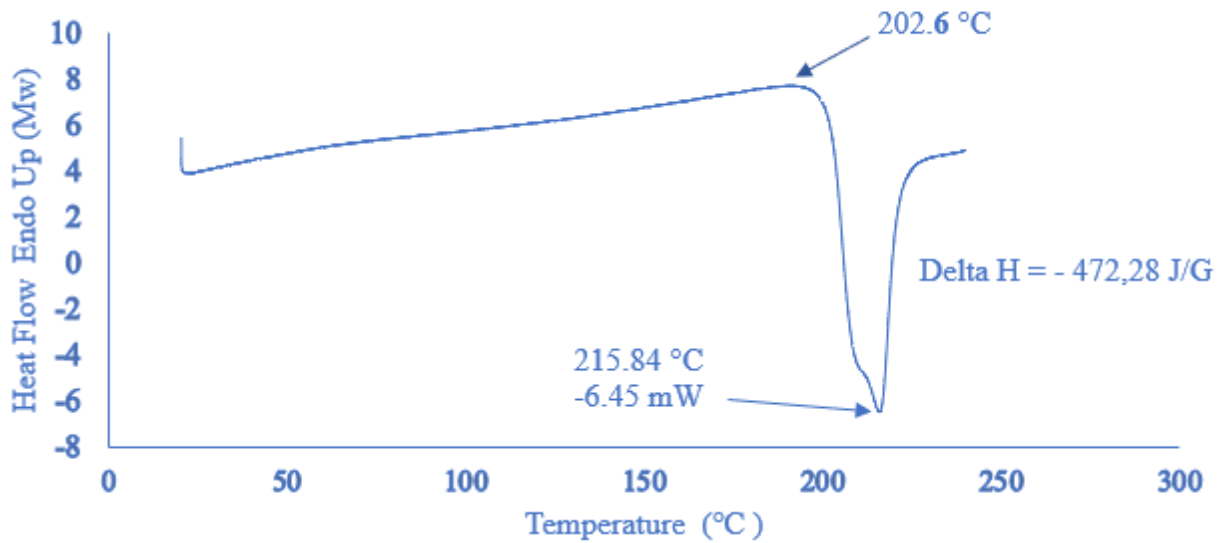


Figure 6.10: Thermogram obtained using DSC analysis of TZD heated at a heating rate of 10 °C/min.

The DSC thermogram of PDX revealed a typical DSC trace, similar to other reported results by Han *et al.* (2016) and Branton and Jana, (2017). DSC analysis of PDX showed an endothermic peak at 213.56 °C, followed with immediate thermal degradation with an onset of 214.59 °C. Furthermore, it is in correlation with the HSM and TGA results. The PDX experimental melting point is relatively close to the known PDX melting point which is between 202 - 212 °C and melting with decomposition as denoted in Chapter 2. The PDX melted sample released the energy equaling to 140.76 J/g as depicted in Figure 6.11.

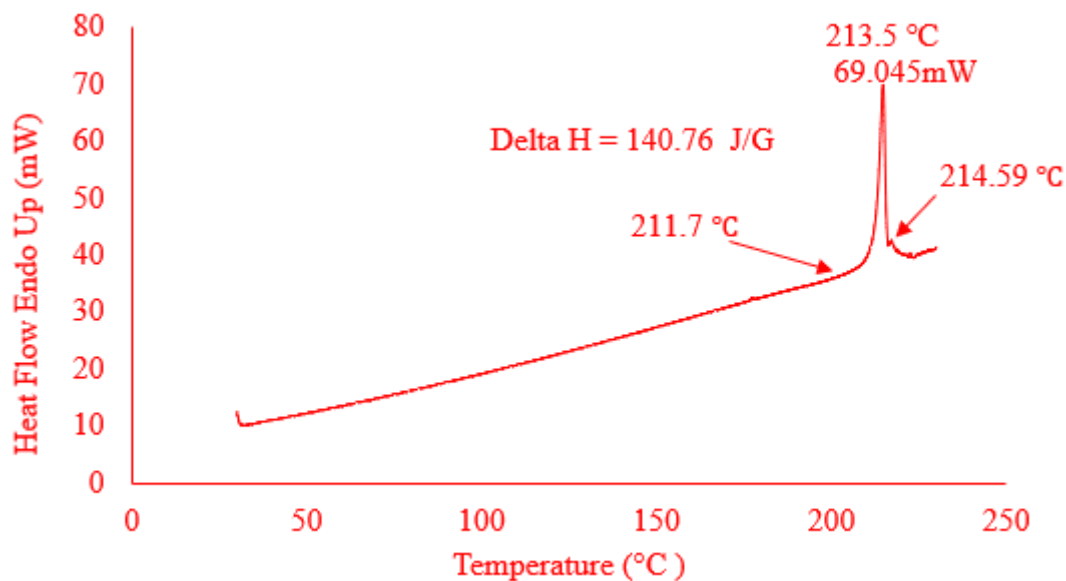


Figure 6.11: DSC thermogram obtained with PDX during heating at 10 °C/min across a temperature range of 30 – 230 °C.

6.2.4 Equilibrium solubility of TZD and PDX in various solvents

Based on the fact that this is a solid-state form study which relied heavily on the physicochemical properties of the two compounds under investigation, it was imperative to investigate the equilibrium solubility of TZD and PDX in various solvent systems. The equilibrium solubility of both compounds was subsequently investigated in organic solvents as well as typical pharmaceutical relevant aqueous buffered solvents. Table 6.3 provides an outline of the obtained solubility results obtained for TZD and PDX at a temperature of 25 °C ± 2 °C. It became apparent that TZD is very poorly soluble in most solvents with the highest solubility concentration achieved in distilled water (888.60 ± 35.08 µg/ml) followed by pH 1.2 (355.47 ± 17.16 µg/ml). Based on these obtained solubility concentrations as well as the BCS (Chapter 3), TZD can be classified as a poorly soluble drug. In correlation with literature PDX proved to be highly soluble in pH 6.8 buffered aqueous solvent and based on the BCS and just as literature dictates PDX is characterised as a highly soluble drug.

Table 6.3: Equilibrium solubility obtained for TZD and PDX in various solvent systems at 25 °C

Solvent	TZD concentration ($\mu\text{g/ml}$) \pm STDEV	PDX concentration ($\mu\text{g/ml}$) \pm STDEV
Methanol	76.37 \pm 2.98	3948.98 \pm 96.79
Ethanol	100.31 \pm 4.83	2023.49 \pm 32.17
Acetonitrile	28.54 \pm 1.45	15.27 \pm 29.70
Acetone	128.22 \pm 8.08	4025.55 \pm 96.79
pH 1.2 (0.1 N HCl)	355.47 \pm 17.16	3388.29 \pm 7.02
pH 4.5	0.00 \pm 0.00	8152.99 \pm 15.85
pH 6.8	72.59 \pm 10.03	11318.31 \pm 85.52
Distilled water	888.60 \pm 35.08	5100.49 19.33

6.3 Physicochemical characterisation of TZD and PDX in combination

The possibility of the combination of TZD and PDX as molecular modifications which would allow TZD and PDX to co-exist as either a co-crystal or a co-amorphous solid-state form was further investigated. It was therefore important to determine the compatibility of the two compounds with one another. This compatibility study was conducted by preparing a physical mixture of TZD and PDX in a 1:1 w/w ratio through light grinding of the mixture using a mortar and pestle. Subsequently, this mixture was analysed applying FT-IR and Raman spectroscopy, PXRD and thermal analysis.

The FTIR was used to investigate the nature and the extent of intermolecular bonding between TZD and PDX. From Figure 6.12 as well as the data outlined in Table 6.4 it was observed that the

FTIR spectrum obtained with the TZD:PDX physical mixture presented replication of functional bonds from the parent compounds. Alcohol functional bonds from PDX were observed at 3321, 3326 and 2809 cm^{-1} and the strong ketones stretch at 1706 cm^{-1} and alkene stretch at 1643 cm^{-1} emanating from the TZD molecule could be observed. The following absorbance bands associated with TZD disappeared: 2873, 1035.52, 760.71, 734.56. The out-of-plane -CH bends of 929 and 836 cm^{-1} were still observed in the TZD:PDX physical mixture. The absorbance band at 1732 cm^{-1} associated with PDX were also not observed in the FT-IR spectrum obtained for the mixture. No new absorbance bands which could signify new bond formation were observed. Furthermore, based on the fact that the mixture was prepared through light mixing without any external factors such as heat, solvents, or any other source of kinetic energy added which could induce intermolecular bond formation, it was deduced that the disappearance of some of the absorbance bands could be linked to the solid-state dilution of each compound.

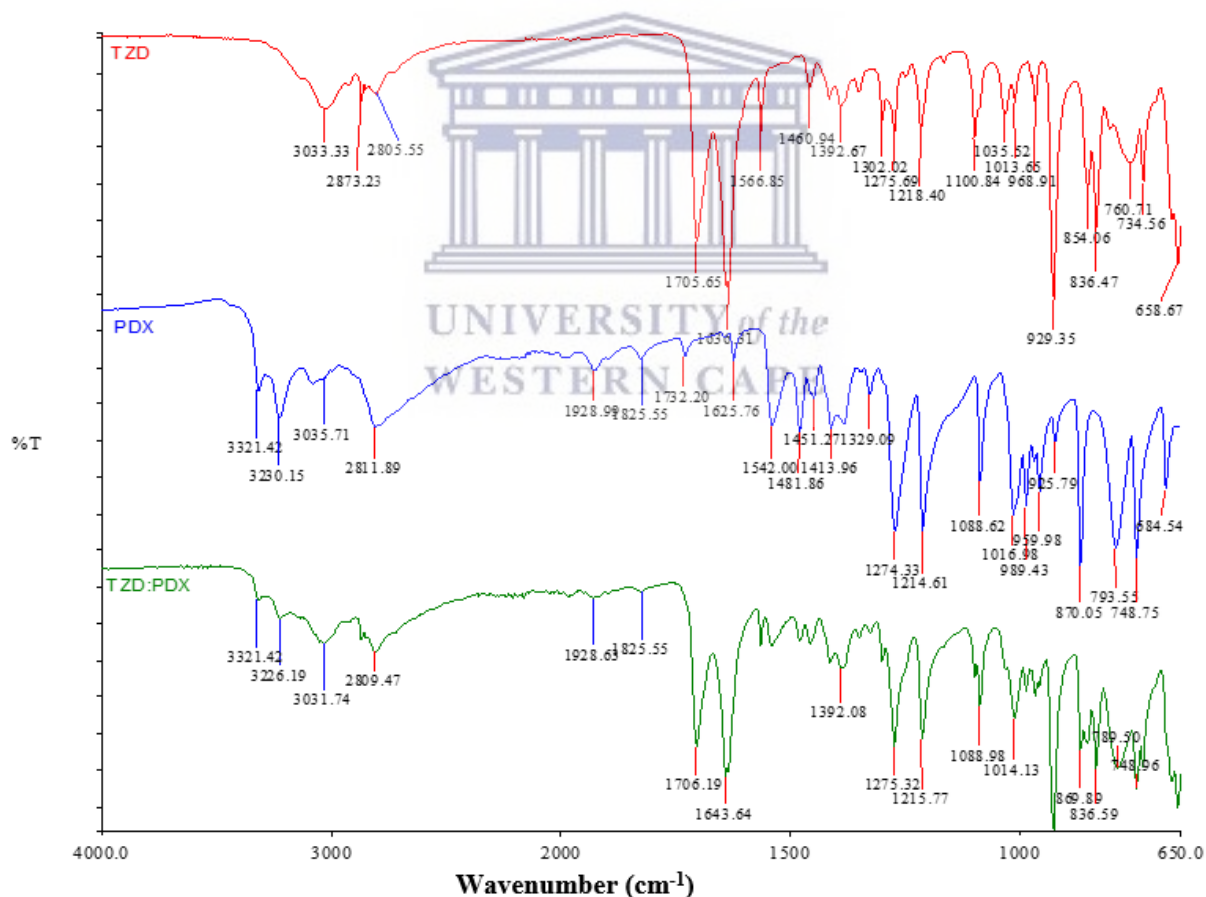


Figure 6.12: Overlay of FTIR spectra obtained for TZD, PDX and the TZD:PDX physical mixture 1:1 (w/w).

Table 6.4: Investigation of appearance and disappearance of wavenumbers of spectra of TZD, PDX and TZD:PDX (1:1 w/w).

TZD Wavenumber (cm ⁻¹)	PDX Wavenumber (cm ⁻¹)	TZD:PDX (1:1 w/w) Wavenumber (cm ⁻¹)
-	3321.42	3321.42
-	3230.15	3226.19
3033.33	3035.71	3031.74
2873.23	-	Disappearance
2805.55	2811.89	2809.47
-	1928.99	1928.63
-	1825.55	1825.55
-	1732.20	Disappearance
1705.65	-	1706.19
1636.81	1625.76	1643.64
1566.85	-	1566
-	1542.00	1542
-	1481.86	1481
1460.94	1451.27	1451
1392.67	1392.09	1392.08
1302.02	-	1302
1275.69	1274.33	1275.32
1218.40	1214.61	1215.77
1100.84	1088.62	1088.98
1035.52	-	Disappearance
1013.65	1016.98	1014.13
-	989.43	989.43
968.91	959.98	968.91
929.35	925.79	929.35
-	870.05	869.89
854.06	-	854.06
836.47	-	836.59
	793.55	789.50
760.71	-	Disappearance
-	748.75	748.96
734.56	-	Disappearance
-	684.54	Disappearance
658.67	-	658.67

Figure 6.13 depicts an overlay of the Raman spectra obtained for TZD, PDX and the combination of the two compounds and revealed a disappearance of the peak at wavenumber 692 cm⁻¹ which

signifies the C=C-C functional group associated with PDX. Only a small peak at 702 cm^{-1} was observed for the TZD:PDX mixture. However, the C-O group associated with the TZD molecule observed in the wavenumber interval of $1300 - 1000\text{ cm}^{-1}$ remained identifiable within the TZD:PDX mixture as well as the asymmetric strong stretch of alkene at 1644 cm^{-1} . The disappearance or shift of the 692 cm^{-1} peak, associated with PDX was ascribed to solid-state dilution.

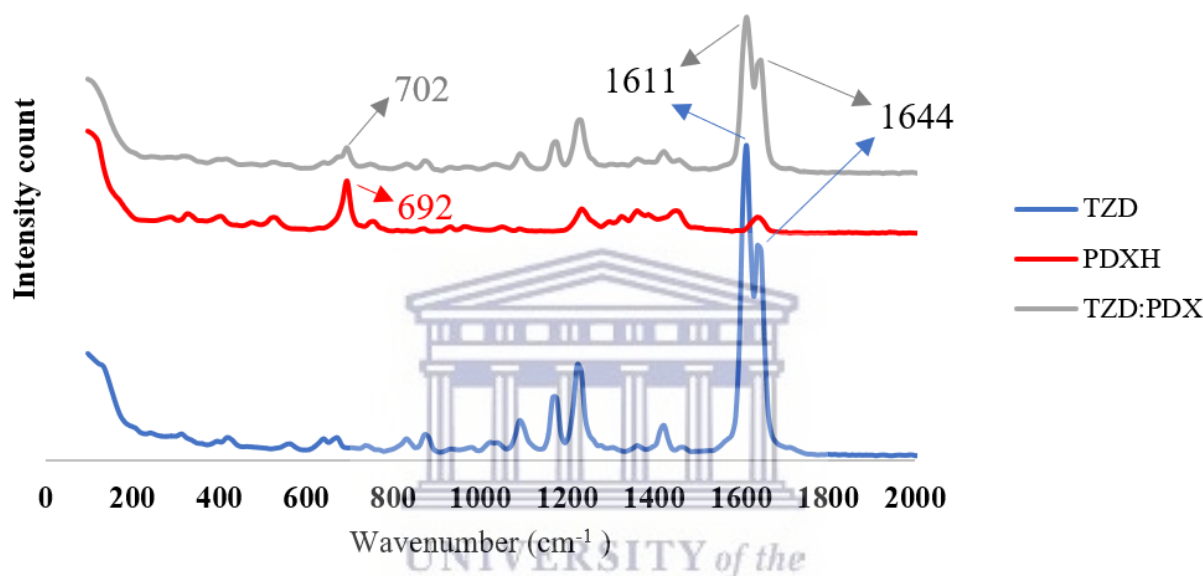


Figure 6.13: Raman spectra overlay of TZD, PDX and TZD:PDX physical mixture.

Figure 6.14 depicts an overlay of the PXRD diffractograms obtained with PDX, TZD and the TZD:PDX physical mixture. Table 6.5 outlines the diffraction peaks identified for the three investigated samples. Through comparison, it was observed that peaks associated with PDX at diffraction angles 15.56 , 21.11 and $21.95^\circ 2\theta$ disappeared in the physical mixture. At this point this observation was not ascribed to an incompatibility between PDX and TZD due to the fact that this disappearance might be due to dilution of PDX in the solid-state through the mere mixture of the two compounds.

Table 6.5: X-ray diffraction peaks obtained for TZD, PDX and TZD:PDX physical mixture 1:1 (w/w).

TZD	PDX	TZD:PDX
°2θ	°2θ	°2θ
-	10.31	10.43
-	15.56	-
16.33	-	16.39
-	16.92	17.05
18.52	-	18.60
18.88	-	-
19.25	-	-
-	20.65	-
-	20.76	20.82
-	21.11	-
-	21.95	-
23.17	-	-
23.21	-	-
-	23.43	-
23.86	-	-
-	24.19	-
-	25.05	25.07
-	25.93	26.05
-	27.83	27.87
-	29.01	-
-	37.21	-

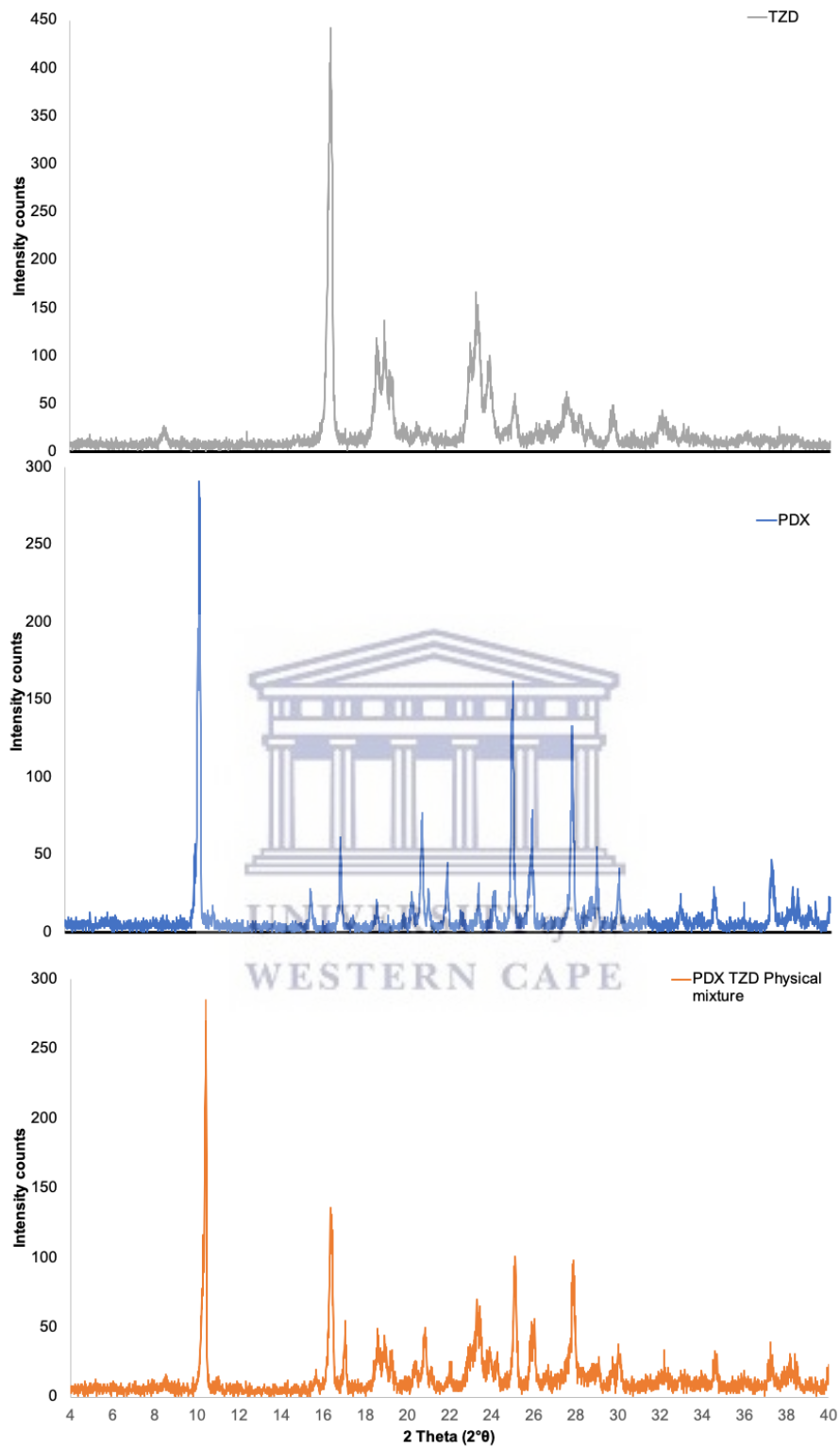


Figure 6.14: PXRD diffractograms of TZD, PDX and TZD:PDX physical mixture 1:1 (w/w).

Figure 6.15 depicts the comparison of the DSC thermograms indicating the thermal changes resulting from simply mixing TZD and PDX. It can be seen from the thermogram obtained with the TZD:PDX mixture, that the exothermic peak of TZD dominated the endothermic peak of PDX, resulting in an exothermic peak at 209.88 °C, which is 6.35 °C lower than that exhibited by TZD alone (Figure 6.10). The physical mixture also marked an earlier thermal event at ± 184 °C resembling a glass transition temperature (T_g). This was an interesting observation since neither TZD nor PDX, as single compounds, presented a T_g .

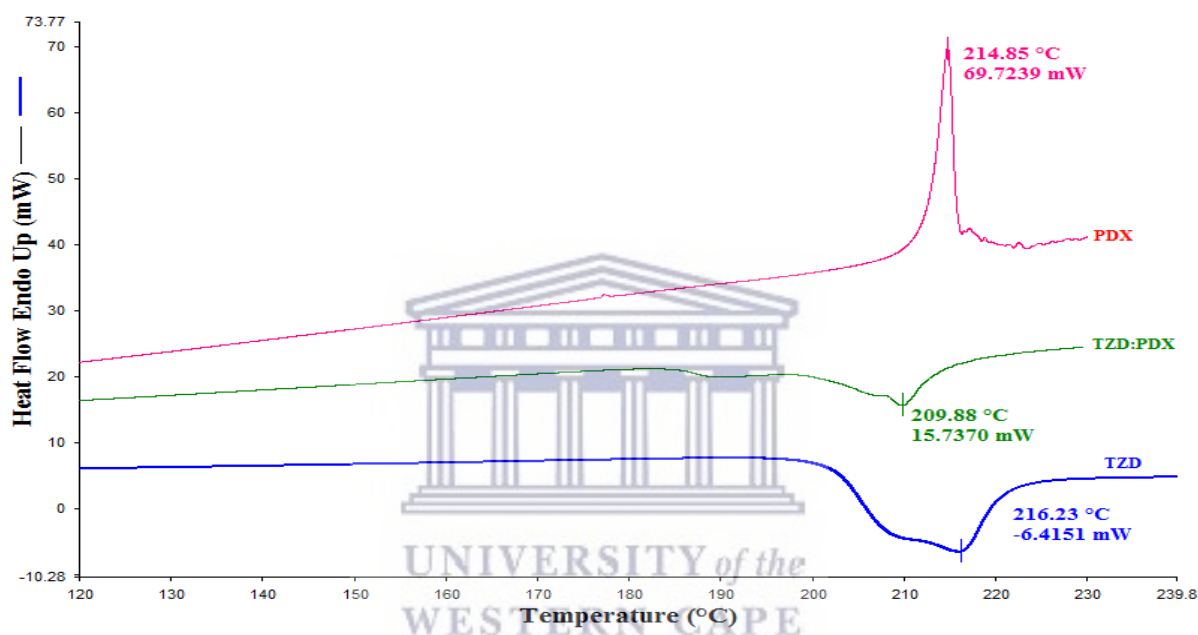


Figure 6.15: Overlay of the DSC thermograms obtained for TZD, PDX and TZD:PDX physical mixture 1:1/ (w/w).

The observed thermal behaviour was further investigated utilising HSM, in an effort to identify the observed T_g and to visually determine whether the melting behaviour of PDX was affected by the degradation behaviour of TZD. HSM revealed onset of degradation of the drug:drug mixture at ± 200 °C which is 10 °C lower than that observed with TZD and PDX alone (Figure 6.16). Since this was a 1:1 w/w ratio it was expected that the melting of PDX would be observable, but HSM did not indicate this and it appeared to be masked by the earlier onset of degradation of the mixture.

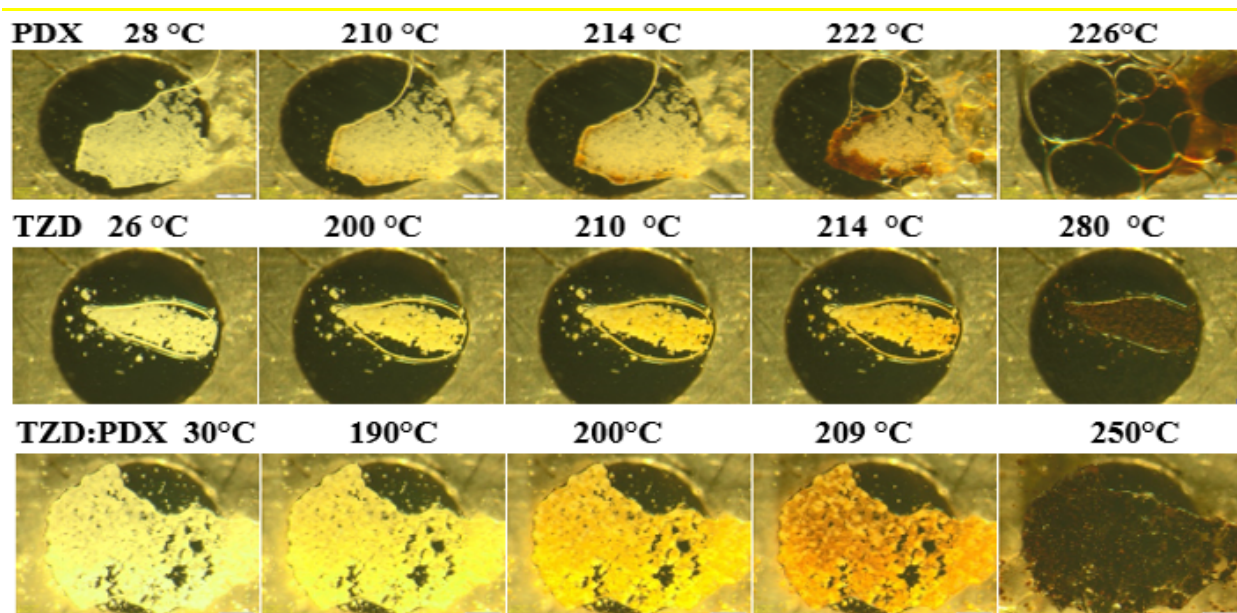


Figure 6.16 : Photomicrographs depicting the thermal behavior of PDX, TZD and TZD:PDX physical mixture 1:1/ (w/w).

Figure 6.17 depicts the thermogram obtained during TGA of the TZD:PDX physical mixture in comparison with the TGA thermograms of TZD and PDX. This result confirmed the onset of degradation of the mixture at a lower temperature (190 °C). Based on the discussed physicochemical data it became apparent that the physical mixture resulted in a quicker onset of degradation. The appearance of a T_g for the TZD:PDX, which did not present in TZD nor PDX alone, as well as the reduction in the intensity of some PXRD diffraction peaks associated with PDX lead to the hypothesis that some amorphous content was generated through the mixing process utilised for the preparation of the TZD:PDX mixture. This was considered to be advantageous since this could be indicative that a co-amorphous solid-state form could possibly be prepared.

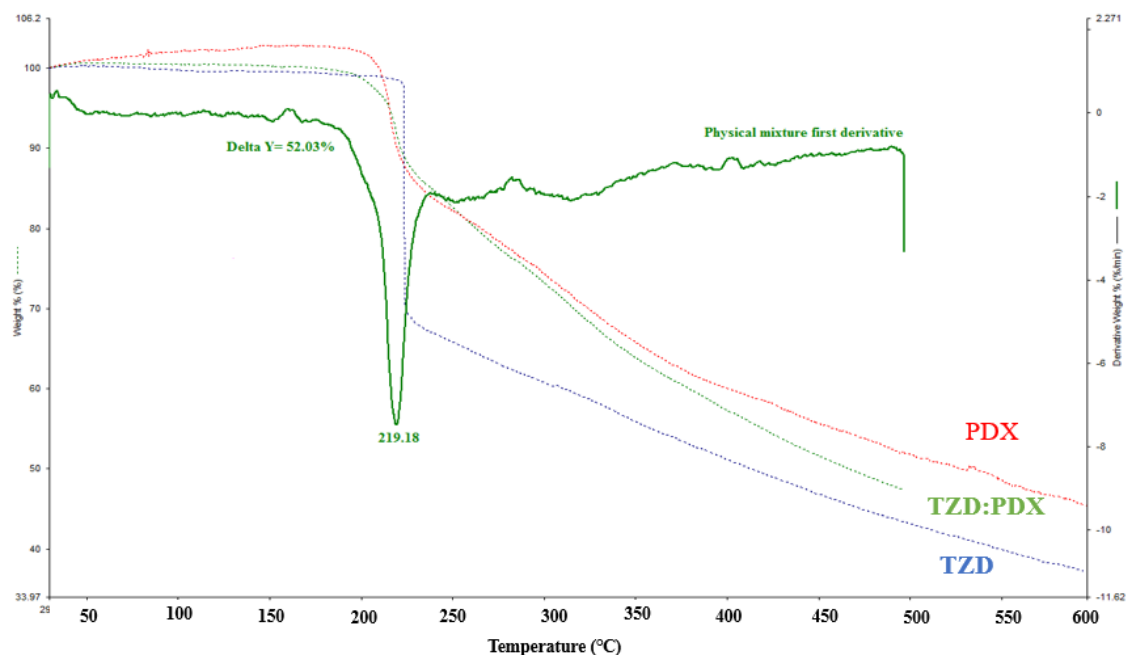


Figure 6.17 : Overlay of the TGA thermograms obtained for TGA, PDX and TZD:PDX physical mixture 1:1/ (w/w).

This being said, the fact that onset of degradation was observed at a lower temperature could also be an indication of compound incompatibility or it could be a positive indication that a metastable molecular modification consisting of the two compounds may exist. The advantage of this would be the possibility to then gain improved aqueous solubility of one or both compounds due to the metastable solid-state form (Dengale *et al.*, 2016). Based on the fact that spectroscopy results did not show any significant changes in molecular bonds it was deduced that the observed thermal events could be ascribed to the generation of amorphous content and not drug-drug incompatibility.

6.4 Investigation of different solid-state form modification techniques to prepare TZD:PDX co-crystals or co-amorphous solid-state forms

Different techniques are available to facilitate the combination of compounds on a molecular level. The techniques were screened based on equipment availability in the laboratory, or whether it is feasible upon consideration of the determined physicochemical properties of TZD and PDX. These

methods are used to enhance the intermolecular bonding between two or more molecules and formation of new solid-state habits and included: (a) solvent evaporation, (b) quench cooling of the melt and (c) liquid assisted grinding (LAG).

6.4.1 Solvent evaporation

Solvent evaporation is a simple and effective method useful in the screening of co-crystal formation on a laboratory scale (small scale). However, a well-known drawback of this solid-state modification method is that it is known to produce environmentally hazardous by-products and it might facilitate the formation of solvates which could then also potentially lead to the inclusion of toxic solvents into the molecular structure (Rodrigues *et al.*, 2018). This method was screened by dissolving the prepared TZD:PDX 1:1 w/w powder mixture in different solvents which were identified as suitable solvents, typically used during pharmaceutical recrystallisation (Chapter 4, paragraph 4.3). The solvents used in this screening process included: acetone, acetonitrile, butanol, DMSO, ethanol, methanol and iso-propanol. As highlighted in Chapter 5 and as experimentally quantified during the equilibrium solubility studies conducted for TZD, the poor solubility of TZD proved to be problematic for solid-state form screening and preparation utilising solvent evaporation. This was due to the fact that TZD is poorly soluble in almost all organic solvents used, except DMSO. The solutions prepared for solvent evaporation resulted in clear phase separation with TZD precipitating out of solution after a period of time and only PDX recrystallised or no recrystallisation was observed with the preparations remaining unchanged for several months. This method was therefore deemed unsuitable for combining the two ingredients and other methods were pursued.

6.4.2 Quench cooling of the melt

This method was pursued in an attempt to form a co-amorphous solid-state modification between TZD and PDX. However, it was found not feasible due to the rapid charring of the sample when heated beyond the melting point of PDX, as already demonstrated in Figure 6.16. The negative outcome of this preparation technique was also not surprising since literature dictates that this

technique is only suitable for compounds which show stability at the melting temperatures of the compounds to be combined or fused together *via* melting (Byrn, Zografi and Chen, 2017).

6.4.3 Liquid assisted grinding (LAG)

During this method the TZD:PDX 1:1 *w/w* powder mixture was grinded in a mortar using a pestle by slowly adding an organic solvent at regular time intervals. The same solvents utilised during the solvent evaporation experiments were used during the LAG process. After the grinding process reached completion the samples were transferred to a sealed polytop vial for subsequent analyses. From all three solid-state form preparation methods, the LAG method proved to be the most successful based on sample yield and no observable sample degradation. The obtained samples were subsequently characterised using FTIR, Raman, PXRD, HSM, TGA and DSC and the results are discussed further in the following section.

6.5 Physicochemical characterisation of TZD:PDX combinations prepared by LAG

6.5.1 FTIR analysis of obtained TZD:PDX LAG samples

To investigate the identity and formation of potential intermolecular bonds, the FTIR spectra obtained with all the LAG prepared samples were compared with the FTIR spectrum of the TZD:PDX mixture. As mentioned before, the disappearance or appearance of absorbance bands would indicate the formation of new functional bonds, which would be indicative of solid-state form modification. The TZD wavenumber of 3035 and 2872 cm^{-1} have either disappeared or overlapped in all the LAG samples. The dominant absorbance bands associated with TZD at 1705 cm^{-1} and 1636 cm^{-1} which are indicative of the ketone and alkene functional groups were still found to be dominant in all the samples prepared through the LAG method. The small peaks of 1929 and 1823 cm^{-1} of pure PDX were still present but smaller in comparison with pure PDX. The broad peak at 2811 cm^{-1} of PDX shifted between 2809-2820 cm^{-1} in all the LAG preparations. The bond of 3083 cm^{-1} associated with PDX shifted to 3039-3054 cm^{-1} and the absorbance band at 3230 cm^{-1} associated with remained the same in the physical mixture but in the LAG prepared samples it was observed in the 3235-3237 cm^{-1} range. From the fingerprint region the strong peak

of 929 cm^{-1} associated with TZD was still present in the mixture and the two strong peaks of PDX at 1274 and 1214 cm^{-1} remained unchanged. The DMSO LAG sample showed a different FTIR spectrum. Where the wavenumber between 2810 - 3321 cm^{-1} became smaller in size and two major peaks from TZD at 1705 and 1636 shifted to 1680 cm^{-1} . In all instances the LAG was conducted over a period of five minutes to enhance formation of new bonds, but the results did not show any new functional bonds present across all the prepared samples. The presence of alcohol functional bond in PDX and amide bond in TZD were expected to form intermolecular bonding which would be detected by either FTIR or Raman spectroscopy.

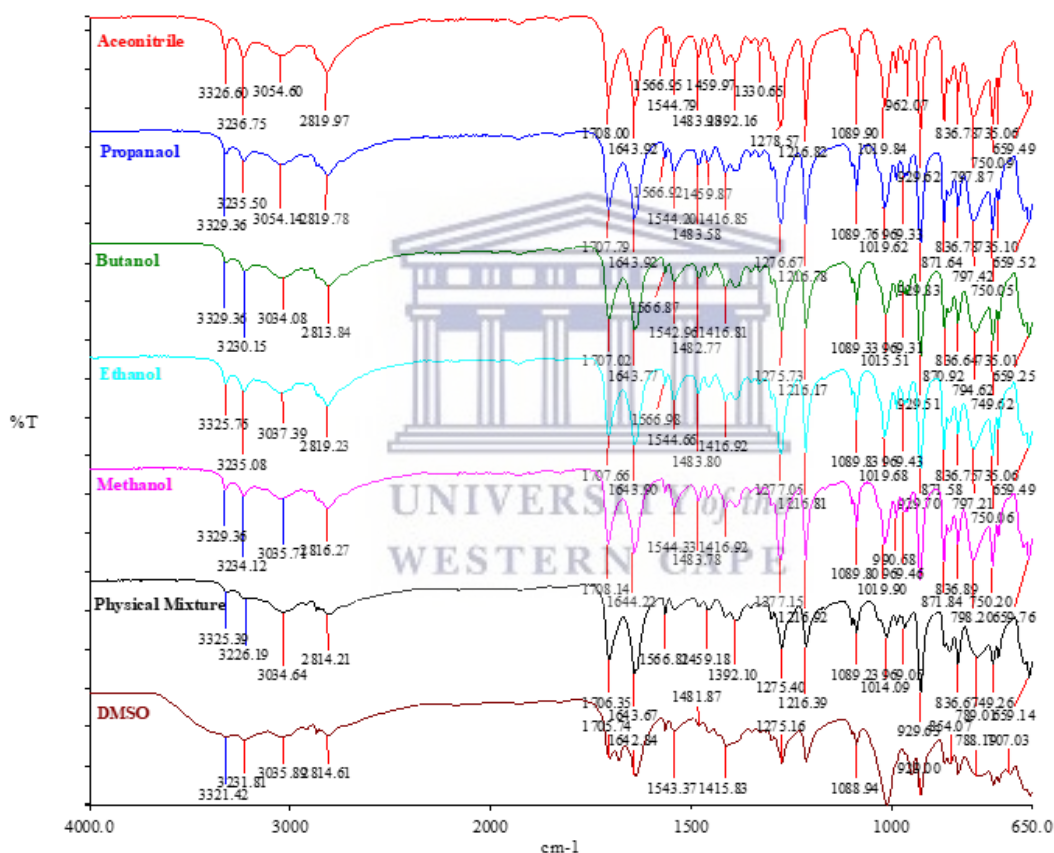


Figure 6.18: FTIR spectrum of binary mixtures 1:1 (w/w) of TZD and PDX prepared by LAG in different solvents.

Table 6.6: Theoretical and experimental FTIR wavenumbers of TZD and PDX LAG mixtures with their respective functional bonds (Smith, 2018; Larkin, 2017).

	Experimental wavenumber (cm ⁻¹)	Theoretical wavenumber (cm ⁻¹)	Associated functional group
Dominant spectrum in mixtures of TZD and PDX as depicted in Fig 6.18	3235-3237	3550-3200	-OH
	3039-3054	3300-3000	-CH ₃
	2872	2962 ±10), 2872 (±10)	-CH ₃
	2820-2809	3200-2700	-OH
	1705	1750 - 1680	-CO-
	1636	1690 - 1630	--C=C-
	1275,1216	1300-1000	-C-O-

UNIVERSITY of the
WESTERN CAPE

6.5.2 Raman spectroscopy of samples obtained during LAG

The Raman shift of pure molecules was compared to the combined binary mixtures to investigate the formation of new bonds as it was done on FTIR. The two major peaks at 1600-1700 cm⁻¹, which is a strong peak of ketone emanating from TZD and at 1100-1300 cm⁻¹ present in the single mixtures are also present in the binary mixtures. The grinding did not induce any bonding between the two drugs as it was also displayed by FTIR. The effect of grinding and LAG did not appear to influence the formation of new functional bonds.

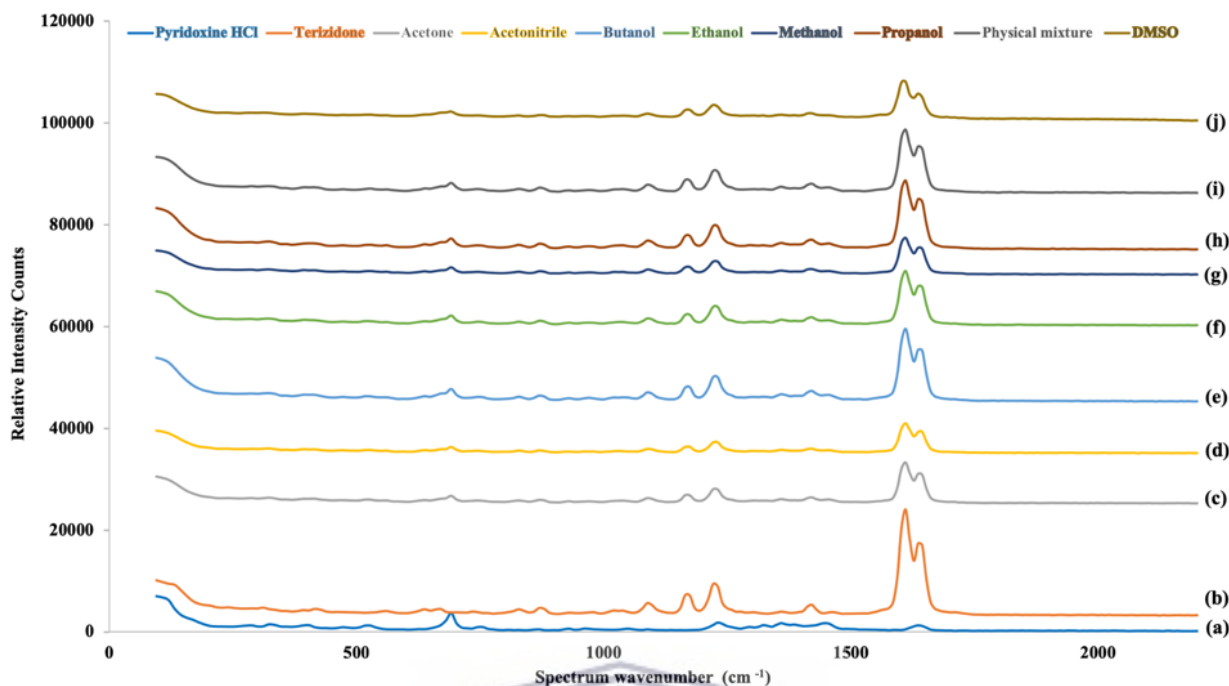


Figure 6.19: Overlay of Raman spectra obtained with (a) PDX, (b) TZD, (c) LAG with acetone, (d) LAG with ACN, (e) LAG with butanol, (f) LAG with ethanol, (g) LAG with methanol, (h) LAG with propanol, (i) TZD:PDX 1:1 w/w mixture and (j) LAG with DMSO.

6.5.3 PXRD of samples manipulated via LAG

Though Raman analysis indicated that no new molecular bonds were formed using the process of LAG and various organic solvents, FTIR analysis showed significant absorbance band broadening for the sample prepared *via* LAG using DMSO as grinding solvent. It was therefore deemed necessary to investigate these preparations using PXRD to ascertain whether new solid-state forms were prepared. Figure 6.20 depicts an overlay of the PXRD diffraction pattern obtained for the acetone LAG preparation in comparison with that of the physical mixture. On comparison it became evident that the LAG process did not result in crystallisation of a new solid-state form since all major diffraction patterns present in the physical mixture were still identifiable in the LAG acetone sample. It was however observed that the sample contained more amorphous content based on the reduction in the overall peak intensities and especially in the reduction of the peak intensity at $10.41^\circ 2\theta$, which showed a 35% reduction in peak intensity.

Figure 6.21 depicts an overlay of the sample prepared using ACN during the LAG process in comparison with the physical mixture. The same diffraction pattern was observed and just as with the sample obtained from LAG with acetone, and it was observed that the level of amorphicity increased during the LAG process. Interestingly though, the diffraction peak at $10.41^\circ 2\theta$ remained the peak exhibiting a 100% intensity in relation to the other diffraction peaks associated with the LAG ACN sample, which is different from that observed with the LAG acetone sample (Figure 6.20). Overall the diffraction peaks signified a 44.78% reduction in peak intensity thus indicating an increase in amorphous content.



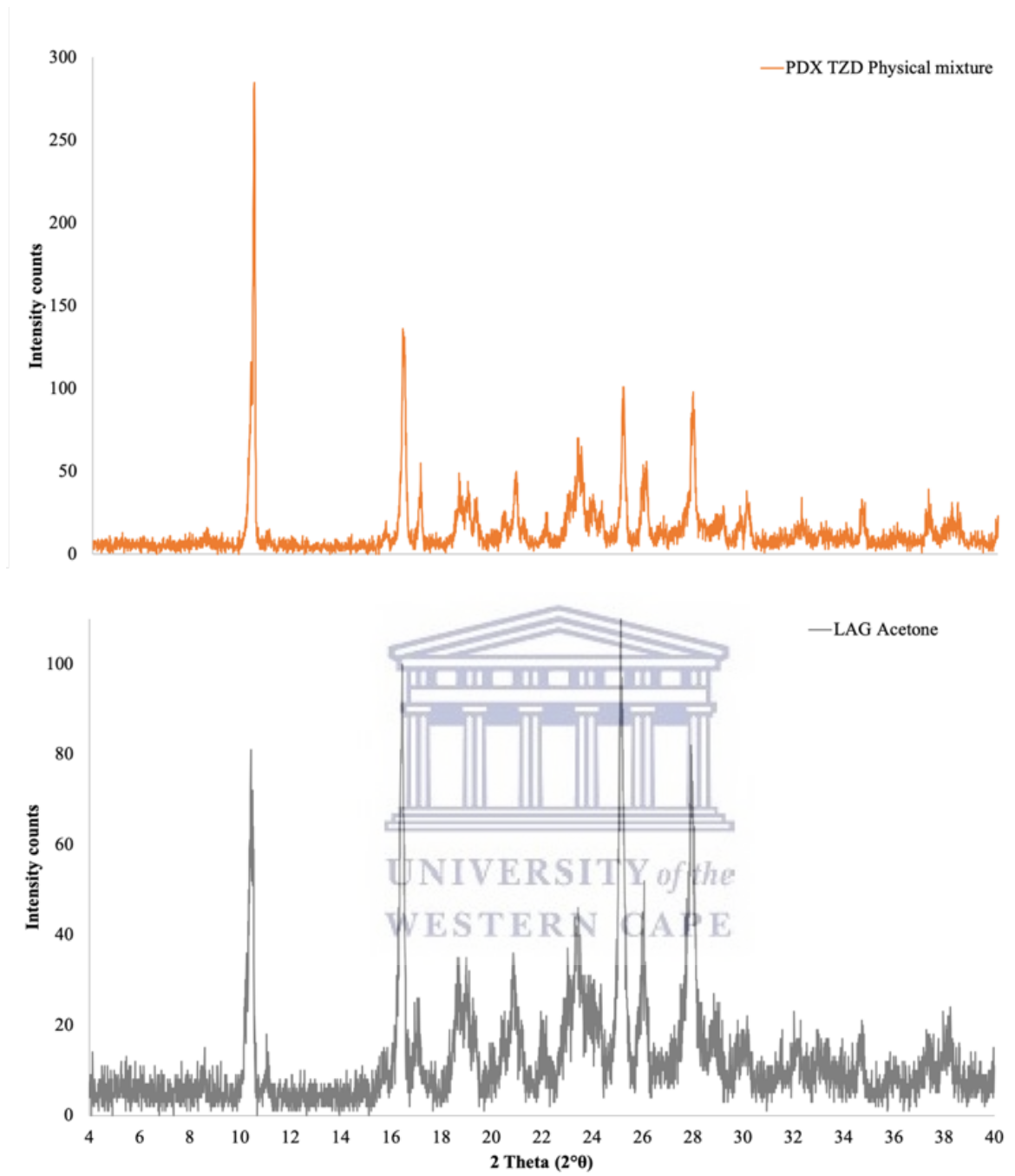


Figure 6.20: Overlay of the PXR D diffractogram obtained for the sample subjected to LAG using acetone as grinding fluid in comparison with the physical mixture.

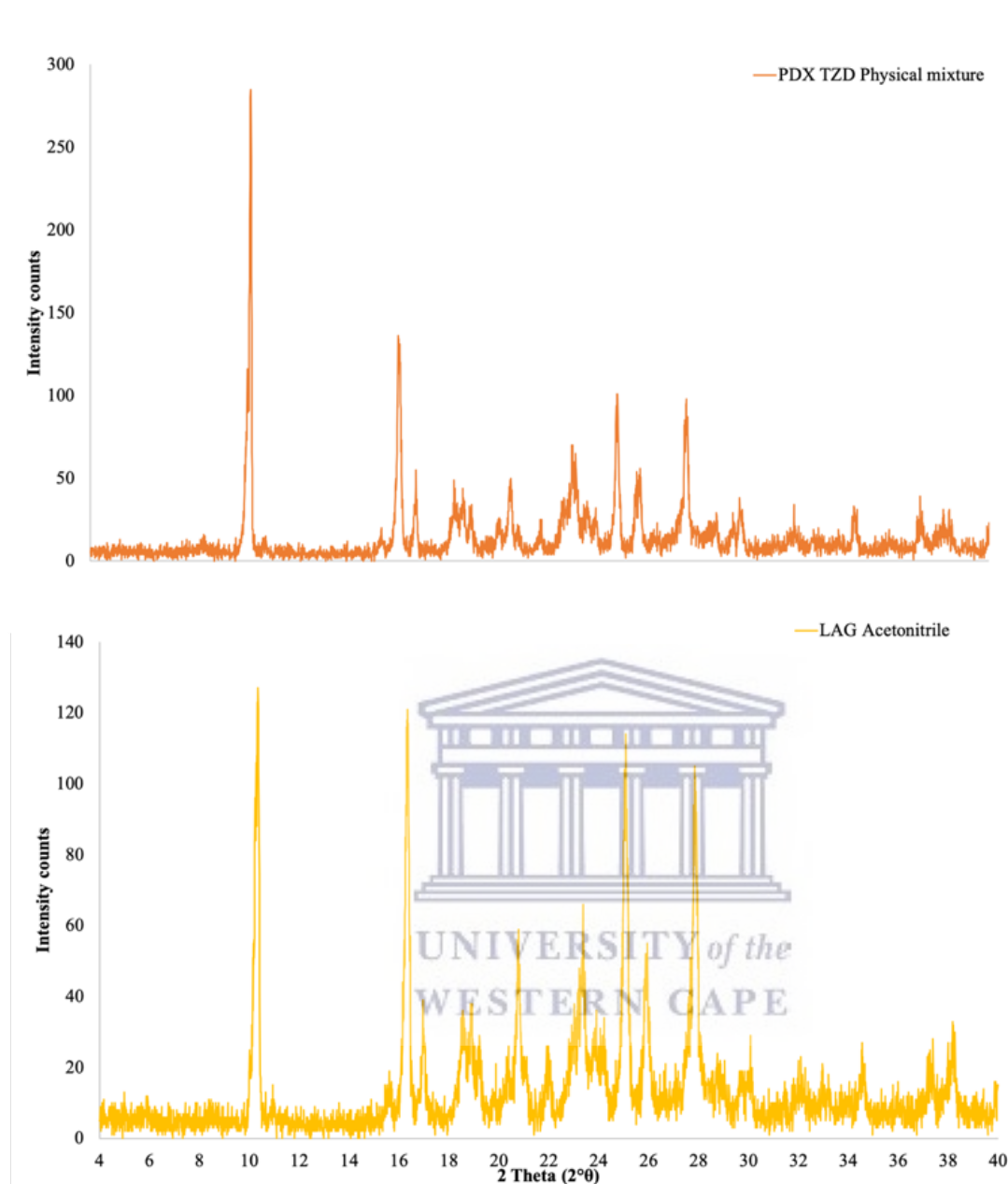


Figure 6.21: Overlay of the PXRD diffractogram obtained for the sample subjected to LAG using ACN as grinding fluid in comparison with the physical mixture.

Very similar diffraction patterns were obtained with the samples manipulated via LAG using butanol (Figure 6.22) and ethanol (Figure 6.23) as grinding fluids. In comparison, the LAG with

ethanol process resulted in a mentionable increase in amorphicity with a 38.52% reduction in the diffraction intensity of the diffraction peak at 10.41 °2 θ .

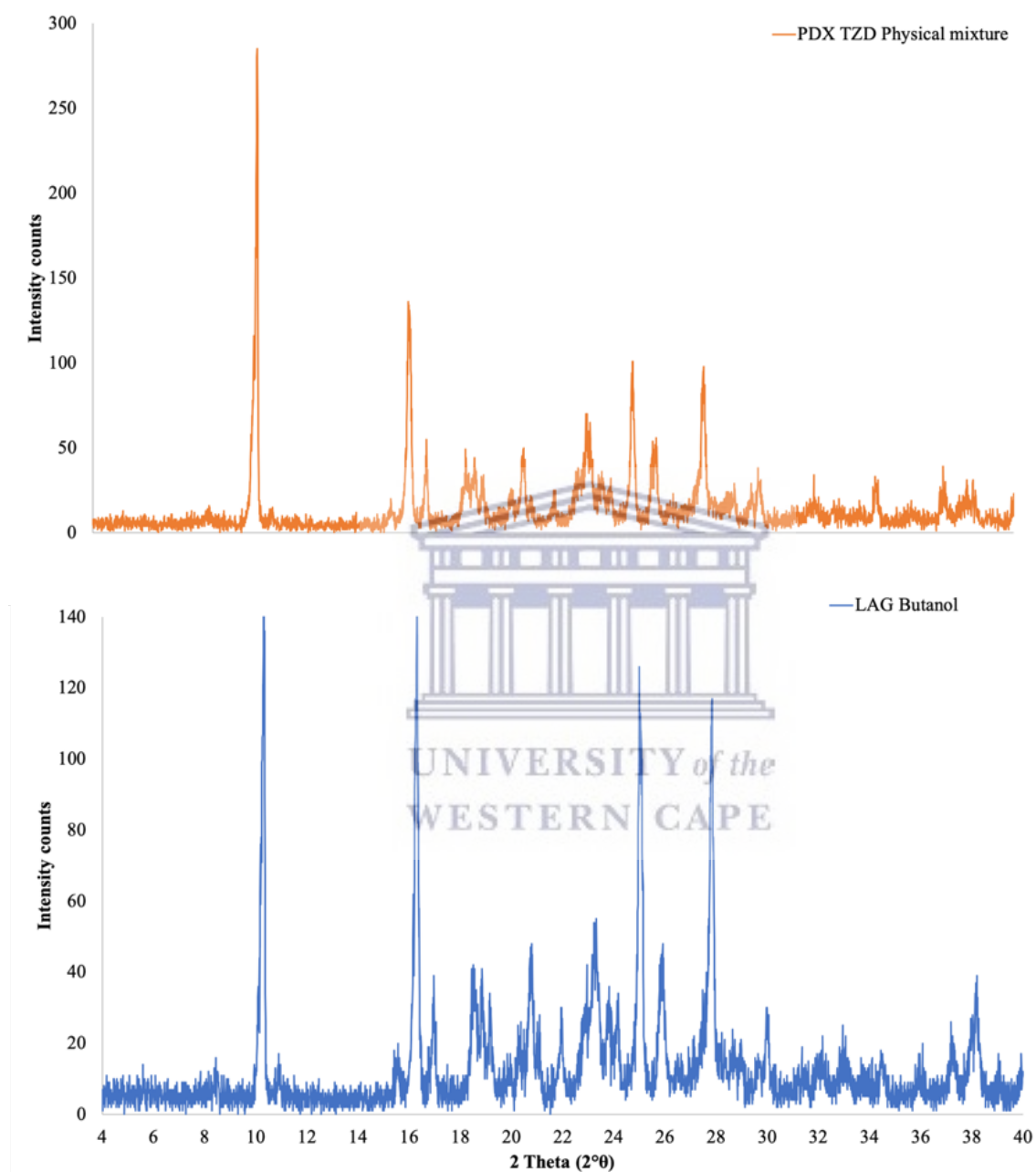


Figure 6.22: Overlay of the PXRD diffractogram obtained for the sample subjected to LAG using butanol as grinding fluid in comparison with the physical mixture.

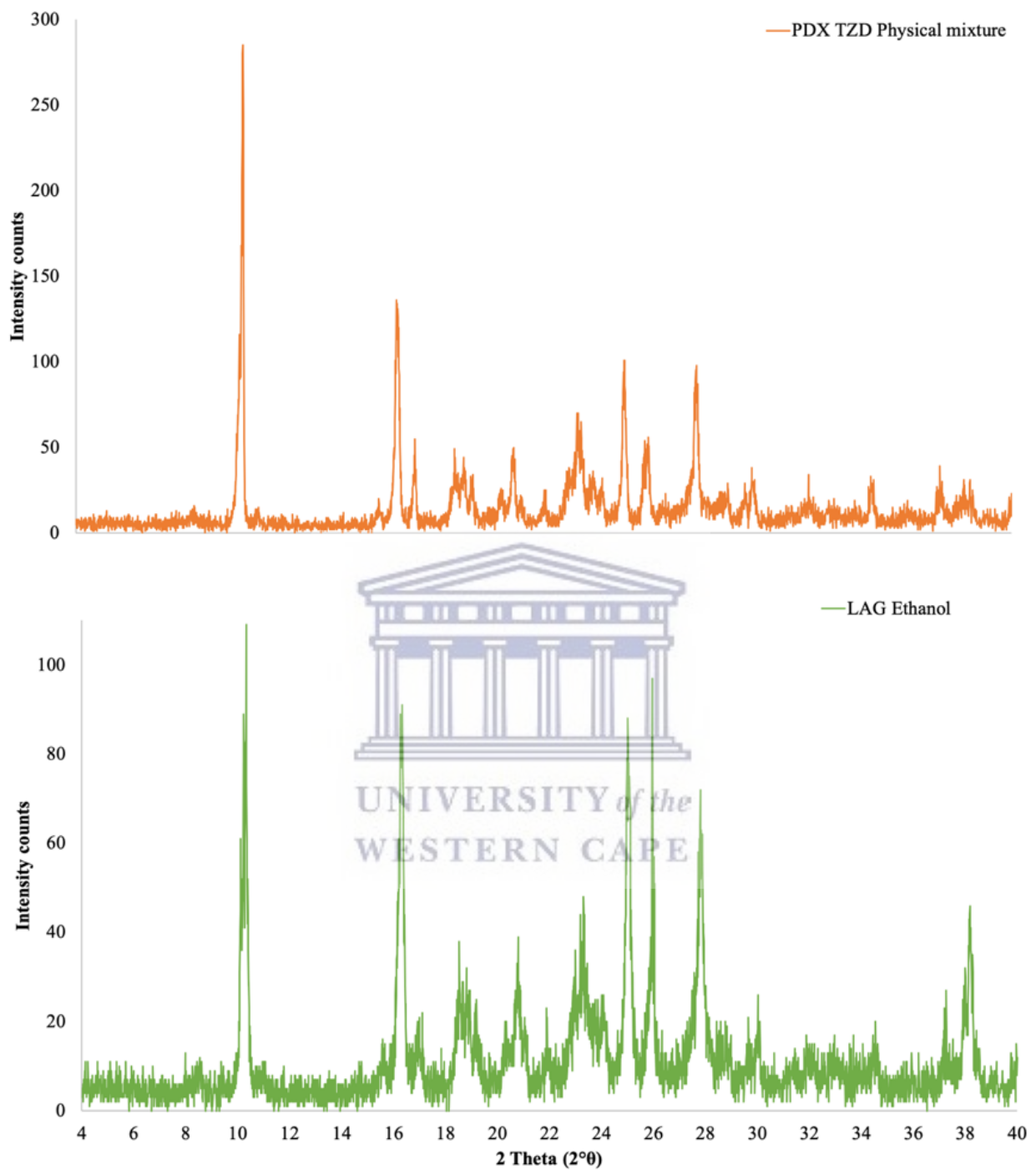


Figure 6.23: *Overlay of the PXR D diffractogram obtained for the sample subjected to LAG using ethanol as grinding fluid in comparison with the physical mixture.*

LAG utilising methanol as grinding fluid also provided a sample exhibiting increased amorphicity (44.17%) and no change in diffraction peak positions, thus signifying that no new solid-state form was prepared (Figure 6.23).

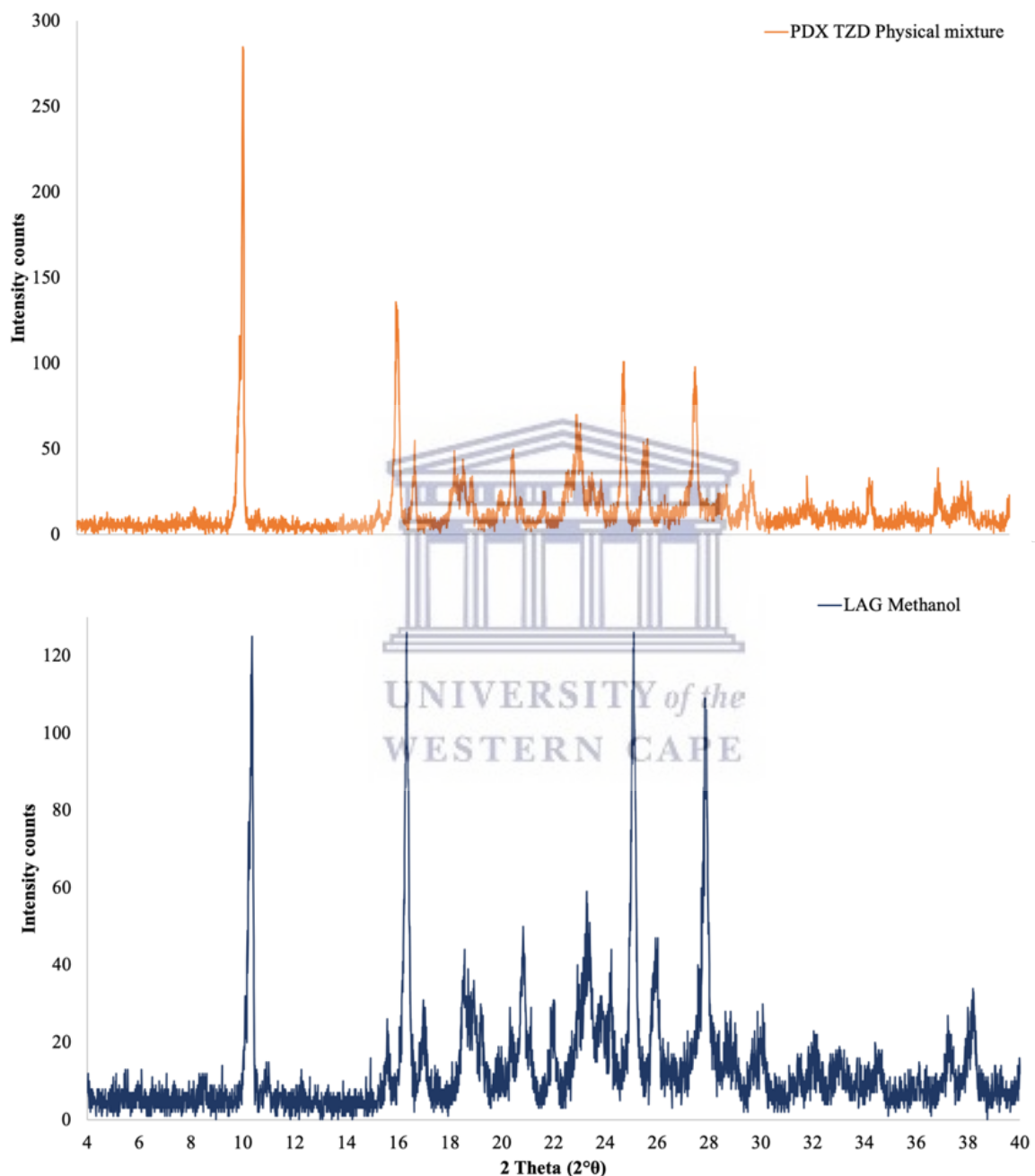


Figure 6.24: Overlay of the PXRD diffractogram obtained for the sample subjected to LAG using methanol as grinding fluid in comparison with the physical mixture.

Finally, the same trend was observed with the samples that were prepared using LAG with isopropanol as grinding fluid (Figures 6.25).

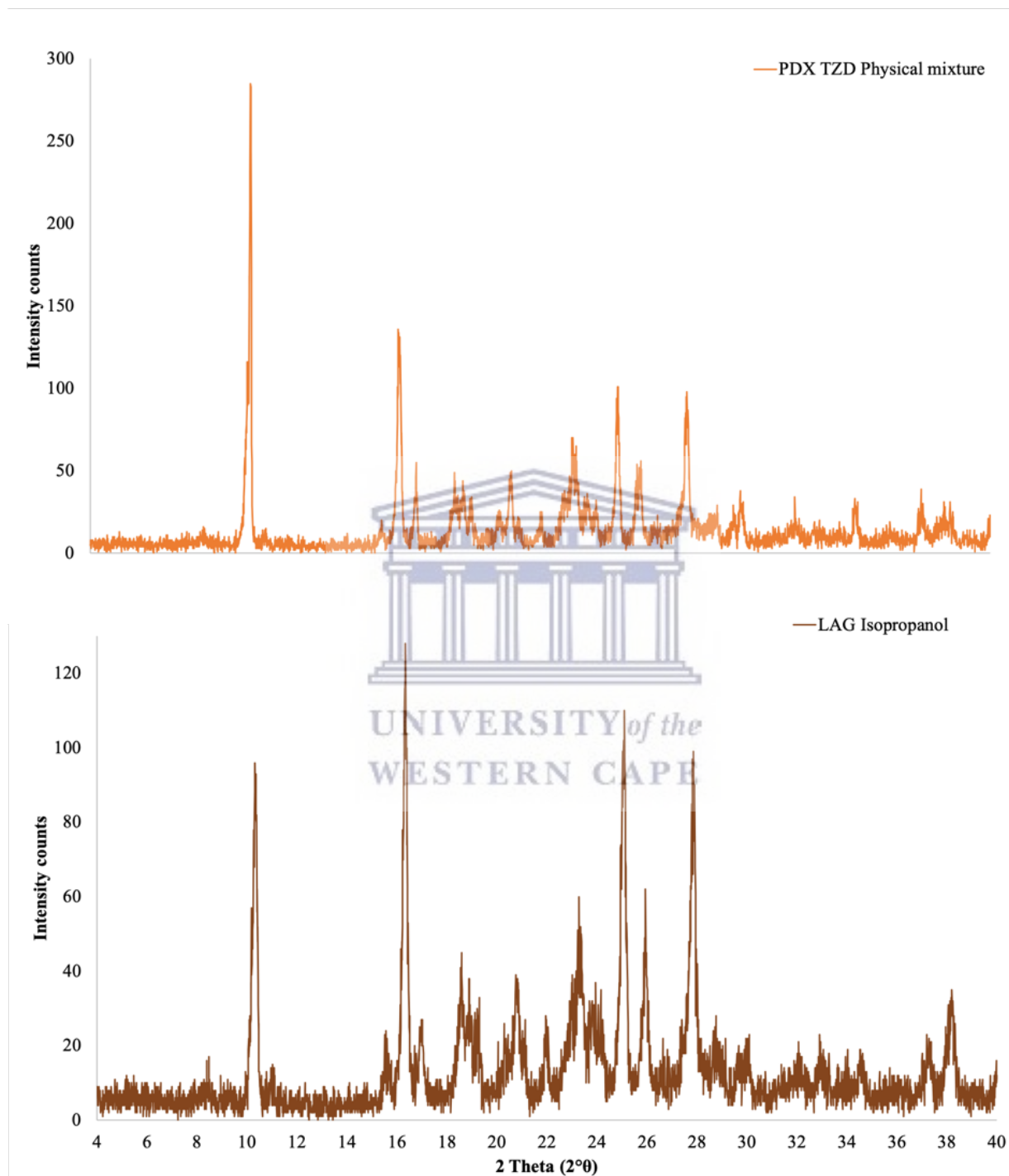


Figure 6.25: Overlay of the PXRD diffractogram obtained for the sample subjected to LAG using isopropanol as grinding fluid in comparison with the physical mixture.

A very different diffraction pattern was observed with the TZD:PDX (1:1 w/w) sample manipulated via LAG using DMSO as solvent. Figure 6.26 depicts an overlay of the diffraction pattern obtained with this sample and that of the physical mixture. This sample exhibited a definitive amorphous habit ascribed to the lack of clear diffraction patterns and a typical amorphous halo.

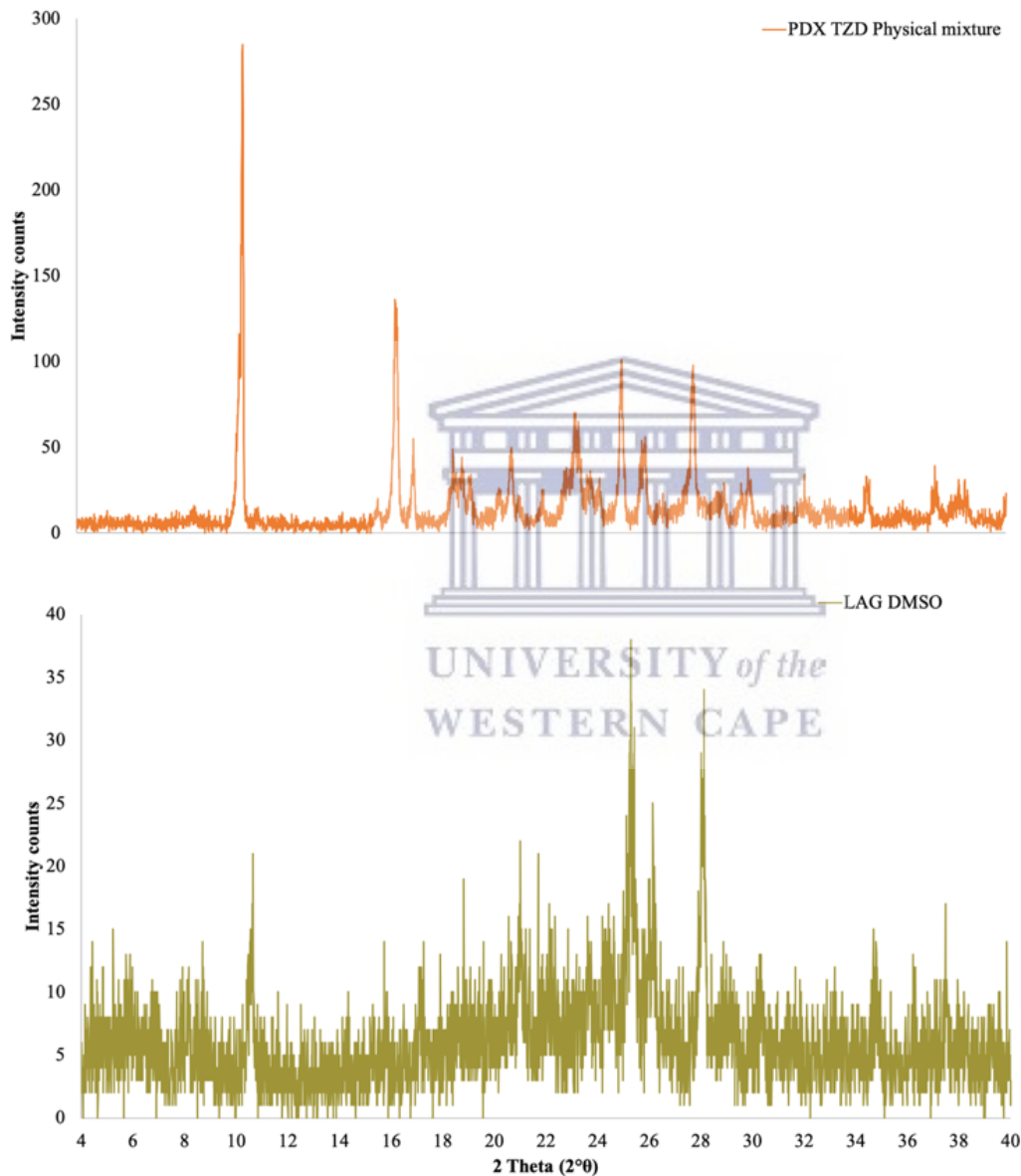


Figure 6.26: *Overlay of the PXRD diffractogram obtained for the sample subjected to LAG using DMSO as grinding fluid in comparison with the physical mixture.*

From the spectroscopy and PXRD data it was deduced that the LAG preparation process did not result in the co-crystallisation of TZD and PDX, in fact it became evident that the opposite occurred with the generation of amorphous content. All the LAG prepared samples showed very similar spectroscopic data and in reference to the obtained FTIR data it was only the LAG sample prepared with DMSO which exhibited absorbance band broadening and the disappearance of absorbance bands. In reference to the Raman spectroscopic data no differences were identified between the different samples (Figure 6.19), whilst PXRD data obtained with the sample prepared using DSMO depicted complete amorphisation of the drug:drug mixture (Figure 6.26). This was in good correlation with the absorbance band broadening observed during FTIR analysis (Figure 6.18) and at this point it was concluded that a co-amorphous solid-state form consisting of TZD:PDX was prepared. It was therefore imperative to investigate the thermal properties associated with the prepared samples and for completeness sake all samples prepared via LAG were investigated further.

6.5.4 Thermal behaviour characterisation of TZD:PDX manipulated via LAG

6.5.4.1 Hot stage microscopy (HSM)

HSM of the samples manipulated using LAG involving various solvents as grinding fluids was performed across a temperature range of 30 – 250°C. Figure 6.27 depicts the micrographs obtained for all the analysed samples. In all instances it was observed that the onset of degradation which is signified by discolouration of the sample, occurred at temperatures significantly lower than that observed for the TZD:PDX physical mixture. Table 6.7 outlines the observed temperature differences. Interestingly, the differences in the onset of degradation temperatures were relatable with the amorphicity of the samples. With the DMSO LAG sample, which showed the greatest degree of amorphicity showing the most significant difference in terms of onset of degradation. This may be linked to the metastable nature of the prepared amorphous form since amorphous forms are known to exhibit lower stability due to the higher level of Gibbs free energy associated with such solid-state forms. However, these instabilities are usually associated with physical stability, in other words how stable the physical solid-state form will remain. The observed discolouration of the samples and



associated degradation signifies chemical instability. This observation therefore warranted further investigation.

Table 6.7: Visually observed onset of degradation of samples prepared using LAG in comparison with the TZD:PDX (1:1 w/w) physical mixture.

Sample	Onset of degradation temperature (°C)	Temperature difference (°C)
TZD:PDX (1:1 w/w) physical mixture	≈ 190	-
Acetone LAG	≈ 175	≈ 15
ACN LAG	≈ 181	≈ 9
Butanol LAG	≈ 152	≈ 38
Ethanol LAG	≈ 169	≈ 21
Methanol LAG	≈ 175	≈ 15
propanol	≈ 174	≈ 16
DMSO LAG	≈ 125	≈ 65



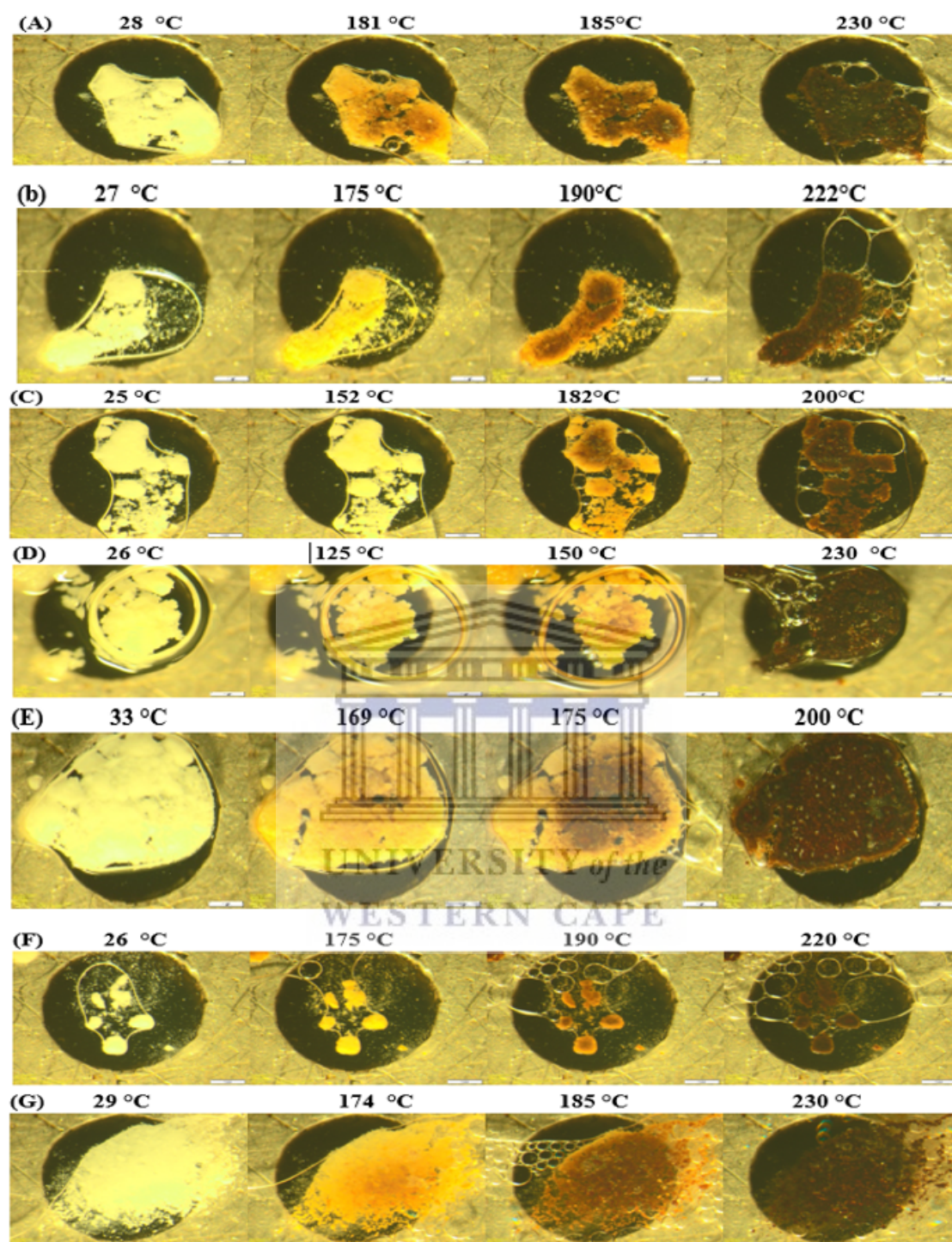


Figure 6.27: HSM data of binary mixtures of TZD and PDX prepared by LAG (1:1(w/w)) indicating the initial, the onset, the peak and the end of the main thermal events (left-to-right) in the following solvents: A: acetone, B: acetonitrile, C: Butanol, D: DMSO E: Ethanol, F: Methanol, and G: Propanol.

6.5.4.2 Thermogravimetric analysis (TGA)

The TGA results corroborated the visual findings of the HSM results. All the samples prepared via LAG exhibited onset of degradation at lower temperatures than observed for TZD, PDX and the TZD:PDX physical mixture. Table 6.8 provides an outline of the onset of degradation temperatures and calculated percentage weight loss (%) associated with each sample prepared via the LAG method.

Table 6.8: TGA onset of degradation and percentage weight loss (%) of samples prepared using LAG in comparison with the TZD:PDX (1:1 w/w) physical mixture.

Sample	Onset of degradation (°C)	Percentage weight loss (%)
TZD:PDX physical mixture	190	52.60
Acetone LAG	180	49.85
ACN LAG	175	49.48
Butanol LAG	180	49.75
Ethanol LAG	175	53.83
Methanol LAG	176	54.54
Propanol LAG	179	52.39
DMSO LAG	130	56.95

6.5.4.3 Differential scanning calorimetry (DSC)

The DSC thermogram series depicted in Figure 6.28 showed very interesting thermal behaviour. For all LAG samples, except the DMSO LAG sample two exothermic events were observed and in all instances the onset of the first exothermic event occurred at a significantly lower temperature than that observed with the TZD:PDX (1:1 w/w) physical mixture. Based on the HSM data (Figure 6.27) the exothermic events were all associated with compound degradation but all thermograms indicated lower onset of degradation (<200°C) just as observed with HSM and TGA. This is attributed to the grinding effect and the solvent involvement which lowers the kinetic energy. It increases the surface area, therefore resulting in early degradation of the compounds. The disappearance of the endothermic peak of PDX and the appearance of two exothermic peaks highlight the possibility of compound interaction which was not considered that significant up until reviewing this data. As mentioned the DSC thermogram obtained with the DMSO LAG sample appeared to be different with an indication of a T_g at 203.7 °C. The formed product also exhibited a different colour attributed to the DMSO solvent. TZD shows the highest solubility in DMSO than in any other organic solvents

and this could be the reason why the outcome for the LAG process is different for DMSO than any of the other solvents used.

This being said, the fact that the LAG samples prepared using acetone, ACN, butanol, ethanol, methanol and isopropanol exhibited two degradation events which is significantly different from that observed with the physical mixture, remained unexplained. Based on the data it was not possible to identify which compound contributed to the first or second degradation events and it was not clear whether this thermal behaviour is due to potential interaction between TZD and PDX. To address these uncertainties TZD and PDX were investigated further by subjecting TZD alone and PDX alone to LAG and the results of this investigation is discussed in paragraph 6.6.



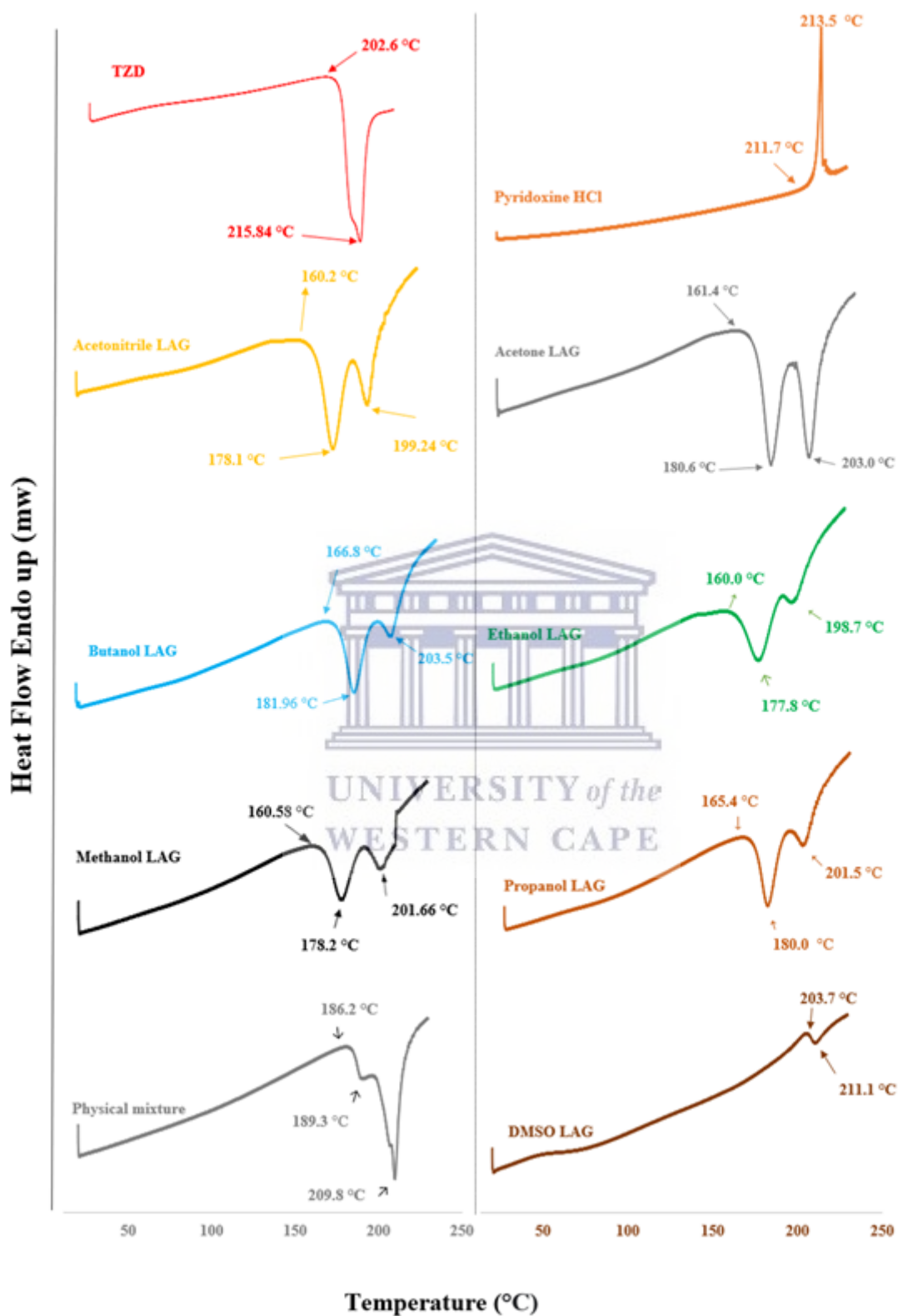


Figure 6.28: DSC thermograms obtained with all samples prepared via LAG in comparison with pure TZD, pure PDX and the TZD:PDX (1:1 w/w) mixture.

6.6 The investigation of the effect of LAG on TZD and PDX as single compounds using HSM and DSC analyses

During this investigation, TZD and PDX were subsequently individually subjected to LAG to investigate the unexplained thermal behaviour of the samples observed during DSC analyses. As control samples, both TZD and PDX were also grinded separately without the addition of any solvent (dry grinding). This was done to aid in comparison with the TZD LAG and PDX LAG samples. Figure 6.29 depicts an overlay of the DSC thermograms obtained for the TZD LAG samples. For all the samples, except the DMSO LAG, a single exothermic thermal event was observed at 214°C. DSC analysis of the DMSO LAG sample revealed a T_g at 110 °C, which is different from that observed for the TZD:PDX DMSO LAG sample (Figure 6.27). The DSC results were found to be in good agreement with the HSM results obtained (Figure 6.2).

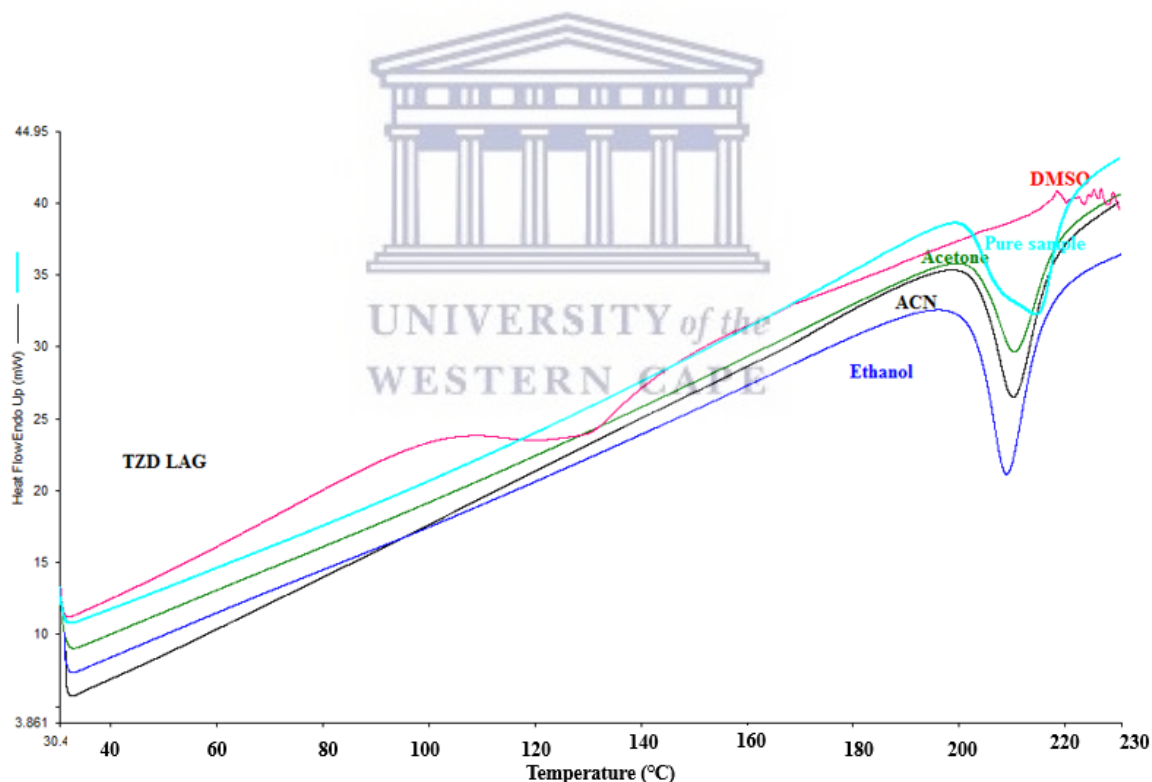


Figure 6.29: DSC thermograms obtained with TZD subjected to LAG using acetone, ACN, ethanol, DMSO and no solvent (dry grinding).

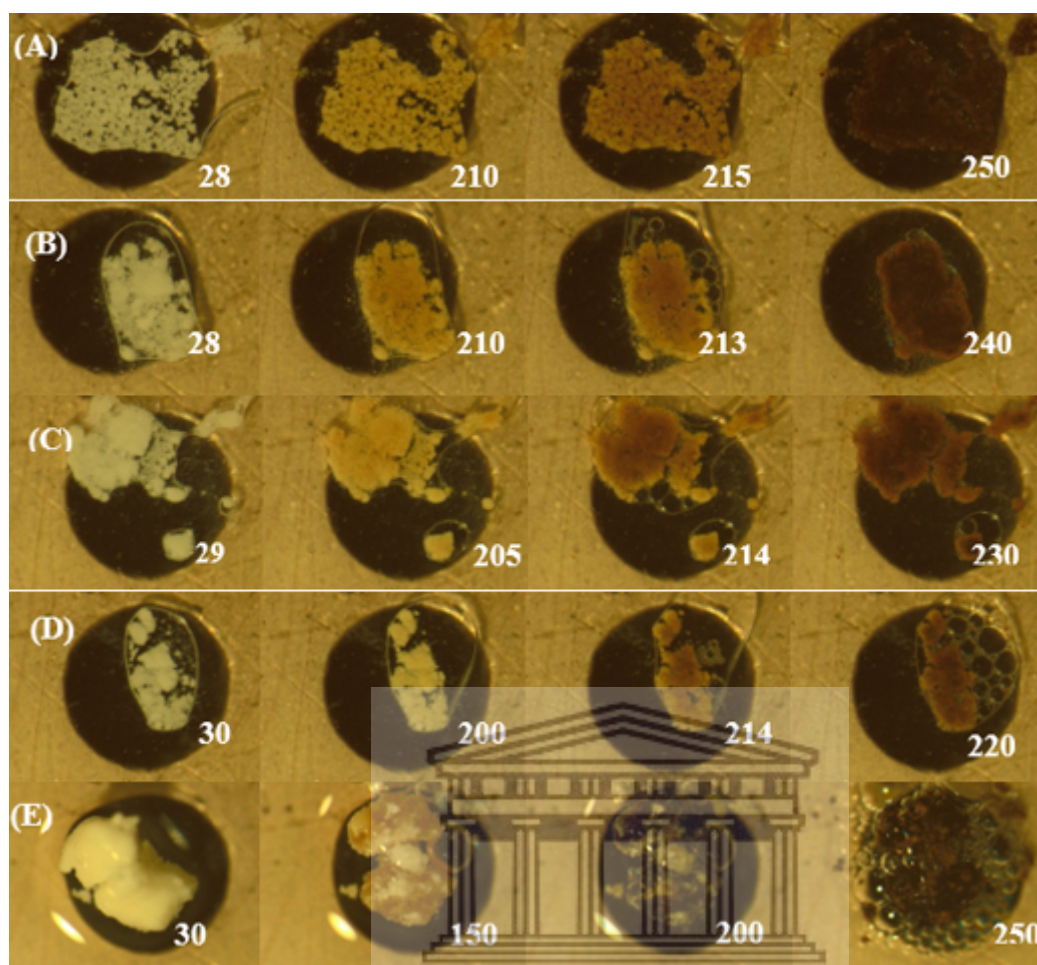


Figure 6.30: HSM micrographs depicting the thermal behaviour ($^{\circ}\text{C}$) of TZD samples prepared by LAG with (A) grinded TZD - without solvent, (B) acetone, (c) ethanol, (D) ACN, (E) DMSO heated at $10^{\circ}\text{C}/\text{min}$ under silicone oil.

For all TZD LAG samples, except the DMSO LAG sample, onset of degradation was observed from around $205 - 210^{\circ}\text{C}$, which is in accordance with the DSC thermograms (Figure 6.28). The micrographs obtained for the TZD DMSO LAG sample showed liquefaction at $\pm 150^{\circ}\text{C}$ thus corresponding to the DSC data.

Figure 6.31 depicts an overlay of the DSC thermograms obtained during the LAG process with PDX alone. Once again, in all instances, except with the PDX DMSO LAG sample, melting endotherms ranging between 217 and 220°C were observed. The PDX DMSO LAG sample exhibited a T_g at $\approx 200^{\circ}\text{C}$. Figure 6.29 depicts the micrographs obtained during HSM of all the investigated samples. All PDX LAG samples, except the DMSO LAG sample showed onset of melting at $\approx 214^{\circ}\text{C}$. The PDX DMSO LAG sample marked a thermal event at a lower

onset temperature of $\approx 193^{\circ}\text{C}$. This observed thermal event was not ascribed to melting but rather an onset of degradation of the PDX sample.

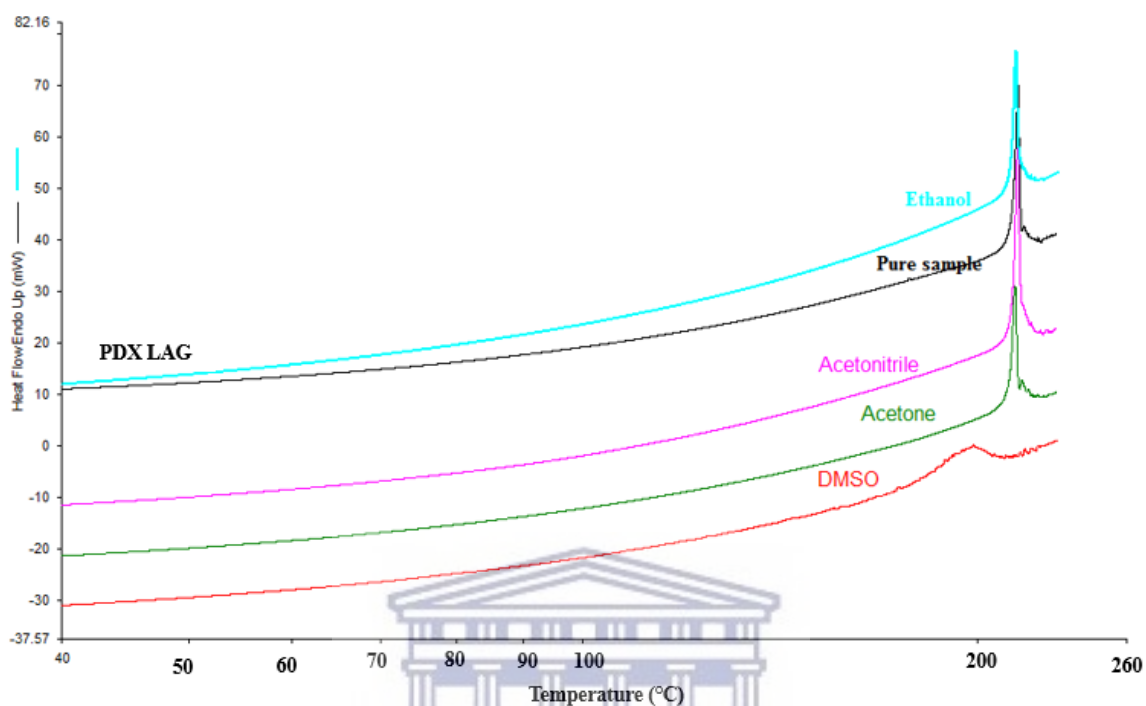


Figure 6.31: Overlay of DSC thermograms of PDX prepared by LAG using acetone, ACN, ethanol and DMSO as grinding fluids and dry grinding as a control sample.

UNIVERSITY of the
WESTERN CAPE

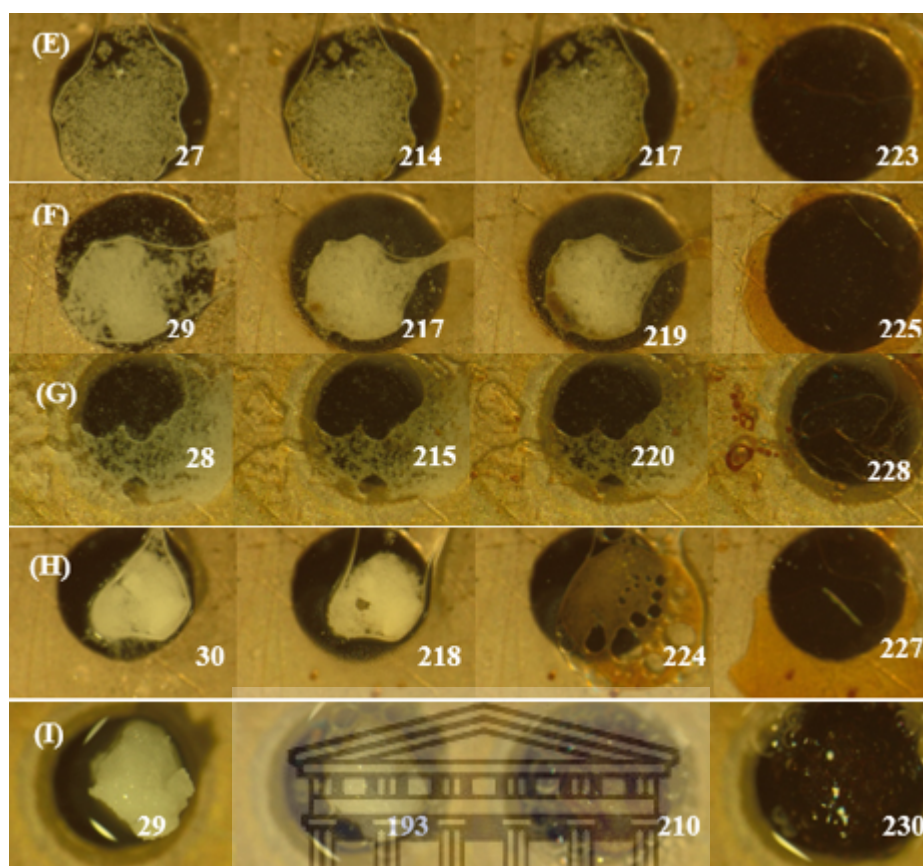


Figure 6.32: HSM micrographs depicting thermal events displayed in (°C) for PDX samples prepared by LAG with (E) grinded PDX alone, (F) acetone (G) ACN, (H) ethanol and (I) DMSO heated at 10 °C per min under silicon oil.

From the described thermal data it became apparent that there was no difference between the thermal behaviour of the dry grinded samples versus the LAG samples prepared with acetone, ACN and ethanol. In fact, the single LAG samples (TZD alone and PDX alone) compared well with the dry grinded samples and presented in each instance with a single thermal event. The TZD samples showed a single degradation event, whilst the PDX samples showed a single melting endotherm. Considering this, it could be concluded that the multiple degradation events observed for the TZD:PDX LAG samples could be attributed to an interaction and potentially an incompatibility between the two compounds.

On the other hand, the samples grinded using DMSO as grinding fluid exhibited thermal behaviour very different from that of all the other LAG samples, irrespective of whether the compounds were investigated alone or in combination with one another. It was therefore hypothesised that DMSO might potentially be the best solvent option since it was the only solvent which rendered the TZD:PDX combination into a co-amorphous solid-state form.

However, based on the observation that a potential incompatibility may exist between TZD and PDX this aspect had to be investigated and needed to be confirmed since an incompatibility shall have detrimental effects, should an FDC product consisting of the two APIs be formulated.

6.7 Compatibility study of TZD and PDX in combination with another

A thorough compatibility study subsequently commenced. Firstly, all the TZD:PDX LAG samples as prepared and discussed in section 6.5 were assayed to determine the drug purity after the LAG process. This was performed to ascertain whether compound degradation due to the LAG process might have occurred. Table 6.9 provides the quantified percentage drug purity (%) for each LAG sample. It was observed that each LAG sample, except the DMSO LAG sample, still contained each drug in a percentage proportionally close to the theoretical 100% each LAG sample started out from. The DMSO LAG sample showed severe degradation of both compounds with a calculated 96.08% and a 23.36% reduction in the purity of TZD and PDX, respectively.

Table 6.9: Onset of degradation and percentage weight loss (%) of samples prepared using LAG in comparison with the TZD:PDX (1:1 w/w) physical mixture

Sample	% TZD \pm STDEV	% PDX \pm STDEV
LAG Acetone	95.24 \pm 1.13	107.28 \pm 0.26
LAG ACN	97.64 \pm 0.24	102.70 \pm 2.23
LAG Butanol	98.68 \pm 0.00	107.02 \pm 0.23
LAG Ethanol	96.18 \pm 0.38	109.26 \pm 1.35
LAG Methanol	96.59 \pm 0.08	109.95 \pm 0.51
LAG Propanol	96.94 \pm 0.26	106.18 \pm 1.47
LAG DMSO	3.92 \pm 0.24	76.64 \pm 1.86

Based on these results further investigation was warranted due to the fact that the quantified drug purity in each LAG sample, except the DMSO LAG sample, did not explain the observed thermal behaviour (Figure 6.27), yet. A compatibility study of the TZD:PDX combination at elevated temperature was therefore pursued, in an attempt to accelerate any adverse chemical interaction, which may exist between the two drugs. This resulted in the isothermal storage of pure TZD, pure PDX and the TZD:PDX (1:1 w/w) mixture at 60 °C \pm 0.5 °C for a period of 28 days. Samples were analysed on a weekly basis utilising TGA, to determine the onset of

degradation, FTIR to ascertain whether any molecular interactions occurred and finally the drug content was determined to identify and quantify any chemical degradation.

The TGA data were analysed by measuring the % total weight loss which occurred during the heating run, to determine the effect of the heat stress over a period of 28 days on the control samples as well as the drug-drug combination. The peak temperature at which degradation occurred was also documented. For all documented results, the *p*-values were determined utilising the Excel ANOVA Toolpak, and the data presenting with *p* > 0.05 was reported as not statistically significant (Kennedy-Shaffer, 2017). Across the 28-day testing period, PDX marked an average weight loss of 51.21 ± 5.8 % and the calculated *p*-value of 0.89 showed the slight deviations in the average calculated weight loss to be insignificant. It was however noted that the peak degradation temperature associated with PDX increased from 215.61 °C to 223.58 °C from day 0 to day 28 (Table 6.10).

The average % weight loss documented for TZD across the 28 day testing period showed an average of 57.12 ± 5.88 % with a *p*-value of 0.74 which was also not statistically significant. The variation observed in the TZD peak degradation temperature was also not found to be significant. The same trends were observed with the TZD:PDX physical mixture stored isothermally at 60 °C for 28 days (Table 6.11). Therefore, based on thermal degradation behaviour the combination of TZD:PDX showed to be stable and compatible.

The FTIR analyses conducted for PDX (Figure 6.33), TZD (Figure 6.34) and TZD:PDX (1:1 w/w) mixture (Figure 6.35) did not detect any changes in the molecular conformations, as the FTIR data did not show any shifts in wavenumbers. This proves that there was no chemical interference induced by the heat as the FTIR spectra remained unchanged from day 0 to day 28 for all the samples.

Table 6.10: TGA compatibility data of pure PDX, pure TZD and TZD:PDX (1:1 w/w) combination stored at 60 °C and analysed on a weekly basis for a period of 28 days.

	Day 0	Day 7	Day 14	Day 21	Day 28
PDX					
Weight loss (%)	54.71	46.13	54.01	43.97	57.25
Peak degradation temperature (°C)	215.61	223.7	223.58	223.70	222.17
TZD					
Weight loss (%)	62.67	49.67	53.98	55.80	63.49
Peak degradation temperature (°C)	222.65	215.00	212.44	221.95	219.17
TZD:PDX (1:1 w/w)					
Weight loss (%)	58.29	55.17	49.84	36.46	46.72
Peak degradation temperature (°C)	216.18	216.91	216.81	214.20	215.81

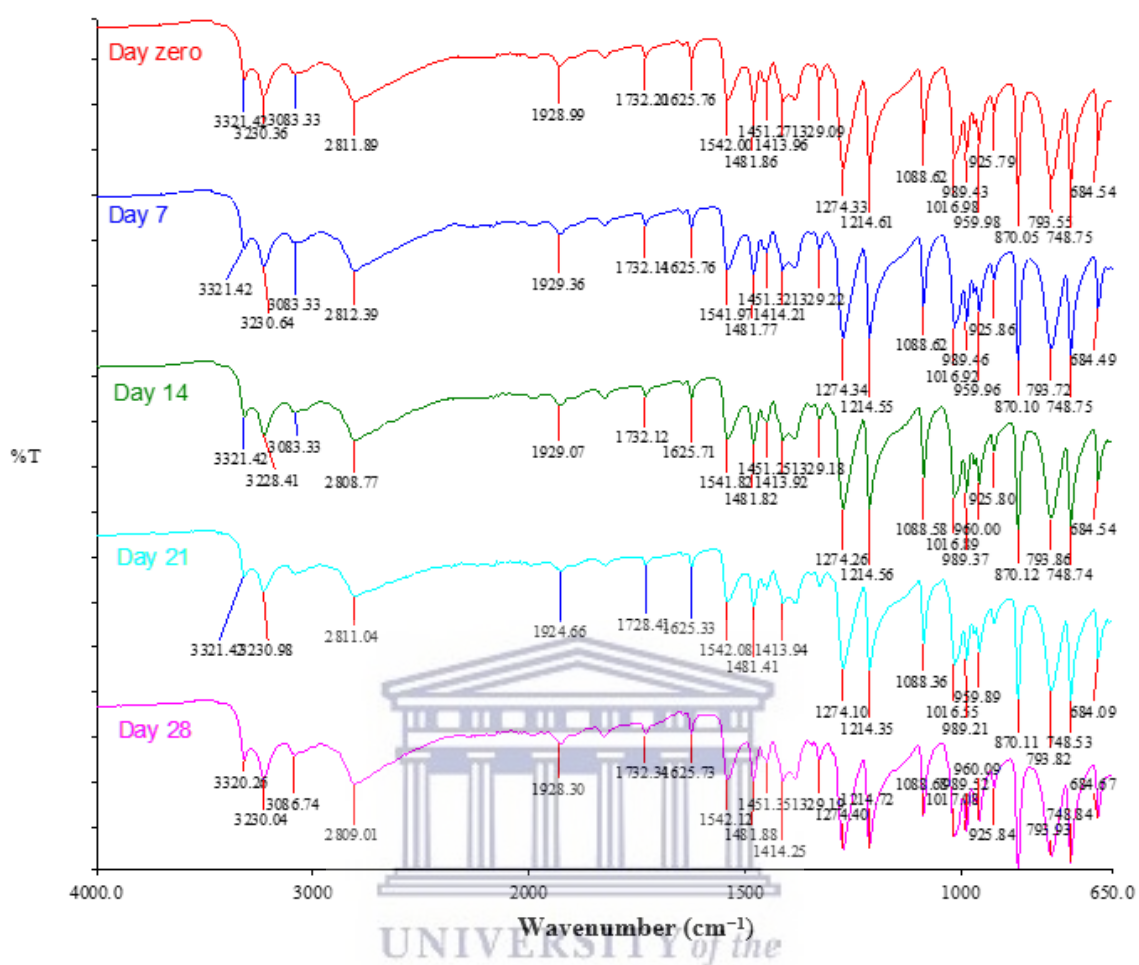


Figure 6.33: Overlay of the obtained FTIR spectra obtained for PDX during isothermal storage at 60 ± 0.5 °C and analysed on a weekly basis for a period of 28 days.

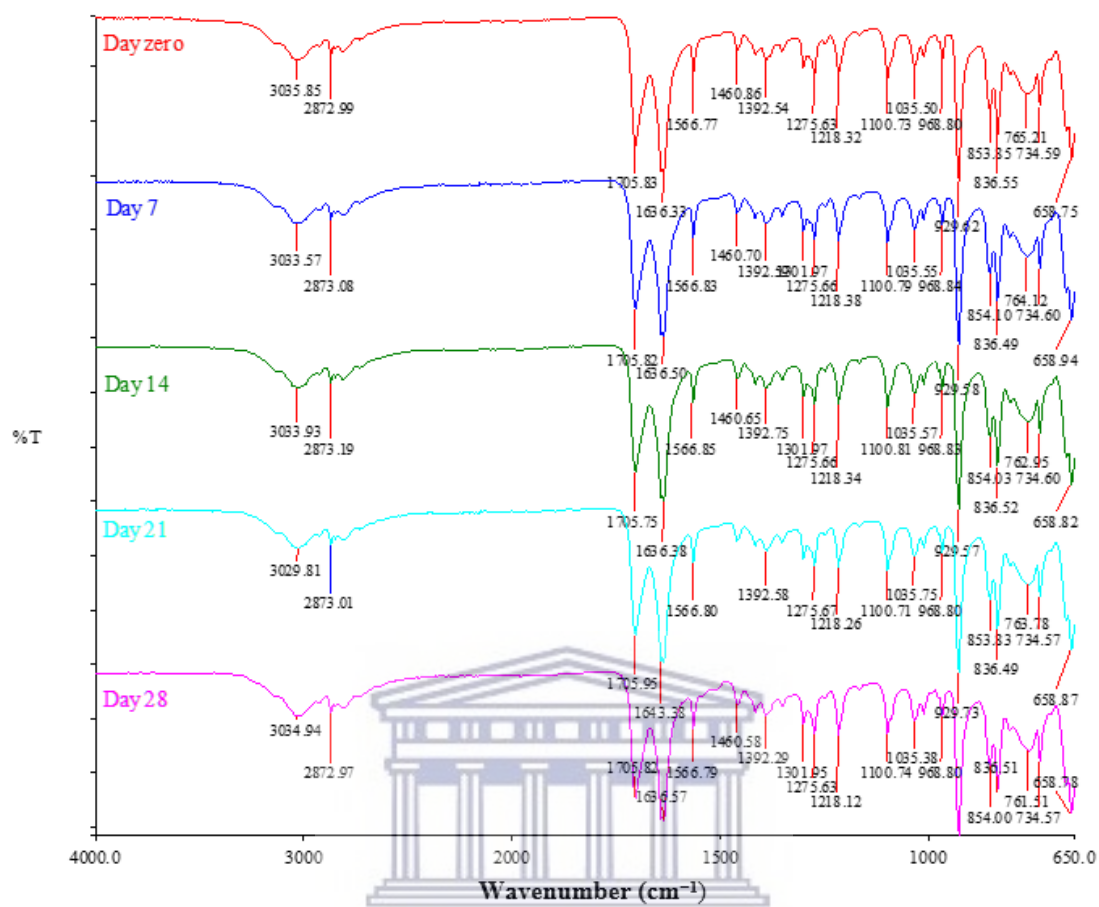


Figure 6.34: Overlay of the obtained FTIR spectra obtained for TZD during isothermal storage at 60 ± 0.5 °C and analysed on a weekly basis for a period of 28 days.

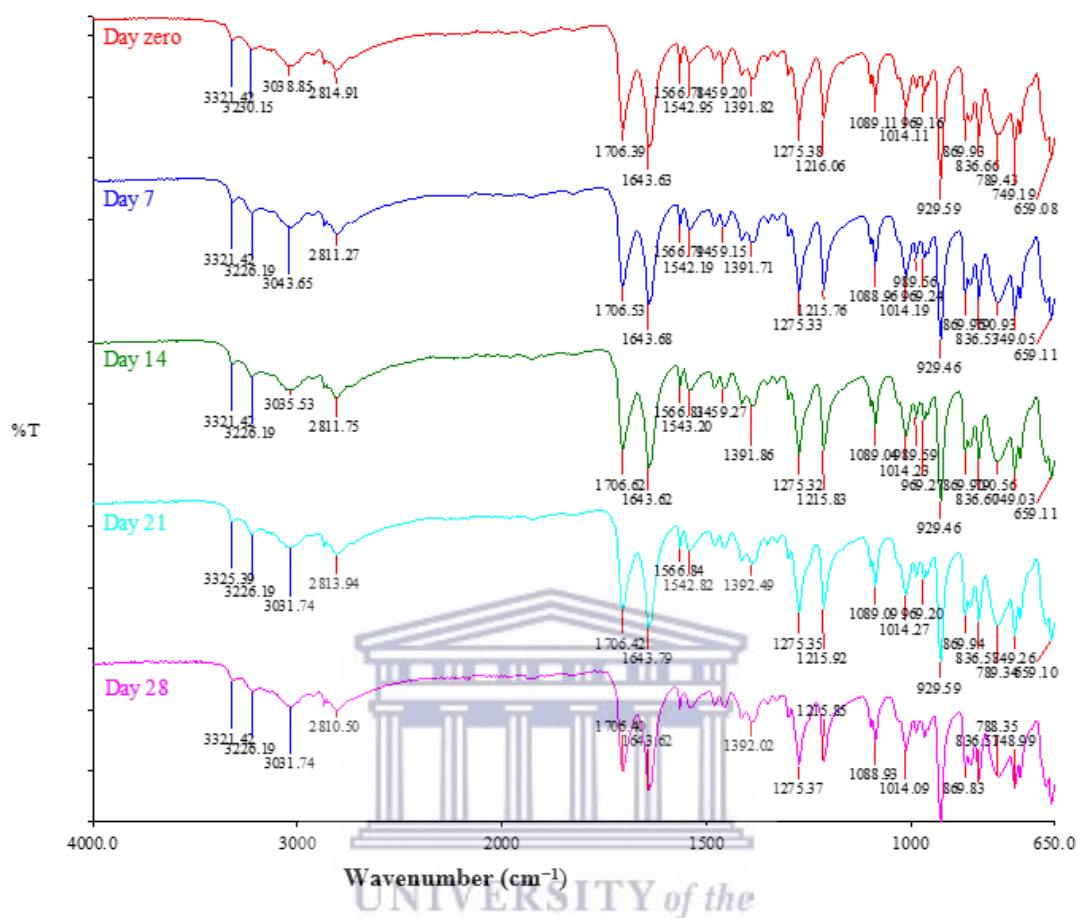


Figure 6.35: Overlay of the obtained FTIR spectra obtained for the TZD:PDX (1:1 w/w) mixture during isothermal storage at 60 ± 0.5 °C and analysed on a weekly basis for a period of 28 days.

The samples were subsequently also assayed to determine the drug purity of the stored samples and the obtained data is provided in Table 6.11. From this data it became apparent that pure PDX starts to degrade after a week of storage at 60 °C but when present in the TZD:PDX combination it did not exhibit the same level of degradation and remained stable. Significant degradation of the single (pure) compounds was observed at 14 days of storage but interestingly the same level of degradation was not observed for the two drugs when part of the drug-drug mixture. The overall degradation quantified for the two compounds as part of the physical mixture across the 28 days could be correlated with the degradation of each individual compound and therefore it was deduced that these two drugs are compatible with one another.

Table 6.11: Determined drug purity for TZD, PDX and both compounds in the TZD:PDX (1:1 w/w) mixture during isothermal exposure of the samples to 60 ± 0.5 °C

Day	Pure TZD		Pure PDX		TZD:PDX (1:1 w/w)			
					TZD		PDX	
	%	STDEV	%	STDEV	%	STDEV	%	STDEV
0	101,51	0.06	102.77	0.12	102.41	0.62	100.18	0.37
7	99.67	0.46	86.76	0.15	103.64	0.22	100.74	0.15
14	73.97	2.65	73.06	0.17	102.94	0.11	100.67	0.93
21	51.70	0.01	43.36	0.09	62.81	1.87	54.76	0.03
28	42.87	0.09	32.78	0.53	59.66	0.53	43.99	0.67

6.8 Conclusion

TZD marked conflicting results with its solid-state behavior. Its thermal analysis: HSM, TGA and DSC demonstrated an amorphous nature with an observed degradation temperature at 214°C which is not a melting point as was mentioned previously in the literature. The PXRD diffraction pattern of TZD showed a partially crystalline pattern. Thermal analyses of PDX showed a melting point, followed by immediate degradation as observed under HSM, TGA and DSC. These thermal results obtained for PDX were corroborated by literature reports. Spectroscopic analysis confirmed both the identity of PDX and TZD.

Equilibrium solubility testing of TZD proved this drug to be poorly soluble in most organic solvents which informed towards challenges that will thus be experienced during typical molecular modification processes. The poor solubility behaviour made the process of solvent evaporation as a co-crystallisation process impossible, due to phase separation occurring between the highly soluble PDX and the poorly soluble TZD. The fact that TZD did not exhibit a melting point and only degradation made a molecular fusing of TZD and PDX through the process of melting impossible. The fact that PDX also degraded almost immediately post melting made this process even more difficult. The molecular modification process of LAG

showed the most promise from a processing perspective, since this process doesn't involve the application of heat nor relies on the solubilisation of the individual compounds. Samples manipulated using LAG didn't show any achieved molecular modifications since spectroscopic and PXRD data remained similar with that of the drug-drug physical mixture. The only sample which showed promise of a co-amorphous solid-state form was the DMSO LAG preparation but as the study progressed it was unequivocally interpreted as compound degradation leading to the formation of an amorphous structure.

Thermal data collected for all the LAG preparations suggested that TZD and PDX could be incompatible when exposed together to processing parameters, such as elevated temperatures and certain solvents. This was investigated in-depth and it was realised that the effect of LAG had no effect on the pure samples separately but only when manipulated together using solvents, thermal behaviour changes were observed. This being said, the LAG process did not affect the chemical purity of the samples, except for the DMSO LAG preparation. It was therefore hypothesised that the manipulation of the TZD:PDX combination through the addition of organic solvents could lead to some level of molecular relaxation and structuring of the molecules in a more disorganised manner. This was evident from the observed increase of amorphous content in all LAG preparations. It was then further hypothesised that this higher level of entropy (molecular disorganisation) potentiates the degradation behaviour of both TZD and PDX when subjected to very high temperatures, such as during DSC analyses, which possibly result in the detection of two distinct degradation events.

This study proved that molecular combinations of TZD and PDX are challenging due to the inherent physicochemical properties of the two drugs. Due to a very thorough and in-depth compatibility study involving these two drugs, it was concluded that TZD and PDX are compatible with one another. This informed the potential of formulating a simple FDC product formulation consisting of the two drugs as a possibility. In conclusion, an FDC combination of the two drugs on molecular level, ie. co-crystals or co-amorphous solid-state forms is not possible but a simple pharmaceutical tablet or capsule formulation containing both TZD and PDX may soon be a reality.

6.9 References

- Aboul-Enein, H.Y. and Loutfy, M.A.** 1984. Pyridoxine hydrochloride. In: Florey, K. (ed.). *Analytical Profiles of Drug Substances*. Vol. 13. New York: Academic Press, pp. 447-486.
- Blomberg, B., Spinaci, S., Fourie, B. and Laing, R.** 2001. The rationale for recommending fixed-dose combination tablets for treatment of tuberculosis. *Bulletin of the World Health Organization*, 79: 61-68.
- Branton, A., Jana, S.** 2017. Evaluation of the Effect of the Energy of Consciousness Healing Treatment on Physico-chemical and Thermal Properties of Pyridoxine Hydrochloride. *American Journal of Physical Chemistry*, 6(4): p.49-58. doi: 10.11648/j.ajpc.20170604.11.
- British Pharmacopeia.** 2013. Department of Health, Great Britain. Stationery office.
- Byrn, S.R., Zografis, G. and Chen, S.** 2017. Product development. In: Byrn, S.R., Zografis, G. and Chen, S. Ed(s). *Solid state properties of pharmaceutical materials*. Hoboken, NJ: Wiley, 69-87.
- Chadha, R. and Bhandari, S.** 2014. Drug–excipient compatibility screening—role of thermoanalytical and spectroscopic techniques. *Journal of pharmaceutical and Biomedical Analysis*, 87:82-97. Doi: <https://doi.org/10.1016/j.jpba.2013.06.016>.
- Cimpoi, C., Casoni, D., Hosu, A., Miclaus, V., Hodisan, T. and Damian, G.** 2005. Separation and identification of eight hydrophilic vitamins using a new TLC method and Raman Spectroscopy. *Journal of Liquid Chromatography & Related Technologies*, 28(16):2551-2559. Doi: <https://doi.org/10.1080/10826070500189737>.
- Dengale, S., Grohgan, H., Rades, T. and Löbmann, K.** 2016. Recent advances in co-amorphous drug formulations. *Advanced Drug Delivery Reviews*, 100:116-125. <https://doi.org/10.1016/j.addr.2015.12.009>.
- Han, D., Li, X., Wang, H., Wang, Y., Du, S., Yu, B., Liu, Y., Xu, S. and Gong, J.** 2016. Determination and correlation of pyridoxine hydrochloride solubility in different binary mixtures at temperatures from (278.15 to 313.15) K. *The Journal of Chemical Thermodynamics*, 94:138-151.
- Joshi, D.R. and Adhikari, N.** 2019. An overview on common organic solvents and their toxicity. *Journal of Pharmaceutical Research International*. 1-18. Doi: 10.9734/jpri/2019/v28i330203.
- Kennedy-Shaffer, L.,** 2017. When the alpha is the omega: P-values, “substantial evidence,” and the 0.05 standard at FDA. *Food and Drug Law Journal*, 72(4):595–635.

Köse, D.A., Zumreoglu-Karan, B., Sahin, O. and Büyükgüngör, O. 2014. Boric acid complexes with thiamine (vitamin B1) and pyridoxine (vitamin B6). *Inorganica Chimica Acta*, 413:77-83. Doi: <https://doi.org/10.1016/j.ica.2013.12.045>.

Larkin, P. 2017. Basic principles. In: Larkin, P. *Infrared and Raman spectroscopy: principles and spectral interpretation*. 2nd ed. Elsevier, pp7-27.

Pubchem. 2021. *Terizidone.* [online] Available at: <https://pubchem.ncbi.nlm.nih.gov/compound/Terizidone> [Accessed 28 July 2021].

Radoman, T.S., Džunuzović, J.V., Grgur, B.N., Gvozdrenović, M.M., Jugović, B.Z., Miličević, D.S. and Džunuzović, E.S. 2016. Improvement of the epoxy coating properties by incorporation of polyaniline surface treated TiO₂ nanoparticles previously modified with vitamin B6. *Progress in Organic Coatings*, 99: 346-355. Doi:10.1016/j.porgcoat.2016.06.014.

Scifinder. 2021. *SciFinder® Login.* [online] Available at: <https://scifinder.cas.org/scifinder/view/scifinder/scifinderExplore.jsf> [Accessed 25 June 2021].

Smith, B. 2018. *Infrared spectral interpretation: a systematic approach.* CRC press, pp. 1-163.

Van der Meer, F. 2018. Near-infrared laboratory spectroscopy of mineral chemistry: A review. *International Journal of Applied Earth Observation and Geoinformation*, 65: 71-78. Doi: <https://doi.org/10.1016/j.jag.2017.10.004>.

Vippagunta, S.R., Brittain, H.G. and Grant, D.J. 2001. Crystalline solids. *Advanced Drug Delivery Reviews*, 48(1): 3-26. Doi: [https://doi.org/10.1016/S0169-409X\(01\)00097-7](https://doi.org/10.1016/S0169-409X(01)00097-7).

Vora, A. 2010. Terizidone. *Journal of Association Physician of India.* Volume 58.

Chapter 7

Concluding remarks , limitations, and recommendations

It was reiterated throughout the study that the physicochemical characteristics of API(s) are fundamental for preformulation and formulation as the preformulation knowledge influence the formulation development process and it is used to predict process-induced transformations caused by manufacturing process. Furthermore, they ultimately have an effect on clinical benefits associated with the API(s) (Acharya *et al.*, 2018). The importance of compatibility studies, which are part of preformulation studies sought to characterise and establish the physicochemical properties of compounds was discussed and investigated. Each chemical has its own intrinsic chemical and physical properties; therefore, it is evaluated before being mixed with other pharmaceutical ingredients (Kulkarni, Sharma, and Agrawal, 2015).

As part of this study, the latest literature of *Mtb* and MDR-TB epidemiology was reviewed. The progress made, up until this point in time in terms of TB treatment as well as the current progress of introducing new treatment regimens were discussed. The ever-remaining challenge of poor patient adherence due to the significant “pill-burden” experienced by TB-patients has been highlighted. This was linked to the approach of exploiting solid-state modification of drugs and the inclusion of such molecular modifications to either prepare FDCs or to modify the raw materials to achieved enhanced drug solubility and bioavailability. .

Throughout this study, knowledge in terms of the physicochemical characteristics of TZD, a molecule obtained from the condensation of two molecules of cycloserine (Hwang *et al.*, 2013), was expanded upon. PXRD data revealed that TZD exists as a partly crystalline solid-state form. This study proved that TZD doesn't present with a definitive melting point, which contradicts the single literature source that reported a melting point range of 204 - 205 °C (Scifinder, 2019). On the other hand, PDX melted within the range of 210 °C to 220 °C followed by a rapid onset of degradation. It was found to be highly crystalline and highly water soluble which is in alignment with the reviewed literature. Equilibrium solubility results proved that TZD is poorly soluble in almost all organic solvents.

The study investigated the feasibility of a convenient FDC between TZD and PDX obtained through molecular modification and the formation of a novel solid-state form such as a co-crystal or co-amorphous form. Based on the solubility behaviour of TZD as well as the

combined thermal behaviour observed for TZD and PDX it was concluded that molecular modification techniques involving the solubilisation of both compounds will be problematic. Further to this, based on the thermal behaviour of TZD as well as the rapid decomposition of PDX immediately after melting it was realized that the well-known method of quench cooling of the melt won't be a feasible option to facilitate novel solid-state form preparation. The only viable technique identified was that of LAG. This method was investigated further and preparations generated from this method were analysed for intermolecular bonding between the two compounds involving techniques such as thermal analysis, spectroscopy, PXRD as well as assay testing..

Anomalous thermal behaviour was obtained with almost all the LAG preparations, except the LAG with DMSO. Initially, the LAG with DMSO sample was characterised as a co-amorphous solid-state form, based on the obtained PXRD data but more in-depth investigation revealed that LAG with DMSO resulted in significant compound degradation. This beckon the question whether compound degradation also occurred during the LAG process involving the other organic solvents and therefore a very thorough and in-depth compatibility study between TZD and PDX was conducted. Spectroscopy, thermal analyses as well as drug purity determinations proved that TZD and PDX are indeed compatible with one another.

The project necessitated the simultaneous analysis of TZD and PDX and this resulted in the development and successful validation of a novel HPLC method following ICH guidelines. This method can be used for identification and quantification of TZD and PDX either separately or simultaneously.

A limitation of this study was the fact that only the 1/1: *w/w* ratio of TZD to PDX was studied. The recommended dose for both drugs, as dicussed in Chapter 2, is 50 mg PDX for every 250 mg TZD. Considering this a further study would be important to investigate different ratios, either based on stoichiometry or weight per weight. This being said, the technique of spray-drying should also be considered as a technique to potentially prepare a co-amorphous solid-state form of TZD:PDX. Spray-drying is a versatile technique that allows the formation of powder particles from complex solution systems and to achieve effective spray-drying complete solubilisation of the compounds to be spray-dried is not a necessity. Another solid-state form modification technique which could prove to be advantageous would be that of hot-melt extrusion. This method would allow the mixing of both compounds with a molten

polymer solution. However, based on the thermal behaviour of both TZD and PDX one would have to be cautious when this method is utilised as to not trigger compound degradation.

As mentioned, cycloserine is the parent compound of TZD, and it would therefore be informative to compare its physicochemical characteristics behavior with that of TZD. Furthermore, the potential molecular interaction between PDX and cycloserine might be potentially more successful, especially if cycloserine exhibits very different thermal and solubilization behaviour compared to TZD. Furthermore, during this study only the salt form of PDX could be sourced and not the free base as well. A potential future study could investigate the impact of using the free base of PDX as a co-crystal or co-amorphous co-former rather than the hydrochloride salt. The TZD solubility data obtained, showed it to be poorly soluble in almost all aqueous buffered solutions and most of the organic solvents. This study didn't focus on *in vitro* behavior of the two drugs when in combination with one another and therefore yet another gap in the knowledge base has been identified. Future studies could potentially investigate and correlate *in vitro* behaviour of TZD and PDX when in combination with drug permeation and *in vivo* studies of pharmacokinetics of the two drugs to have a complete understanding of the observed physicochemical characteristics.

Overall, This study provided critical, fundamental information for any future project focusing on the preformulation and formulation of FDCs combining TZD and PDX.

UNIVERSITY OF
WESTERN CAPE

7.1 References

Acharya, P.C., Shetty, S., Fernandes, C., Soares, D., Maheshwari, R. and Tekade, R.K. 2018. Preformulation in Drug Research and Pharmaceutical Product Development. In: Tekade R.K. (Ed). *Dosage Form Design Considerations*. Amsterdam: Elsevier, 1-55. Doi: <https://doi.org/10.1016/B978-0-12-814423-7.00001-0>.

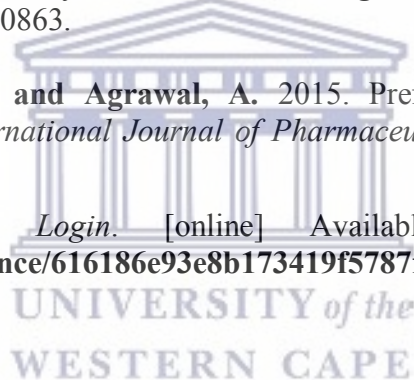
Albanna, A.S., Smith, B.M., Cowan, D. and Menzies, D. 2013. Fixed-dose combination antituberculosis therapy: a systematic review and meta-analysis. *European Respiratory Journal*, 42(3), 721-732. Doi: 10.1183/09031936.00180612.

Fernández-García, R., Prada, M., Bolás-Fernández, F., Ballesteros, M.P. and Serrano, D.R. 2020. Oral fixed-dose combination pharmaceutical products: Industrial manufacturing versus personalized 3D printing. *Pharmaceutical Research*, 37(7):1-22. Doi: <https://doi.org/10.1007/s11095-020-02847-3>.

Hwang, T.J., Wares, D.F., Jafarov, A., Jakubowiak, W., Nunn, P. and Keshavjee, S. 2013. Safety of cycloserine and terizidone for the treatment of drug-resistant tuberculosis: a meta-analysis. *The International Journal of Tuberculosis and Lung Disease*, 17(10):1257-1266. Doi: <https://doi.org/10.5588/ijtld.12.0863>.

Kulkarni, S., Sharma, S.B. and Agrawal, A. 2015. Preformulation-a foundation for formulation development. *International Journal of Pharmaceutical, Chemical & Biological Sciences*, 5(2). 403-406.

Scifinder. 2019. *SciFinderⁿ Login*. [online] Available at: <<https://scifinder-n.cas.org/searchDetail/substance/616186e93e8b173419f5787f/substanceDetails>> [Accessed 9 October 2021].



Appendix

*The following paper was compiled from research conducted as part of this study and was submitted to the ISI-accredited journal Analytica for peer-review. The paper was compiled following the published instructions to authors:
<https://www.mdpi.com/journal/analytica/instructions>*



The development and validation of a RP-HPLC method for the simultaneous detection and quantification of pyridoxine and terizidone

Ngabo Yves Musafili ¹, Halima Samsodien ¹ and Marique Aucamp ^{1,*}

¹ School of Pharmacy, Faculty of Natural Sciences, University of the Western Cape, Robert Sobukwe Drive, Bellville, Cape Town, South Africa.

* Correspondence: maucamp@uwc.ac.za.

Abstract: Tuberculosis (TB) remains a life-threatening infection and it is well-known that effective TB treatment is associated with multiple drugs administered to infected patients on a daily basis. Terizidone (TZD) is an anti-TB drug used in the treatment of multi-drug resistant and extensively drug-resistant TB but presents with polyneuropathic adverse effects in some patients. To counteract these adverse effects, TZD is typically prescribed with pyridoxine (PDX), well-known as Vitamin B₆. As part of a pre-formulation study investigating the potential to co-formulate these two compounds, it became necessary to have a simple and reliable reversed-phase high-performance liquid chromatography (RP-HPLC) method. Optimal, simultaneous separation and detection of TZD and PDX was obtained using a mobile phase of ultrapure water and acetonitrile (30 :70 %v/v) with 1 mL glacial acetic acid. The stationary phase was a Discovery[®] C₁₈, 150 x 4.6 mm, 5 μm column maintained at ambient temperature. A detection wavelength of 260 nm was used. The method was validated in terms of linearity, accuracy, precision, limit of detection (LOD), limit of quantification (LOQ), specificity, robustness, and solution stability. Validation proved this method to be acceptable and reliable for the simultaneous accurate detection and quantification of TZD and PDX.

Citation: Lastname, F.; Lastname, F.; Lastname, F. Title. *Analytica* **2021**, *2*, Firstpage–Lastpage.
<https://doi.org/10.3390/xxxxx>

Keywords: Terizidone; pyridoxine; RP-HPLC; simultaneous detection; method validation; solution stability, aqueous buffered media

Academic Editor: Firstname Lastname

Received: date
Accepted: date
Published: date

Publisher's Note: MDPI stays neutral with regard to jurisdictional claims in published maps and institutional affiliations.



Copyright: © 2021 by the authors. Submitted for possible open access publication under the terms and conditions of the Creative Commons Attribution (CC BY) license (<https://creativecommons.org/licenses/by/4.0/>).

1. Introduction

Tuberculosis (TB) is a communicable infectious disease that is caused by *Mycobacterium tuberculosis*, and it produces silent, latent infection and active disease. It is an infection that mainly affects the lungs (pulmonary TB) but other sites in the human body may also be affected which is then termed extrapulmonary TB [1]. Currently, on a global level, TB is ranked among the top ten causes of death, and it is the leading cause of death from a single infection [2]. A substantial amount of research is being dedicated to the effective treatment and possible eradication of TB, and the World Health Organization (WHO) has set out an end-TB strategy, which is to reduce TB deaths by 95% and incidence rates by 90% from 2014 to 2035 [2].

Terizidone (TZD) is a WHO categorized group IV anti-TB drug (Figure 1(a)). It is effective against both *Mycobacterium tuberculosis* and *Mycobacterium avium*. TZD is used as a second-line treatment option in multi-drug resistant TB (MDR-TB) and extensively drug-resistant TB (XDR-TB) for non-psychotic adult or pediatric patients. However, it is principally known to cause polyneuropathic side effects [3, 4]. Pyridoxine hydrochloride (PDX), also known as Vitamin B₆, is a water-soluble molecule involved in several enzymatic reactions in the human body. The molecular structure thereof is depicted in

<http://etd.uwc.ac.za/>

Figure 1(b). It is prevalent in brewer's yeast, eggs, chicken, carrots, fish, meat, peas, wheat germ and walnuts. A vitamin B₆ deficiency may cause anemia, nerve damage, seizures, skin problems, and sores in the mouth [5,6]. It is recommended that patients considered to be at risk for developing polyneuropathy, such as those with alcohol dependency, malnutrition, diabetes, and human immunodeficiency virus infection, receive daily PDX supplementation. It is often prescribed in TB patients taking isoniazid and TZD to reduce the occurrence of the polyneuropathic side effects [7,8]. TZD is a poorly studied drug and very little is known of its solubility and physico-chemical properties. In order to investigate the physico-chemical properties of a drug, it is necessary to quantify and qualify the drug under investigation. During a physico-chemical and compatibility study involving the combination of TZD with PDX, it became necessary to have a sensitive analytical method that will allow the simultaneous detection of the two compounds. Currently, there are only three literature sources discussing the HPLC analysis of TZD. One of these studies reports the detection and quantification of TZD in human plasma, utilizing a gradient elution setup [9], another reports a stability indicating RP-HPLC method for the determination of TZD from bulk material [10] and finally, another study reports the impurity profiling of TZD using HPLC in combination with mass spectrometry [11]. Presently, no study reporting the simultaneous detection and quantification of TZD and PDX exists. Because these two drugs are typically prescribed together, the possibility of the development of a suitable fixed-dose combination dosage form might bring relief to the significant pill-burden that TB patients experience. The need for a sensitive, simple, cost-effective as well as stability indicating RP-HPLC method was thus identified which led to the development and validation of this method.

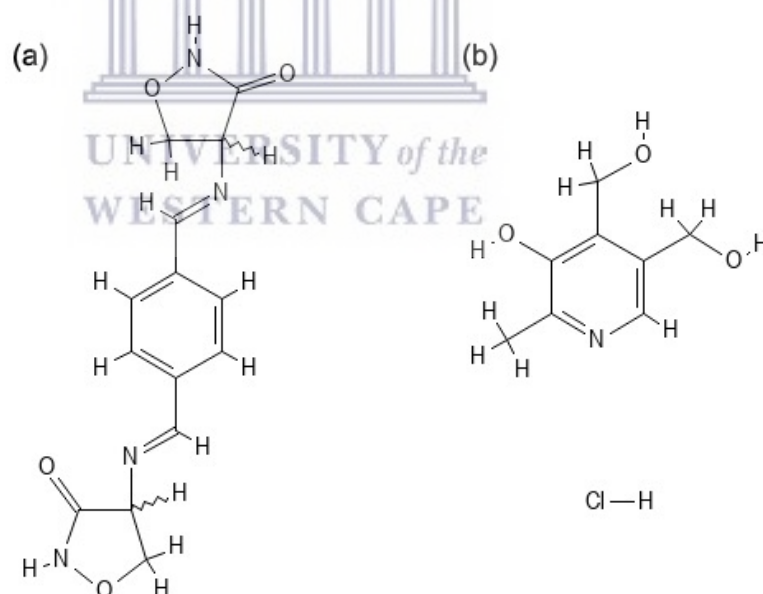


Figure 1. Molecular structures of (a) TZD and (b) PDX [12,13].

The validation of a simple and cost-effective HPLC method, which allows the simultaneous detection of TZD and PDX when present in the proposed diluent and in aqueous buffered media (pH 1.2, 4.5 and 6.8), typically used in pharmaceutical quality control testing, is described here.

2. Materials and Methods

2.1 Reagents

TZD bulk material was an in-kind donation from Chemical Process Technologies (Pretoria, South Africa) and a TZD certified reference standard (lot number: 2-MJK-168-2)

with a purity of 99.5% (Toronto Research Chemicals, Canada) was purchased from Industrial Analytical (Johannesburg, South Africa). PDX, dimethyl sulfoxide (DMSO), sodium hydroxide (NaOH), hydrochloric acid (HCl), anhydrous sodium acetate, disodium hydrogen orthophosphate, potassium dihydrogen orthophosphate and glacial acetic acid were purchased from Sigma-Aldrich (Johannesburg, South Africa). For mobile phase, standard and sample solution preparation, ultrapure water with a resistivity of 18.2 M Ω was obtained from a Purite water purification system (Lasec, Johannesburg, South Africa). Chromatography grade acetonitrile was purchased from Merck (Johannesburg, South Africa).

2.2 HPLC instrumentation and chromatographic conditions

The method development and validation were performed using a Knauer Azura DAD (Berlin, Germany) HPLC system equipped with an autosampler, quaternary pump, photodiode array detector and column thermostat. The ClarityChrom[®] software package was used for data processing purposes. A Supelco[™] (Bellefonte, United States) Discovery[®] C₁₈, 150 x 4.6 mm, 5 μ m, was used as stationary phase and was purchased from Sigma-Aldrich (Johannesburg, South Africa). Throughout the method validation process, the column temperature was maintained at ambient temperature. An isocratic flow of the mobile phase was utilized with the mobile phase consisting of 30:70 v/v acetonitrile: HPLC grade water with 1 mL of glacial acetic acid added. The following mobile phase flow rate program was utilized: 0.5 mL/min from 0 to 4 min, followed by an increase of the flow rate to 1.5 mL/min from 4.1 min to 8 min. An injection volume of 10 μ L and a detection wavelength of 260 nm was used. A run time of 8 minutes was employed.

2.3 Preparation of standard stock and working solutions

Stock solutions containing 200 μ g/mL TZD and PDX, respectively were prepared using a 50:50 v/v acetonitrile : ultrapure water solution as solvent. Due to the poor solubility of TZD in almost all organic solvents, it was necessary to dissolve TZD first in DMSO. For every 10 mg of TZD used, 150 μ L of DMSO was used as solubilizing solvent. Subsequently, serial dilutions of the stock solutions were made to achieve solutions in the concentration range of 50.0 – 800.0 μ g/mL. Solutions were filtered using a 0.22 μ m syringe filter.

2.4 Method validation

Method validation was performed by evaluating the linearity, accuracy, precision which included repeatability and reproducibility, limit of detection (LOD), limit of quantification (LOQ), specificity, robustness, and solution stability. The method was validated based on the International Conference on Harmonisation (ICH) guideline on the validation of analytical procedures Q2(R1) [14].

2.4.1 Linearity

The linearity of this analytical method was determined by analyzing five standard solutions of varying concentrations across the range of 50.0 – 800.0 μ g/mL for both compounds. Calibration curves for TZD and PDX were achieved by plotting the obtained peak areas versus the concentrations. The obtained correlation plot was used to determine the correlation coefficient (r^2), slope and intercept associated with each compound.

2.4.2 Accuracy

Accuracy of this analytical method was investigated through recovery studies which were performed by the spiking of a standard solution, resulting in five solutions at the following concentration levels: 50, 100, 200, 300 and 400 μ g/mL for both TZD and PDX. These solutions were analyzed against a reference solution of known concentration at

100% concentration level. The percentage recovery for TZD and PDX at each concentration level was subsequently quantified.

2.4.3 Precision

The precision associated with this analytical method was determined on two levels: repeatability, also termed intra-assay precision and reproducibility also termed intermediate precision. Method precision was determined over a series of measurements of a single sample and was thus conducted by analyzing six replicates of solutions containing 200 µg/mL of TDZ and PDX in combination. Reproducibility (inter-day precision) is based on variation which may include the variation obtained on different days, associated with different analysts, or equipment [14]. Reproducibility of both TZD and PDX analyzed using this method was determined through a consecutive analysis across three days with solutions containing 200 µg/mL TDZ and PDX in combination.

2.4.4 Limit of detection (LOD) and limit of quantification (LOQ)

During LOD and LOQ determinations, TZD and PDX were analyzed across a concentration range of 50.00 – 800.00 µg/mL. Subsequently, the LOD and LOQ for TZD and PDX were calculated based on the standard deviation of the response and the slope as recommended by the ICH guidelines on analytical method development and validation [14], using ANOVA statistical analysis and applying the following equations:

$$\text{LOD} = 3.3\sigma / b \quad (1)$$

$$\text{LOQ} = 10\sigma / b \quad (2)$$

With σ being the standard deviation of the response values across the concentration range used to determine linearity and range of the analytical method and b being the slope of the calibration curve.

2.4.5 Specificity

Firstly, the respective peak of each compound was identified through the analysis of samples, containing only one compound, at a time. Subsequently, TZD and PDX were combined, and these solutions were analyzed to ascertain whether a shift in retention time could be identified or any other peak interference due to the combination. Further to this, the specificity of both compounds was studied when combined with typical pharmaceutical dissolution media. Different solvents, namely hydrochloric acid (pH 1.2), buffered distilled water (pH 4.5 and pH 6.8) and pure distilled water were injected separately to ascertain whether any peak interference will occur once TZD and PDX are diluted in these solvents.

2.4.6 Robustness

During the validation process, robustness of the method was analyzed by deliberate adjustment of the following parameters: column temperature ranging from ambient (25°C ± 0.3°C) to 40°C ± 0.3°C, and wavelength variation of 230, 250 and 280 nm. The influence of these deliberate changes on peak area, peak symmetry, and retention time for both PDX and TZD was subsequently documented.

2.4.7 Solution stability

These stability studies were conducted over a course of three days, under four storage conditions: photosensitivity, where the sample was exposed to direct sunlight, refrigeration (5°C ± 0.5°C), ambient temperature (25°C ± 2.0°C), and heat (60°C ± 2.0°C). Furthermore, the stability of the TZD and PDX in the sample solution were investigated through exposing the solution to stress conditions which included the addition of 200 µL of either acid (0.1N HCl), alkaline (1N NaOH) and oxidation (3% H₂O₂) to three sample

vials. Six HPLC vials containing a solution with a concentration of 200 µg/mL of TZD and PDX, respectively were prepared and analyzed over a period of three days.

3. Results

3.1. Linearity

The linearity of this analytical method was established by creating a correlation plot of the obtained peak areas versus the TZD and PDX concentrations (50.0 – 800.0 µg/mL), respectively. The correlation coefficients (R^2) for TZD and PDX were calculated to be 0.9998 and 0.9996, respectively. Figure 2 depicts the regression plots obtained for both compounds. From these plots and resulting correlation coefficients, it was deduced that an acceptable correlation exists between the analytical response and the analyte concentration.

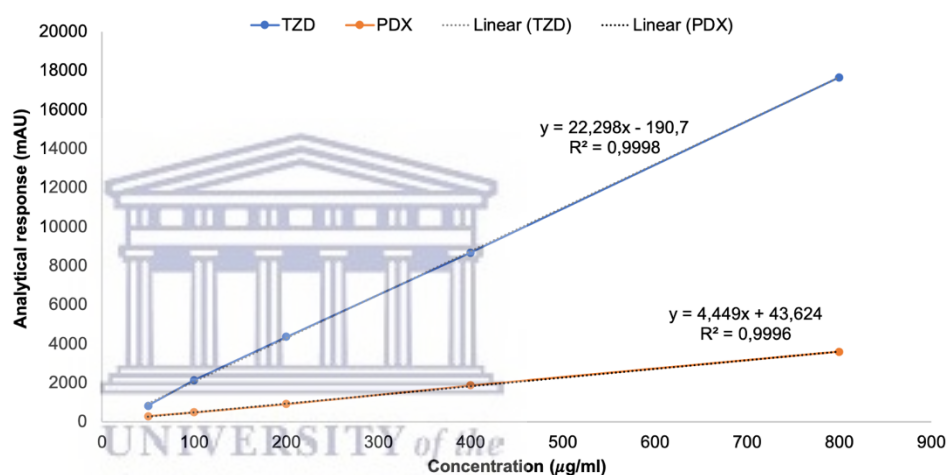


Figure 1. Regression plot obtained for TZD and PDX across a concentration range of 50.00 – 800 µg/mL.

3.2. Accuracy

The accuracy of this analytical method was investigated through recovery studies, which was performed by the spiking of a standard solution, resulting in five solutions at five concentration levels 50, 100, 200, 300 and 400 µg/mL. The obtained accuracy results are disseminated in Table 1. Based on the fact that this method was developed to allow the quantification of TZD and PDX as part of typical pharmaceutical assay and dissolution testing, recovery ranges of 98.0 – 102.0% (for assay) and 95.0 – 105.0% (for dissolution) should be applied and adhered to [15]. It was therefore found that the proposed method is sufficiently accurate for the quantification of TZD in the concentration range of 100.0 – 400.0 µg/mL and for the quantification of PDX a concentration range of 50.0 – 300.0 µg/mL will produce accurate results.

Table 1. Accuracy results obtained for TZD and PDX determined at 50, 100, 200, 300 and 400 µg/mL

Expected concentration (µg/mL)	TZD		PDX	
	% Recovery	Concentration (µg/mL)	% Recovery	Concentration (µg/mL)
50.00	92.04	46.48 ± 0.05	102.04	51.53 ± 0.05
104.00	101.74	105.81 ± 0.77	98.04	101.96 ± 0.54
202.10	100.25	202.61 ± 0.87	100.37	202.85 ± 2.56
312.00	99.55	310.60 ± 0.25	98.62	307.69 ± 0.60
404.00	99.77	403.07 ± 0.54	97.23	392.81 ± 0.16

3.3. Precision

Precision was assessed on two levels through the determination of repeatability (intra-day) and intermediate precision (inter-day or reproducibility). Repeatability was assessed across the concentration range of 100.00 – 300.00 µg/mL for both TZD and PDX and was found to be within the validation limits of ≤ 2.0%. Tables 3 and 4 outlines the inter-day precision testing of TZD and PDX. The percentage recovery and percentage relative standard deviation (%RSD) associated with the recovery of both compounds across a period of three days was found to be acceptable, proving that the method will provide precise analytical outputs when attempted on different days and by different analysts.

Table 2. Results obtained during repeatability testing of the analytical method

Concentration (µg/mL) (n = 12)	TZD Peak Area	Peak area (Average ± %RSD)	PDX Peak Area	Peak area (Average ± %RSD)
101.00	2420.34	2408.78 ± 0.09	793.77	795.86 ± 0.22
	2378.18		795.69	
	2427.83		798.12	
208.00	4824.74	4823.49 ± 0.04	1615.32	1619.26 ± 0.26
	4820.50		1616.09	
	4822.94		1622.28	
	4826.31		1616.42	
	4823.83		1626.20	
	4822.63		1620.67	
303.00	7023.60	7032.03 ± 0.11	2449.71	2454.94 ± 0.16
	7039.47		2459.21	
	7033.03		2455.89	

Table 3. Results obtained during inter-day precision testing of TZD

219

Concentration ($\mu\text{g/mL}$) (n = 9)	Day 1 % Recovery	Day 2 % Recovery	Day 3 % Recovery
104.00	102.40	98.53	102.64
	100.62	97.19	101.23
	100.62	100.85	101.33
Mean	101.21	98.86	101.73
%RSD	0.83	1.53	0.63
208.00	98.53	98.05	99.34
	97.48	98.11	99.37
	98.05	98.08	99.26
Mean	98.02	98.08	99.32
%RSD	0.44	0.02	0.05
303.00	99.51	101.89	100.44
	100.06	102.33	100.98
	98.98	101.67	100.51
Mean	99.52	101.96	100.64
%RSD	0.44	0.27	0.24

220

Table 4. Results obtained during inter-day precision testing of PDX

221

Concentration ($\mu\text{g/mL}$) (n = 9)	Day 1 % Recovery	Day 2 % Recovery	Day 3 % Recovery
102.00	97.09	103.63	100.31
	98.72	102.64	98.95
	98.98	102.14	100.55
Mean	98.26	102.80	99.94
%RSD	0.85	0.60	0.70
209.00	102.12	98.09	100.23
	102.35	98.06	100.78
	102.14	98.56	101.02
Mean	102.28	98.24	100.71
%RSD	0.11	0.23	0.29
301.00	100.06	101.51	99.77
	100.17	100.67	99.04
	100.99	100.86	99.81
Mean	100.41	101.01	99.54
%RSD	0.41	0.35	0.36

3.4. Limit of detection (LOD) and limit of quantification (LOQ)

222

Equations 1 and 2 have been applied for LOD and LOQ determination. For TZD the LOD and LOQ were quantified as 13.49 $\mu\text{g/mL}$ and 44.95 $\mu\text{g/mL}$ respectively, and for PDX, the LOD and LOQ were quantified as 21.49 $\mu\text{g/mL}$ and 71.64 $\mu\text{g/mL}$ respectively. This means that the amount lower than 13.49 $\mu\text{g/mL}$ for TZD and 21.49 $\mu\text{g/mL}$ for PDX will not be accurately detected by the developed method.

223

224

225

226

227

3.4. Specificity

228

The specificity of this method was investigated by injecting the mobile phase and several buffered aqueous media (pH 1.2, 4.5 and 6.8) as well as distilled water using an injection volume of 10 μL . From these injections, it was apparent that neither the

229

230

231

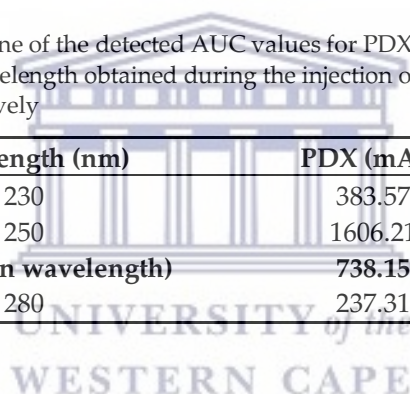
solvents nor the mobile phase was interfering with either the PDX or the TZD peak, and accurate identification and quantification of the two compounds will be possible irrespective of the solvent used (Figure 2).

3.5. Robustness

The robustness testing for this method applied deliberate adjustments to the chromatographic parameters. Adjustments were made to the detection wavelength, resulting in the testing of chromatographic response at 230, 250 and 280 nm. Table 5 provides an outline of the obtained area under the curve (AUC) values for both PDX and TZD. From these deliberate changes, it was observed that PDX exhibits a higher AUC at wavelength 250 nm whilst TZD shows the highest AUC response at 280 nm. Based on these results it was concluded that using a detection wavelength of 260 nm provides the best detection for both compounds. Deliberate changes to the column temperature were also tested during robustness testing. The column temperatures were varied from ambient temperature to 40°C. It was noted that changes in the column temperature did not affect the retention time of each of the compounds significantly, and therefore not identified as a critical chromatographic parameter for this method.

Table 5. Outline of the detected AUC values for PDX and TZD after deliberate adjustments in the detection wavelength obtained during the injection of a solution containing 100 µg/mL PDX and TZD, respectively

Wavelength (nm)	PDX (mAU)	TZD (mAU)
230	383.57	4808.23
250	1606.21	2157.37
260 (chosen wavelength)	738.15	4627.39
280	237.31	4834.05



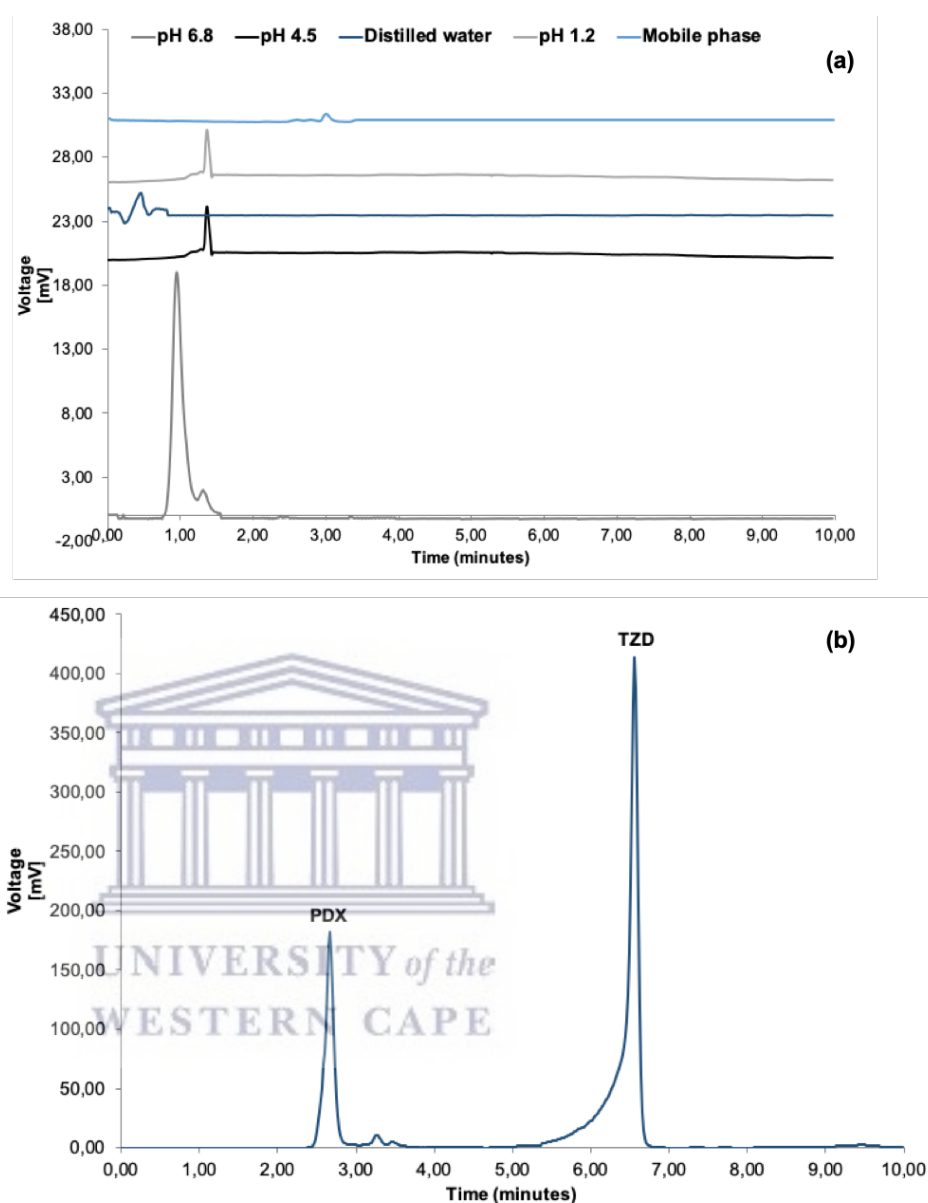


Figure 2. Overlay of chromatograms obtained with (a) mobile phase, pH 1.2, pH4.5, pH 6.8 buffered media and distilled water; (b) PDX and TZD dissolved in the described diluent.

3.6. Solution stability

During solution stability testing, it became apparent that this method is sensitive towards the detection of degradation products associated with the two drug compounds. Table 6 provides a summary of the quantified concentrations of both compounds during exposure to various storage conditions, as well as to conditions that would accelerate the degradation of both drugs. It was observed that both PDX and TZD showed stability when stored in the fridge (5°C). In terms of stability at ambient storage conditions, it was found that PDX degraded $\approx 10\%$ during the three-day testing period, whilst TZD remained stable at room temperature. The sample stored at 60°C showed a 65.06% decrease in PDX purity after the first day of storage and complete degradation thereafter. The appearance of an unknown peak was also observed at 3.13 minutes (Figure 3). This observation is contradictory to stability data reported in literature which states that PDX remains stable during exposure to heat [16,17]. However, it should be noted that this stability was not tested in solution, neither in this specific solvent system nor in combination

with TZD. Quantification of TZD in the sample stored at 60°C showed an increase in the drug concentration and this could be ascribed to possible solvent evaporation. TZD completely degraded upon exposure to 60°C in combination with PDX for a period of three days. PDX is reported to be sensitive to light when it is in neutral or alkaline solutions [16, 17]. This behavior was confirmed during this validation process, since PDX was extensively degraded during exposure to sunlight when combined with TZD (Figure 4). The same behavior was observed for TZD, and this was noted to be different to that reported by Gandhi, Shevale and Choudhari [10]. Stability of both compounds were observed when exposed to acidic conditions. Following these findings that are different from that dictated by literature were observed in terms of the stability of PDX in strong alkali. PDX showed marked degradation (% purity loss of 35.1%) across the solution stability testing period in an alkaline environment (Table 6). It was also noticed that PDX is sensitive towards oxidative species based on a purity loss of 19.5% across a period of 3 days. On the other hand, TZD remained stable during exposure to an alkaline environment as well as to oxidative species.

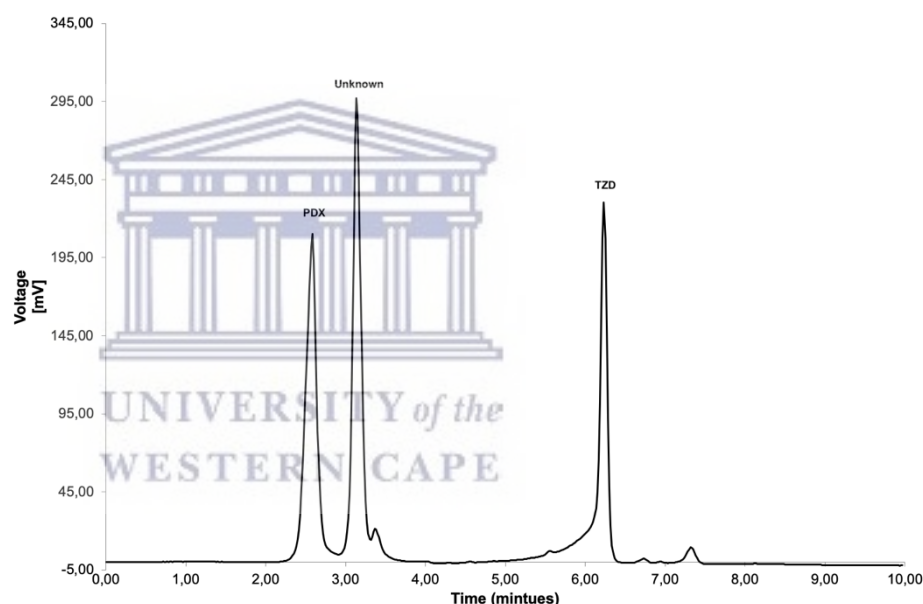


Figure 3. Chromatogram obtained with a solution containing 200 µg/mL PDX and TZD, respectively after exposure to a storage temperature of 60.0°C for a period of 24 hours.

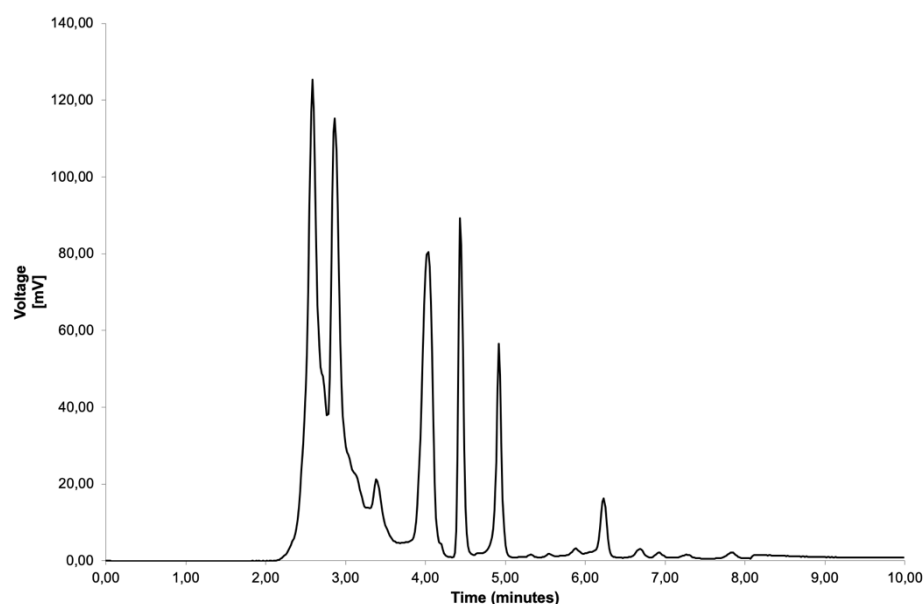


Figure 4. Chromatogram obtained with a solution containing 200 µg/mL PDX and TZD, respectively after exposure to direct sunlight for a period of 24 hours.

Table 6. Percentage purity (%) calculated for PDX and TZD during exposure to various storage conditions as well as harsh environments for a period of three days

Conditions	5°C	25°C	60°C	Photolysis	Acid hydrolysis	Alkaline hydrolysis	Oxidation
PDX (% purity)							
Day 1	100.00	100.00	100.00	100.00	100.00	100.00	100.00
Day 2	98.08	94.87	34.94	1.81	100.02	70.84	94.15
Day 3	95.13	90.41	0	0	93.75	64.91	80.95
TZD (% purity)							
Day 1	100.00	100.00	100.00	100.00	100.00	100.00	100.00
Day 2	97.50	97.43	127.67	0	99.86	101.97	100.39
Day 3	97.59	97.58	72.76	0	99.56	100.63	99.94

4. Discussion

Due to the high pill-burden experienced by many patients suffering from TB infection, many strategies are being investigated and employed to reduce the number of drugs these patients need to consume daily. PDX is usually prescribed together with TZD to reduce the polyneuropathic side-effects that TZD treatment is associated with. It is therefore justifiable to co-formulate these two active pharmaceutical ingredients into a single dosage form. However, as a new dosage forms are formulated, it also requires an establishment of a suitable analytical method which would allow accurate, reliable detection and quantification of the compounds included into the new pharmaceutical product. Currently, there is no analytical method which allows for the simultaneous detection and quantification of PDX and TZD. A reliable robust RP-HPLC method that allows for the simultaneous detection and quantification of PDX and TZD was developed and validated. The validation process and obtained parameters proved the method to be suitable for the quantification of PDX and TZD across a relative wide concentration range. Recovery studies as part of the accuracy testing of this analytical method proved that this method will be appropriate for typical assay and dissolution testing of both compounds when combined into a single preparation. Selectivity testing proved that no interference on the PDX or TZD peak occurs when different solvent types are being used, making this

method suitable for typical drug release testing. Moreover, a thorough solution stability study proved that once combined with one another, these two compounds exhibit stability behavior different to that reported by other studies which investigated these two compounds alone. It was however deduced from the solution stability study, that this method is stability indicating since it is sensitive to the detection of degradation compound peaks. In conclusion, this method meets the requirements provided by regulating bodies and can be categorized as a suitable validated analytical method [14].

Author Contributions: Conceptualization, M.A and Y.M.; methodology, Y.M and M.A.; validation, M.A and Y.M; resources, M.A and H.S.; writing—original draft preparation, Y.M; writing—review and editing, M.A, Y.M and H.S.; supervision, M.A and H.S; project administration, M.A.

All authors have read and agreed to the published version of the manuscript.

Data Availability Statement: All relevant data are provided within this manuscript.

Conflicts of Interest: The authors declare no conflict of interest.

References

1. Wells, B.G.; Dipiro, J.T.; Schwinghammer, T.L.; Dipiro, C. *Pharmacotherapy Handbook*, 9th ed.; McGraw-Hill Education: New York, United States of America, 2015; pp. 476-489.
2. World Health Organization. Global tuberculosis report 2021. Available online: <https://www.who.int/teams/global-tuberculosis-programme/tb-reports/global-tuberculosis-report-2021> (accessed on 21 October 2021).
3. Riccardi, N.; Canetti, D.; Rodari, P.; Besozzi, G.; Saderi, L.; Dettori, M.; Codesca, L.R.; Sotgiu, G. Tuberculosis and pharmacological interactions: A narrative review. *CRPHAR* **2021**, *2*, 100007:1-10. <https://doi.org/10.1016/j.crphar.2020.100007>.
4. Huynh, J.; Thwaites, G.; Marais, B.J.; Schaaf, H.S. Tuberculosis treatment in children: The changing landscape. *Paediatr. Respir. Rev* **2020**, *36*, 33-43.
5. Bernstein, A.L.; Dinesen, J.S. Effect of pharmacologic doses of vitamin B6 on carpal tunnel syndrome, electroencephalographic results, and pain. *J Am College Nutr* **1989**, *12*, 73-76.
6. Leklem, J.E.. Vitamin B6. In *Modern nutrition in health and disease*, 9th ed.; Shils, M.E., Olson, J.A., Shike, M., Ross, A.C., Eds.; Williams and Wilkins: Philadelphia, USA, 1999; pp. 413-421.
7. Van der Watt, J.; Harrison, T.; Benatar, M.; Heckmann, J. Polyneuropathy, anti-tuberculosis treatment and the role of pyridoxine in the HIV/AIDS era: a systematic review. *Int J Tuberc Lung Dis* **2011**, *15*(6), 722-728.
8. Court, R.; Centner, C.M.; Chirehwa, M.; Wiesner, L.; Denti, P.; de Vries, N.; Harding, J.; Gumbo, T.; Maartens, G.; McIlleron, H. Neuropsychiatric toxicity and cycloserine concentrations during treatment for multidrug-resistant tuberculosis. *IJID* **2021**, *105*, 688-694. <https://doi.org/10.1016/j.ijid.2021.03.001>
9. Mulubwa, M.; Mugabo, P. Analysis of terizidone in plasma using HPLC-UV method and its application in a pharmacokinetic study of patients with drug-resistant tuberculosis. *Biomed Chromatogr* **2018**, *32*:e4325, 1-7. <https://doi.org/10.1002/bmc.4325>.
10. Gandhi, S.V.; Shevale, V.P.; Choudhari, G.B. Development and validation of a stability indicating RP-HPLC method for the determination of terizidone. *IAJPS* **2018**, *05*(03), 1353-1361.
11. Vanavi, P.J.; Rajput, S.J. Impurity profiling of first line anti-TB drug – Terizidone using chromatographic and related techniques. *Int. j. pharm* **2021**, *13*(5), 83-95.
12. National Center for Biotechnology Information. Available online: <https://pubchem.ncbi.nlm.nih.gov/compound/Terizidone> (accessed on 21 October 2021).
13. National Center for Biotechnology Information. Available online: <https://pubchem.ncbi.nlm.nih.gov/compound/Pyridoxine-hydrochloride> (accessed on 21 October 2021).
14. International Conference of Harmonisation. [https://www.gmp-compliance.org/guidemgr/files/Q2\(R1\).pdf](https://www.gmp-compliance.org/guidemgr/files/Q2(R1).pdf) (accessed on 21 September 2021).
15. LoBrutto, R.; Patel, T. Method validation. In *HPLC for pharmaceutical scientists*, 1st ed.; Kazakevich, Y., LoBrutto, R.; John Wiley and Sons: New Jersey, USA, 2007; pp. 455-502.
16. Harris, R.S. General discussion on the stability of nutrients. In *Nutritional evaluation of food processing*, Karmas, E., Harris, R.; Springer: Dordrecht, 1988; pp. 3-5.
17. Aboul-Enein, H.Y.; Loutfy, M.A. Pyridoxine hydrochloride. In *Analytical profiles of drug substances*, Florey, K.; Academic Press: New York, USA, 1984; pp.447-486.